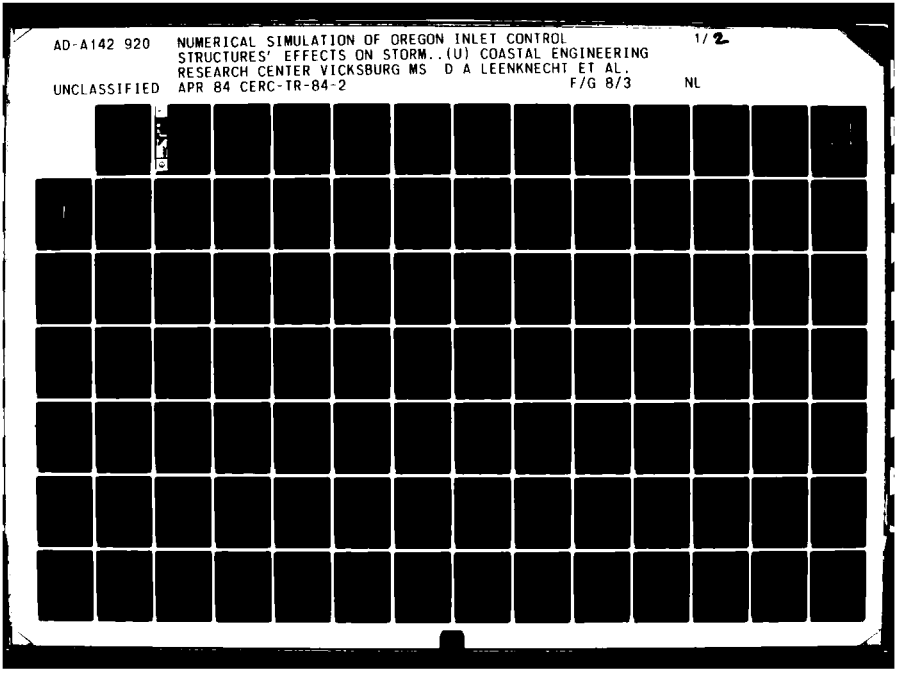
AD-A142 920
NUMERICAL SIMULATION OF OREGON INLET CONTROL STRUCTURES' EFFECTS ON STORM..(U) COASTAL ENGINEERING RESEARCH CENTER VICKSBURG MS D A LEENKNECHT ET AL.
1/2
UNCLASSIFIED
APR 84 CERC-TR-84-2
F/G 8/3
NL

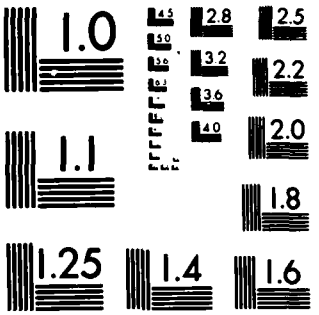

MICROCOPY RESOLUTION TEST CHART
NATIONAL BUREAU OF STANDARDS-1963-A

US Army Corps of Engineers

COASTAL ENGINEERING RESEARCH CENTER

TECHNICAL REPORT CERC-84-2

NUMERICAL SIMULATION OF OREGON INLET CONTROL STRUCTURES' EFFECTS ON STORM AND TIDE ELEVATIONS IN PAMLICO SOUND

by

David A. Leenknecht, Jeff A. Earickson, and H. Lee Butler

Coastal Engineering Research Center
U. S. Army Engineer Waterways Experiment Station
P. O. Box 631, Vicksburg, Miss. 39180

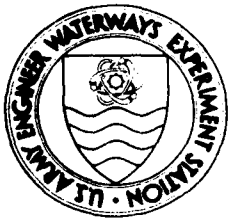

April 1984
Final Report

Approved For Public Release; Distribution Unlimited

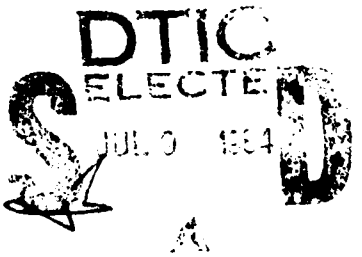

Prepared for U. S. Army Engineer District, Wilmington
Wilmington, N. C. 28402

Unclassified

SECURITY CLASSIFICATION OF THIS PAGE (When Data Entered)

REPORT DOCUMENTATION PAGE	READ INSTRUCTIONS BEFORE COMPLETING FORM
1. REPORT NUMBER: Technical Report CERC-84-2	2. GOVT ACCESSION NO.: AD-A142 920
	3. RECIPIENT'S CATALOG NUMBER
4. TITLE (and Subtitle): NUMERICAL SIMULATION OF OREGON INLET CONTROL STRUCTURES' EFFECTS ON STORM AND TIDE ELEVATIONS IN PAMLICO SOUND	5. TYPE OF REPORT & PERIOD COVERED: Final Report
	6. PERFORMING ORG. REPORT NUMBER
7. AUTHOR(s): David A. Leenknecht, Jeff A. Earickson, H. Lee Butler	8. CONTRACT OR GRANT NUMBER(s)
9. PERFORMING ORGANIZATION NAME AND ADDRESS: U. S. Army Engineer Waterways Experiment Station, Coastal Engineering Research Center, P. O. Box 631, Vicksburg, Miss. 39180	10. PROGRAM ELEMENT, PROJECT, TASK AREA & WORK UNIT NUMBERS
11. CONTROLLING OFFICE NAME AND ADDRESS: U. S. Army Engineer District, Wilmington, P. O. Box 1890, Wilmington, N.C. 28402	12. REPORT DATE: April 1984
	13. NUMBER OF PAGES: 163
14. MONITORING AGENCY NAME & ADDRESS(if different from Controlling Office)	15. SECURITY CLASS. (of this report): Unclassified
	15a. DECLASSIFICATION/DOWNGRADING SCHEDULE

16. DISTRIBUTION STATEMENT (of this Report)

Approved for public release; distribution unlimited.

17. DISTRIBUTION STATEMENT (of the abstract entered in Block 20, if different from Report)

18. SUPPLEMENTARY NOTES

Available from National Technical Information Service, 5285 Port Royal Road, Springfield, Va. 22161

19. KEY WORDS (Continue on reverse side if necessary and identify by block number)

Hydrodynamics--Mathematical models. (LC)
Hydraulic structures--Evaluation. (LC)
Sediment transport. (LC)
Simulation methods. (LC)
Oregon Inlet (North Carolina). (LC)

20. ABSTRACT (Continue on reverse side if necessary and identify by block number)

Three numerical hydrodynamic models with progressively finer grid resolutions, utilizing the finite difference code WIFM, were developed for the purpose of evaluating the influence of proposed structures under storm conditions and providing elevation and velocity data for concurrent numerical sediment transport studies at Oregon Inlet, North Carolina. The offshore model encompassed the entire Carolina coast over the continental

(Continued)

DD FORM 1 JAN 73 1473 EDITION OF 1 NOV 65 IS OBSOLETE

Unclassified

SECURITY CLASSIFICATION OF THIS PAGE (When Data Entered)

20. ABSTRACT (Continued).

shelf and was used to propagate storm effects from deep water to the finer resolution models. The nearshore model extended from Cape Henry to Cape Lookout, and provided finer detail along the Outer Banks, within Pamlico and Albemarle Sounds, and at Oregon Inlet. This model was used for both tide and surge simulations and was the primary tool for establishing structural effects under storm conditions in the Oregon Inlet vicinity. It also was used to provide boundary conditions for the most detailed model of the study known as the shore process model. The shore process model emcompassed less than 85 square miles centered about Oregon Inlet and provided high resolution at the inlet and in the surf zone. It provided more realistic circulation patterns of the inlet, the effects of jetties on inlet flow, and hydrodynamic data for concurrent numerical sediment transport studies.

Data collected for previous physical model studies were supplemented by additional data from NOAA and unpublished SAW letter reports for satisfactory calibration and verification of the models under existing tidal conditions and for two severe storms of record: the March 1962 northeaster and Hurricane Donna (1960). Two structural alternatives (involving parallel jetties with 2,500- and 5,000-ft-wide spacings) were studied, and their effects were determined to be limited to the inlet under tidal conditions and to the immediate inlet vicinity under circumstances approximating Hurricane Donna. The maximum possible influence attributable to inlet restriction was determined by simulations with complete inlet closure (this was not under consideration as an improvement plan) under Hurricane Donna conditions, and no changes were noted beyond a 12-mile radius of the inlet. Within that distance, elevation increases of 2.4 ft and 1.4 ft were indicated at the Pea Island Coast Guard Station and Oregon Inlet Marina, respectively, with total inlet closure under Donna-like conditions. For 2,500- and 5,000-ft-wide jetty alternatives, no significant changes were noted during Donna simulations, the 2,500-ft case producing water-elevation increases of 0.6 ft and 0.3 ft, respectively, for the above stations. Tidal simulations with structural alternatives indicated local variations to be limited to the inlet.

Simulations at very fine grid resolution were made using the shore process model to provide hydrodynamic data for numerical sediment transport studies covering the normal range of tides with no jetties, four structural alternatives with a mean tide, and the historical March 1962 northeaster with no jetties.

PREFACE

This study was authorized by the U. S. Army Engineer District, Wilmington (SAW), and conducted at the U. S. Army Engineer Waterways Experiment Station (WES). The study was performed, and this report prepared, by Messrs. David Leenknecht, Jeff Earickson, and H. Lee Butler of the Wave Dynamics Division (WDD), Hydraulics Laboratory. Providing general supervision were Mr. H. B. Simmons, Chief of the Hydraulics Laboratory, and Dr. R. W. Whalin and Mr. C. E. Chatham, Jr., former and acting Chiefs of the Wave Dynamics Division. The WWD and its personnel were transferred to the Coastal Engineering Research Center (CERC) of WES on 1 July 1983 under the supervision of Dr. Whalin, Chief of CERC.

This report describes the application of numerical hydrodynamic models to Pamlico Sound and adjacent areas. Following model calibrations and verifications, an evaluation of proposed jetty configurations for Oregon Inlet was made. All numerical computations were performed on the CRAY 1 and Control Data Cyber computers of Boeing Computer Services in Bellevue, Washington.

Commanders and Directors of WES during this investigation and the preparation and publication of this report were COL Nelson P. Conover, CE, and COL Tilford C. Creel, CE. Technical Director was Mr. F. R. Brown.

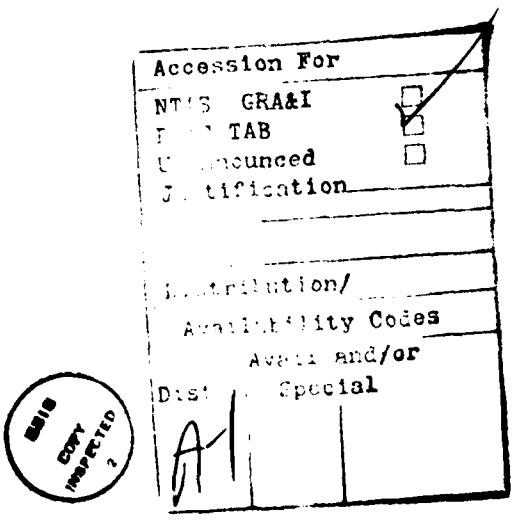

TABLE OF CONTENTS

CONVERSION FACTORS, U. S. CUSTOMARY TO METRIC (SI) UNITS OF MEASUREMENT

U. S. customary units of measurement used in this report can be converted to metric (SI) units as follows:

Multiply	By	To Obtain
cubic feet per second	0.02831685	cubic metres per second
feet	0.3048	metres
feet per second	0.3048	metres per second
knots (international)	0.5144444	metres per second
miles (U. S. nautical)	1.852	kilometres
miles (U. S. statute)	1.609344	kilometres
square miles (U. S. statute)	2.589988	square kilometres

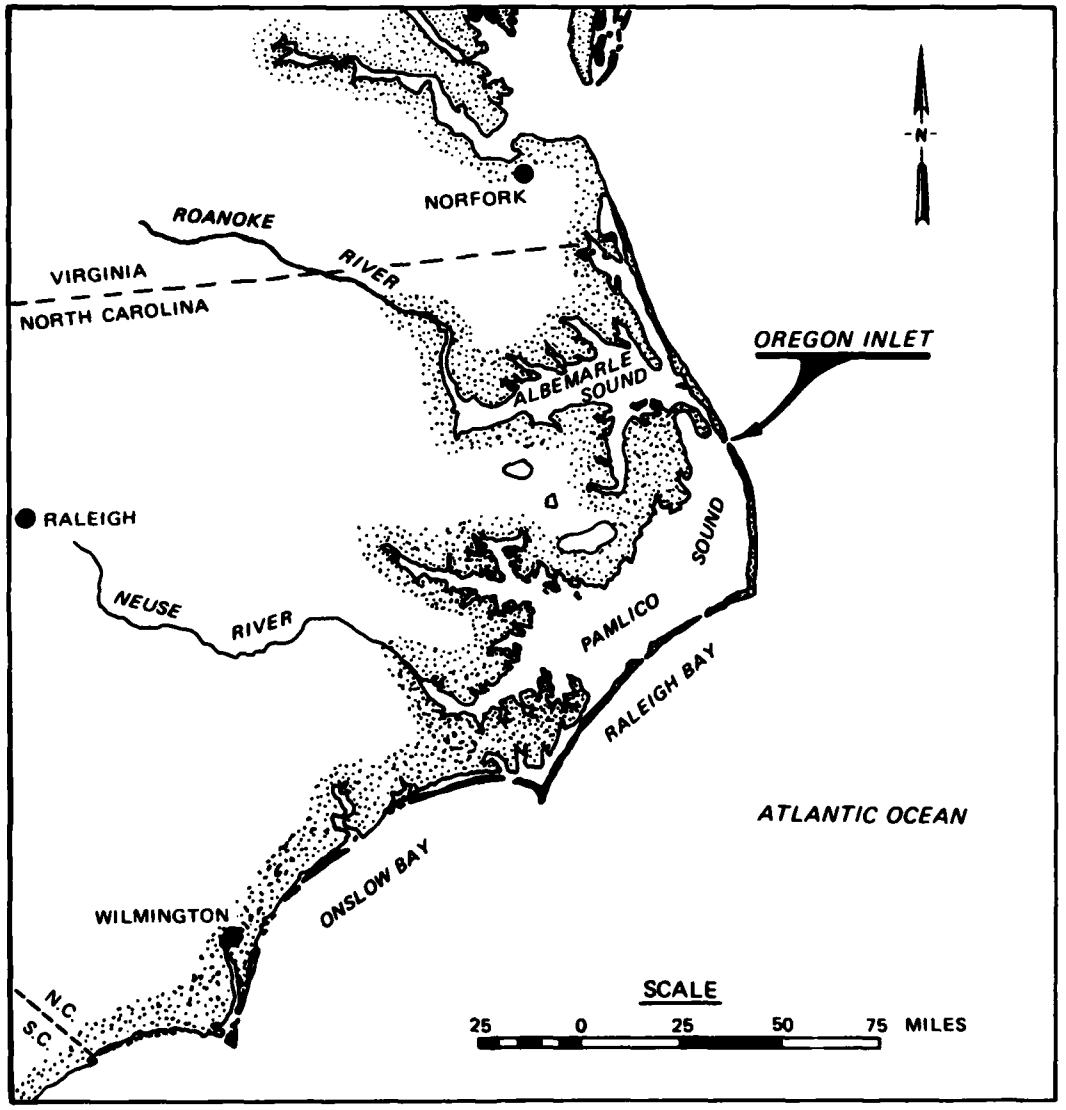

Figure 1. Location map

NUMERICAL SIMULATION OF OREGON INLET CONTROL STRUCTURES' EFFECTS ON STORM AND TIDE ELEVATIONS IN PAMLICO SOUND

PART I: INTRODUCTION

Background and Objectives

1. North Carolina's Atlantic coast has two large lagoons, Pamlico Sound and Albemarle Sound, separated from the ocean by a strand of barrier islands known as the Outer Banks (Figure 1). The Outer Banks stretch approximately 190* miles between Virginia Beach, Virginia; Cape Hatteras, and Morehead City, North Carolina. Only three openings in the barrier islands provide navigational access between Pamlico Sound and the Atlantic: Hatteras, Ocracoke, and Oregon Inlet. Oregon Inlet, the northernmost of the three openings, provides the fishermen and boaters of Roanoke Island and Albemarle Sound the only practical means of reaching the ocean. Since the creation of the present-day Oregon Inlet by a hurricane in 1846, navigation there has remained hazardous due to channel movements and shoals. Location of the channel also has moved steadily south due to sediment transport by alongshore currents in the past 100 years.

2. In 1970, Congress authorized the Manteo (Shallowbag) Bay project which included the stabilization of Oregon Inlet with a dual jetty system. Since the addition of jetties will change the hydrodynamics of the inlet, proposed structures need to be evaluated for their impact on normal tidal conditions and storm surges.

3. This study evaluates several proposed jetty configurations for Oregon Inlet with numerical hydrodynamic models of the entire lagoon system and the area around the inlet. The models are calibrated by computing tides and adjusting model parameters until the computations match observed tides. The calibrations are verified by storm surge simulations of two historical storms (Hurricane Donna in 1960 and the March 1962 northeaster) that affected the inlet. These calculations are shown to agree with marigrams recorded during the storms at several tide stations on the Atlantic coast and in the bays.

---

* A table of factors for converting U. S. customary units of measurement to metric (SI) units is presented on page 3.

After verification, the effects of the jetties are estimated with the models for both tide and storm conditions.

Approach

4. The numerical hydrodynamic code used in this study is WIFM, the WES Implicit Flooding Model (Butler, in preparation). WIFM employs finite difference methods to approximate the vertically integrated Navier-Stokes equations. Several special features of WIFM are important to this study. The flooding and drying of tidal flats and low-lying lands are accurately simulated in WIFM. Variably spaced finite difference grids are used to maximize accuracy in the hydrodynamic simulations, without increasing computer costs. WIFM can approximate jetties, and other small topographic details, as thin barriers between computational cells. The implicit formulation used in WIFM's solution scheme allows for larger time-steps than do explicit solution schemes.

5. The hydrodynamic features of the Carolina coast and Oregon Inlet are simulated to three levels of accuracy in this study by the use of three different finite difference grids that cover different portions of the study area (Figure 2). The three grids can be linked together, wherein an internal boundary in a larger grid can provide boundary conditions to the next smallest grid. The offshore grid (Figure 3) approximates the entire Carolina coast with 3,186 cells, making computations with it inexpensive. This grid extends seaward to the continental shelf in order to model the effects of long-wave shoaling caused by the shelf. Oregon Inlet is only approximated by one cell in the offshore grid, so computations from this model can only provide rough estimates of hydrodynamics in the sounds. The nearshore grid (Figure 4) models the Outer Banks in much finer detail with 9,009 cells. Tides and surges can be accurately simulated throughout the bays and inlets with this grid. Oregon Inlet is modeled with enough detail in this grid to allow for calculations with crude jetty approximations. This grid provides all boundary conditions to the most detailed of the three grids used in this study, the shore process grid.

6. The shore process grid (Figure 5) covers less than 85 square miles around Oregon Inlet with 4,620 computational cells. This model provides high resolution at the inlet and in the surf zone. The shore process model predicts circulation patterns at the inlet, predicts effects of jetties on inlet flow,

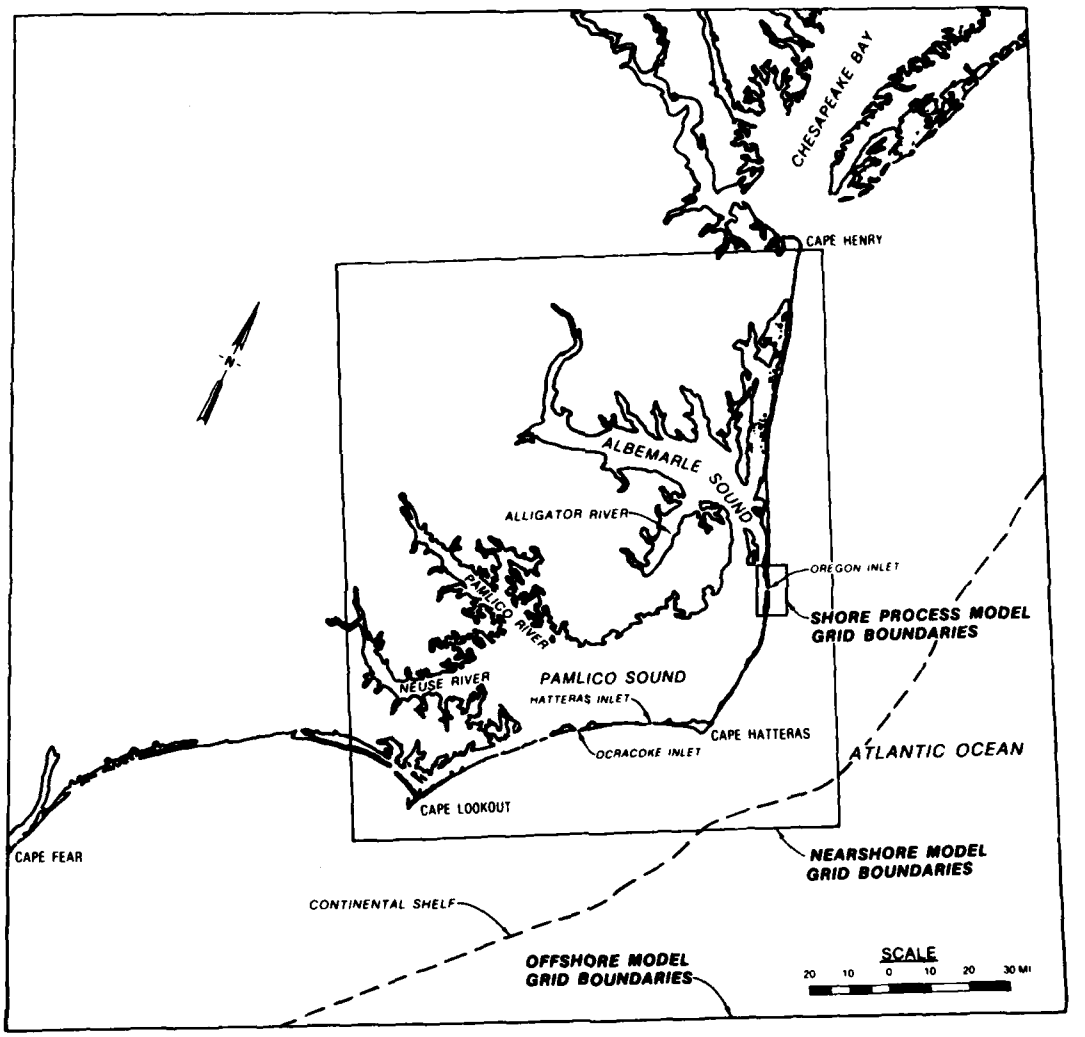

Figure 2. Numerical model grid boundaries

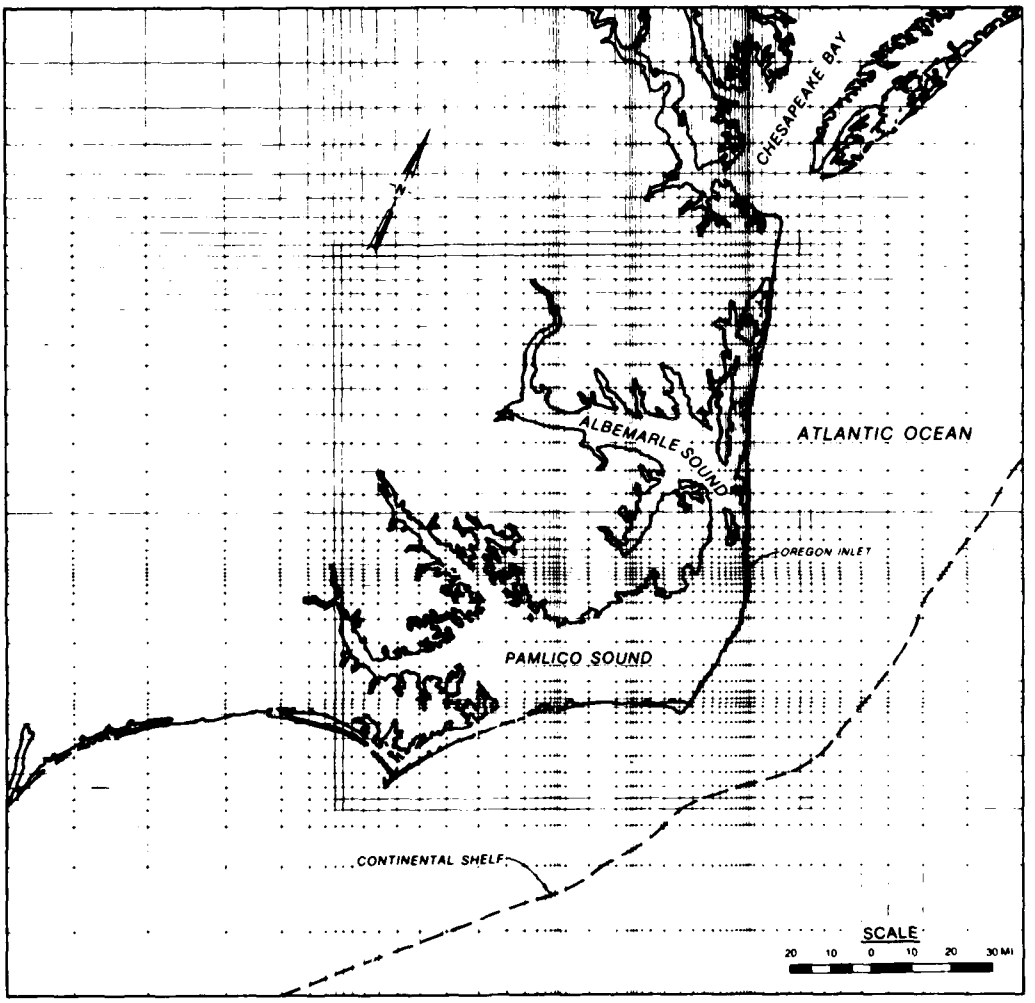

Figure 3. Offshore model computational grid

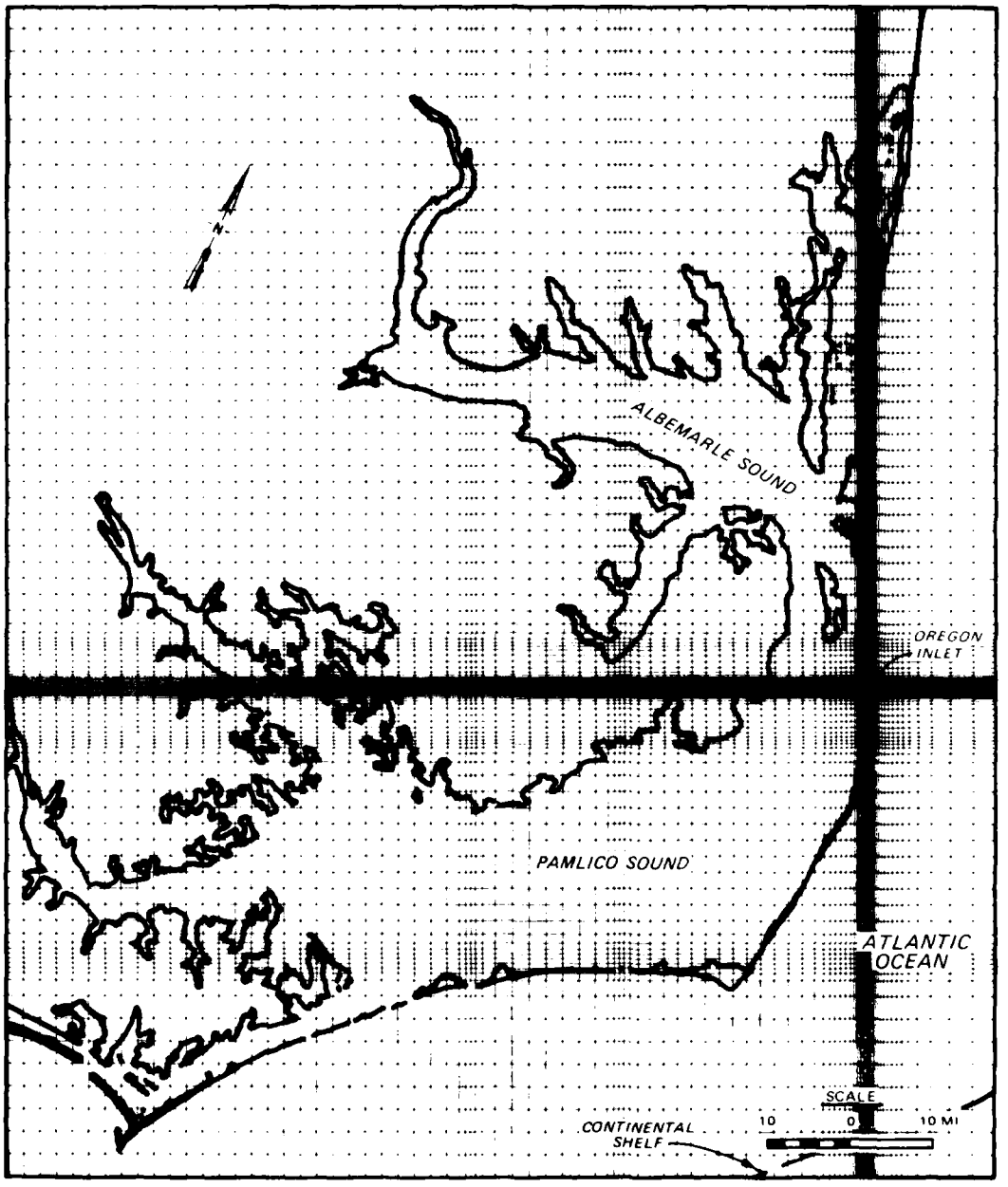

Figure 4. Nearshore model computational grid

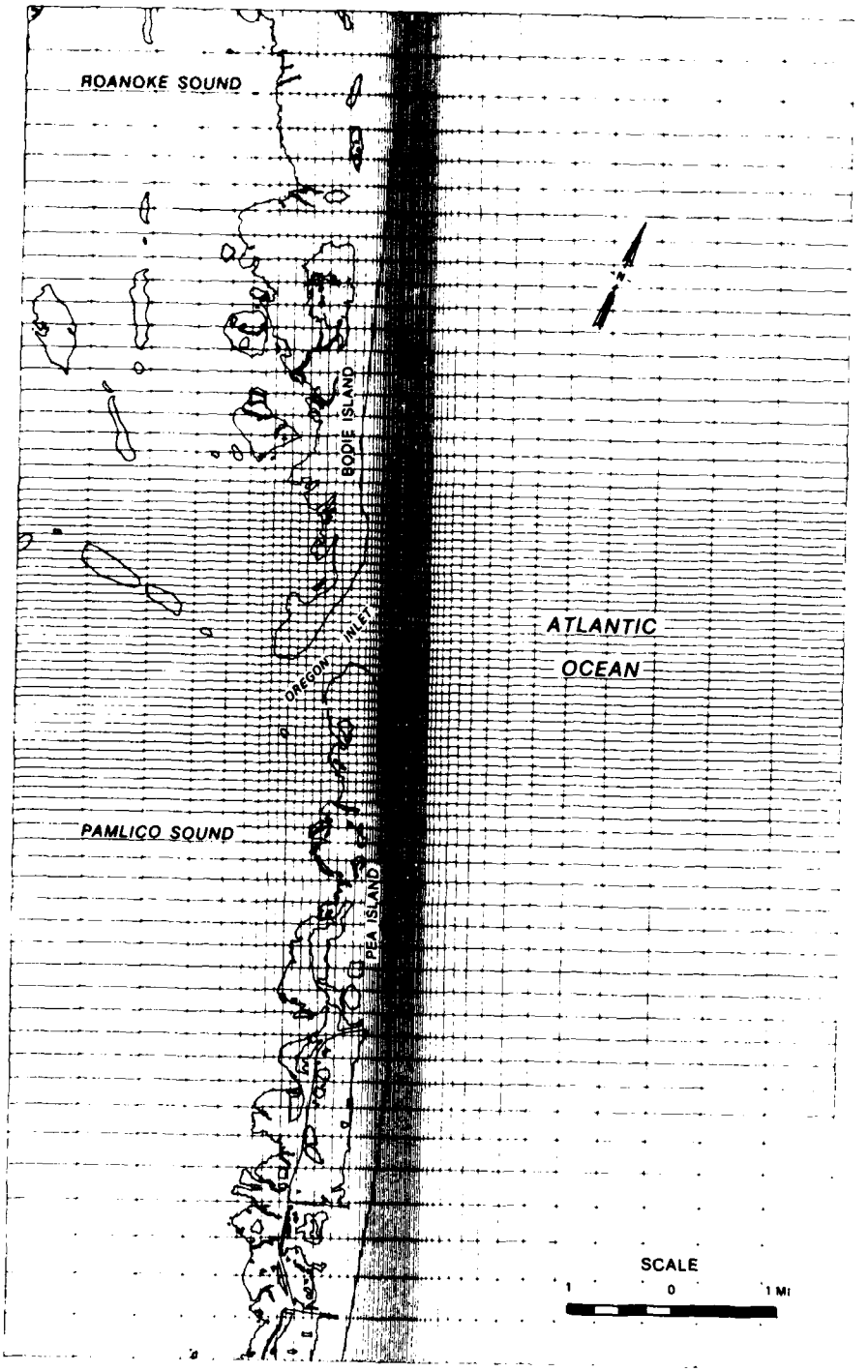

Figure 5. Shore process model computational grid

and provides flow data for the sediment transport studies of Houston (in preparation). The effects of channel dredging can also be studied with this model.

7. Storm simulations in WIFM require the input of wind stresses and barometric pressures into the computations. The wind and pressure fields for Hurricane Donna are simulated with the Standard Project Hurricane (SPH) model (Graham and Nunn 1959; National Oceanic and Atmospheric Administration (NOAA) 1972; Schwerdt, Ho, and Watkins 1979). SPH is a parametric model that characterizes a hurricane by its radius to maximum winds, central pressure deficit, forward speed, and other variables. The parameters needed to reproduce a historical storm can be collected from surface weather charts. The winds and pressures of the March 1962 northeaster are estimated from digitized data provided by the Wave Information Study (WIS) at the U. S. Army Engineer Waterways Experiment Station (WES) (Corson, Resio, and Vincent 1980; Resio, Vincent, and Corson 1982). WIS data are referenced to an earth-coordinate system, and a computer code was developed to interpolate this information to WIFM grids. Wind velocities and pressures for each WIFM cell are read in during the hydrodynamic calculations, and WIFM converts wind velocities in surface stress by Charnock's relation (Garrett 1977).

and provides flow data for the sediment transport studies of Houston (in preparation). The effects of channel dredging can also be studied with this model.

7. Storm simulations in WIFM require the input of wind stresses and barometric pressures into the computations. The wind and pressure fields for Hurricane Donna are simulated with the Standard Project Hurricane (SPH) model (Graham and Nunn 1959; National Oceanic and Atmospheric Administration (NOAA) 1972; Schwerdt, Ho, and Watkins 1979). SPH is a parametric model that characterizes a hurricane by its radius to maximum winds, central pressure deficit, forward speed, and other variables. The parameters needed to reproduce a historical storm can be collected from surface weather charts. The winds and pressures of the March 1962 northeaster are estimated from digitized data provided by the Wave Information Study (WIS) at the U. S. Army Engineer Waterways Experiment Station (WES) (Corson, Resio, and Vincent 1980; Resio, Vincent, and Corson 1982). WIS data are referenced to an earth-coordinate system, and a computer code was developed to interpolate this information to WIFM grids. Wind velocities and pressures for each WIFM cell are read in during the hydrodynamic calculations, and WIFM converts wind velocities in surface stress by Charnock's relation (Garrett 1977).

PART II: COMPUTATIONAL TECHNIQUES

Equations of Motion

8. The hydrodynamics of the numerical model WIFM are derived from the Navier-Stokes equations in a Cartesian coordinate system (Figure 6). The

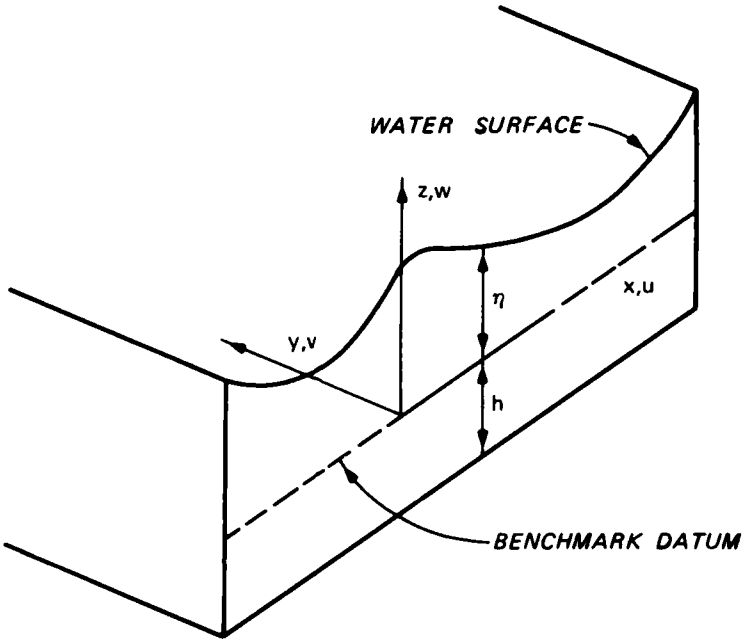

Figure 6. Coordinate system for problem formulation

long wave approximations of small vertical accelerations and a homogenous fluid yield vertically integrated two-dimensional equations of continuity and momentum:

Continuity

$$\frac{\partial \eta}{\partial t} + \frac{\partial}{\partial x}(ud) + \frac{\partial}{\partial y}(vd) = R \tag{1}$$

Momentum

$$\frac{\partial u}{\partial t} + u\frac{\partial u}{\partial x} + v\frac{\partial u}{\partial y} - fv + g\frac{\partial}{\partial x}(\eta - \eta_a) + \frac{gu}{C^2 d}(u^2 + v^2)^{1/2} - \varepsilon\left(\frac{\partial^2 u}{\partial x^2} + \frac{\partial^2 u}{\partial y^2}\right) + F_x = 0 \tag{2}$$

$$\frac{\partial v}{\partial t} + u \frac{\partial v}{\partial x} + v \frac{\partial v}{\partial y} + fu + g \frac{\partial}{\partial y} (\eta - \eta_a) + \frac{gv}{C^2 d} (u^2 + v^2)^{1/2}$$

$$- \varepsilon \left(\frac{\partial^2 v}{\partial x^2} + \frac{\partial^2 v}{\partial y^2} \right) + F_y = 0 \qquad (3)$$

The dependent variables in the problem are η , u , and v , which represent the water-surface elevation above datum and the vertically averaged water velocities in the x- and y-directions, respectively.* The other variables in the equations are: h , the local ground (cell) elevation above datum; $d = \eta - h$, the total water depth; t , time; f , the Coriolis parameter; C , the Chezy coefficient for bottom friction; ε , the eddy viscosity coefficient; g , the acceleration due to gravity; and R , the rate of water volume change in the system due to rainfall or evaporation. The coefficient η_a accounts for hydrostatic water elevations due to atmospheric pressure differences, and F_x and F_y are terms representing external forces such as wind stress.

9. The computational grid used for the finite difference approximations in WIFM employs a stretching transformation for each of the two coordinate directions (x and y). This transformation from physical space to computational space offers the major advantage of allowing increased grid resolution in areas of interest, by controlling the arbitrary constants a , b , and c in the equation:

$$x = a + b\alpha^c \qquad (4)$$

Physical distances are defined by x , and the computational grid lines in each direction are defined by positive integer values of α . The values of a , b , and c are determined not only from desired grid resolutions, but also from the requirement that the derivative $\frac{\partial x}{\partial \alpha}$ be continuous everywhere. Many stability problems commonly associated with variable grid schemes are eliminated due to this continuity constraint. The transformation is applied

---

* For convenience, symbols and unusual abbreviations are listed and defined in the Notation (Appendix A).

to each coordinate direction independently in order to maximize grid resolution in areas of hydrodynamic importance and to minimize computational cells in the far field.

Numerical Method

10. The alternating-direction-implicit (ADI) method has been used by Leendertse (1970) and others to solve the two-dimensional equations of motion. When the advective terms are included in the momentum equations (Equations 1-3) the ADI method has encountered stability problems. Weare (1976) indicates that the problem arises from approximating advective terms with one-sided differences in time, and suggests the use of a centered scheme with three time-levels. WIFM employs a centered stabilizing-correction (SC) scheme which is second-order accurate in space and time, and boundary conditions can be formulated to the same order accuracy. Details of the SC scheme can be found in Butler (in preparation) and a general development is presented in the following paragraphs.

11. The linearized equations of motion can be written in matrix form as:

$$U_t + AU_x + BU_y = 0 \tag{5}$$

where

$$U = \begin{bmatrix} \eta \\ u \\ v \end{bmatrix}, \quad A = \begin{bmatrix} o & d & o \\ g & o & o \\ o & o & o \end{bmatrix}, \quad B = \begin{bmatrix} o & o & d \\ o & o & o \\ g & o & o \end{bmatrix}$$

The SC scheme for solving Equation 5 is

$$(1 + \lambda_x)\, U^* = (1 - \lambda_x - 2\lambda_y)\, U^{k-1} \tag{6}$$

$$(1 + \lambda_y)\, U^{k+1} = U^* + \lambda_y\, U^{k-1} \tag{7}$$

where

$$\lambda_x = \frac{1}{2}\frac{\Delta t}{\Delta x} A\delta_x \quad \text{and} \quad \lambda_y = \frac{1}{2}\frac{\Delta t}{\Delta y} B\delta_y$$

The quantities δ_x and δ_y are centered difference operators and the superscript k counts time-levels. The starred quantities can be considered intermediate values for variables at the $(k+1)$ time-level.

12. The first step in the SC procedure computationally sweeps the grid in the x-direction, with the second step sweeping the y-direction. Completing both sweeps constitutes a full time-step, advancing the solution from the k^{th} time-level to the $(k+1)$ time-level. The form of the difference equations for the x-sweep is given by

$$\frac{1}{2\Delta t}(\eta^* - \eta^{k-1}) + \frac{1}{2\Delta x}\delta_x(u^*d + u^{k-1}d) + \frac{1}{\Delta y}\delta_y(v^{k-1}d) = 0 \tag{8}$$

$$\frac{1}{2\Delta t}(u^* - u^{k-1}) + \frac{g}{2\Delta x}\delta_x(\eta^* + \eta^{k-1}) = 0 \tag{9}$$

$$\frac{1}{2\Delta t}(v^* - v^{k-1}) + \frac{g}{\Delta y}\delta_y(\eta^{k-1}) = 0 \tag{10}$$

and the y-sweep by

$$\frac{1}{2\Delta t}(\eta^{k+1} - \eta^*) + \frac{1}{2\Delta y}\delta_y(v^{k+1}d - v^{k-1}d) = 0 \tag{11}$$

$$u^{k+1} = u^* \tag{12}$$

$$\frac{1}{2\Delta t}(v^{k+1} - v^*) + \frac{g}{2\Delta y}\delta_y(\eta^{k+1} - \eta^{k-1}) = 0 \tag{13}$$

13. Noting that v^* in Equation 10 is only a function of previously computed variables at the $(k-1)$ time-level, its substitution into Equation 13 and the substitution of u^* (Equation 12) into Equations 8 and 9 yield the simplified forms

x-sweep

$$\frac{1}{2\Delta t}(\eta^* - \eta^{k-1}) + \frac{1}{2\Delta x}\delta_x(u^{k+1}d + u^{k-1}d) + \frac{1}{\Delta y}\delta_y(v^{k-1}d) = 0 \tag{14}$$

$$\frac{1}{2\Delta t}(u^{k+1} - u^{k-1}) + \frac{g}{2\Delta x}\delta_x(\eta^* + \eta^{k-1}) = 0 \tag{15}$$

y-sweep

$$\frac{1}{2\Delta t}\left(\eta^{k+1} - \eta^{*}\right) + \frac{1}{2\Delta y}\ \delta_y\left(v^{k+1}{}_d - v^{k-1}{}_d\right) = 0 \tag{16}$$

$$\frac{1}{2\Delta t}\left(v^{k+1} - v^{k-1}\right) + \frac{g}{2\Delta y}\ \delta_y\left(\eta^{k+1} + \eta^{k-1}\right) = 0 \tag{17}$$

14. The details of applying the SC scheme to Equations 1-3 can be found in a report by Butler (in preparation). The diffusion terms of Equations 2 and 3 are also represented with time-centered approximations. The inclusion of diffusion terms contributes to the numerical stability of the scheme (Vreugdenhill 1973), and serves to somewhat account for turbulent momentum dissipation at the larger scales. While the resulting finite difference forms of Equations 1-3 appear cumbersome, they are efficient to solve. Application of the appropriate equation to one row or column of the grid (the "sweeping" process) results in a system of linear algebraic equations whose coefficient matrix is tridiagonal. Tridiagonal matrix problems can be solved directly, without the cost and effort of matrix inversion.

15. The computational time-step for the SC scheme in WIFM is largely governed by simple mass and momentum conservation principles. The maximum time-step for a problem is characterized by:

$$\Delta t = \frac{n\Delta S}{V} \tag{18}$$

where V is the largest flow velocity to be encountered at a cell with its smallest side length ΔS. The parameter n is of order 1. So, the time step is constrained by the smallest cell width which contains the highest flow velocity. In physical terms, Equation 18 requires that the flow cannot move substantially farther than one cell width in one time-step.

Boundary Conditions

16. WIFM allows a variety of boundary conditions to be specified, which can be classified into three groups: open boundaries, land-water boundaries, and thin-wall barriers.

Open boundaries

17. When the edge of the computational grid is defined as water, such

as a seaward boundary or a channel exiting the grid, either the water elevation or the flow velocities can be specified as an open boundary-condition. This information can be input to WIFM as tabular data, or constituent tides can be calculated within the code during the time-stepping process. Open boundaries for a grid can be saved from a specified internal boundary of another grid so that computational grids can be linked together. Grid linking is used in this study in order to model large coastal areas inexpensively and to supply correct boundary conditions to the shore-processes grid.

Land-water boundaries

18. WIFM allows land-water boundaries to be either fixed or variable to account for flooding in low-lying terrain. Fixed boundaries specify a no-flow condition at the cell face between land and water. The position of a variable boundary is determined by the relationship of the water elevation at a "wet" cell to the land elevation at a neighboring "dry" cell. Once a water elevation rises above the level of adjacent land height, water is initially moved onto the "dry" cell by using a broad-crested weir formula (Reid and Bodine 1968). When the water level on the dry cell exceeds some small value, the boundary face is treated as open and computations for η, u, and v are made at the now "wet" cell. Drying is the inverse process, and mass is conserved in these procedures.

Thin-wall barriers

19. These barriers are defined along cell faces and are of three types: exposed, submerged, and overtopping. Exposed barriers allow no flow across a cell face. Submerged barriers control flow across a cell face by using a time-dependent friction coefficient. Overtopping barriers are dynamic: they can be completely exposed, completely submerged, or they can act as broad-crested weirs. The barrier character is determined by its height and the water elevations in the two adjoining cells.

Grid Connections

20. Application of the embedded grid concept employed in this study requires a transfer of hydrodynamic information from one grid to another. Specifically, data are transferred from the offshore grid to the nearshore grid and thence to the shore process grid. In practice, the shore process model was always driven by a nearshore model simulation, and the offshore

model was used to drive the system only for storm events.

21. The two embedded grids utilized in this study (nearshore and shore process) contain successively finer resolution with resultant greater detail. Therefore stability requirements as governed by Equation 18 necessitate the use of successively smaller time-steps in simulations with these models. Data are transferred between coupled grids at the outer boundary cells of the embedded grid. Coupling grids are designed such that the cell size Δx and the derivative $\frac{\partial x}{\partial \alpha}$ (in the direction orthogonal to the coupling boundary) are equivalent in the coupling cells of both the driving and driven grids. In the direction normal to the coupling boundary, cell expansion and contraction are allowed to proceed independently, thus requiring spatial interpolation of the transferred data. A temporal interpolation is also required due to the small time-step needed by the embedded grid. Care must be taken to ensure that coupling grids contain similar water volumes within the embedded grid coverage, particularly at the coupling boundaries in order to preserve hydrodynamics between the grids.

22. The data transferred between models consist of η, u, and v at each coupling cell. A utility program performs the necessary spatial and temporal interpolations between coupling grids. It should be noted that connections are not totally dynamic in the sense that the simulations are independent and not concurrent. Communication is unidirectional from the driving to the driven model.

PART III: PROTOTYPE DATA

23. Field measurement data required for model calibrations and verification were taken from existing data bases. No new collection efforts were undertaken during the course of this study. The following is a summary of the prototype data used in the investigation and its sources.

Tidal Data

24. A hydraulic model study to determine effects of Oregon Inlet stabilization by jetties was conducted at WES and reported by Hollyfield, McCoy, and Seabergh (1983). Representatives of the National Ocean Survey (NOS), U. S. Army Engineer District, Wilmington (SAW), and WES formulated a data collection program. Field surveys were carried out in the spring and summer of 1975. Efforts included collecting tide and current data, primarily in the vicinity of Oregon Inlet, and prototype hydrography/topography data within the area reproduced in the hydraulic model. The tide data were subsequently analyzed for their tidal constituents. Constituent data form allows for isolating the astronomical event and was used both to force the WIFM model and for comparison with model results. Tide elevation data outside the Oregon Inlet area were obtained (in constituent form) from NOS. Figure 7 (page 24) shows locations of field stations in the offshore grid region. Since the M_2 constituent contains about 90 percent of the tidal energy in the Pamlico Sound area, calibration computations were simplified by considering only an M_2 tide. Table 1 delineates the M_2 amplitude and epoch (relative to Greenwich) for each field station.

Storm Surge Data

25. Two historical storms were modeled in this study: Hurricane Donna in 1960 and the extratropical March 1962 storm. Meteorological data for Hurricane Donna were obtained from NOS. These included a list of storm parameters, track definition, and surface windfield analysis. Table 2 presents a time variation of these storm parameters. The coincident predicted astronomical tide was reconstructed from constituent tidal data (particularly at Capes Fear, Lookout, Hatteras, and Henry) obtained from NOS. Comparison

water level and wind data at various model locations were obtained from a CE letter report on Hurricane Donna dated 28 April 1961.

26. Meteorological data for the March 1962 storm were obtained from a data base constructed for the WIS project at WES (Resio, Vincent, and Corson 1982). Comparison water levels and wind data were obtained from a CE letter report on the March 1962 storm dated 6 September 1962.

PART IV: NUMERICAL MODEL CALIBRATION

Procedure

27. The three models in this study were calibrated against the tides of the Carolina coast. The tide along the Outer Banks is semidiurnal in nature, with the M_2 constituent predominating. To calibrate the computational models, four parameters were adjusted in WIFM: (a) the depths or elevations assigned to each cell, (b) the Chezy friction coefficients for each cell, (c) the choice of cells used as marigram stations, and (d) the boundary condition imposed on the grids. The water depth or land elevation of a cell was estimated from maps, and only a few depths were changed slightly during calibration. Except in shallow water and at flow constrictions, the models' hydrodynamics were fairly insensitive to changes in Chezy coefficients. The choice of which cells to serve as marigram stations was sometimes arbitrary due to shoreline approximations and the size of cells relative to hydrodynamic details in the prototype. For a model that was adjusted to the point where only one WIFM gage disagreed slightly with prototype data, this discrepancy was removed by changing the gage's placement in the grid.

28. Calibrations largely involved the development of proper boundary conditions for the models. For a tide, seaward boundary conditions were estimated by wave speed calculations and shoaling factors. With initial estimates, the development of correct boundary conditions proceeded through three steps: (a) computations with WIFM using the latest estimate, (b) comparison of computed marigrams to prototype data, and (c) refinement of the boundary conditions. Successive iterations were performed to match computed tides against prototype data. The other parameters in WIFM were also adjusted during the refinement of the boundary conditions.

29. The model's ability to accurately reproduce prototype data was limited by cell sizes used in the grid (which governed how well topography was simulated) and by any approximations used for the boundary conditions. In this study, the prototype tides were approximated with just the M_2 constituent. For the North Carolina coast, this approximation provided a good representation of the entire tide while keeping the expenses of calibration to a minimum. The number of iterations needed in the boundary condition refinement process soars when multiconstituent tides are used, because of the increased

number of variables that must be adjusted.

Offshore Model

30. The tides of two time periods were simulated in the calibration of the offshore model: 5-10 March 1962 (the March 1962 northeaster) and 11 and 12 September 1960 (Hurricane Donna). Predicted highs and lows for several stations along the coast were taken from U. S. Coast and Geodetic Survey (1962) tide tables for these two times to serve as prototype data. Four stations (Capes Fear, Lookout, Hatteras, and Henry) yielded the initial estimates for boundary conditions and served as the primary comparisons with WIFM computations during the calibration process. Estimates of the M_2 amplitudes and epochs for the grid boundaries were chosen so that the computed one-constituent tide would represent the entire predicted tide, and not just the M_2 portion of the signal. In order to easily see the agreement between WIFM computations and the prototype data, computed marigrams were plotted against spline-fit curves of the predicted highs and lows.

31. Boundary conditions were first refined to match the predicted tides of the March 1962 storm. The beginning of the WIFM computation was chosen to be midnight Greenwich Mean Time (GMT) on 5 March 1962. A 3-min time-step was used in WIFM, and 111 hr of the tide were computed. Plate 1 shows computed marigrams versus prototype curves for the four Cape stations. There are small variances between the peaks of the computed and prototype tides due to the lack of other constituents in the grid boundary conditions, but the two tides match well for these gages. To check that the model correctly represents the prototype tide at other points along the Outer Banks, other stations are compared with computations (Plate 2). Virginia Beach shows an excellent match, while the calculated amplitudes at the Currituck Beach Lighthouse are about 1/2 ft higher than predicted. This increase is caused by the shoreline approximation made in the grid for the barrier island at Currituck, and by the proximity of the WIFM gage to this shore.

32. Plates 2 and 3 illustrate how the crude approximations of the three inlets in the offshore grid (each inlet is only one cell wide) induce some local amplification of the computed tide. However, the basic hydrodynamic properties of the inlets are preserved in this model because the cross-sectional areas of the inlets match observations (Jarrett 1976). Tidal wave

energy does enter the bays properly, and the marigrams calculated within Pamlico and Albemarle Sounds (Plate 3) agree with the information in the tide tables. While the NOAA tide tables do not list highs and lows for the bays, they note that "In Albemarle and Pamlico Sounds, except near the inlets, the periodic tide has a mean range less than one-half foot" (p. 226, 1962 Tide Tables).

33. After calibration of the offshore model with the March 1962 tide, boundary conditions were developed to simulate the predicted tides for Hurricane Donna. The starting time of this simulation was noon GMT on 11 September 1960, and WIFM computed 33 hr of tides with a 3-min time-step. The boundary refinement process was cycled through again, but no minor parameters were changed in WIFM. Plate 4 shows that the computed amplitudes at Cape Fear fall about 1 ft below predictions. This result comes as a compromise: when boundary amplitudes were increased in the offshore model near Cape Fear to raise the computed peaks, the tide range throughout the model became too large to match predictions at other stations. Plates 5 and 6 compare computations with predictions for other stations along the Outer Banks and illustrate the tides within the bays. As with the March 1962 tide, these plates show agreement at Virginia Beach and Currituck, local increases at the inlets, and the proper tides within the bays.

Nearshore Model

34. The calibration of the nearshore model was accomplished using constituent tide data resulting from harmonic analysis of gage records at 14 stations within the grid coverage. Although no data collection was performed for this study, data from previous collection efforts were available at 10 stations in the vicinity of Oregon Inlet, and these were supplemented by NOAA data at four additional open-coast locations. Because of its predominance, the M_2 (lunar-semidiurnal) constituent was selected as a representative parameter for model calibration. A summary of gage locations with M_2 amplitudes and epochs is presented in Table 1. Gage locations are depicted in Figures 7 and 8.

35. Initial efforts at calibrating the nearshore model were performed using a mean tide from January 1981. First estimates for bathymetry and open boundary adjustments were determined using this simulation period. Grid

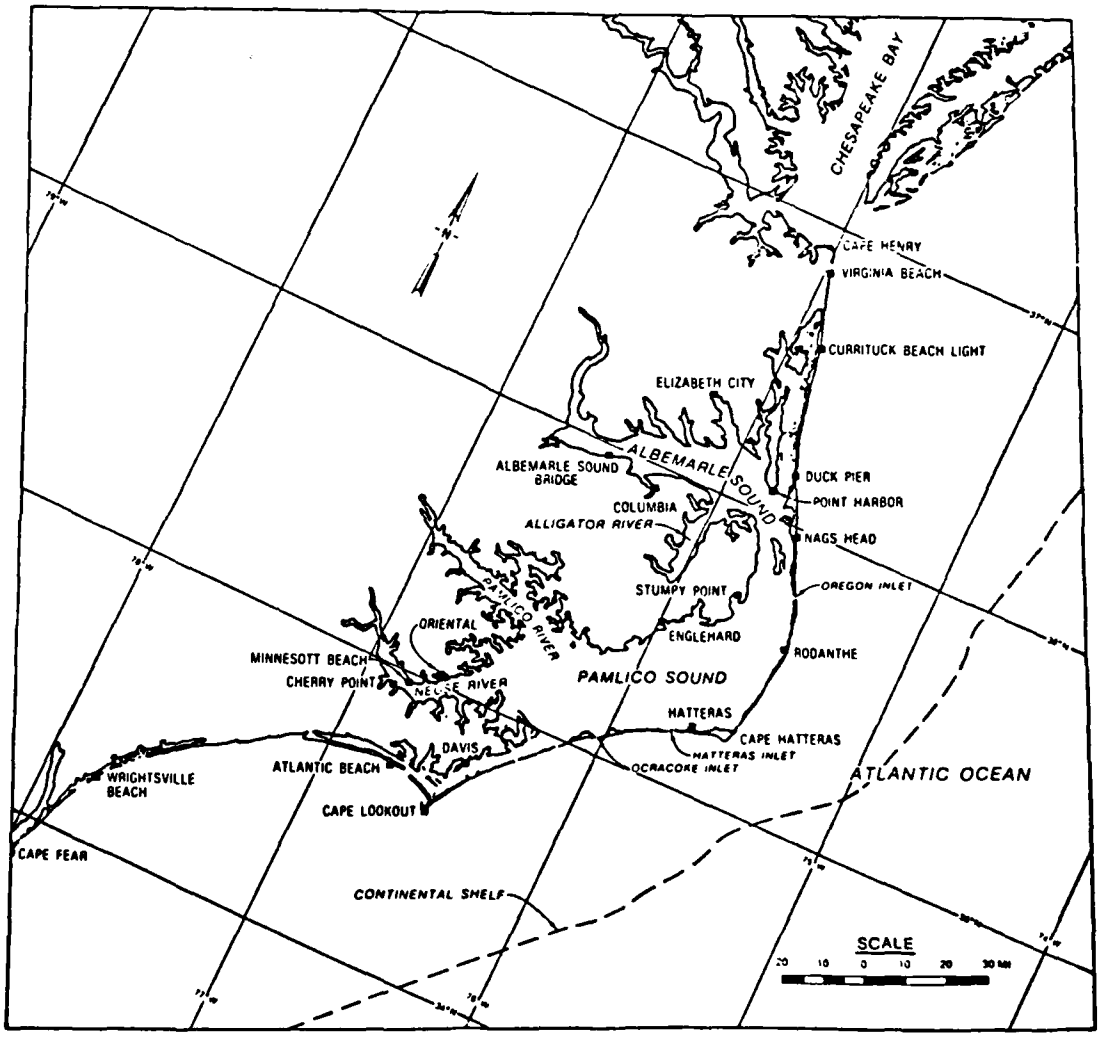

Figure 7. Offshore and nearshore model gage locations

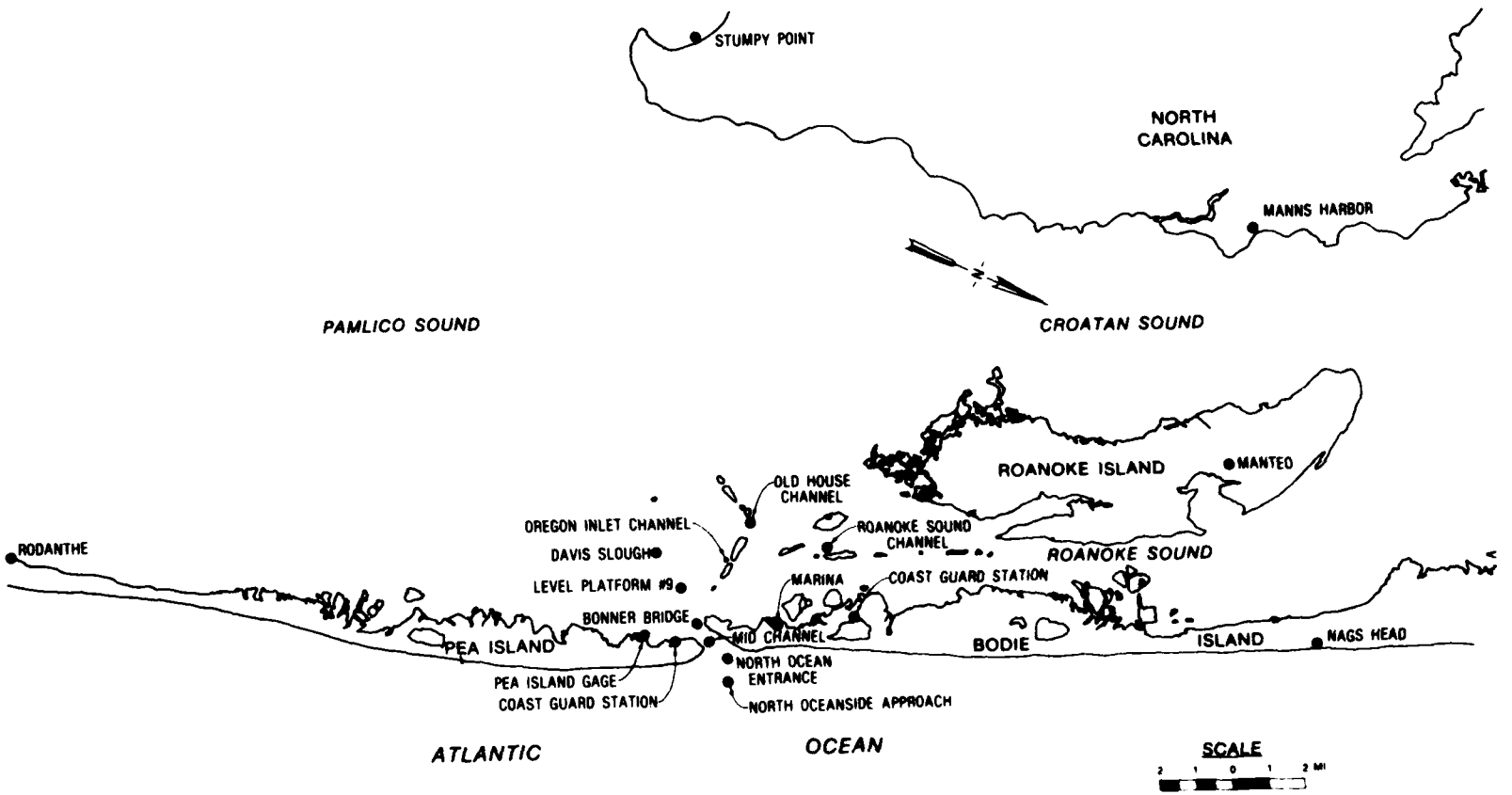

Figure 8. Nearshore and shore process model gage locations

resolution in the Oregon Inlet vicinity was modified to relax stability exigencies, economize simulations, and yet preserve major inlet features. Final adjustments of boundary conditions and friction characteristics were performed using a tidal period of 19-22 May 1975 which is coincident with data from the previous physical model study (Hollyfield, McCoy, and Seabergh 1983) of Oregon Inlet.

36. Marigrams presenting model versus prototype M_2 amplitudes appear in Plates 7-10 starting at 0300 (GMT) 20 May 1975. The model quite accurately reproduces the open-coast tide as observed at all available stations. Model performance at Oregon Inlet is characterized by good agreement at Bonner Bridge and the Pea Island Coast Guard Station. The remaining stations present comparisons at bayside locations in the inlet vicinity. They also show good agreement with amplitude variances less than 0.1 ft and some slight phase shifting attributed to channel and shoal features subscale to grid resolution.

Shore Process Model

37. Unlike the coarser models used in the study, the shore process model presented a unique case for calibration. Open-boundary conditions were not adjustable since they were transferred from simulations on the nearshore model. Because the primary function of this model was to provide hydrodynamics for sediment transport studies, cell depth changes were restricted in order to maintain the same bathymetry for these two modeling efforts. Friction values were adjusted to coincide with representations in the nearshore model. The inclusion of the momentum advection terms and the very fine grid resolution (Δx_{min} = 100 ft) with the resultant small time-step ($\Delta t \leq 15$ sec) required careful adjustments of the eddy viscosity coefficient to achieve simulation stability, and yet produce realistic circulation currents and horizontal eddies evident at the inlet under normal and proposed configurations. Calibration efforts for this model were performed for mean tides produced by nearshore model simulations in the aforementioned May 1975 period. Results are discussed in PART V, and model gage locations are shown in Figure 8.

PART V: NUMERICAL MODEL VERIFICATION

38. After calibration, the ability of the models to simulate the hydrodynamics of storm surges was verified with the two historical storms. Hurricane Donna and the March 1962 northeaster produced some of the highest surges recorded along the Outer Banks, and they had severe effects on Oregon Inlet. These storms were considered rigorous tests for the models of the North Carolina coast.

39. The eye of Hurricane Donna passed just west of Pamlico Sound during the storm's movement north (Figure 9), with the highest winds concentrated over the Sound. During the peak of the storm, 60- to 80-knot winds blew across Pamlico Sound from the south and southwest, causing a large surge to pile up along the bay side of the barrier islands near Oregon Inlet. The elevation difference between the surge in the bay and the level of the Atlantic Ocean created a 10-ft head across the inlet, which caused an enormous flow through the inlet. The surge in the bay also caused extensive flooding at the barrier islands, Roanoke Island, and the nearby mainland.

40. The March 1962 storm derived its force not from high peak winds but from sustained gales over several days. The low pressure system which drove the storm remained along the eastern seaboard for over a week, generating 35- to 50-knot winds from the north and northeast from 6 March to 8 March. These gales caused a surge on the Atlantic side of the Outer Banks near Oregon Inlet and a drawdown on the east side of Pamlico Sound. The head difference at the inlet caused a large flow into the bay through an entire tidal cycle on 7 March, which, together with setup, created flooding in nearby Roanoke Island and the mainland.

41. The storm simulations used the historical tides developed during calibration as initial and boundary conditions for the nearshore and offshore models. The initial conditions for a WIFM storm run were supplied by data sets (dubbed "hotstarts") saved during tidal computations. Hotstarts contain the free-surface elevations and horizontal velocities at every point in a grid, which enables one to start WIFM calculations with this information as a realistic, dynamic initial condition. The same tidal boundary conditions were also used during storm simulations, so that the tide appears throughout each storm hydrograph. Hence, computed hydrographs can be directly compared with historical marigrams.

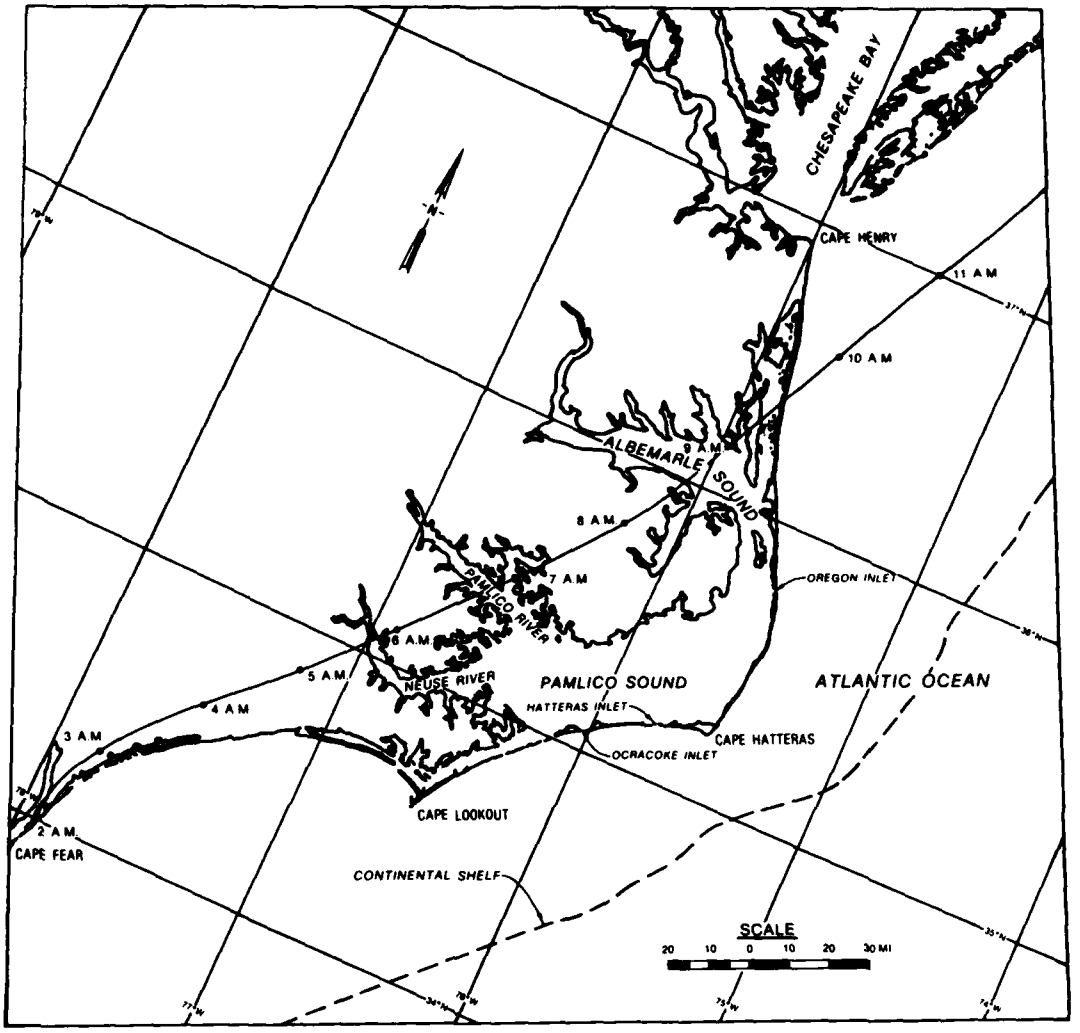

Figure 9. Track of Hurricane Donna

42. With the boundary and initial conditions for a storm simulation specified by tides, the meteorological forces appear in the computations as the terms F_x , F_y , and η_a in Equations 2 and 3. These terms represent the shear (wind stress) and normal (barometric pressure differential) forces applied to the water surface during the storm. WIFM obtains values for the wind and pressure fields from datasets created by other computer codes, such as the SPH Program. Wind velocity and pressure head values for every grid cell are read into WIFM every few time-steps, and then WIFM converts the wind velocity into surface shear stress by Charnock's linear relation (Garrett 1977). The drag coefficient for Charnock's method is:

$$C_D = 0.00075 + 0.000067W \tag{19}$$

where W is the 10-metre wind speed in metres per second. The surface stress is calculated by Taylor's (1916) equation:

$$\tau = \rho\, C_D W^2 \tag{20}$$

where ρ is the air density, assumed constant for this study. The total surface stress then is resolved into components for the F_x and F_y terms in WIFM.

43. Due to the increase in flow velocities through Oregon Inlet during the storms, the computational time-step in WIFM had to be adjusted for the nearshore model. Both Hurricane Donna and the March 1962 northeaster were simulated with a 3-min time-step in the offshore model (the same as for the tide runs). The March 1962 computation begins at midnight GMT on 5 March and goes to noon GMT on 9 March. The Hurricane Donna simulation begins at noon GMT on 11 September 1960 and computes to 9 p.m. GMT on 12 September. For the nearshore model, the time-step was reduced to 50 sec but the same starting and ending times were kept. The March 1962 storm was simulated with a 60-sec time-step from hours 33 to 78 (9 a.m. GMT on 6 March to 6 a.m. GMT on 8 March). The simulation of only 45 hr of this storm greatly reduced computational costs.

44. Two letter reports of SAW (Davidson 1961, Grygiel 1962) contain the prototype storm surge data used in this study. Surge histories for the peak periods (7 March 1962 and 11 and 12 September 1960) for most of the sites in Figure 7 can be found in these reports. No prototype data were available at or near Oregon Inlet, but there are recorded marigrams available from Rodanthe, Nags Head, Stumpy Point, and Point Harbor. These four sites all lie within 25 miles of the inlet, so that agreement between them and calculations can indicate the accuracy of calculations at Oregon Inlet. Tabulated measurements of the tide highs and lows for the months of March 1962 and September 1960 provided independent checks on the accuracy of the surge histories; these two sources agreed completely. The tabulated data also gave an indication as to where a "mean water level" may lie for each prototype gage. An average of the month's highs and lows (excluding the storm period) seldom came close to the datum listed with the tabulations. Differences are mainly attributable

to two factors: datum discrepancies and local superelevation. The datum for all tide gages was based on the National Geodetic Vertical Datum (NGVD), which is not intended to equal the local mean water level. Bench marks used to reference the gages were not tied together by a single survey and hence may not lie in the same datum plane. In addition, local mean water levels, particularly in the sounds, should be above NGVD due to a general rise in sea level, since NGVD was established in 1929, and also due to local superelevation of the bays caused by freshwater inflow into the sounds. Freshwater inflow, and its local effects, was not considered in this modeling effort. In order to account for the above factors, datum adjustments were estimated as differences between the NGVD values and the monthly high/low averages. Table 3 summarizes the sites used in the verification of the two largest models, gages within the grids, and the datum adjustments estimated from the high/low averages. Tabulated data were not available for all of the prototype marigrams, and it must be noted that the March 1962 surge at Nags Head is estimated since the tide gage there was lost during the storm. Grygiel states that the estimate "is based on reliable evidence and should be less than 1 ft in error..." (p. 3).

Offshore Model

45. Plates 11-13 compare the computed storm surge of the March 1962 storm with the prototype data for the 11 sites listed in Table 3. Where datum adjustments are available, they have been subtracted from the prototype records in these plates. While the comparisons agree well, some differences occur due to the shoreline approximations used in the offshore model and due to the presence of wave setup in the prototype data. Computations for Oriental, Rodanthe, Point Harbor, and Columbia exhibit excellent fits to the field records. Minnesott Beach and Cherry Point have computed peak surges that are slightly high due the shoreline approximations made for the Neuse River. The cell sizes in the offshore grid near Stumpy Point Bay also do not allow this small bay to be well represented; therefore the computations and prototype for this site differ. The presence of wind-induced wave setup in the prototype records of Wrightsville Beach, Hatteras, and Englehard can explain why these computations fall below field measurements. The divergence in elevations after hour 60 (the peak of the storm) at Hatteras shows how wave

setup can act to keep the water elevation raised in the prototype data. Since WIFM cannot model this effect, the computed water level at Hatteras begins to fall after the peak of the storm. Prototype data for Nags Head are not available (the tide gage disappeared during the storm) but estimates of the surge have been made by SAW from other information. This estimate appears with computations for Nags Head in Plate 13 with no datum shift estimates removed. The computed and estimated prototype records agree in form, and the roughly 2-ft elevation difference can be accounted for by datum shifts, wave setup, and errors in Grygiel's estimate of the record at Nags Head.

46. Plates 14-16 compare the computed storm surge of Hurricane Donna with prototype data for the offshore model. Ten sites are shown, and the datum shift estimates of Table 3 have been removed from the prototype records. Atlantic Beach and Nags Head, both sites on the open ocean, show the best agreement. For sites in the bay, the effects of wave setup and shoreline approximations play an important role in the agreement between computations and field records. An added factor is the speed at which Hurricane Donna moved across the North Carolina coast. The eye of the storm traversed the distance from Cape Fear to Cape Henry in about 8 hr, causing rapid changes in wind speed and direction for sites in Pamlico and Albemarle Sounds. The rapid movement of the storm, along with the shoreline simplifications of the Neuse and Pasquotank Rivers, caused some phase difference between computations and the prototype records at Cherry Point, Minnesott Beach, and Elizabeth City. Columbia, a site up a narrow recess of Albemarle Sound, also has a phase shift. The prototype records for Hatteras and Nags Head show the effect of wave setup at the peak of Hurricane Donna (hour 22) but these records agree well with computations. Despite the shoreline approximations for Stumpy Point Bay in the offshore grid, the results match well at this site. The computations at Englehard overpredict the surge, but the results agree at hour 22, the time of maximum flow at Oregon Inlet.

47. Plates 11-16 illustrate that the offshore model can simulate both historical northeasters and hurricanes to a reasonable accuracy, with a minimal number of grid cells. Considering the accuracy with which the datum shift adjustments in Table 3 are estimated, the comparisons of computations with field data for the offshore model are quite good.

Nearshore Model

48. Plates 17-19 illustrate the excellent agreement between computations for the March 1962 storm in the nearshore model and the prototype data. Once again, the datum shifts listed in Table 3 are included in the field records. The computations match all 11 sites quite closely. Davis, a gage not represented in the offshore model due to cell sizes, has no datum shift included in the prototype record. It can be expected that any shift would be of the same order as nearby sites such as Wrightsville Beach. The computations of Stumpy Point agree with the prototype because Stumpy Point Bay can be reasonably approximated by the small cells in the nearshore grid.

49. Plate 20 shows the flow patterns through Oregon Inlet for the peak of the March 1962 northeaster (hour 60, or noon GMT on 7 March) in the nearshore model. Plates 21 and 22 show marigrams for eight locations (Figure 8) in Oregon Inlet, while Plates 23-26 show the corresponding velocity records. The velocities at the inlet tell what happened during the storm. The normal ebb-flood cycle of tidal flow through the inlet was halted by the surge seaward of the inlet on 7 March. For a 22-hr period between 8 a.m. GMT on 7 March (hour 56 in the calculations) and 6:00 a.m. GMT on 8 March (hour 78), the flow was entirely into Pamlico Sound. According to computations, the peak flow velocity was about 9 fps, or about twice the normal tidal velocity. At the peak of the storm about 630,000 cfs of water flowed into Pamlico Sound. Figure 10 shows the computed surge contours at noon GMT on 7 March (hour 60) for the area of Oregon Inlet, Roanoke Island, and the nearby mainland. The head difference driving the flow is about 5 to 6 ft.

50. Comparison of the nearshore model calculations of Hurricane Donna with the prototype data can be found in Plates 27-29. Most of the phase differences found in the offshore model computations do not appear in the nearshore model due to the increased resolution in this grid. As with the offshore model, the effects of wave setup appear in the plots for Hatteras and Nags Head. Considering the severity of Hurricane Donna, and the resolution of the grid for the nearshore model, Plates 27-29 show that this model can simulate a historical hurricane.

51. Plate 30 illustrates the severity of the ebb flow through Oregon Inlet at the peak of Hurricane Donna (10:00 a.m. GMT, 12 September, or hour 22 of the computations). Plates 31 and 32 show the surge histories of the

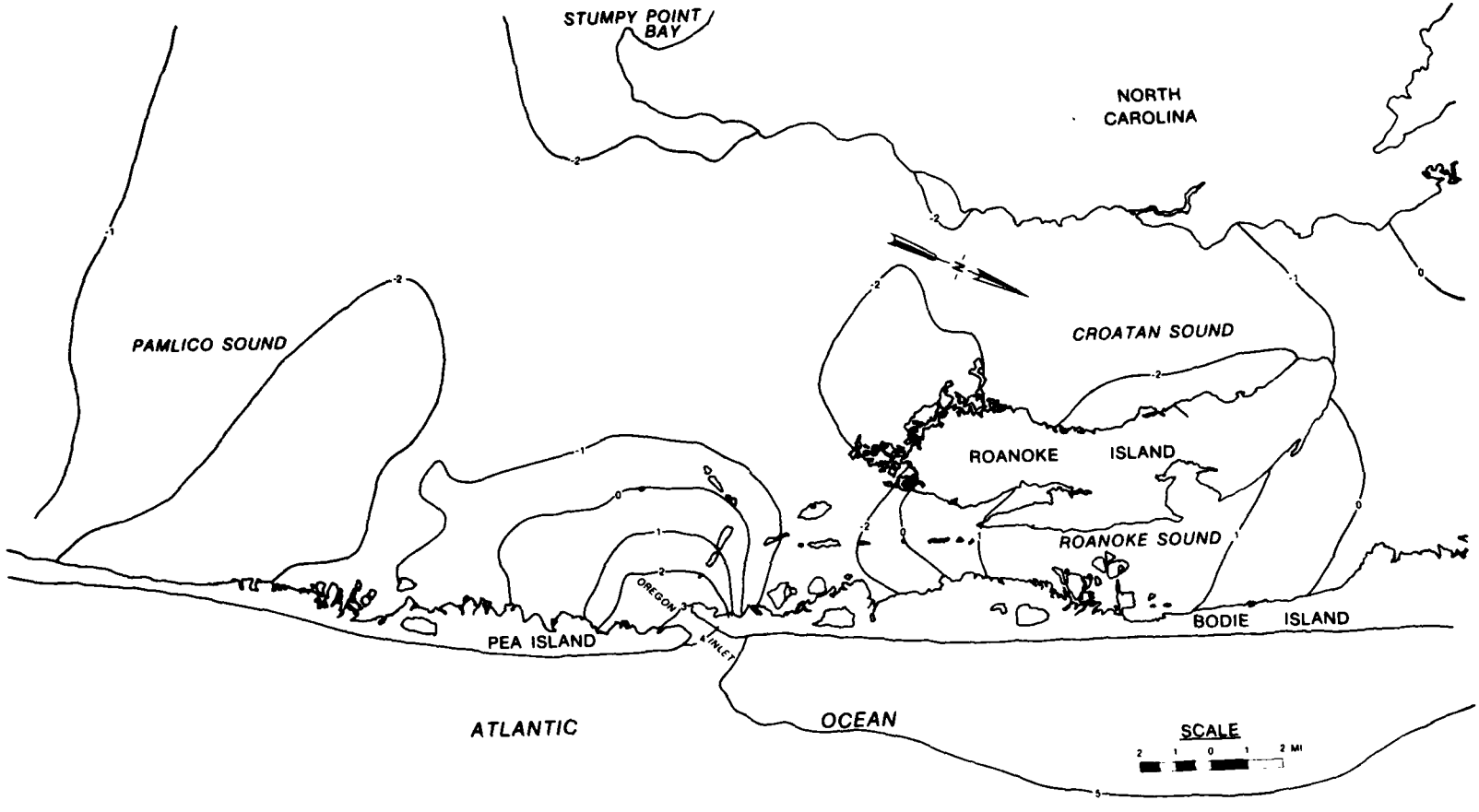

Figure 10. Computed surge contours during March 1962 northeaster (1200 GMT)

locations in Figure 9, while Plates 33-36 show the corresponding velocities. Once again, the velocity records describe how the storm affected the inlet. The buildup of surge in Pamlico Sound on the bayward side of the barrier island caused by the high winds from the southwest drove a violent outflow through the inlet between 7:00 a.m. and 4:00 p.m. GMT on 12 September. Figure 11 shows the computed contours for the area around Oregon Inlet at the peak of Hurricane Donna, and this figure illustrates the 10-ft head difference across the inlet which caused the ebb flow. Peak velocities of 12 to 14 fps occurred in the inlet, with 18 fps calculated at the north oceanside approach. The nearshore model indicates that about 1 million cfs of water flowed out through Oregon Inlet at the peak of Hurricane Donna.

Shore Process Model

52. Prototype storm data were unavailable for the relatively small region encompassed by the shore process model. Since it was employed principally for tidal simulations, results were compared for the M_2 constituent tide. Plate 37 shows marigrams for a 16-hr period starting at 1900 (GMT) 20 May 1975. The model produced a good match of elevations with prototype data at locations just seaward, within, and west of the inlet, with variances of less than 0.1 ft, and with slight phase shifts on the bayside due to features subscale to this grid, and to bayside boundary conditions affected by similar scale restrictions in the driving nearshore model. Velocity records (Plate 38) in the inlet and Davis Slough were reproduced with proper phasing of the peak flood and ebb flows and were generally within 0.5 fps of observed data indicating proper tidal exchange. Tidal circulation patterns matched quite well in direction and magnitudes with reported data of the same period as presented by Hollyfield, McCoy, and Seabergh (1983).

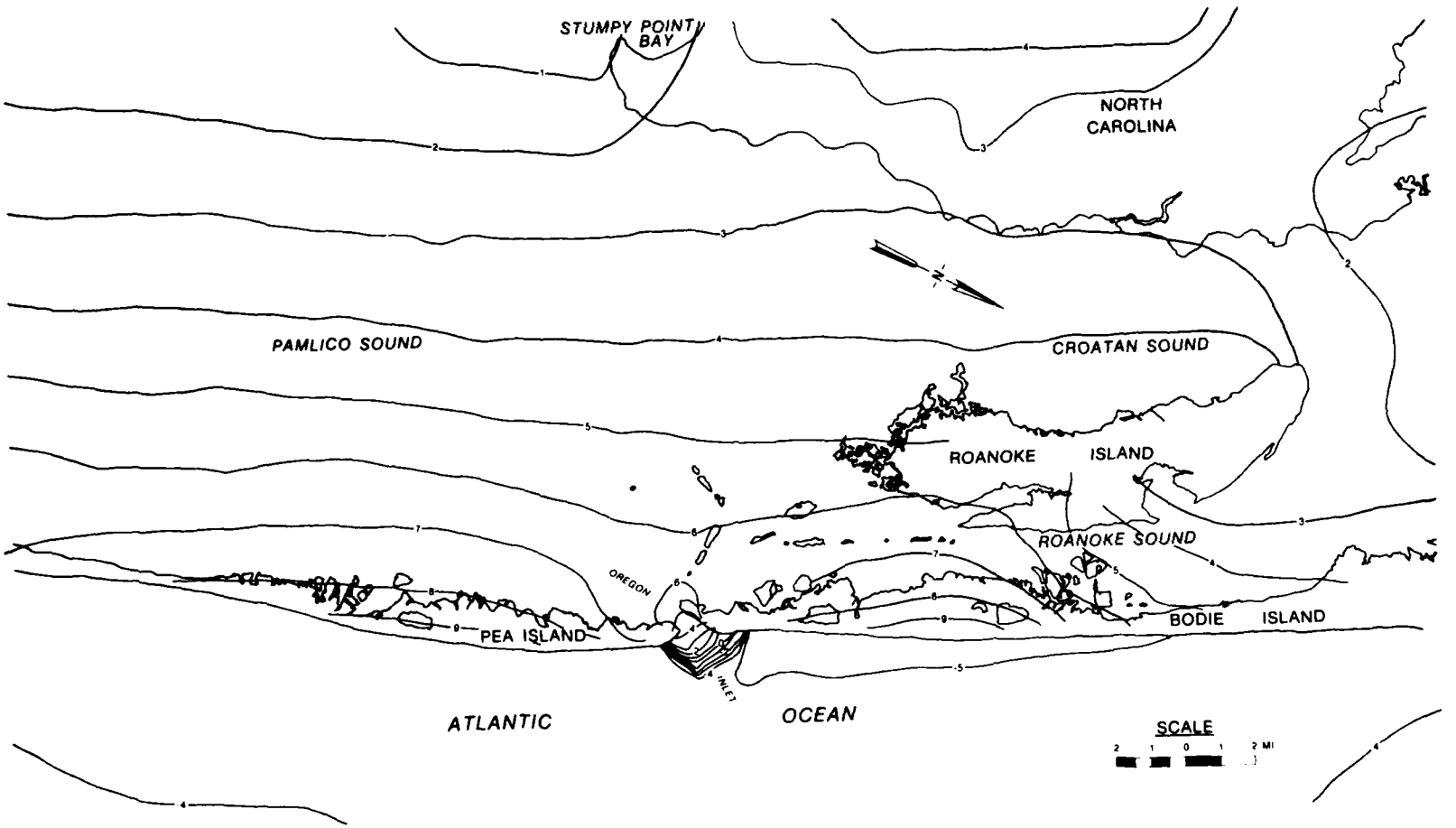

Figure 11. Computed surge contours at peak of Hurricane Donna (1000 GMT, 12 Sept 1960)

PART VI: CONTROL STRUCTURES IMPACT

53. The Oregon Inlet control structures would consist of two parallel jetties extending seaward from the ends of Bodie and Pea Islands. Jetty spacings of 2,500, 3,500, and 5,000 ft (Figure 12) were evaluated in both the nearshore and shore processes model. In the nearshore model, both normal astronomical tides and an extreme meteorological event represented by Hurricane Donna (September 1960) were simulated. The shore processes model was used to develop much finer flow detail around Oregon Inlet for eventual input to the sediment transport simulations. In order to determine the maximum influence changes at Oregon Inlet could have on bay-side storm tides, tests were run with Oregon Inlet closed. These numerical simulations provided good estimates of how the proposed structures at Oregon Inlet would affect surrounding areas during both normal and storm generated tides.

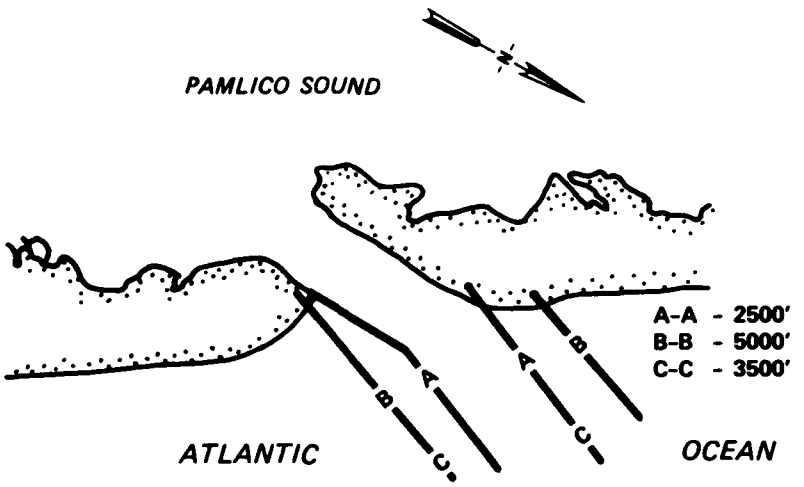

Figure 12. Proposed alternate jetty configurations for Oregon Inlet

Preliminary Tests

54. The eastern edges of the offshore and nearshore grids (Figure 2) were originally placed far enough from Oregon Inlet so that any changes to the inlet would not disturb the boundary values of the models. This assumption was checked with the offshore model by closing the inlet (the severest change) and then simulating Hurricane Donna (the severest surges). Results of this run were then compared with a similar run with the inlet open. The marigrams

at the nearshore grid boundary east of Oregon Inlet agreed completely, indicating that this nearshore boundary was indeed far enough from the inlet.

55. Hurricane Donna also was simulated in the nearshore grid with the inlet closed. This test served to answer the question "What is the maximum radius of influence at which Oregon Inlet can affect a peak storm surge?" A comparison of nearshore computations with existing conditions with the closed inlet case illustrates the effects of closure. Plates 39 and 40 show the two cases for the sites in Figure 8. At the closed inlet the surge differences are, of course, large; but they diminish rapidly away from the opening. The difference is only 1 ft at the Roanoke Sound channel gage, a site 3 miles from the center of the inlet. Figure 13 shows the peak surge contours around Oregon Inlet for the closed inlet and for natural conditions. The surge differences become nil near Rodanthe south of the inlet (13 miles), Manteo north of inlet (12 miles), and 10 miles west of the inlet. So, the closed-inlet computation with the nearshore model indicates that the maximum radius of influence of the inlet is about 10 miles but changes of a foot or more only will occur within a radius of 4 miles from the inlet's center. For example, water elevations at the Pea Island Coast Guard Station and the Oregon Inlet Marina increased by 2.4 ft and 1.4 ft, respectively, under closed inlet conditions. Any nonradical changes to the inlet's hydrodynamics (such as jetties) will exert a minimal influence on peak surge levels, as the jetty computations of this study will show.

Storm Surge Tests

56. All of the storm surge simulations with the jetties were computed in the nearshore model. Hurricane Donna was simulated with the 2,500- and 5,000-ft structures. The 5,000-ft structure changed the surge levels and peak velocities very little from the nearshore simulation with existing conditions at the inlet, while the 2,500-ft structure slightly raised the surges and velocities at the peak of Hurricane Donna.

57. Plate 41 shows the flow patterns through Oregon Inlet at the peak (hour 22) of the high velocities that occurs nearest the north jetty, due to the presence of shallow water near the south structure. Plates 42 and 43 compare marigrams of the 2,500-ft structure to existing conditions for the sites of Figure 8 while Plates 44-47 compare the corresponding velocity records. The

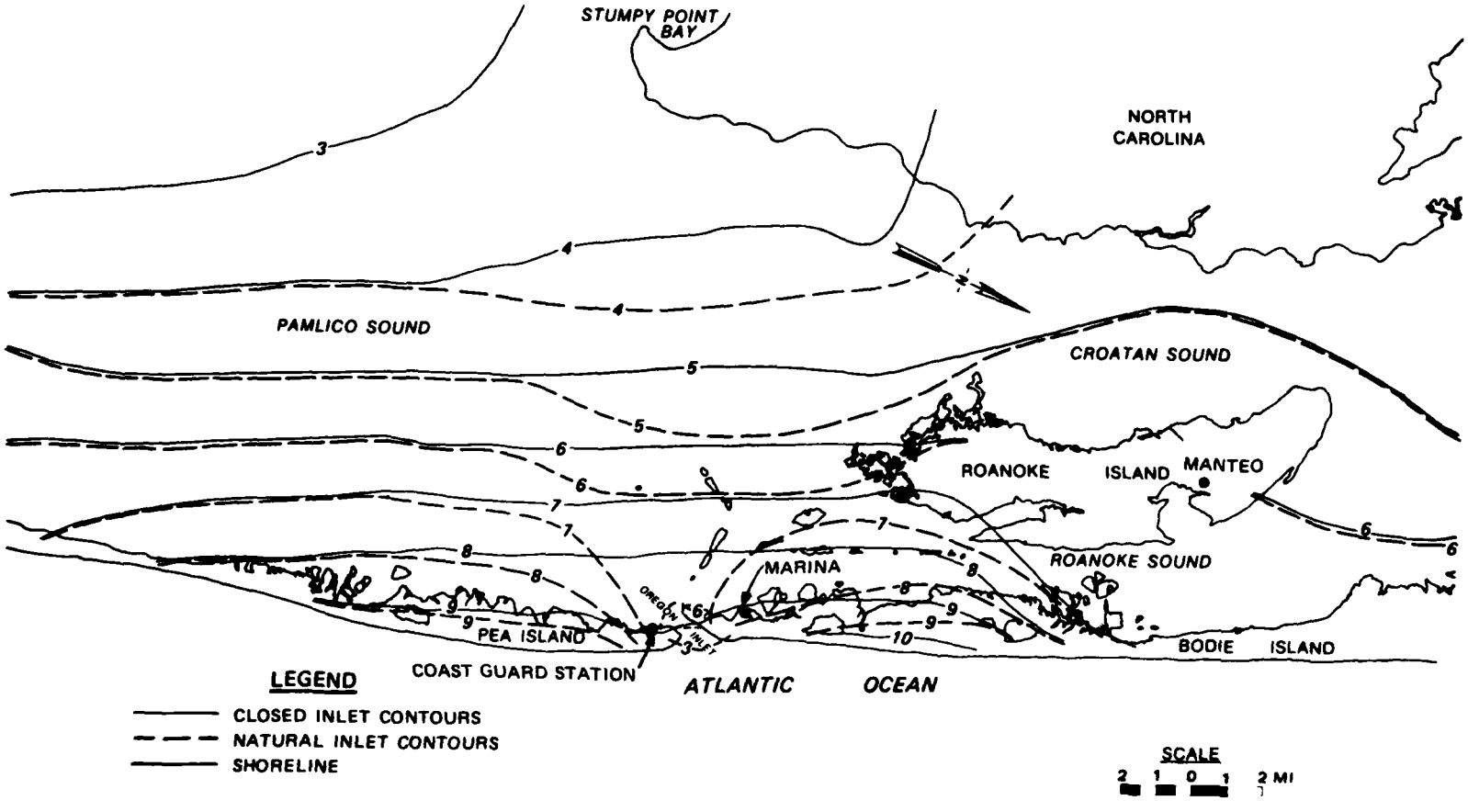

Figure 13. Comparison of computed peak surge contours for Hurricane Donna (natural inlet versus total closure)

largest change in the peak elevations occurs at the North Ocean Entrance, a site at the ends of the jetties. The constricting effects of the structure raise the peak surge about 2 ft in the middle of the inlet, while little difference is noted on the bay side of the opening. Velocities on the bay side are actually reduced by the jetties (i.e. Bonner Bridge) until the flood flow reaches the middle of the inlet. Figure 14 shows a comparison of elevation contours around the inlet for the peak of the storm for this structural alternative.

58. Plate 48 shows the flow patterns at the inlet for the 5,000-ft structure. The shoal in the channel acts to move the fastest velocities near the two jetties. Plates 49 and 50 compare water elevations for this case with existing conditions, while Plates 51-54 compare velocities for the storm. The influence of the jetties on either the surge or the velocities is negligible, even in the channel. Figure 15 shows a comparison of computed surges at the peak of the storm, and clearly indicates that the effects of the 5,000-ft spacing jetties are limited to small variances within the inlet, and no impact on Pamlico Sound, as represented by the nearshore model.

59. A tabular comparison of computed peak surge results for Hurricane Donna at selected Outer Bank locations with the various inlet configurations is presented in Table 4. Results in this comparison also indicate no impact of the structures on peak surge levels within the Albemare/Pamlico Sound systems as recorded along the Outer Banks.

Tidal Tests

60. Tidal simulations with the jetties were conducted with the nearshore and shore process models. A mean tide was simulated with the 2,500-, 3,500-, and 5,000-ft jetties. Structure effects at the inlet vicinity were evaluated with the shore process model, and effects at more distant locations along the Outer Banks were determined with the nearshore model. The jetty configurations were simulated with natural bathymetry features including the offshore shoal and no specific dredging. In general, structure effects were limited to the immediate inlet vicinity with no changes observed at Outer Bank locations.

61. Plates 55-59 present comparisons of natural conditions versus the 2,500-ft jetty alternative for both nearshore and shore process models. Local

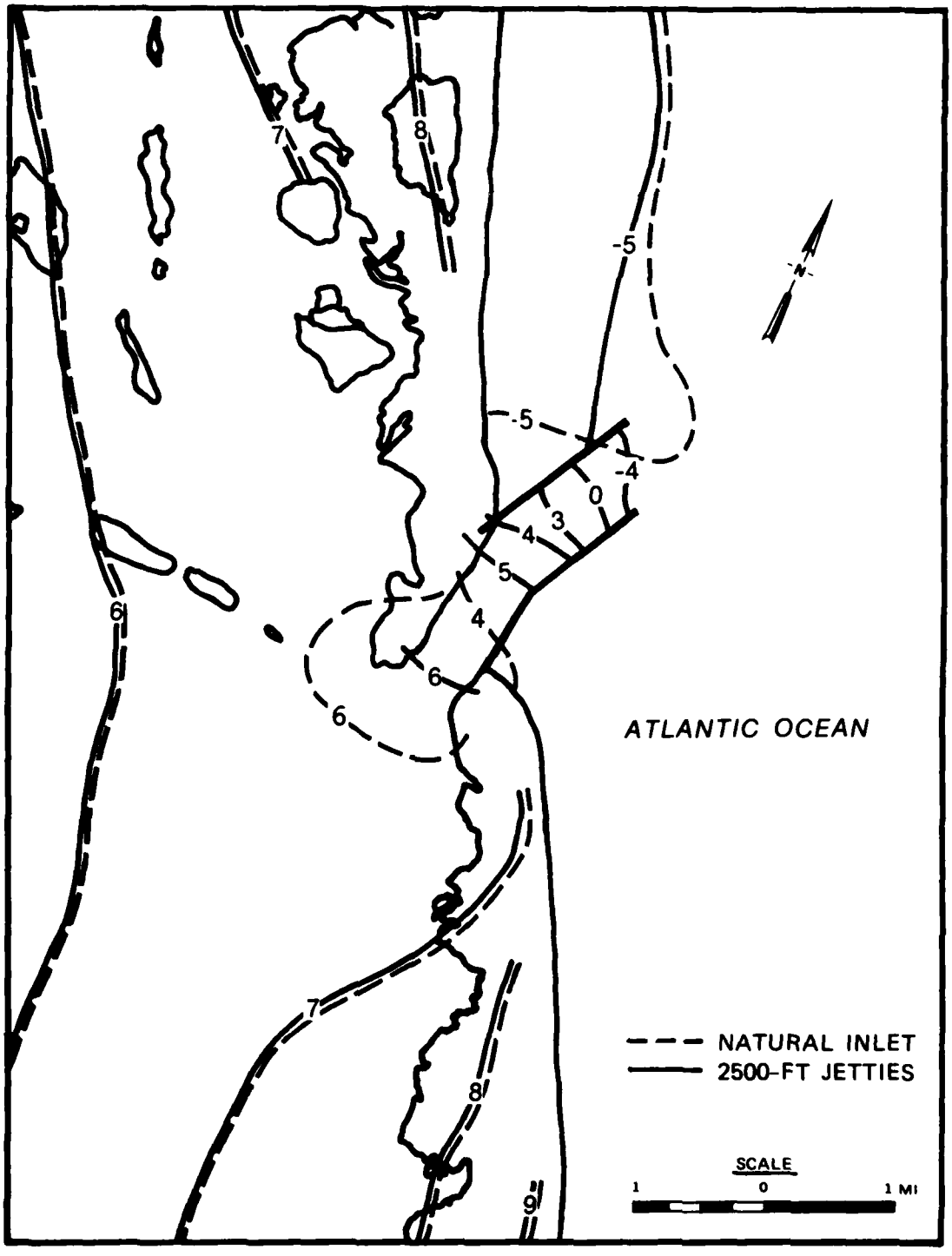

Figure 14. Comparison of computed surge contours at peak of Hurricane Donna (natural inlet versus 2,500-ft jetty spacing)

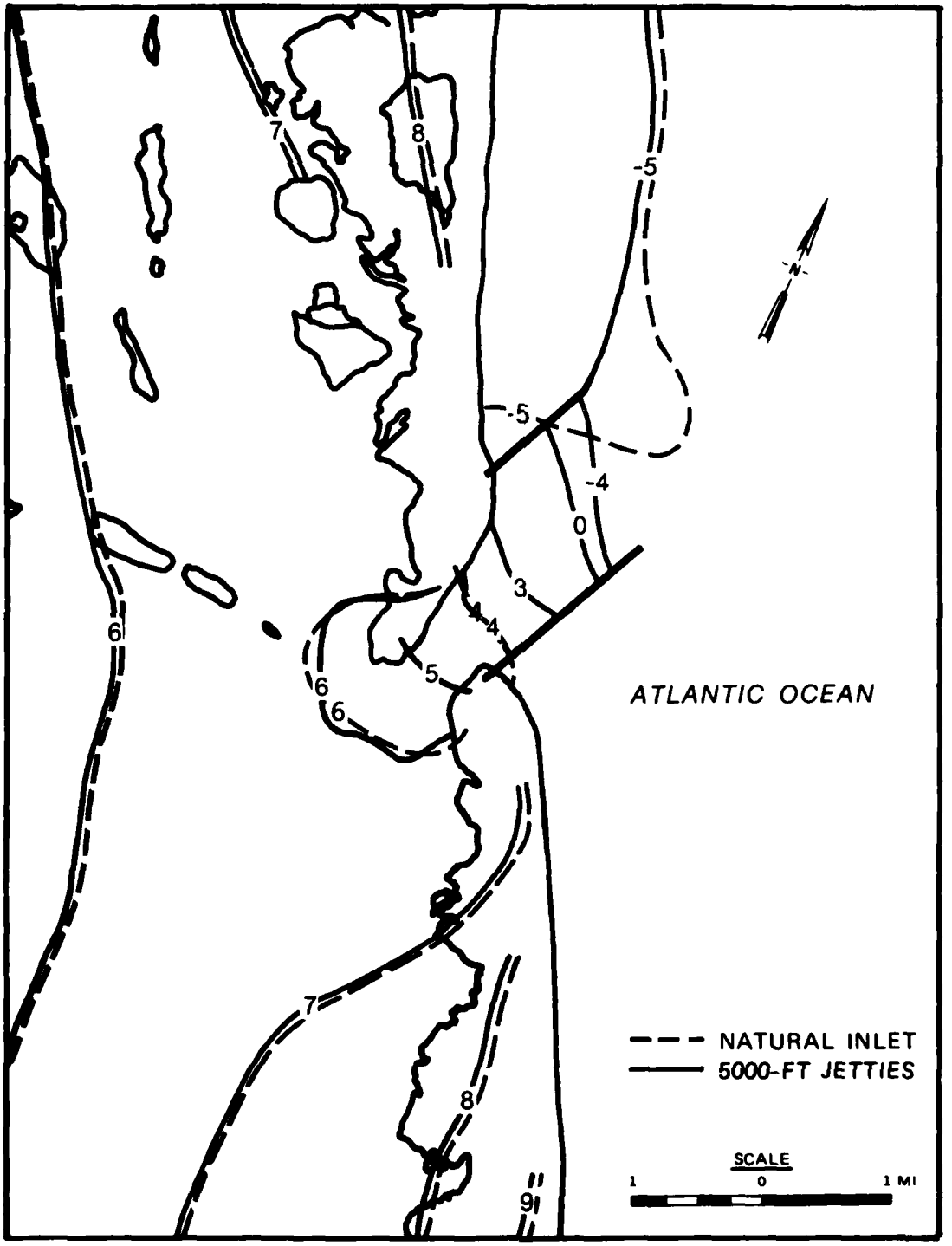

Figure 15. Comparison of computed surge contours at peak of Hurricane Donna (natural inlet versus 5,000-ft jetty spacing)

variations of velocity and elevation were apparent in the inlet and within the jetties. The Pea Island Coast Guard Station experienced range reductions of 0.30 ft while the Davis Slough location experienced a lesser reduction of 0.10 ft. At stations along the Outer Banks such as Bodie Island Coast Guard Station, Nags Head or Rodanthe, amplitude variations were negligible or non-existent. Stations located farther within the Sound showed no variation.

62. Similar comparisons of natural conditions versus the 3,500-ft jetty are shown in Plates 60-64, while Plates 65-69 show the 5,000-ft jetty results. As anticipated, these larger jetty spacings produced smaller variances at the inlet proper, and no discernible changes in range along the outer banks or within the Sound. Plates 70-75 show jetty alignments and flow patterns in the nearshore model at periods of peak flow and ebb tidal flows.

PART VII: SHORE PROCESS MODEL REQUIREMENTS

63. Concurrent with the numerical model efforts described in this report was a study of sediment transport under current and wave-induced current interactions at Oregon Inlet. The application of the WIFM code to the common computational grid used by both studies has been referred to as the shore process model in this report. WIFM was employed to provide elevation and velocity data at 10-min intervals for each cell in the computational grid to the sediment transport models. Such data were required for the following; a mean, spring, and neap tide, a mean tide with 2,500, 3,500-, and 5,000-ft jetty spacings, and south jetty only; and for the March 1962 northeaster.

64. An M_2 constituent tide was again chosen as a boundary condition. The M_2 amplitude was adjusted to represent the full tide values for mean, spring, and neap conditions as reported at Nags Head, North Carolina, by NOAA Tide Tables. Amplitudes of 1.6 ft, 1.9 ft, and 1.3 ft were chosen for the mean, spring, and neap tides, respectively. Appropriate boundary conditions were developed for the nearshore model to produce the proper tides and to provide connecting boundary conditions for the shore process model. Marigrams at typical stations from shore process model simulations under mean tide conditions are presented in Plates 76 and 77. Flow patterns at flood, slack after flood, and ebb portions of the mean tidal cycle at the inlet are shown in Plates 78-80. They indicate the model's ability to realistically produce the rather complicated horizontal flow patterns through the inlet as affected by channelization and shoaling. Similar results for spring tides are presented in Plates 81-85 while neap tide conditions appear in Plates 86-90.

65. The sediment transport studies also required hydrodynamic information for the various structural configurations at the inlet. These alternatives were simulated using the mean tide condition. Simulations with the 2,500-, 3,500-, and 5,000-ft jetty spacings with the nearshore model were used to provide driving boundaries for equivalent cases on the shore process model. Marigrams showing typical shore process model results for these cases are presented in the plates describing structural effects. Flow patterns with the jetties in place for various portions of the tidal cycle appear in Plates 91-99. Flow redistribution around and through the jetties is clearly depicted as well as the local acceleration near the offshore shoal.

66. A fourth structural alternative was simulated for the sediment

transport studies. This was a single structure consisting of the south jetty only from the 5,000-ft spacing alignment. A comparison of the 5,000-ft jetty effects and existing conditions (Plates 100 and 101) demonstrated that the driving boundary conditions from the nearshore model were unaffected by the jetties; therefore a nonstructural mean tide boundary condition from the nearshore model was applied to the shore process model. Marigrams from this simulation appear in Plates 102-104 with the flow patterns presented in Plates 105-107.

67. For sediment transport studies under severe conditions, 24 hr of the March 1962 northeaster were simulated starting at 0600 (GMT) on 7 March. Marigrams at typical stations appear in Plates 108-110 with flow patterns near the peak of the storm at noon shown in Plate 111. The extreme flood flows at the inlet are quite apparent. As indicated in Plate 110, flow through the inlet was unidirectional into the bay for the entire simulation period as observed during the actual storm.

PART VIII: SUMMARY AND CONCLUSIONS

68. Numerical hydrodynamic models were developed and tested for the purposes of evaluating the influence of proposed structures under storm conditions and providing elevation and velocity data for concurrent numerical sediment transport studies at Oregon Inlet, North Carolina. Data collected for previous physical model studies were supplemented by additional data from NOAA and unpublished SAW letter reports for use in calibrating and verifying the models under existing tidal conditions and for two severe storms of record--the March 1962 northeaster and Hurricane Donna (1960). Three models with progressively finer resolution (offshore, nearshore, and shore process) were successfully calibrated (relative to their respective degree of resolution) to replicate an astronomical tidal event. Using a tuned hurricane windfield model for Donna and windfields developed by the Wave Information Study at WES for the March 1962 storm as forcing parameters, the models were able to duplicate observed marigrams throughout the model area. Observed bay-ocean head differentials also were modeled correctly, particularly the 20-hr plus flood event through Oregon Inlet during the peak of the March 1962 storm.

69. Two structural alternatives (involving parallel jetties with 2,500- and 5,000-ft-wide spacings) were studied under tidal and storm conditions. Structural effects were determined to be limited to the inlet under tidal conditions and to the immediate inlet vicinity under circumstances approximating Hurricane Donna. The maximum possible influence exerted by any changes at the inlet was determined by simulations with the inlet completely closed (this was not actually a proposed improvement plan) under Hurricane Donna conditions. For this case, no change was noted beyond a 12-mile radial distance from the inlet. During Hurricane Donna, peak surge levels at the Pea Island Coast Guard Station and the Oregon Inlet Marina were increased by 2.4 ft and 1.4 ft, respectively, with total closure of Oregon Inlet. These stations are in the immediate inlet vicinity (within a 1.2-mile radius). For the 2,500- and 5,000-ft spacings, peak surge level increases for the nearby stations mentioned above were even smaller, with little or no differences noted at farther distances from the inlet.

70. Finally, simulations at very fine grid resolutions were made to provide hydrodynamic data for the sediment transport studies covering the normal range of tides with no jetties, for four structural alternatives with a mean tide, and for the historical March 1962 northeaster with no jetties.

REFERENCES

Butler, H. Lee. "WIRM-WES Implicit Flooding Model: Theory and Program Documentation" (in preparation), U. S. Army Engineer Waterways Experiment Station, CE, Vicksburg, Miss.

Corson, W. D., Resio, D. T., and Vincent, C. L. "Wave Information Studies of U. S. Coastlines; Surface Pressure Field Reconstruction for Wave Hindcasting Purposes," Report 1 (in preparation), U. S. Army Engineer Waterways Experiment Station, CE, Vicksburg, Miss.

Davidson, R. P. 1961. "Report on the Tropical Hurricane of September 1960 (Donna)," U. S. Army Engineer District, Wilmington, Wilmington, Del.

Garrett, J. R. 1977 (Jul). "Review of Drag Coefficients over Oceans and Continents," Monthly Weather Review.

Grygiel, J. S. 1962. "North Carolina Coastal Areas, Storm of 6-8 March 1962 (Ash Wednesday Storm); Final Post Flood Report," U. S. Army Engineer District, Wilmington, Wilmington, Del.

Graham, H. E., and Nunn, D. E. 1959. "Meteorological Considerations Pertinent to Standard Project Hurricane, Atlantic and Gulf Coasts of the United States," National Hurricane Research Project, NWS Report No. 33.

Hollyfield, N. W., McCoy, J. W., and Seabergh, W. C. 1983 (Jun). "Functional Design of the Oregon Inlet Control Structures; Hydraulic Model Investigation," (Technical Report HL-83-10), U. S. Army Engineer Waterways Experiment Station, CE, Vicksburg, Miss.

Houston, J. R. "Sediment Transport Study of Oregon Inlet" (in preparation), U. S. Army Engineer Waterways Experiment Station, CE, Vicksburg, Miss.

Jarrett, J. T. 1976. "Tidal Prism - Inlet Area Relationships," U. S. Army Corps of Engineers.

Leendertse, J. J. 1970. "A Water-Quality Simulation Model for Well-Mixed Estuaries and Coastal Seas; Principles of Computation," RM-6230-rc, Vol 1, Rand Corporation.

Reid, R. O., and Bodine, B. R. 1968 (Feb). "Numerical Model for Storm Surges in Galveston Bay," Journal, Waterways and Harbors Division, American Society of Civil Engineers, Vol 94, No. WW1, Proceedings Paper 5805, pp 33-57.

Resio, D. T., Vincent, C. L., and Corson, W. D. 1982 (May). "Wave Information Studies of U. S. Coastlines; Objective Specification of Atlantic Ocean Wind Data Fields from Historical Data," WIS Report 4, U. S. Army Engineer Waterways Experiment Station, CE, Vicksburg, Miss.

Schwerdt, R. W., Ho, F. P., and Watkins, R. R. 1979. "Meteorological Criteria for Standard Project Hurricane and Probable Maximum Hurricane Wind Fields, Gulf and East Coasts of the United States," National Weather Serivce, NOAA.

Taylor, G. I. 1916. "Skin Friction of the Wind on the Earth's Surface," Proceedings of the Royal Society of London, A92, pp 196-199.

U. S. Coast and Geodetic Survey, 1962. "Tide Tables - 1962," U. S. Department of Commerce, Washington, D. C.

_____. 1972. "Revised Standard Project Hurricane Criteria for the Atlantic and Gulf Coasts of the United States," Hydrometeorological Branch, National Weather Service, NOAA.

Vreugdenhil, C. B. 1973 (Nov). "Secondary-Flow Computations," Publication No. 144, Delft Hydraulics Laboratory, The Netherlands.

Weare, J. T. 1976 (May). "Instability in Tidal Flow Computational Schemes," Journal, Hydraulics Division, American Society of Civil Engineers, Vol 102, pp 569-580.

Table 1

Summary of Prototype Tide Data from Harmonic Analysis

Gage Name	N. Latitude	W. Latitude	No. of Series	Series Length Days	M_2 Amplitude ft	M_2 Epoch deg
Atlantic Beach	34°41.6'	76°42.7'	1	29	1.78	197.81
Cape Hatteras (Fishing Pier)	35°13.4'	75°38.1'	1	29	1.44	204.20
Nags Head (Jennettes Pier)*	35°54.6'	75°35.5'	1	29	1.48	203.28
Duck Pier (Oceanside)	36°10.9'	75°45.0'	1	365	1.58	207.21
Virginia Beach	36°50.6'	75°58.3'	1	366	1.59	211.47
Bonner Bridge*	35°46.4'	75°32.3'	4	29	0.89	214.50
Pea Island Coast Guard Station*	35°46.1'	75°31.6'	4	29	0.78	216.39
Pea Island*	35°45.4'	75°31.6'	2	29	0.58	219.93
Level Platform #9*	35°45.8'	75°33.0'	4	29	0.53	219.50
Davis Slough*	35°44.9'	75°33.2'	3	29	0.45	229.76
Old House Channel*	35°46.5'	75°34.9'	4	29	0.31	241.49
Roanoke Sound Channel*	35°47.9'	75°35.0'	3	29	0.18	263.31
Oregon Inlet Channel*	35°46.4'	75°33.5'	4	29	0.57	233.40
Oregon Inlet Marina*	35°47.8'	75°33.0'	5	29	0.23	246.46

* Indicates data gathered for physical model studies at WES.

Table 2

Summary of SPH Parameters for Hurricane Donna

Date	Time, GMT	Storm Position, deg Latitude	Storm Position, deg Longitude	Maximum Wind, knots	Inflow Angle deg	Azimuth Angle deg	Radius to Maximum Winds, n.m.
11 September 1960	1200	29.8°	81.0°	91	15	23	32
11 September 1960	1500	30.5°	80.5°	89	15	25	32
11 September 1960	1800	31.2°	80.1°	87	20	3	32
11 September 1960	2100	32.1°	79.2°	85	20	6	33
12 September 1960	0000	33.1°	78.3°	83	15	-14	33
12 September 1960	0300	34.3°	77.8°	83	10	-44	30
12 September 1960	0600	35.1°	76.9°	83	10	-22	30
12 September 1960	0900	36.1°	75.9°	83	15	-12	32
12 September 1960	1200	37.4°	75.2°	83	15	-16	34
12 September 1960	1500	38.8°	74.3°	80	20	-16	41
12 September 1960	1800	40.2°	73.4°	77	20	-16	48
12 September 1960	2100	41.6°	71.9°	77	20	-16	48
13 September 1960	0000	43.0°	71.0°	77	20	-16	48

Central Pressure Deficit = 1.48 in Hg.

Table 3

Summary of Prototype Storm Surge Data and WIFM Gage Placement

Gage Location	Prototype Data for March 1962?	Datum Shift Estimate for March 1962 ft	Prototype Data for Donna?	Datum Shift Estimate for Donna ft	Gage in Offshore Grid?	Gage in Nearshore Grid?	March 1962 Prototype and Offshore Gage?	March 1962 Prototype and Nearshore Gage?	Donna Prototype and Offshore Gage?	Donna Prototype and Nearshore Gage?
Wrightsville Beach	X	0.18			X		X			
Atlantic Beach			X	0.29	X	X			X	X
Davis	X					X		X		
Oriental	X	0.29			X	X	X	X		
Minnesott Beach	X	0.84	X	1.23	X	X	X	X	X	X
Cherry Point	X	0.71	X	1.38	X	X	X	X	X	X
Englehard	X	0.61	X	0.86	X	X	X	X	X	X
Hatteras	X	1.02	X	1.31	X	X	X	X	X	X
Stumpy Point	X	0.41	X	0.63	X	X	X	X	X	X
Rodanthe	X	0.06			X	X	X	X		
Nags Head	X		X	0.66	X	X	X	X	X	X
Columbia	X	0.82	X	1.13	X	X	X	X	X	X
Albemarle Sound Bridge			X	0.82	X	X			X	X
Elizabeth City			X	0.91	X	X			X	X
Point Harbor	X	1.01			X	X	X	X		
				Sites for Verification:			11	11	10	10

Note: An X indicates that prototype data are available or that a grid contains a gage at the site. Davis could not be represented in the offshore grid due to shoreline approximations, and Wrightsville Beach falls outside the nearshore grid. The datum adjustments would be subtracted from a site's prototype data.

Table 4

Comparison of Hurricane Donna Peak Surge Levels Along Outer Banks

Location (Sound Side)	Distance from Oregon Inlet, miles	Existing	Closed	2,500-ft Jetty Spacing	5,000-ft Jetty Spacing
Bodie Island:					
Oregon Inlet Marina	1.2	7.8	9.2	8.1	7.8
Bodie Island Lighthouse	3.0	7.9	8.8	8.1	7.9
Headquarters Island	8.5	6.1	6.4	6.2	6.1
Sound Side (Nags Head)	13.25	6.6	6.8	6.7	6.6
Pea-Hatteras Island:					
U. S. Coast Guard Station	1.0	6.5	8.9	7.1	6.5
Goose Island	4.5	8.4	8.9	8.5	8.4
U. S. Fish & Wildlife Service Headquarters	7.6	8.2	8.4	8.2	8.1
Rodanthe	13.6	7.8	7.8	7.8	7.8

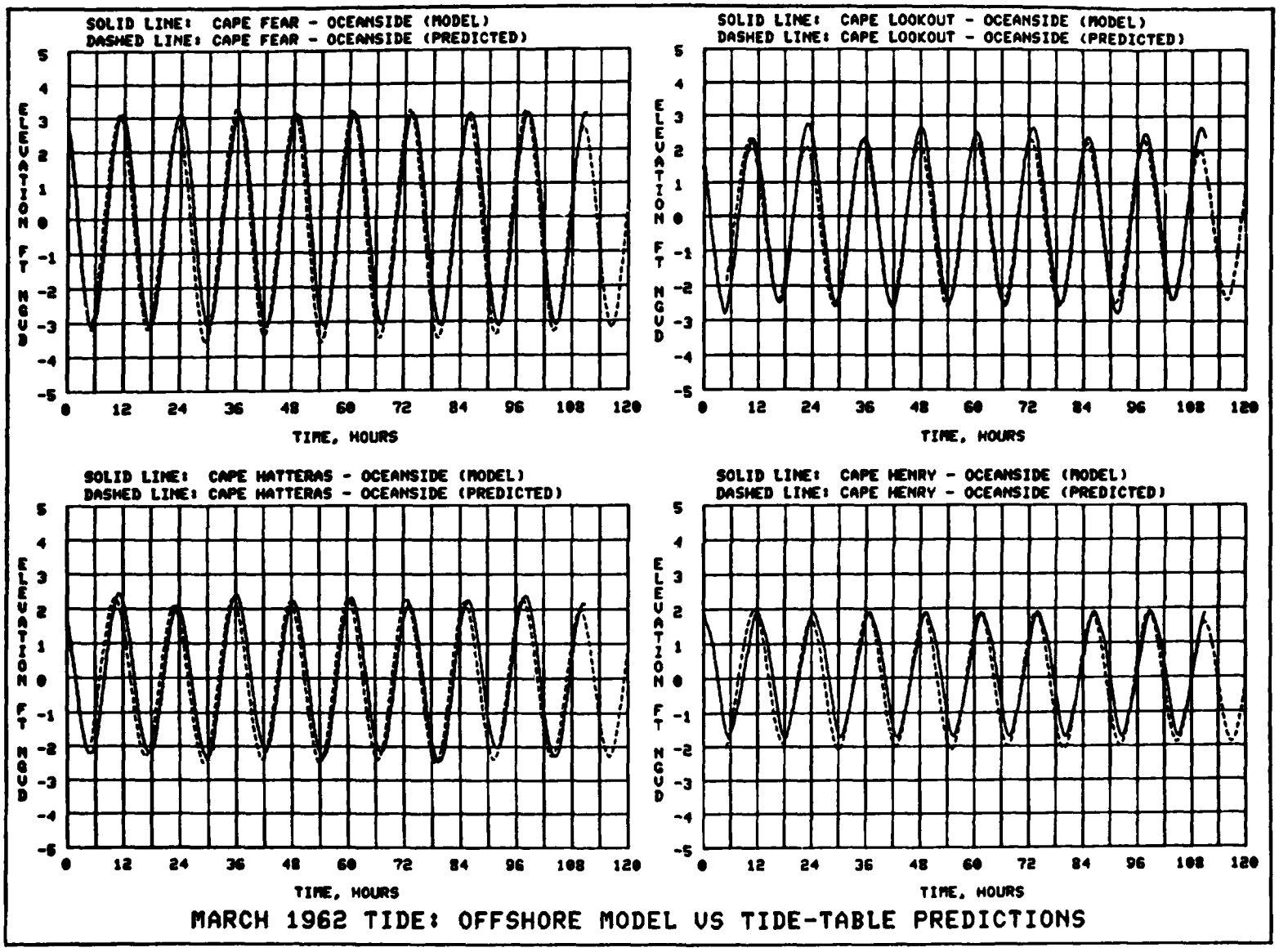

MARCH 1962 TIDE: OFFSHORE MODEL VS TIDE-TABLE PREDICTIONS

PLATE 1

PLATE 2

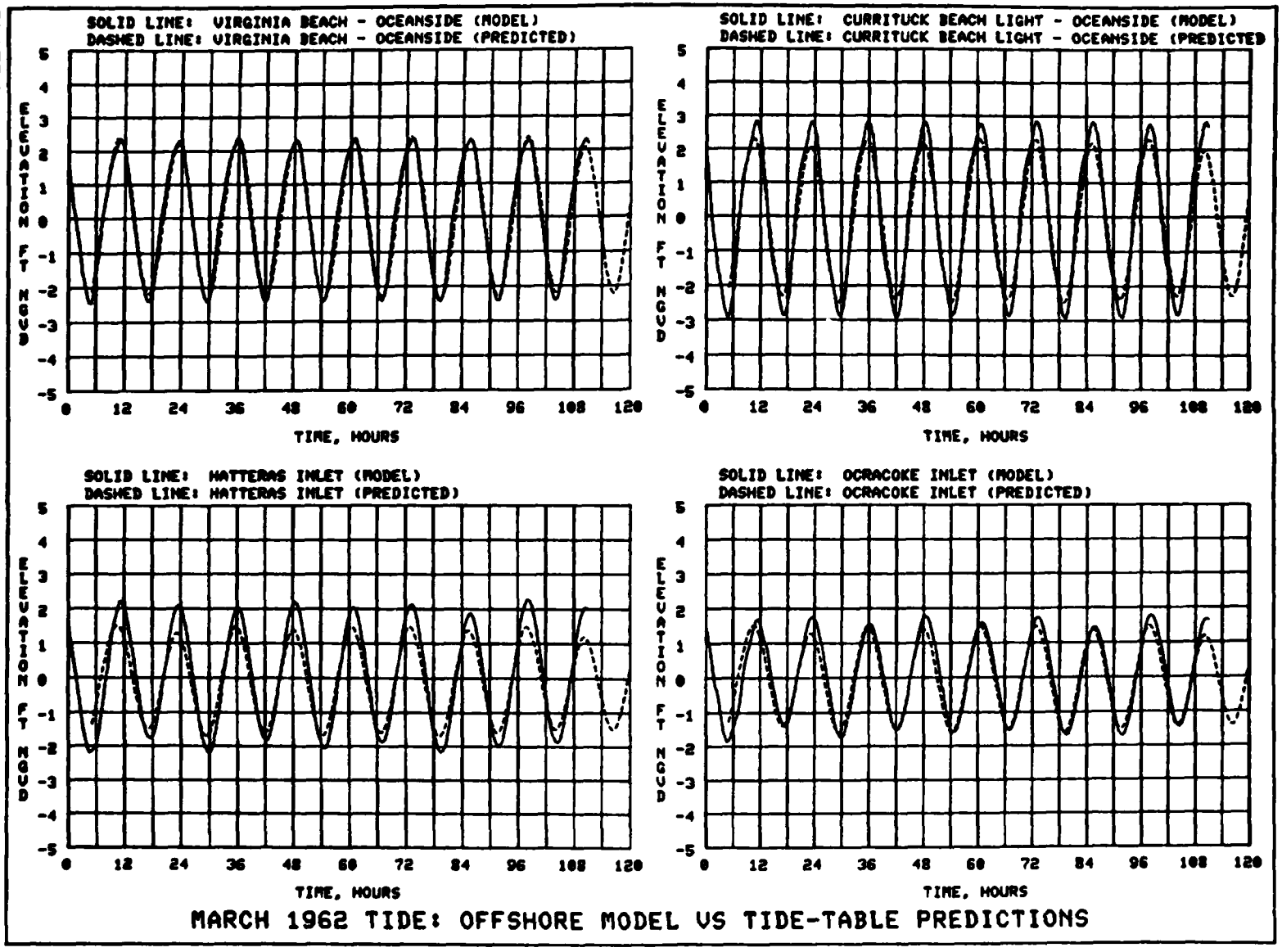
SOLID LINE: VIRGINIA BEACH - OCEANSIDE (MODEL)
DASHED LINE: VIRGINIA BEACH - OCEANSIDE (PREDICTED)
ELEVATION FT NGVD
TIME, HOURS
SOLID LINE: CURRITUCK BEACH LIGHT - OCEANSIDE (MODEL)
DASHED LINE: CURRITUCK BEACH LIGHT - OCEANSIDE (PREDICTED)
ELEVATION FT NGVD
TIME, HOURS
SOLID LINE: HATTERAS INLET (MODEL)
DASHED LINE: HATTERAS INLET (PREDICTED)
ELEVATION FT NGVD
TIME, HOURS
SOLID LINE: OCRACOKE INLET (MODEL)
DASHED LINE: OCRACOKE INLET (PREDICTED)
ELEVATION FT NGVD
TIME, HOURS
MARCH 1962 TIDE: OFFSHORE MODEL VS TIDE-TABLE PREDICTIONS

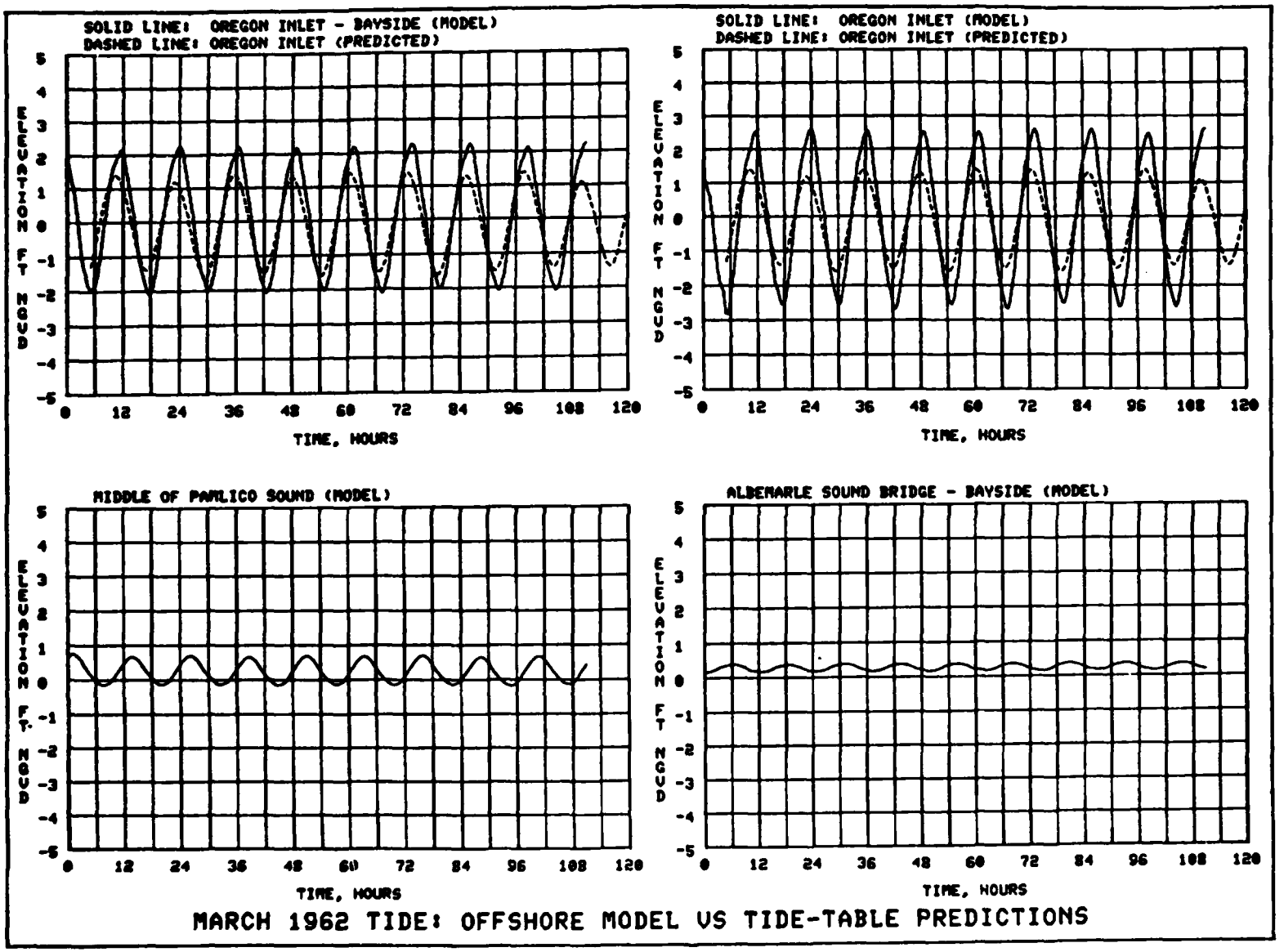
SOLID LINE: OREGON INLET - BAYSIDE (MODEL)
DASHED LINE: OREGON INLET (PREDICTED)
ELEVATION FT NGVD
TIME, HOURS
SOLID LINE: OREGON INLET (MODEL)
DASHED LINE: OREGON INLET (PREDICTED)
ELEVATION FT NGVD
TIME, HOURS
MIDDLE OF PAMLICO SOUND (MODEL)
ELEVATION FT NGVD
TIME, HOURS
ALBEMARLE SOUND BRIDGE - BAYSIDE (MODEL)
ELEVATION FT NGVD
TIME, HOURS
MARCH 1962 TIDE: OFFSHORE MODEL VS TIDE-TABLE PREDICTIONS

PLATE 3

PLATE 4

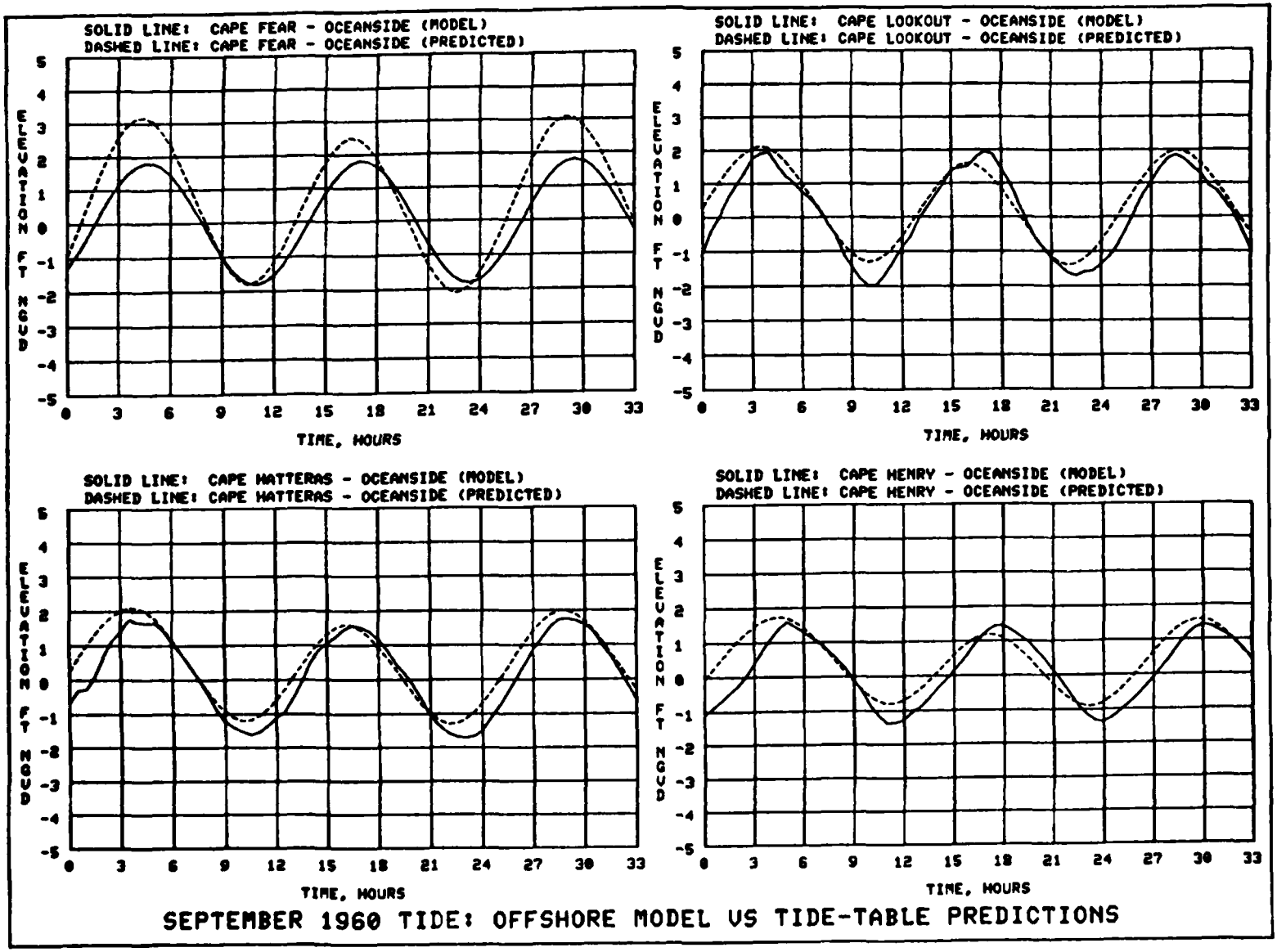

SEPTEMBER 1960 TIDE: OFFSHORE MODEL VS TIDE-TABLE PREDICTIONS

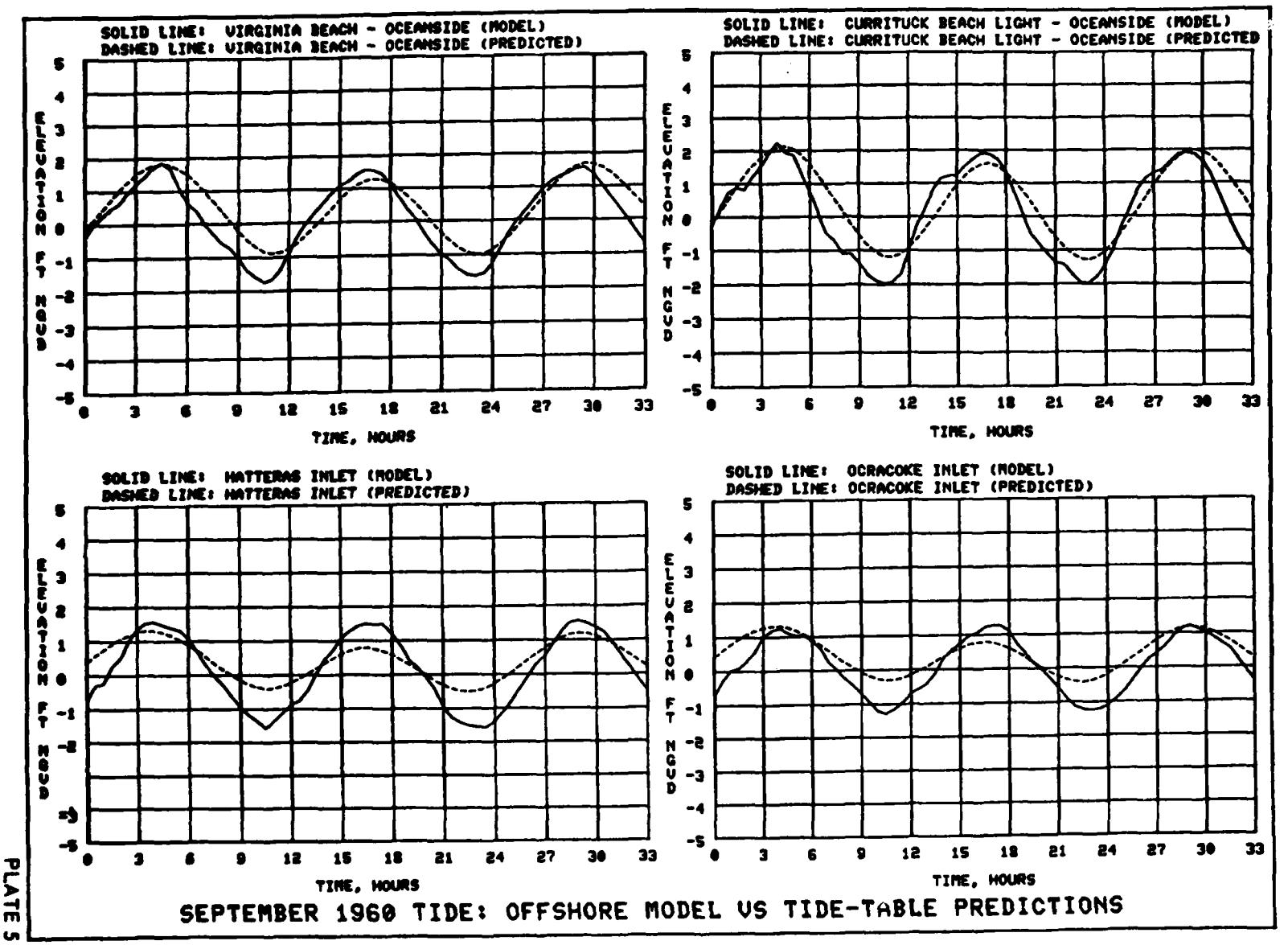

PLATE 5

SEPTEMBER 1960 TIDE: OFFSHORE MODEL VS TIDE-TABLE PREDICTIONS

PLATE 6

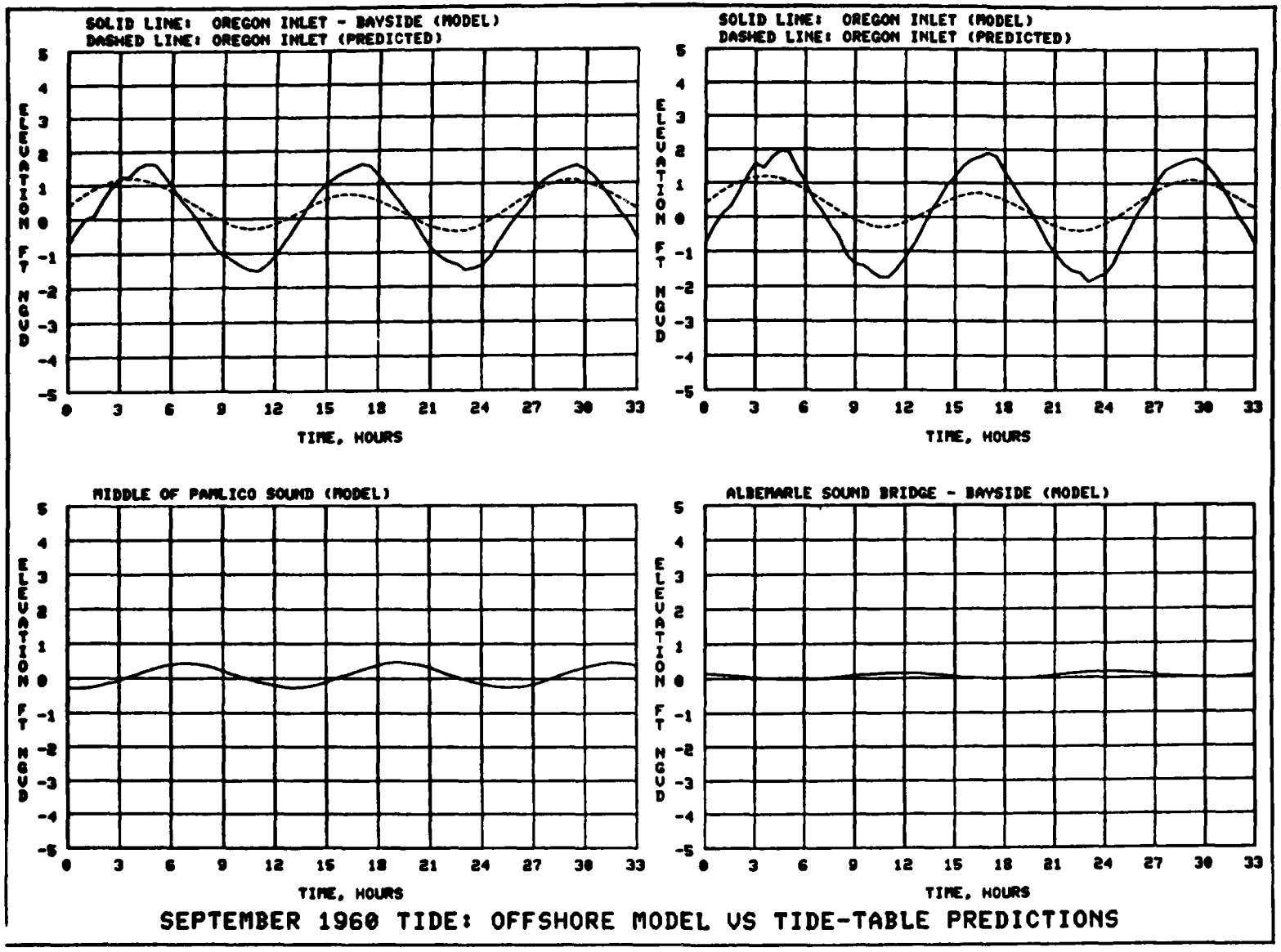

SEPTEMBER 1960 TIDE: OFFSHORE MODEL VS TIDE-TABLE PREDICTIONS

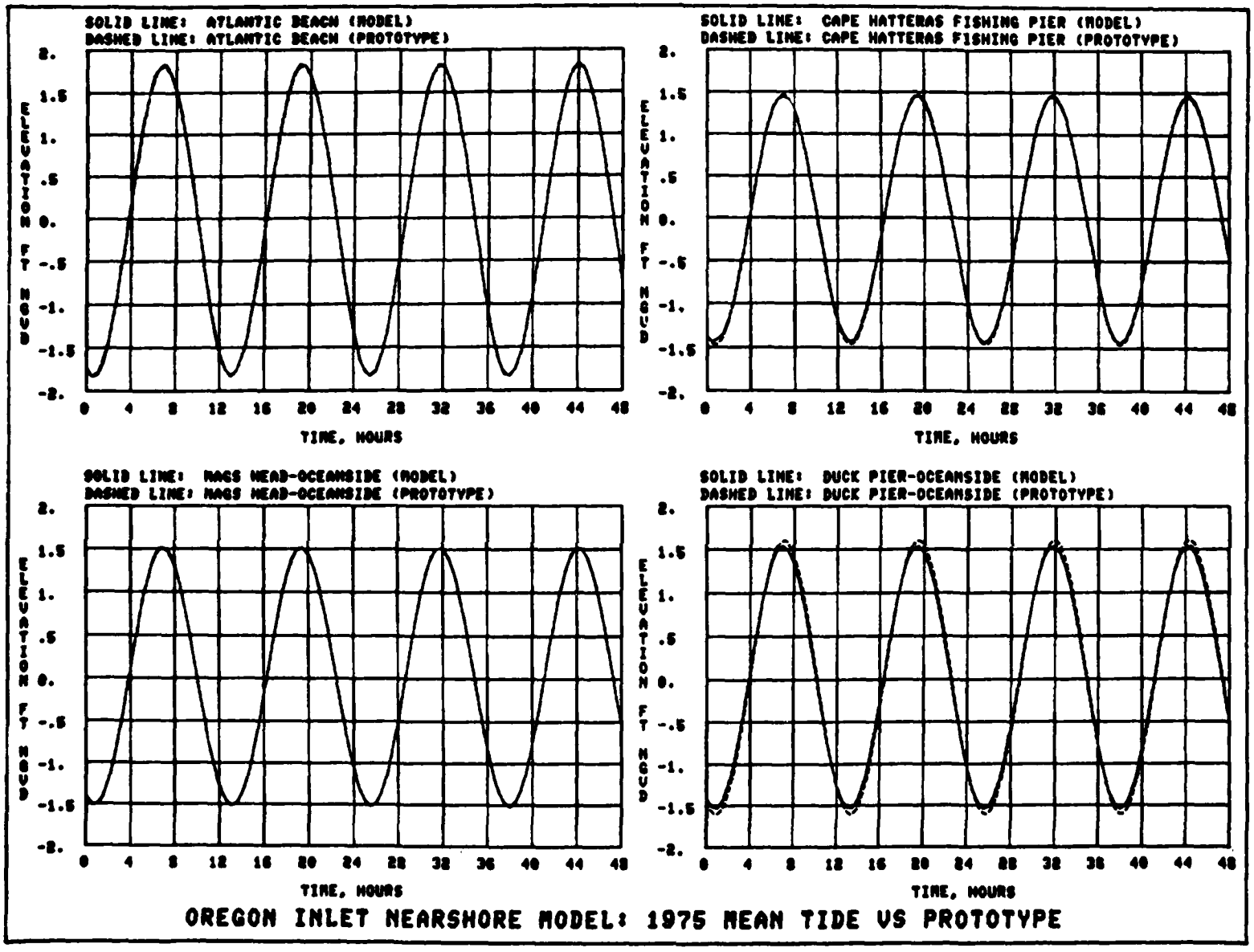

OREGON INLET NEARSHORE MODEL: 1975 MEAN TIDE VS PROTOTYPE

PLATE 7

PLATE 8

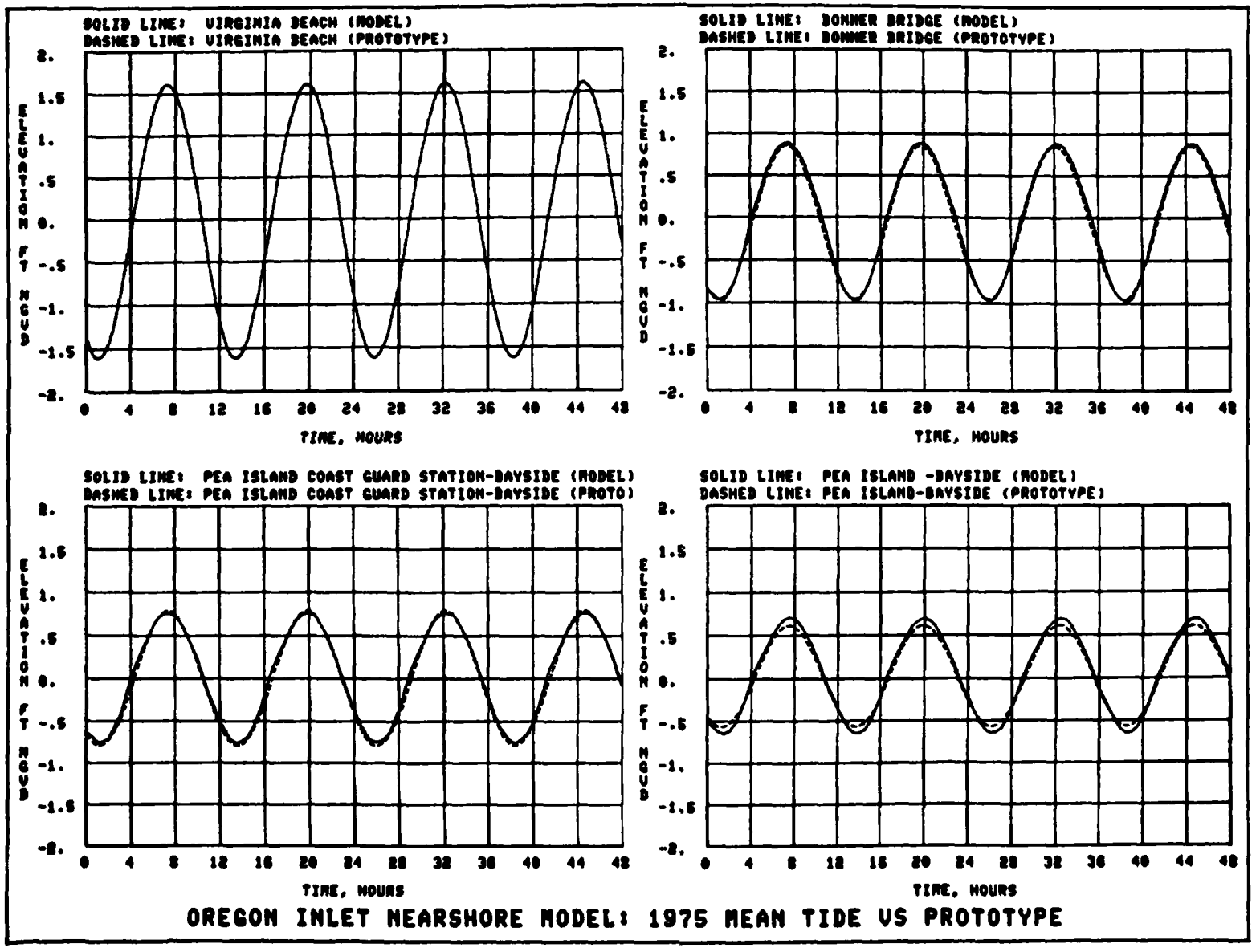

OREGON INLET NEARSHORE MODEL: 1975 MEAN TIDE VS PROTOTYPE

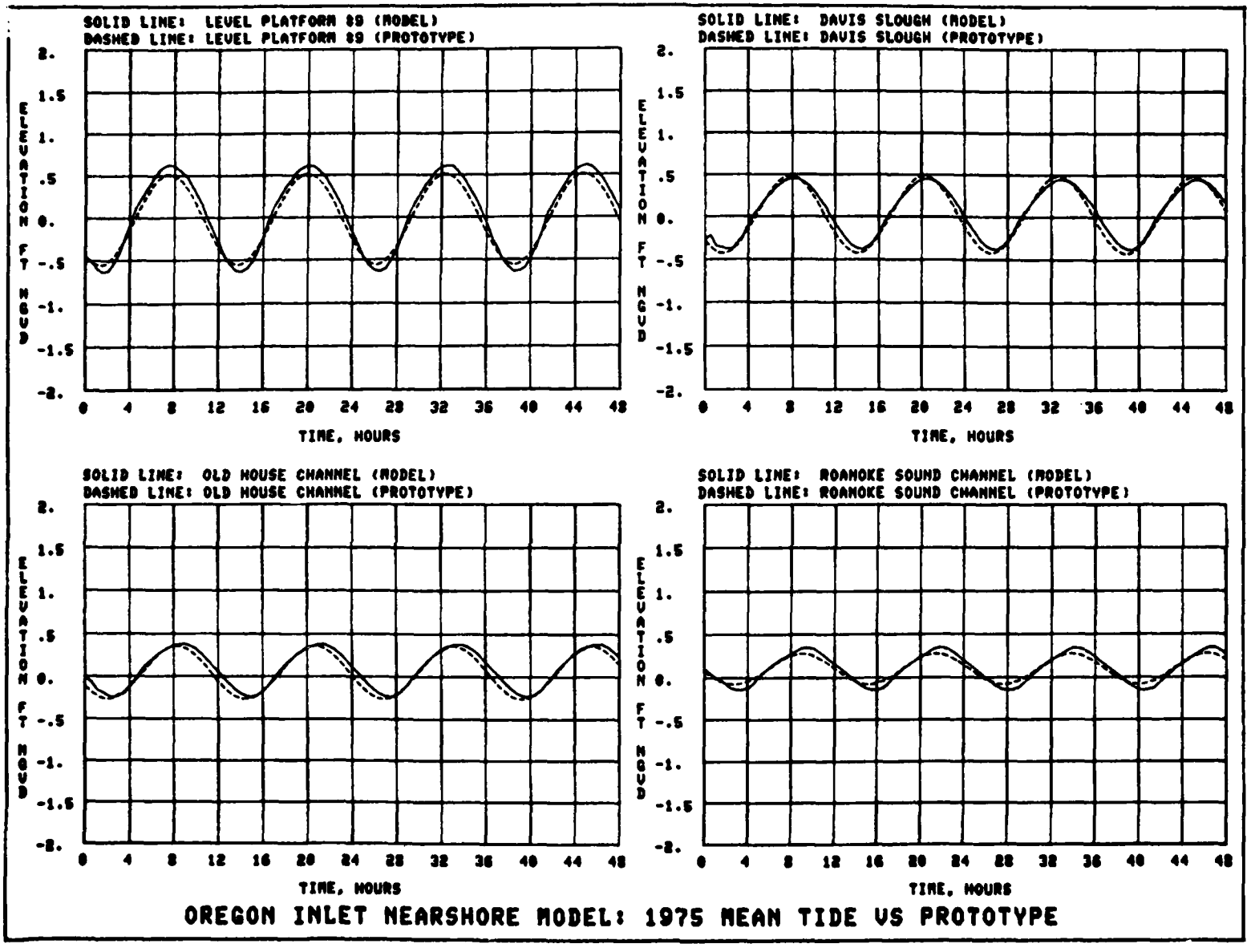

OREGON INLET NEARSHORE MODEL: 1975 MEAN TIDE VS PROTOTYPE

PLATE 9

PLATE 10

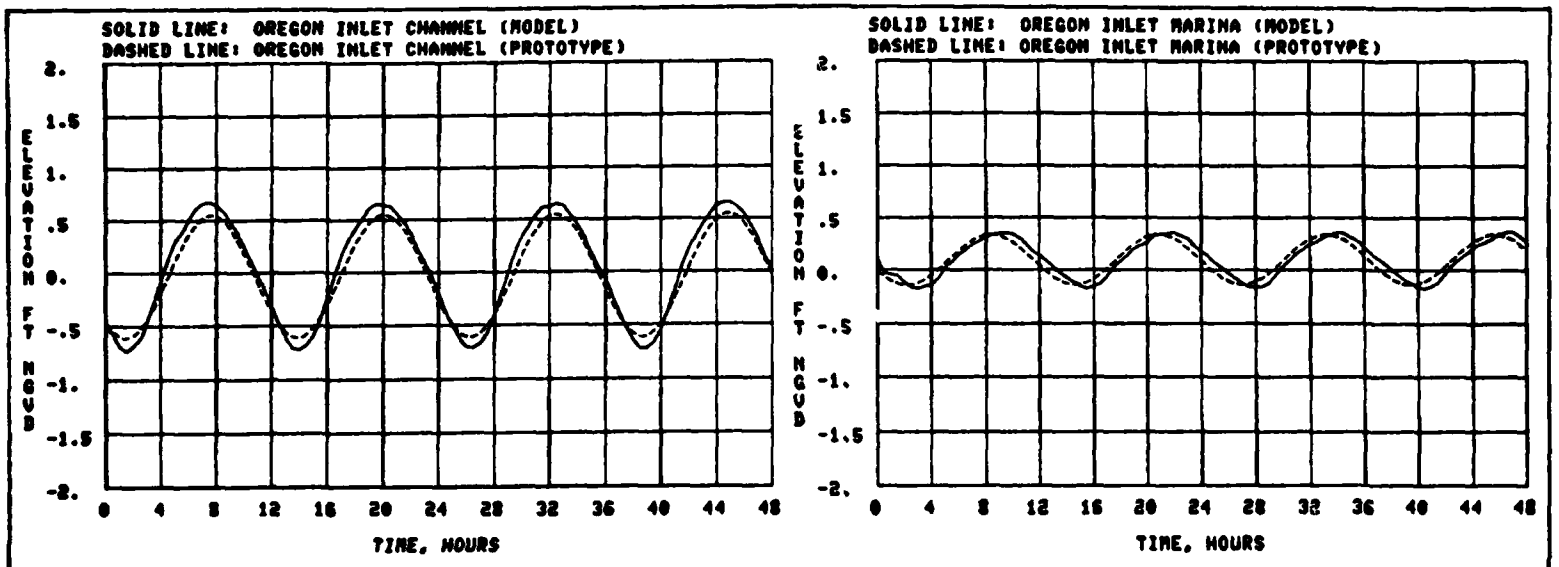

OREGON INLET NEARSHORE MODEL: 1975 MEAN TIDE VS PROTOTYPE

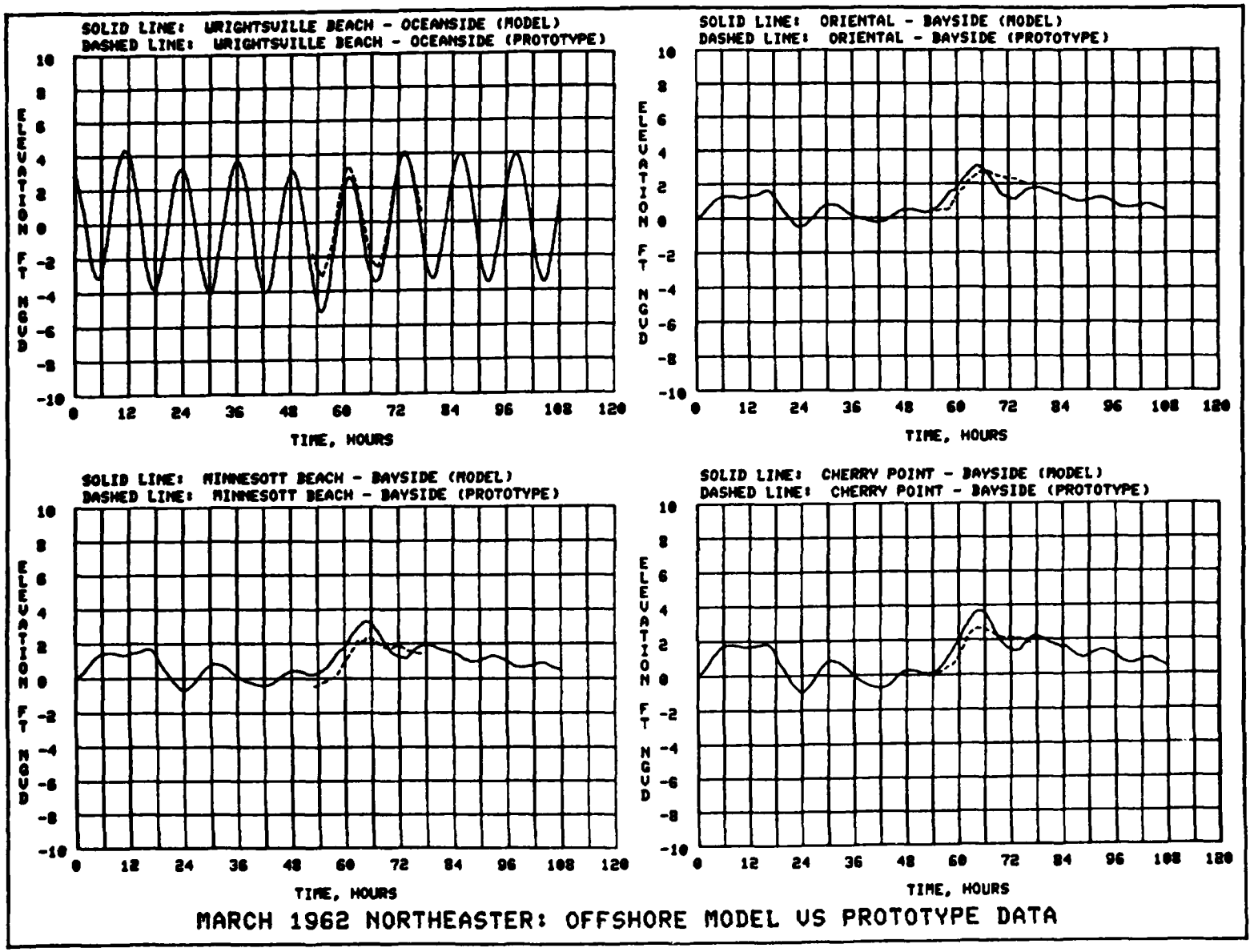

MARCH 1962 NORTHEASTER: OFFSHORE MODEL VS PROTOTYPE DATA

PLATE 11

PLATE 12

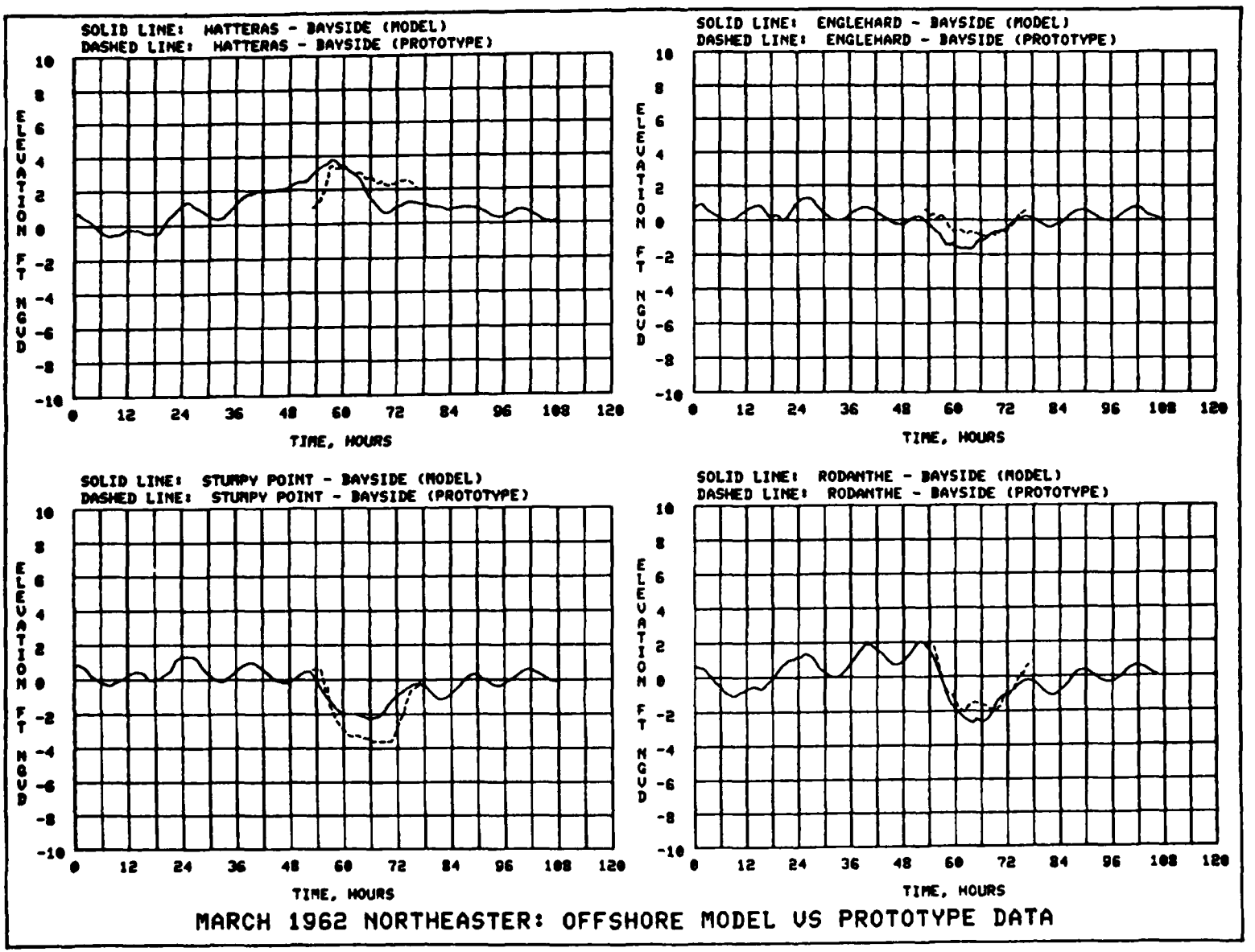

MARCH 1962 NORTHEASTER: OFFSHORE MODEL VS PROTOTYPE DATA

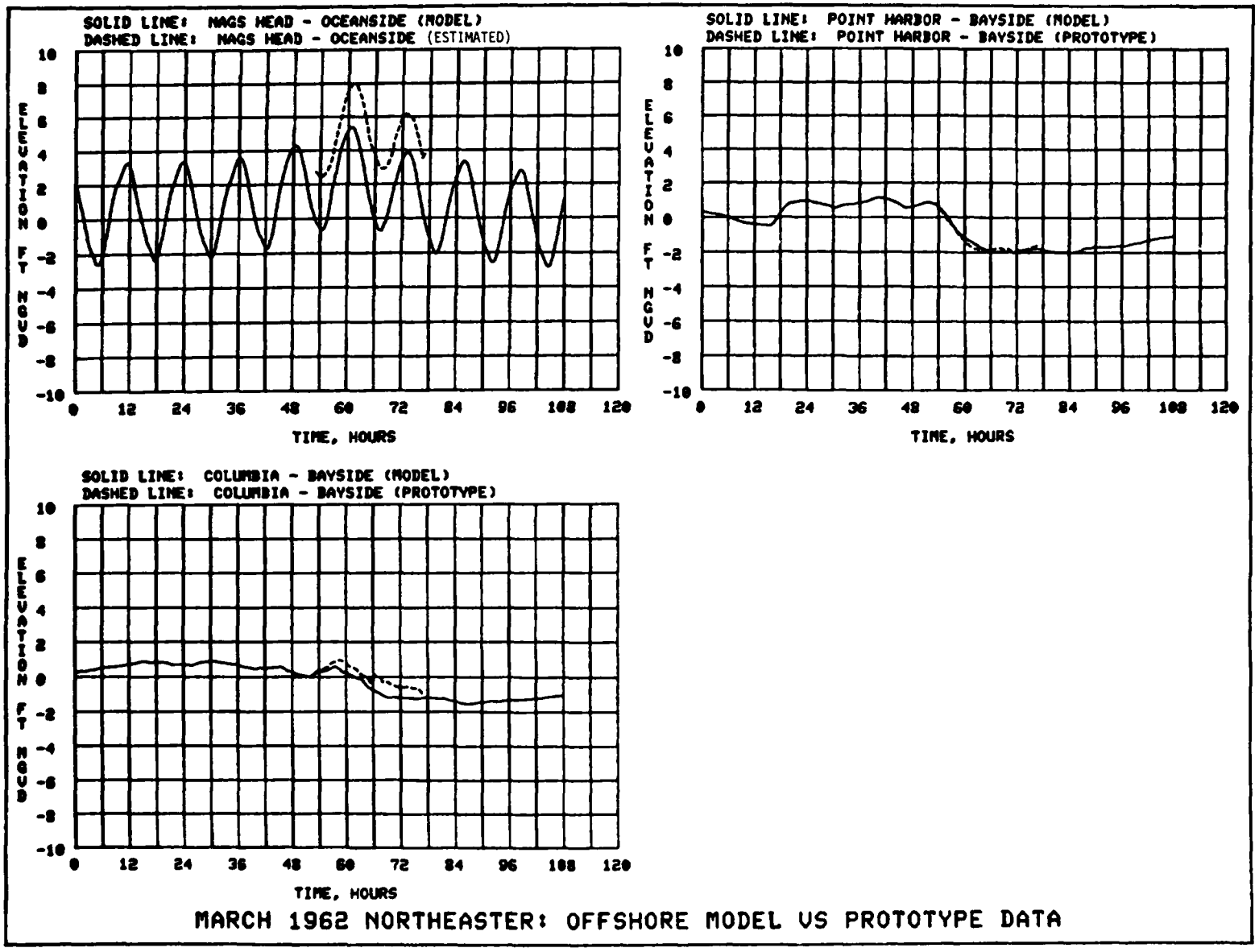

MARCH 1962 NORTHEASTER: OFFSHORE MODEL VS PROTOTYPE DATA

PLATE 13

PLATE 14

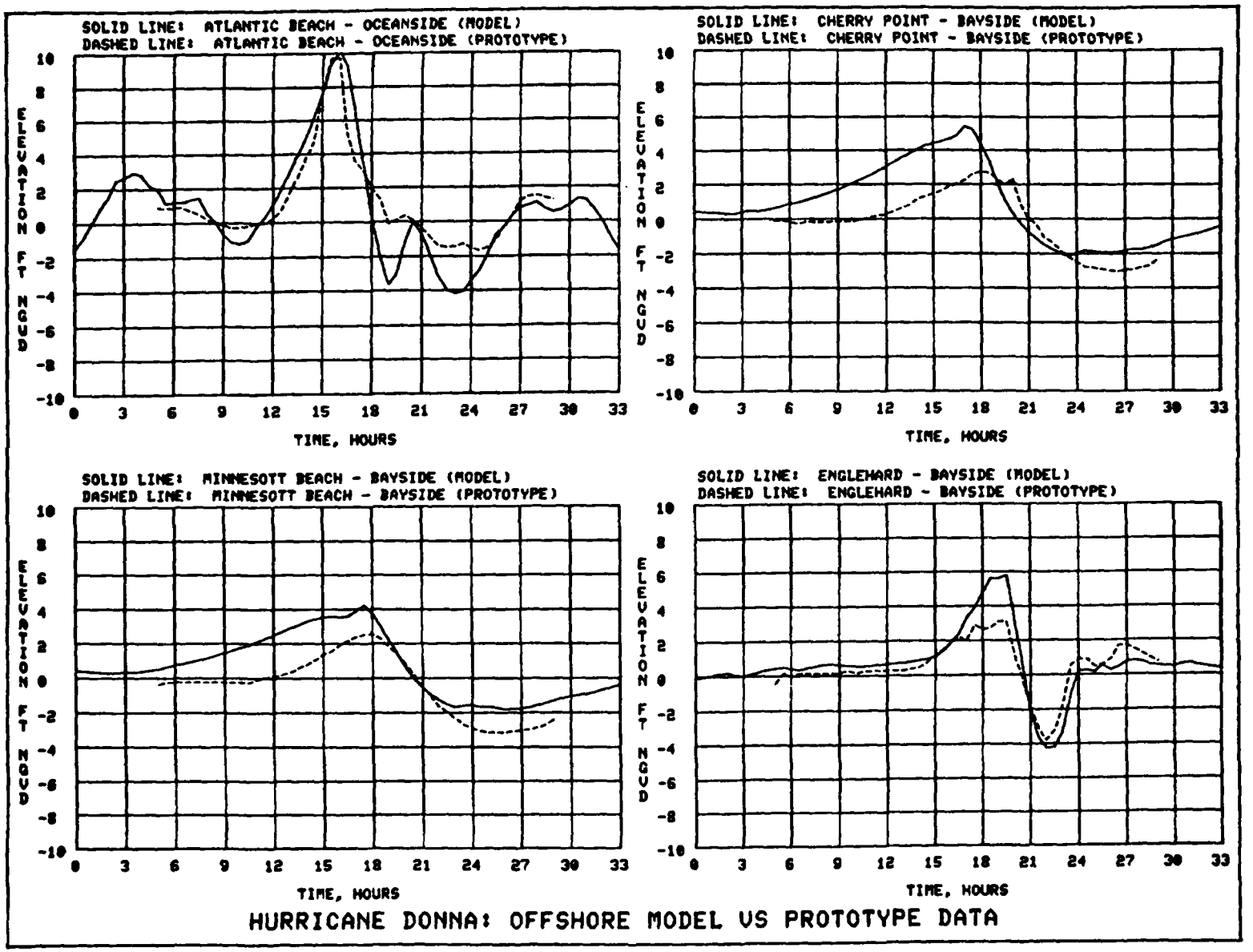

HURRICANE DONNA: OFFSHORE MODEL VS PROTOTYPE DATA

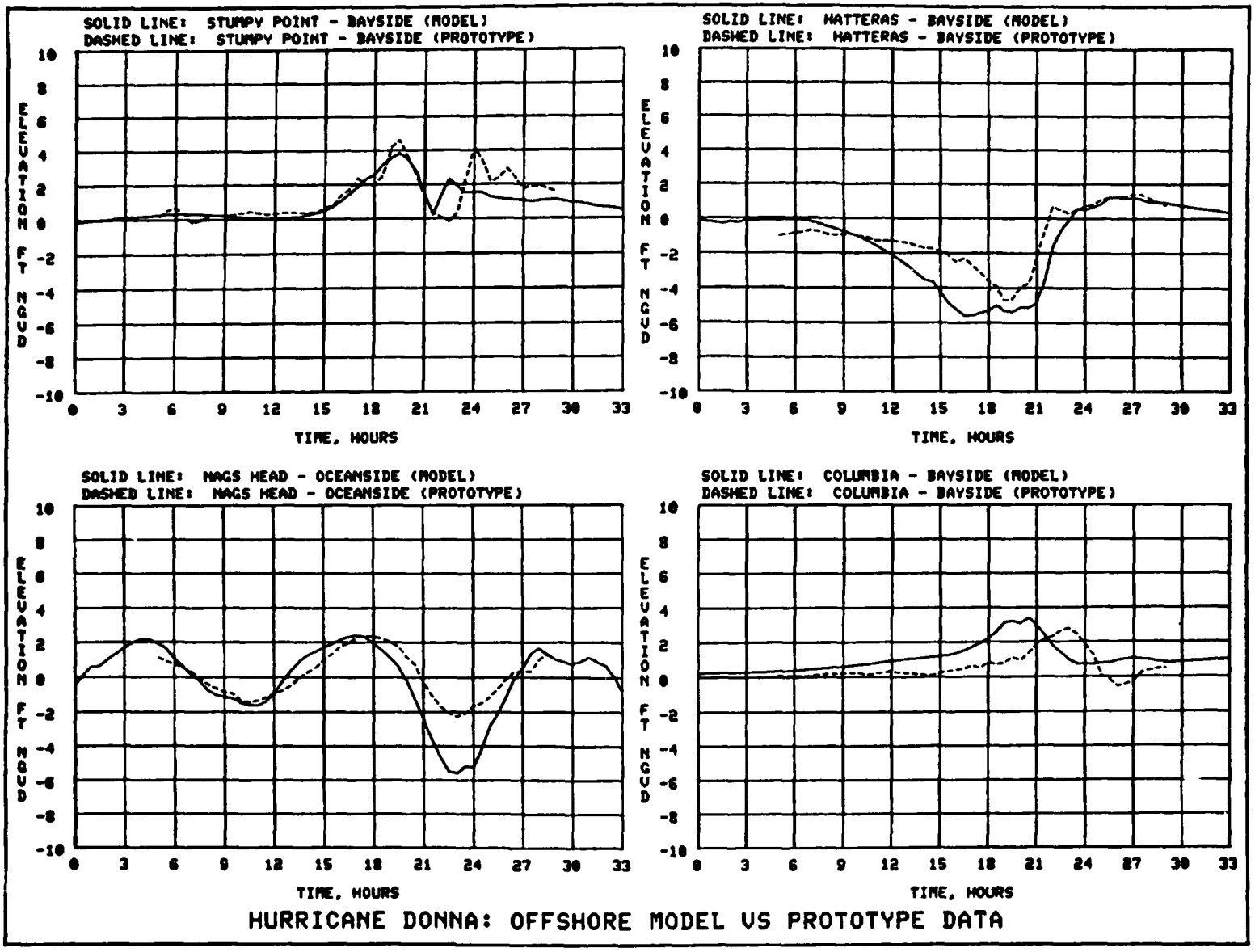

HURRICANE DONNA: OFFSHORE MODEL VS PROTOTYPE DATA

PLATE 15

PLATE 16

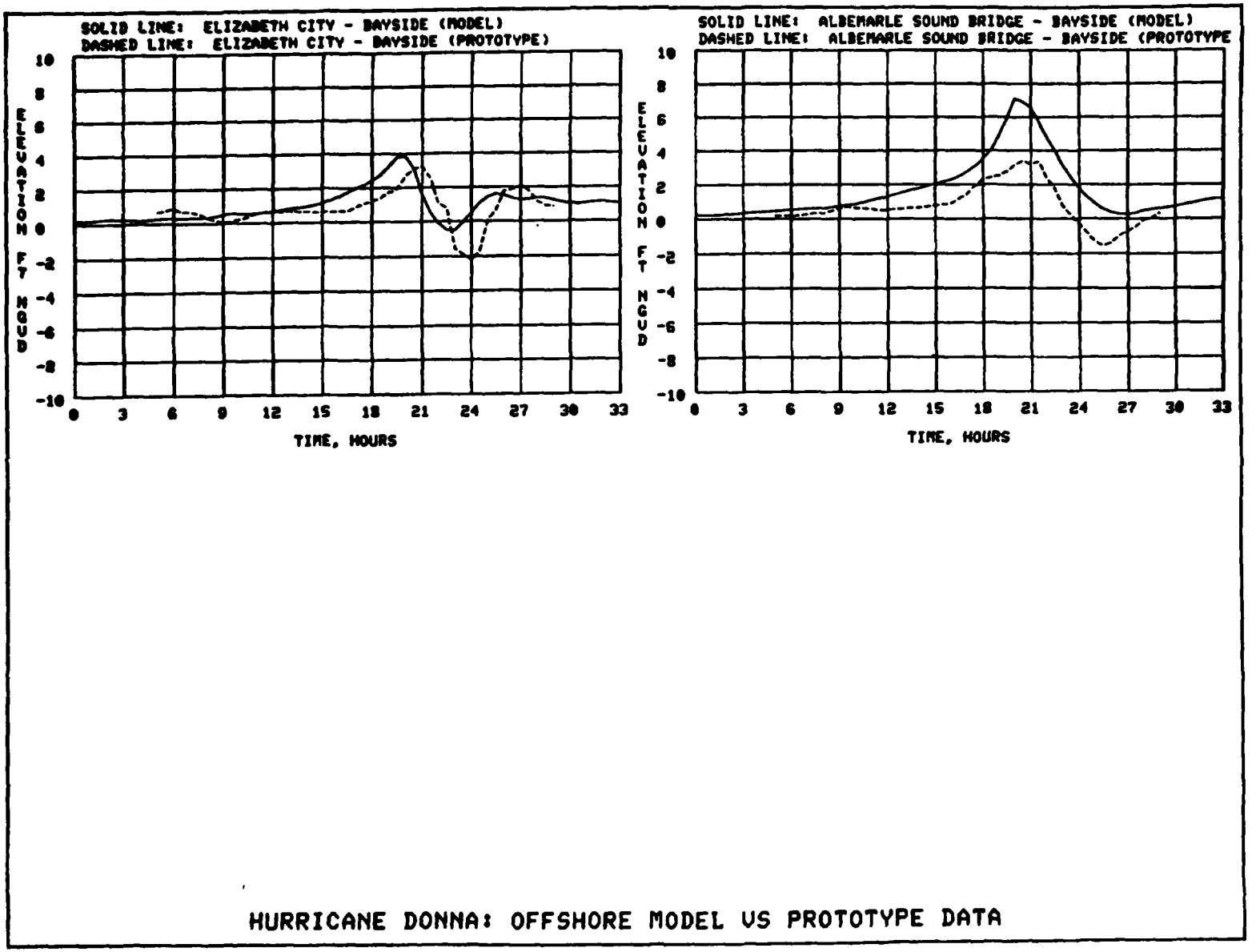

HURRICANE DONNA: OFFSHORE MODEL VS PROTOTYPE DATA

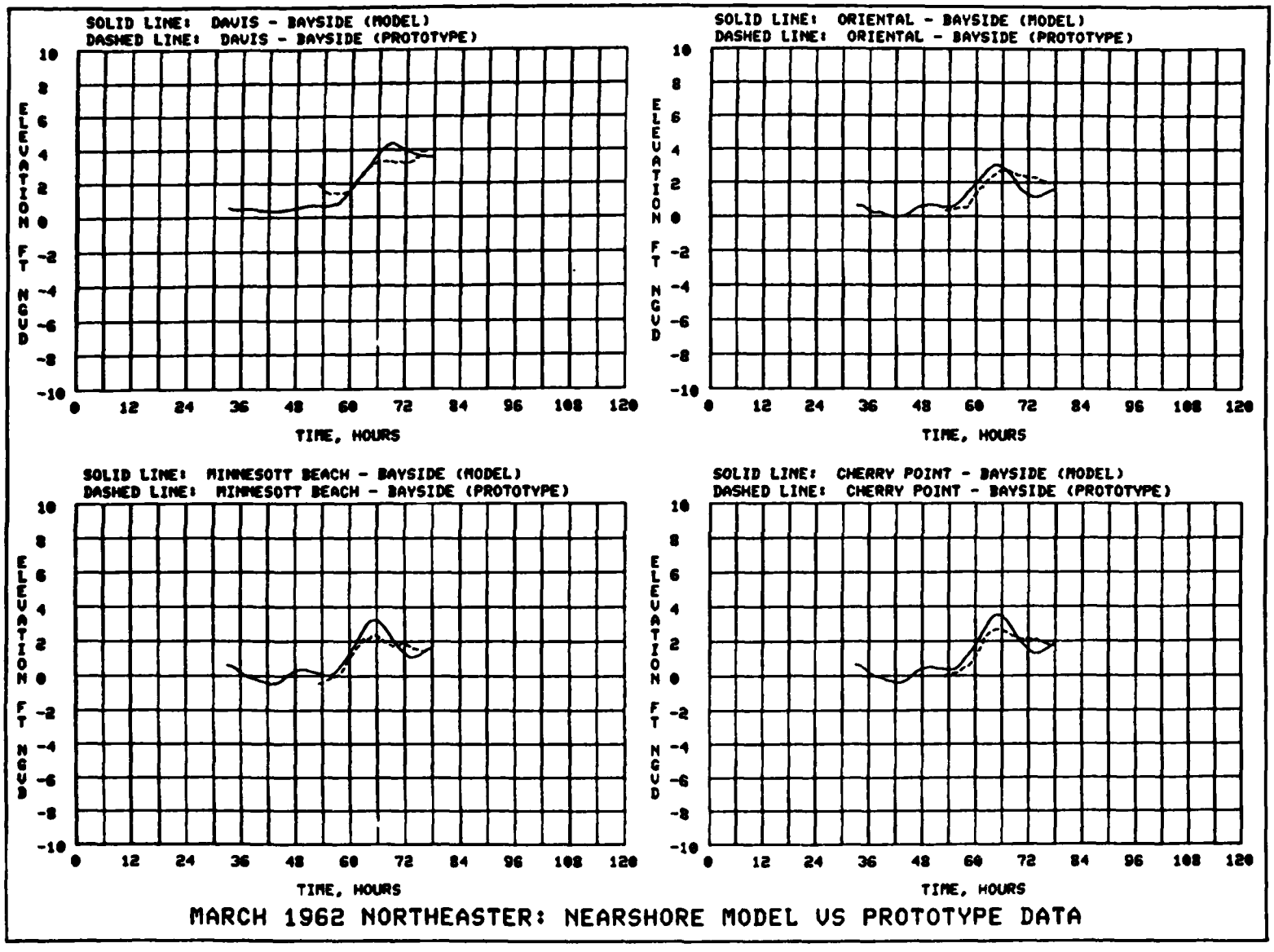

MARCH 1962 NORTHEASTER: NEARSHORE MODEL VS PROTOTYPE DATA

PLATE 17

PLATE 18

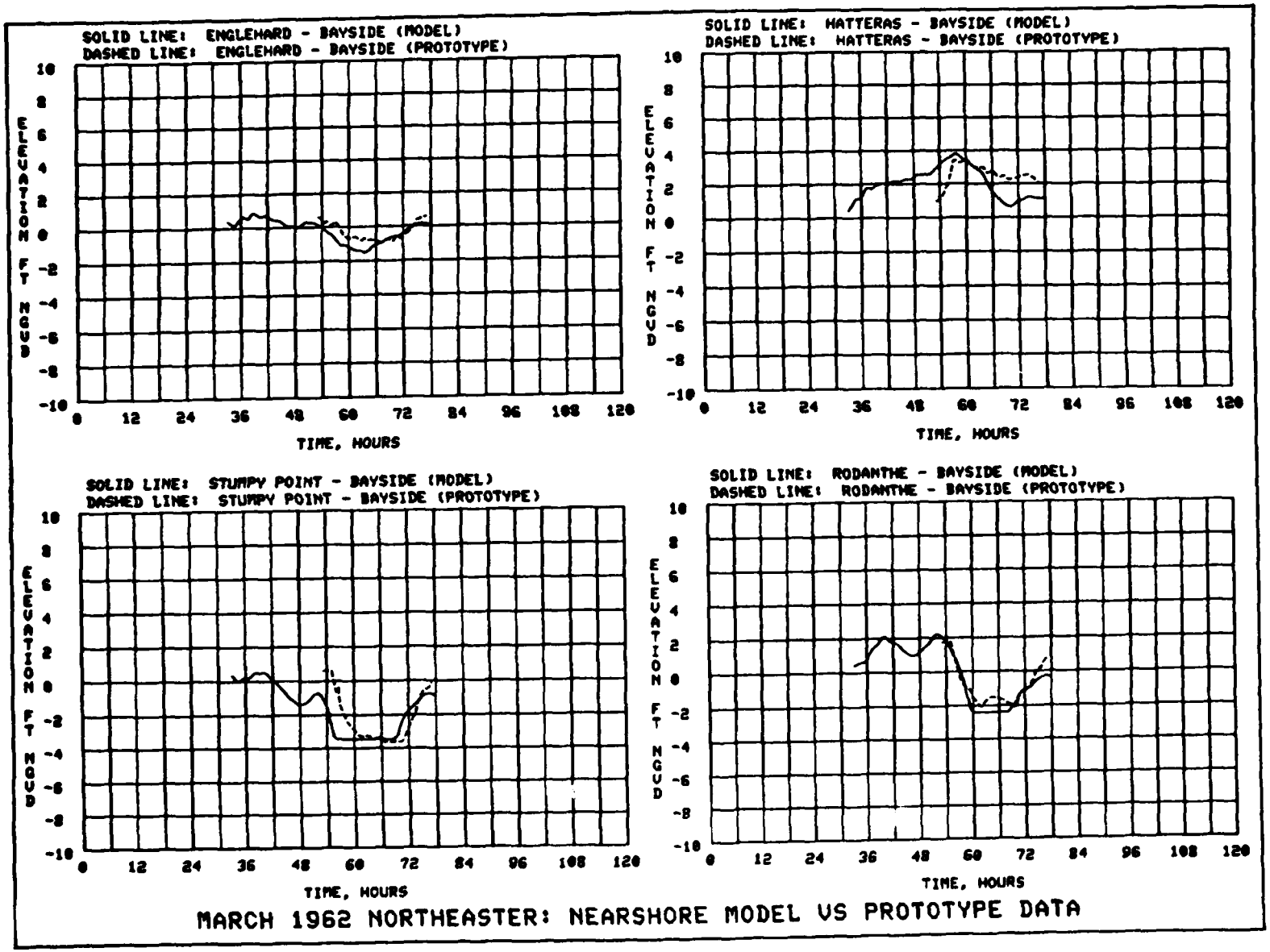

MARCH 1962 NORTHEASTER: NEARSHORE MODEL VS PROTOTYPE DATA

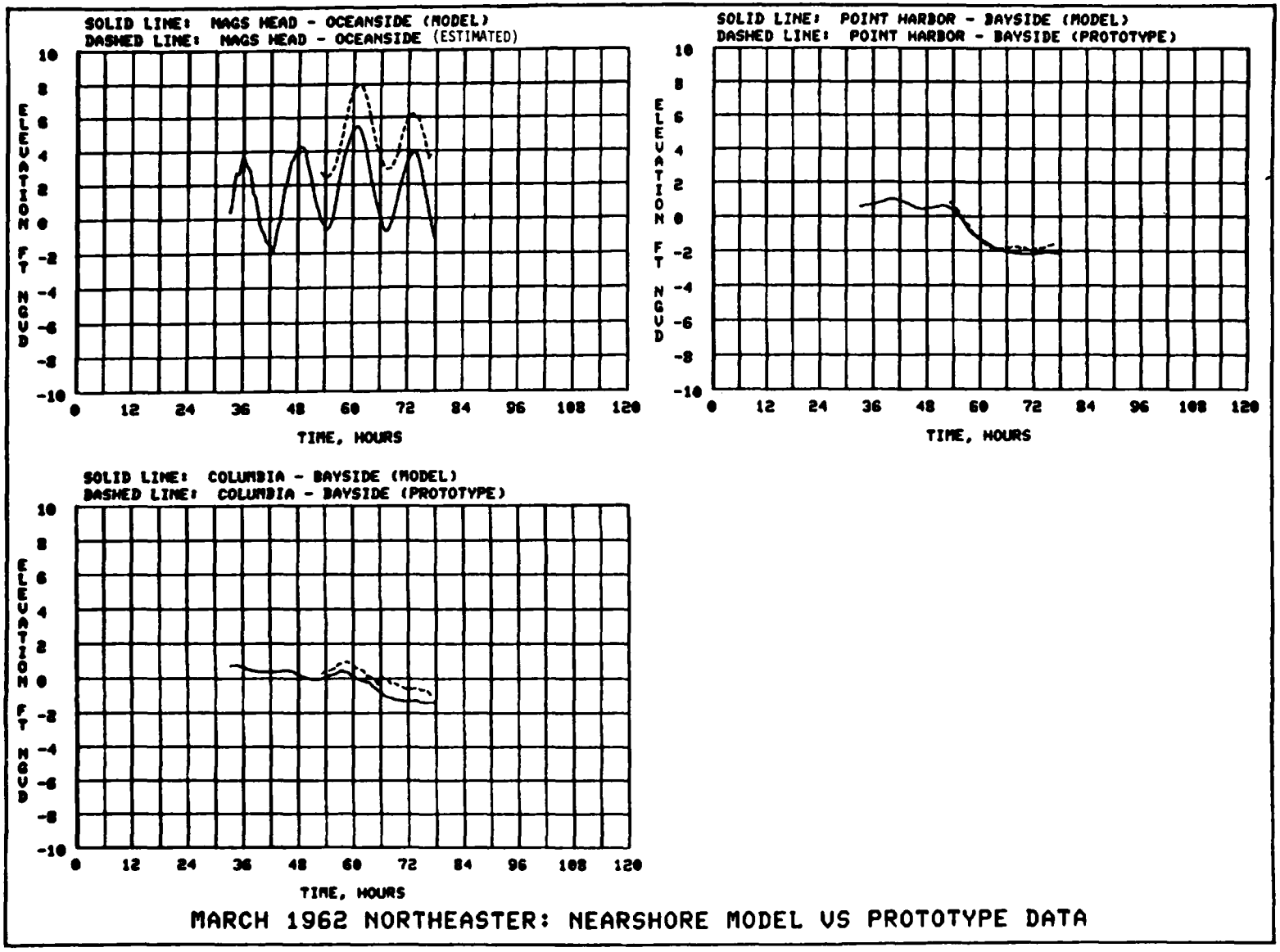

MARCH 1962 NORTHEASTER: NEARSHORE MODEL VS PROTOTYPE DATA

PLATE 19

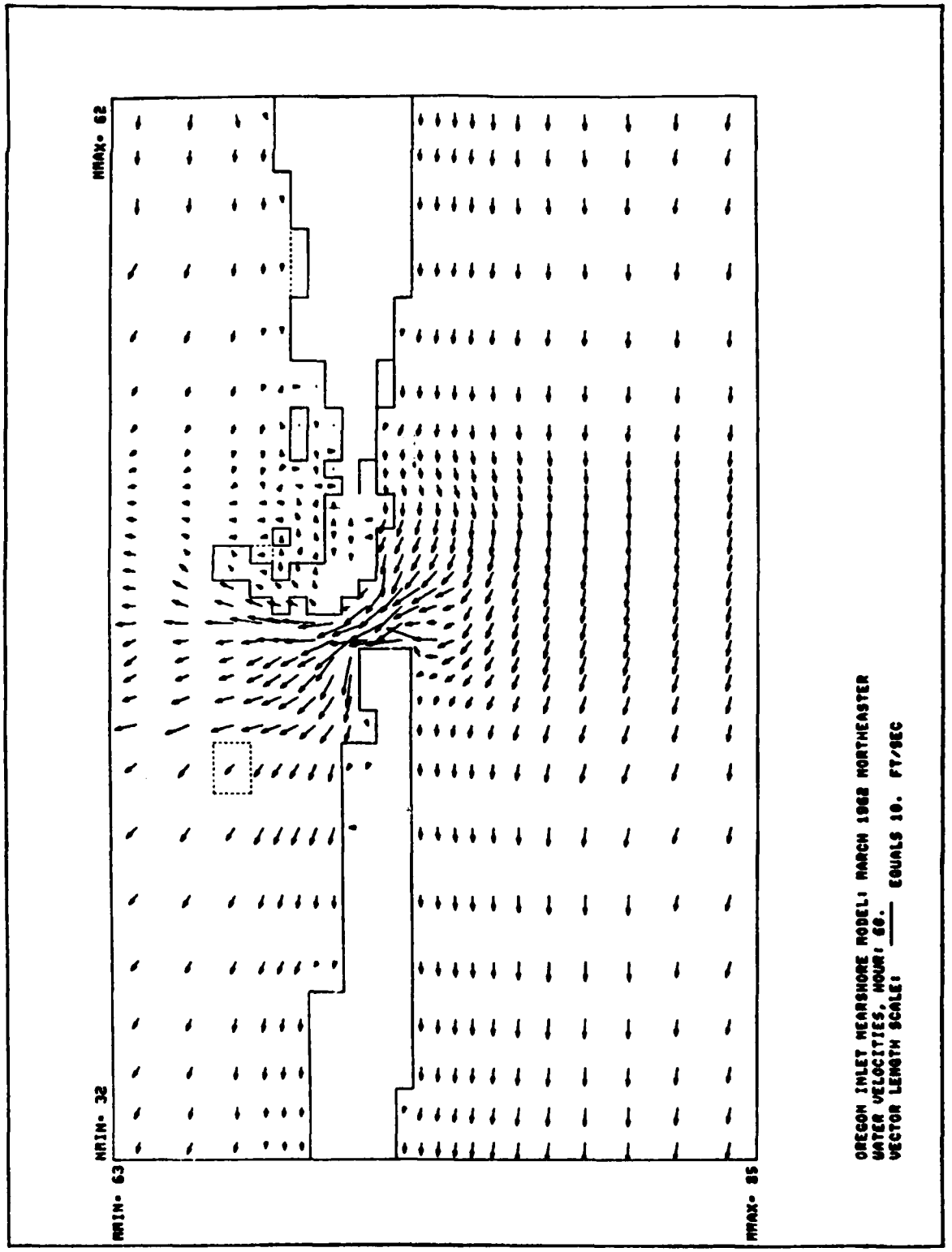
NMAX= 62
NMIN= 32
MMIN= 63
MMAX= 85
OREGON INLET NEARSHORE MODEL: MARCH 1962 NORTHEASTER
WATER VELOCITIES, HOUR: 60.
VECTOR LENGTH SCALE: ____ EQUALS 10. FT/SEC

PLATE 20

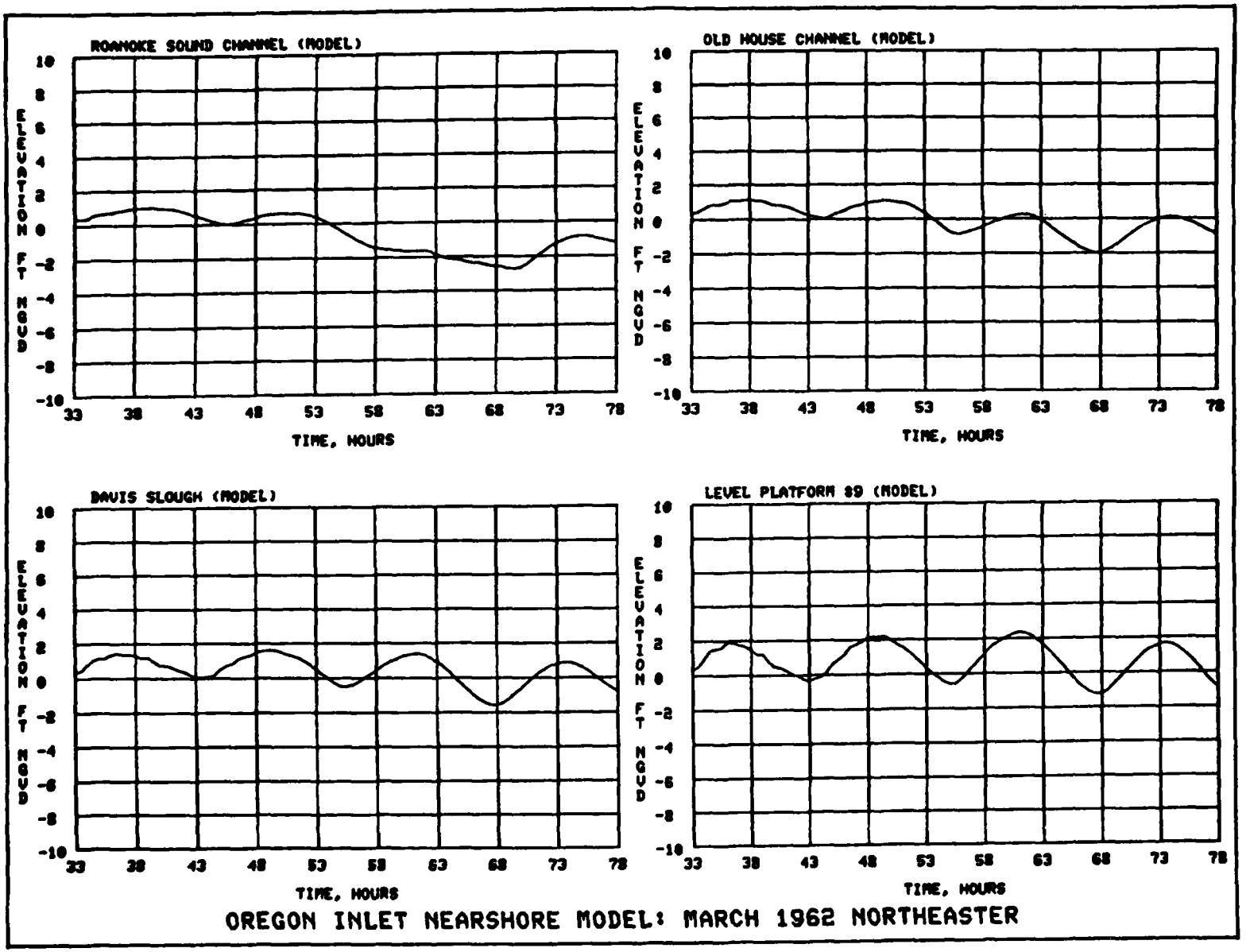

OREGON INLET NEARSHORE MODEL: MARCH 1962 NORTHEASTER

PLATE 21

PLATE 22

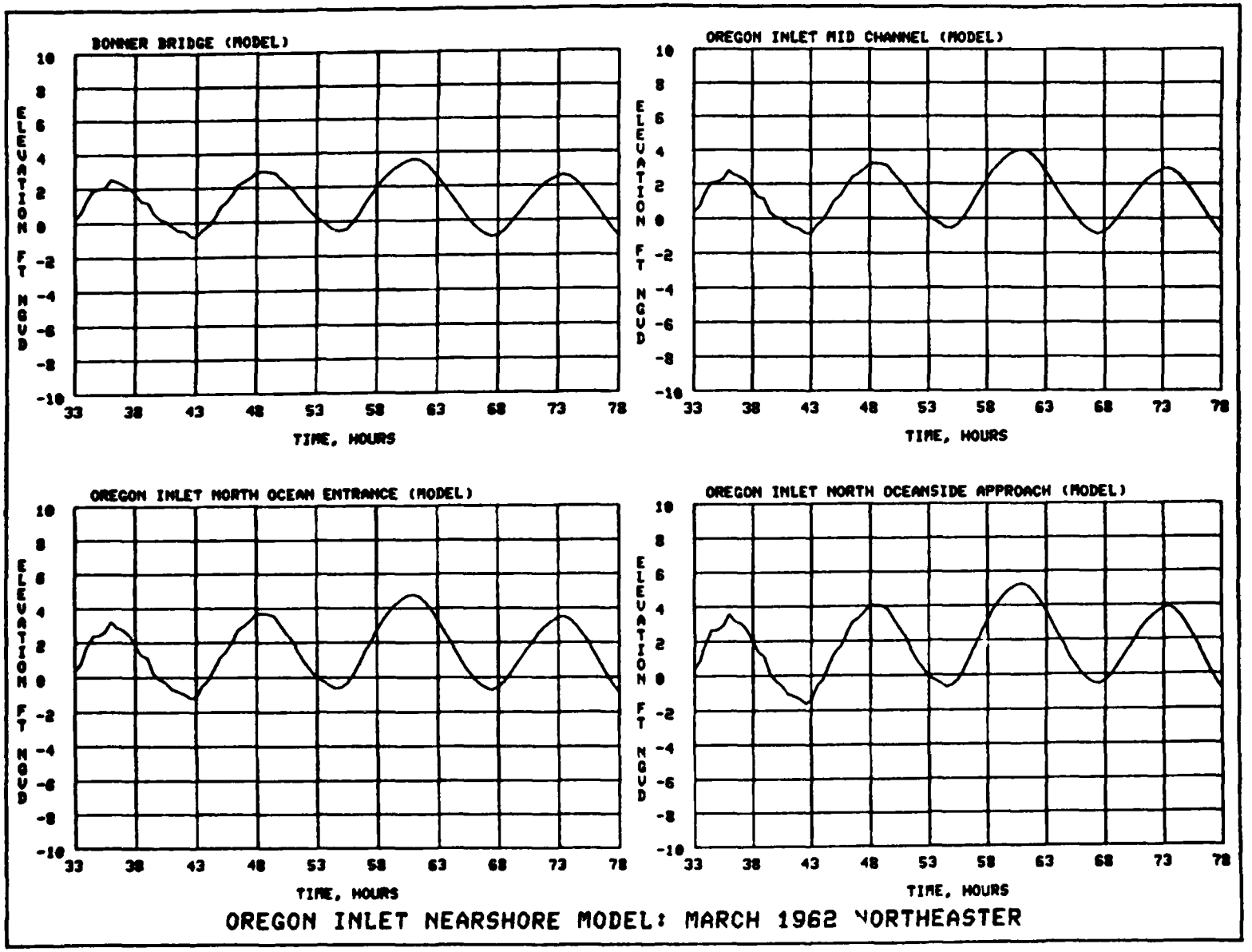

OREGON INLET NEARSHORE MODEL: MARCH 1962 NORTHEASTER

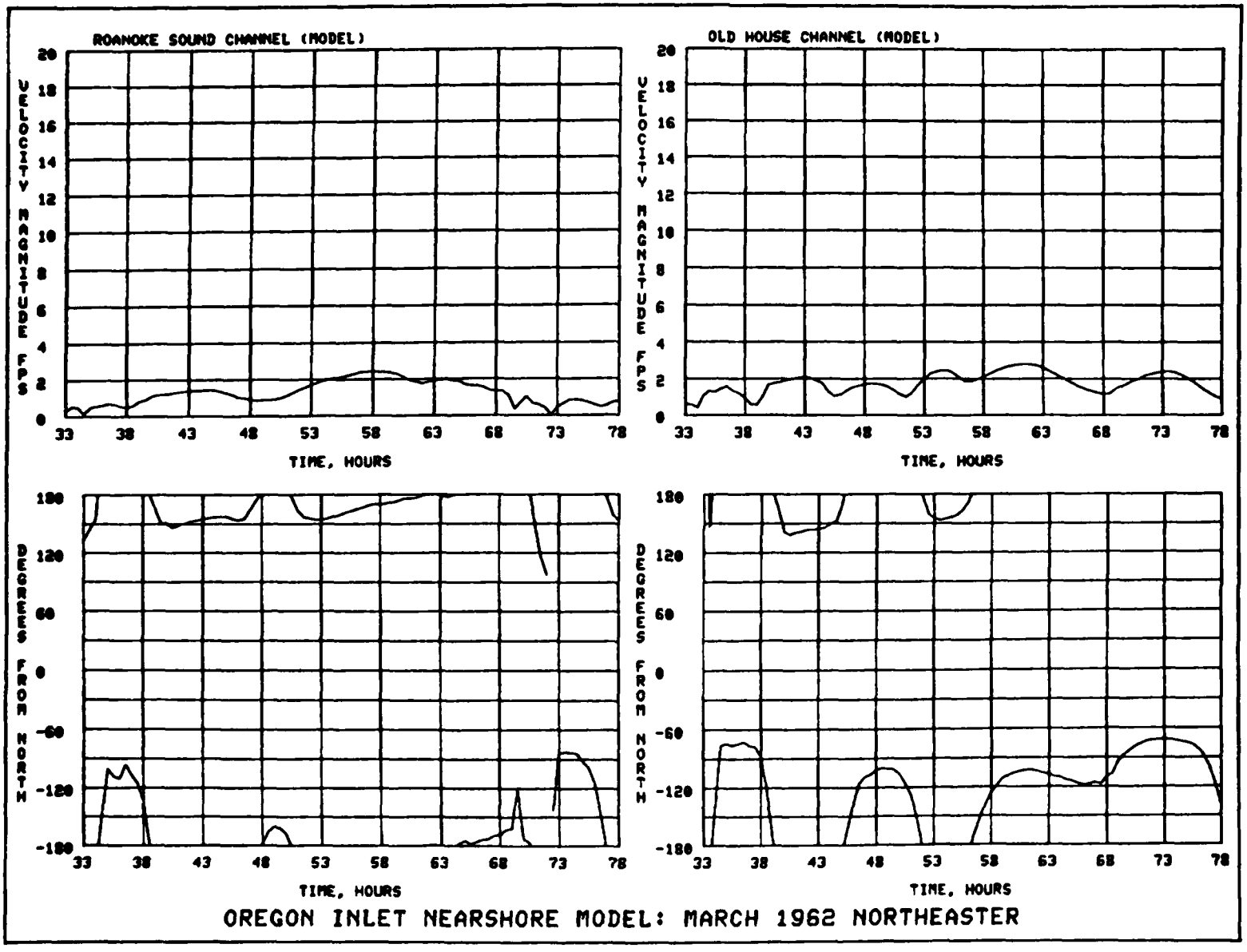

OREGON INLET NEARSHORE MODEL: MARCH 1962 NORTHEASTER

PLATE 23

PLATE 24

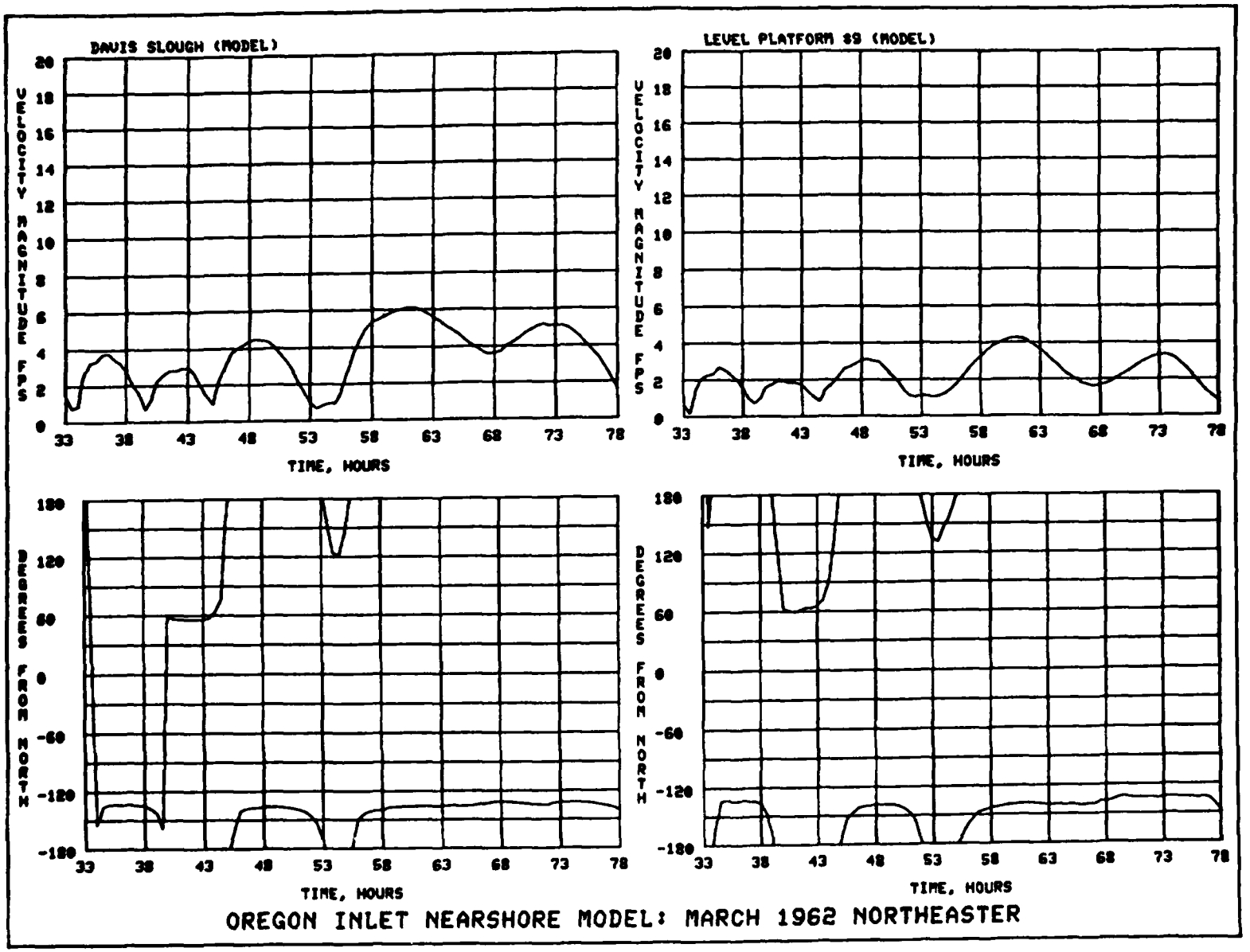

OREGON INLET NEARSHORE MODEL: MARCH 1962 NORTHEASTER

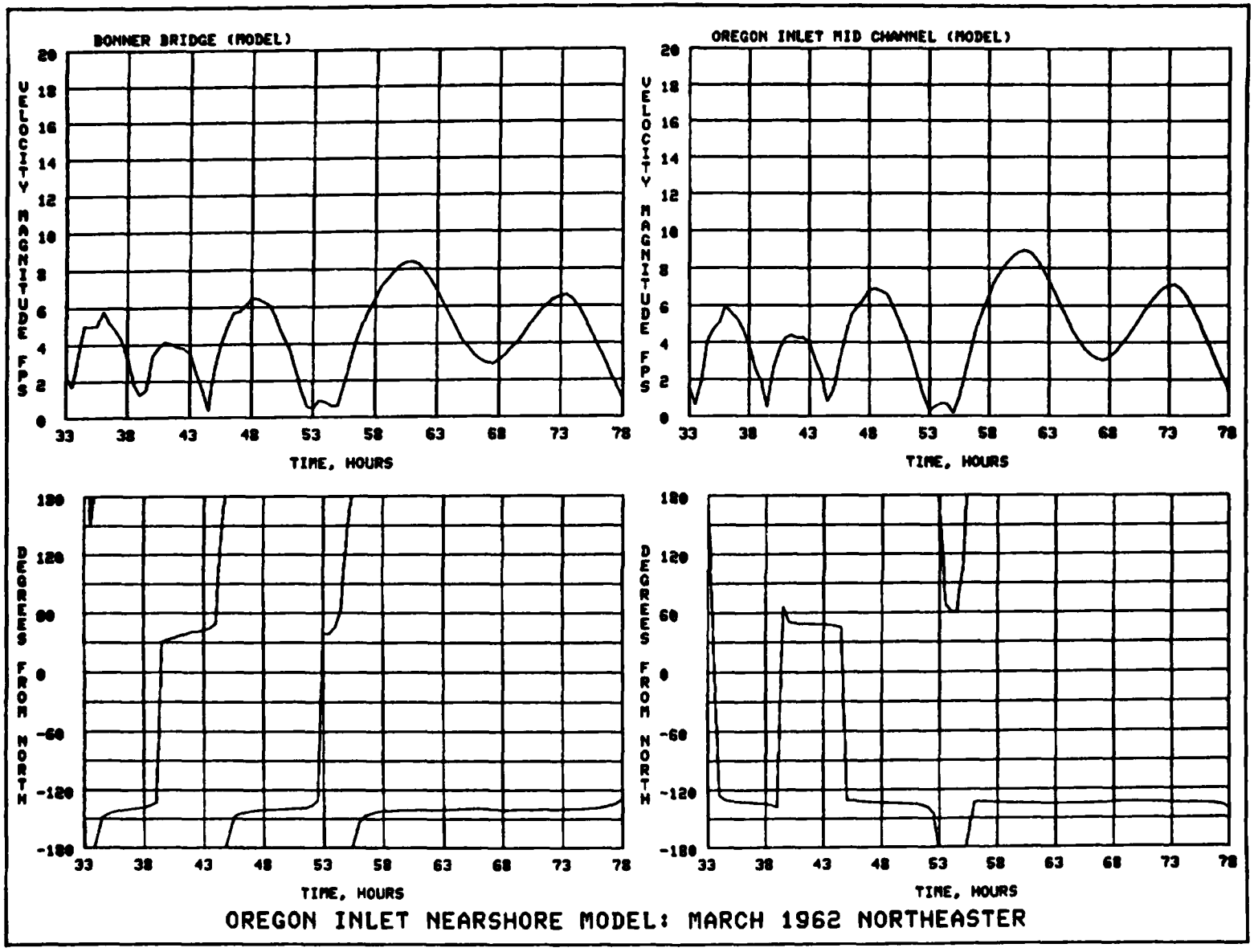

OREGON INLET NEARSHORE MODEL: MARCH 1962 NORTHEASTER

PLATE 25

PLATE 26

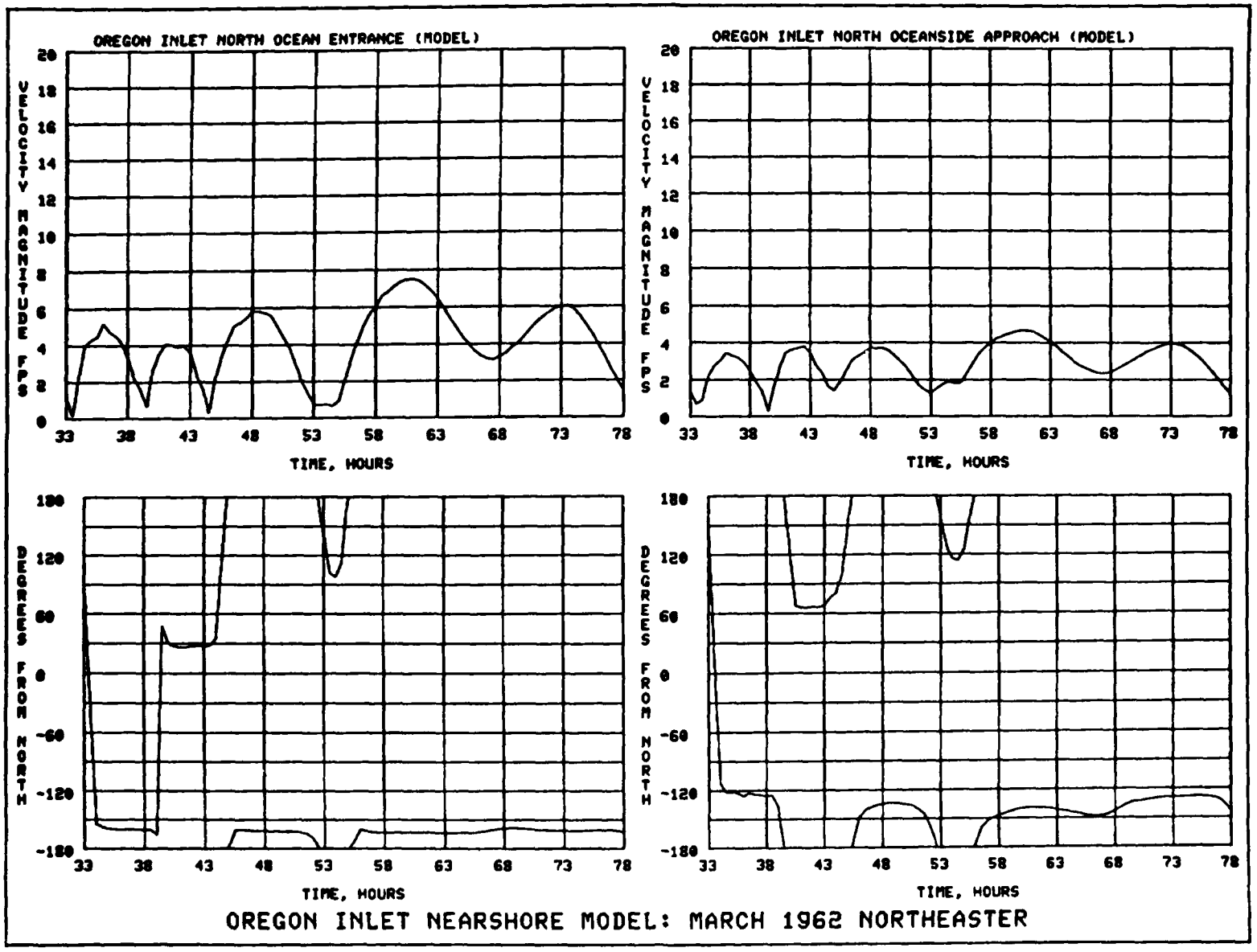

OREGON INLET NEARSHORE MODEL: MARCH 1962 NORTHEASTER

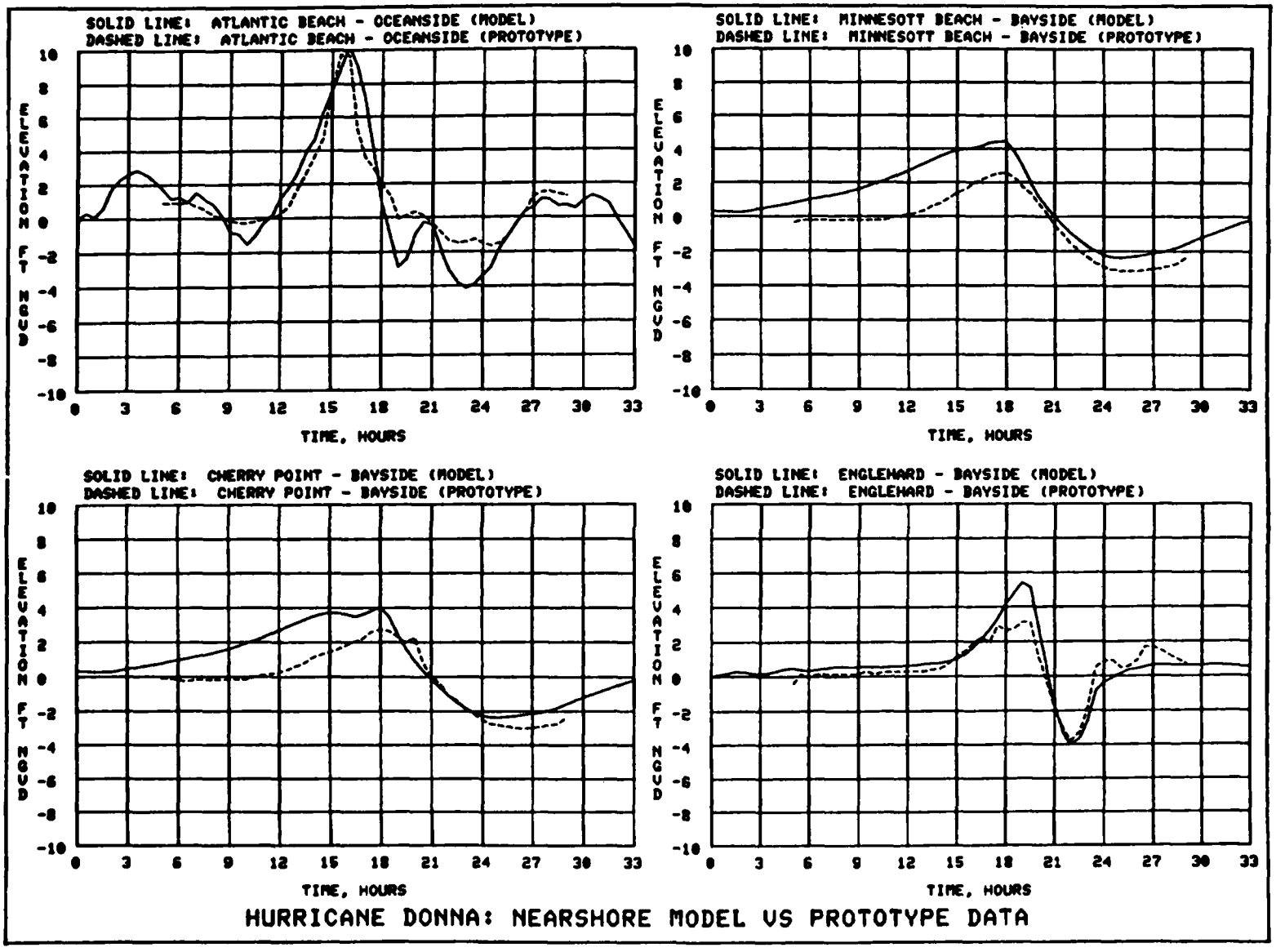

HURRICANE DONNA: NEARSHORE MODEL VS PROTOTYPE DATA

PLATE 27

PLATE 28

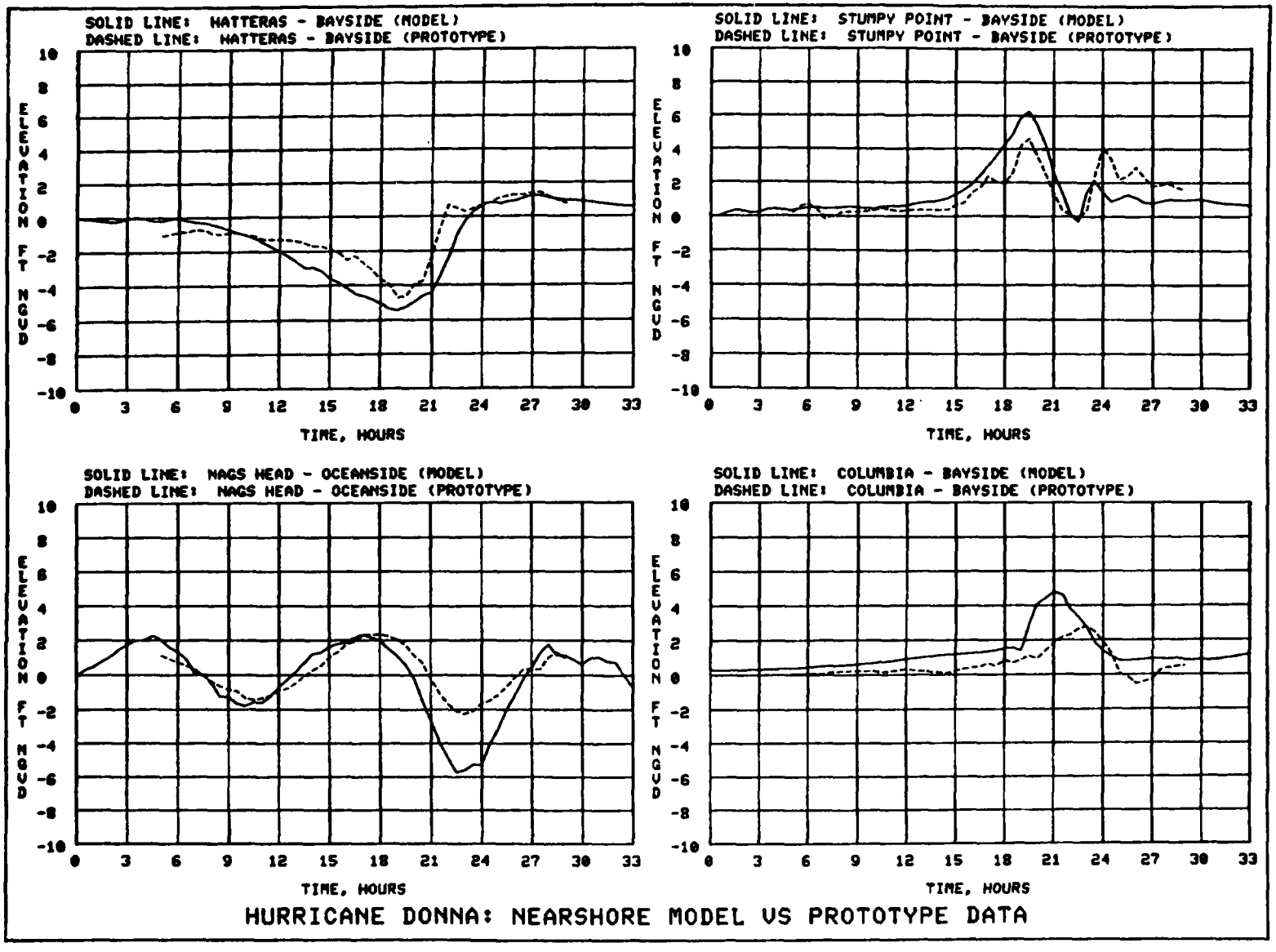

HURRICANE DONNA: NEARSHORE MODEL VS PROTOTYPE DATA

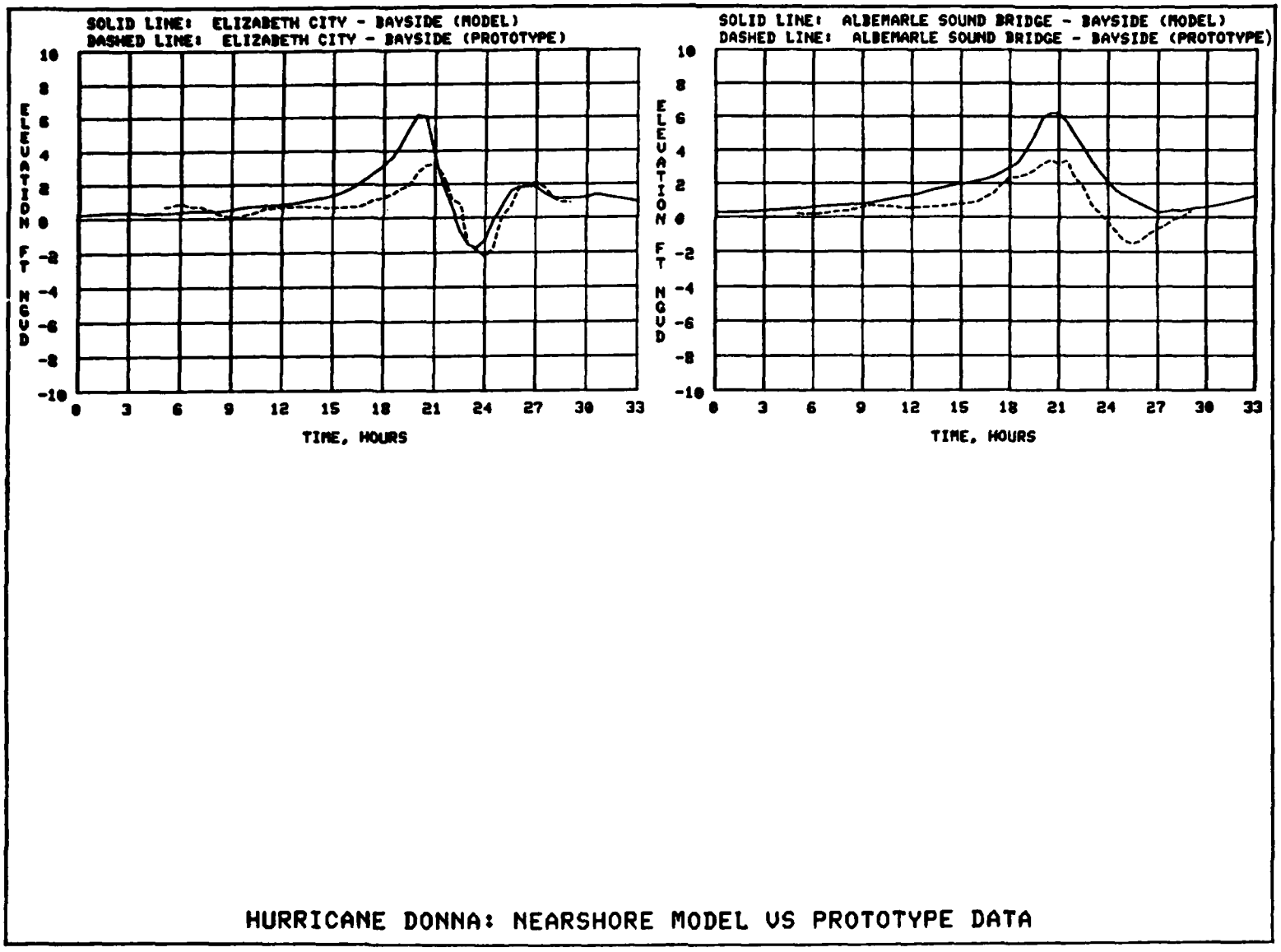

HURRICANE DONNA: NEARSHORE MODEL VS PROTOTYPE DATA

PLATE 29

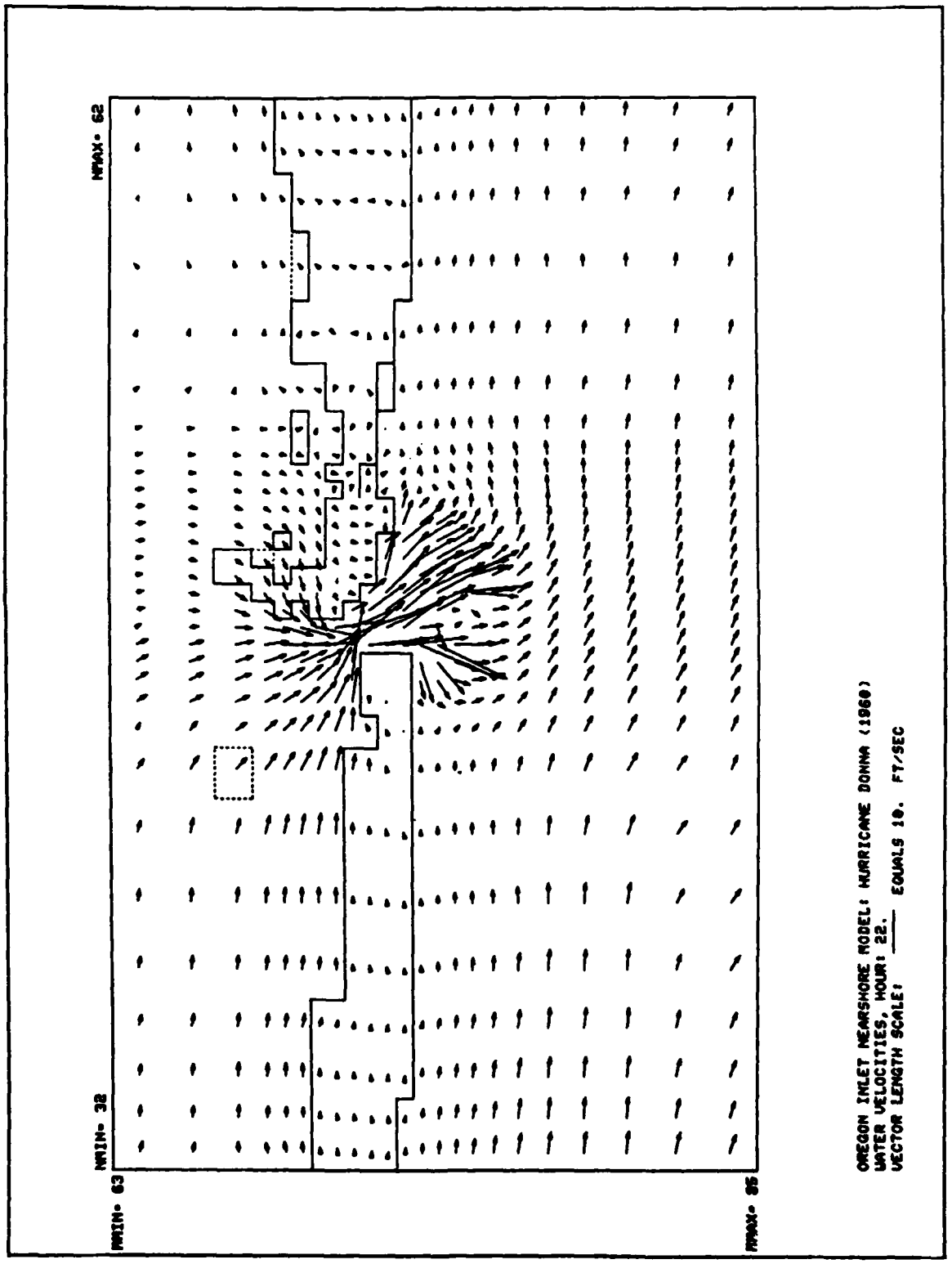
NMAX= 62
NMIN= 38
MMIN= 63
MMAX= 85
OREGON INLET NEARSHORE MODEL: HURRICANE DONNA (1960)
WATER VELOCITIES, HOUR: 22.
VECTOR LENGTH SCALE: ____ EQUALS 10. FT/SEC

PLATE 30

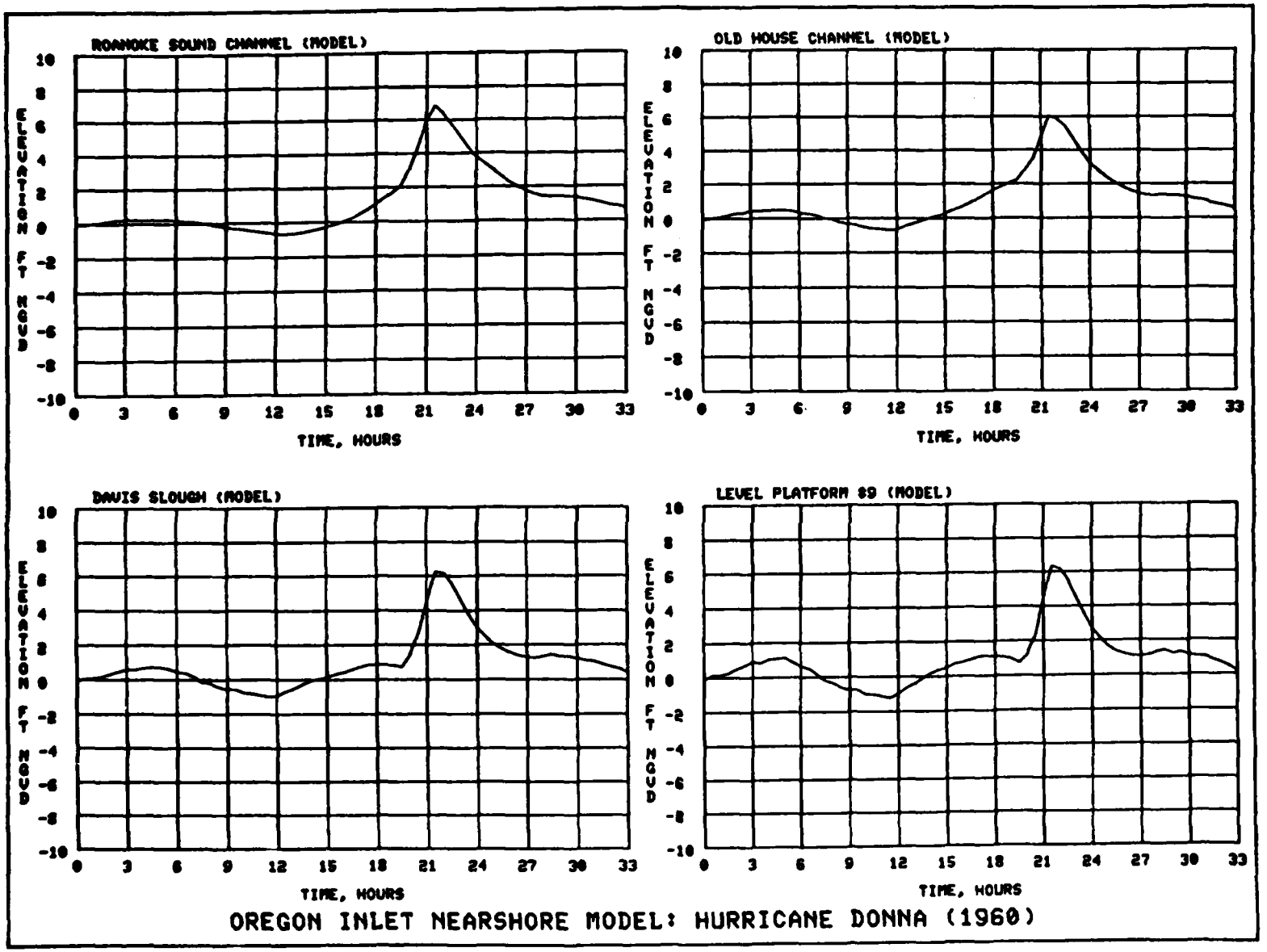

OREGON INLET NEARSHORE MODEL: HURRICANE DONNA (1960)

PLATE 31

PLATE 32

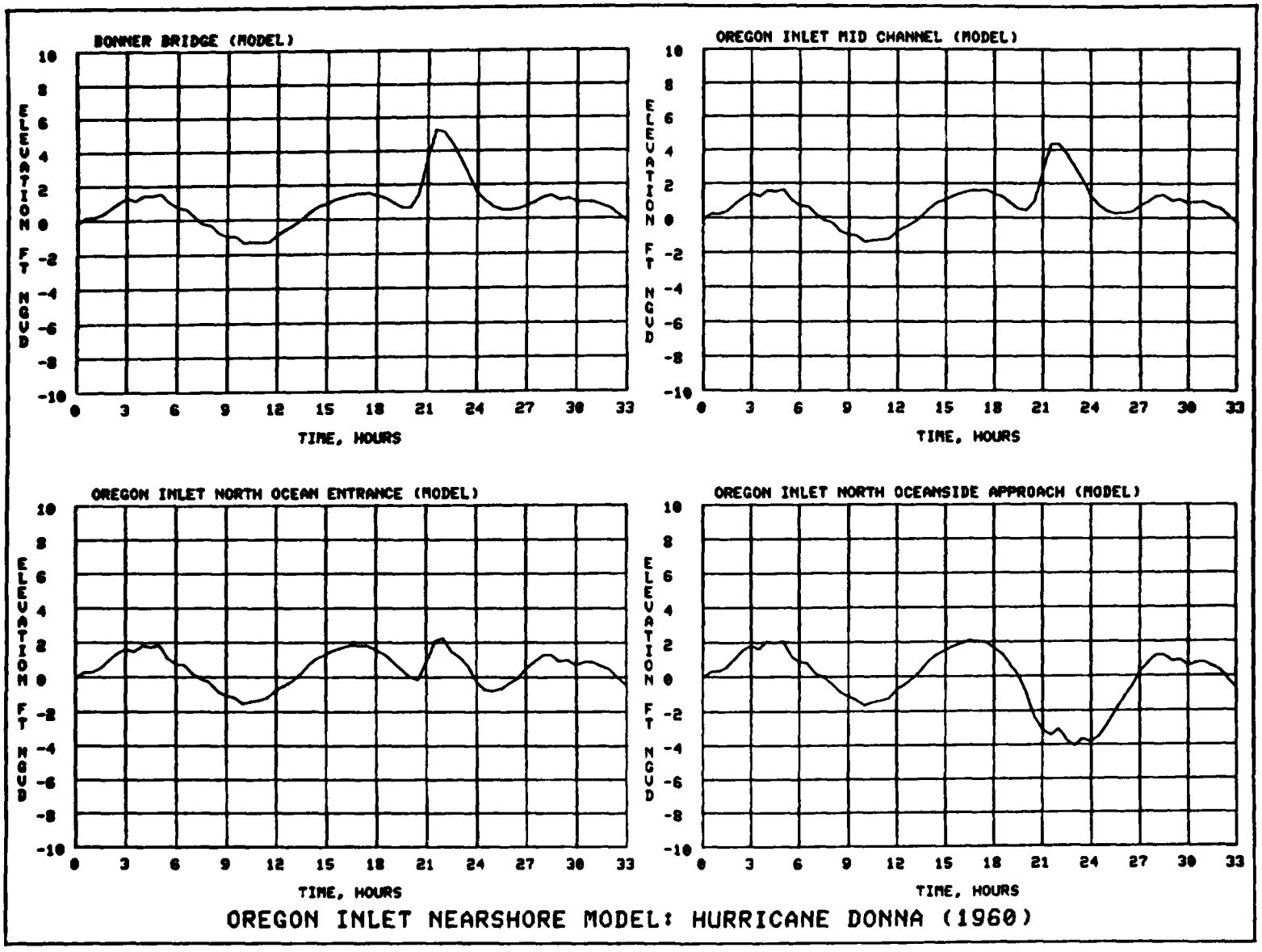

OREGON INLET NEARSHORE MODEL: HURRICANE DONNA (1960)

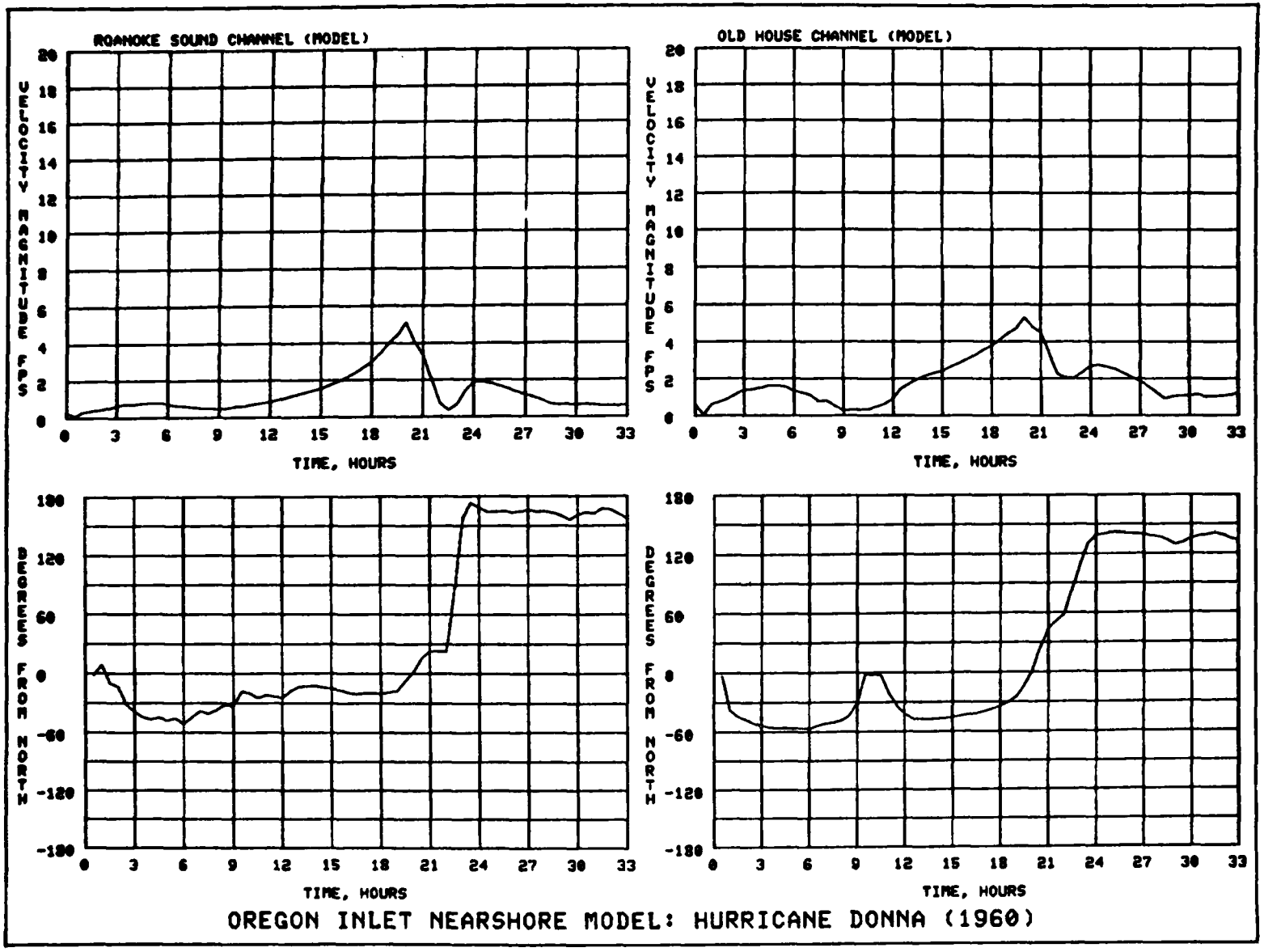

OREGON INLET NEARSHORE MODEL: HURRICANE DONNA (1960)

PLATE 33

PLATE 34

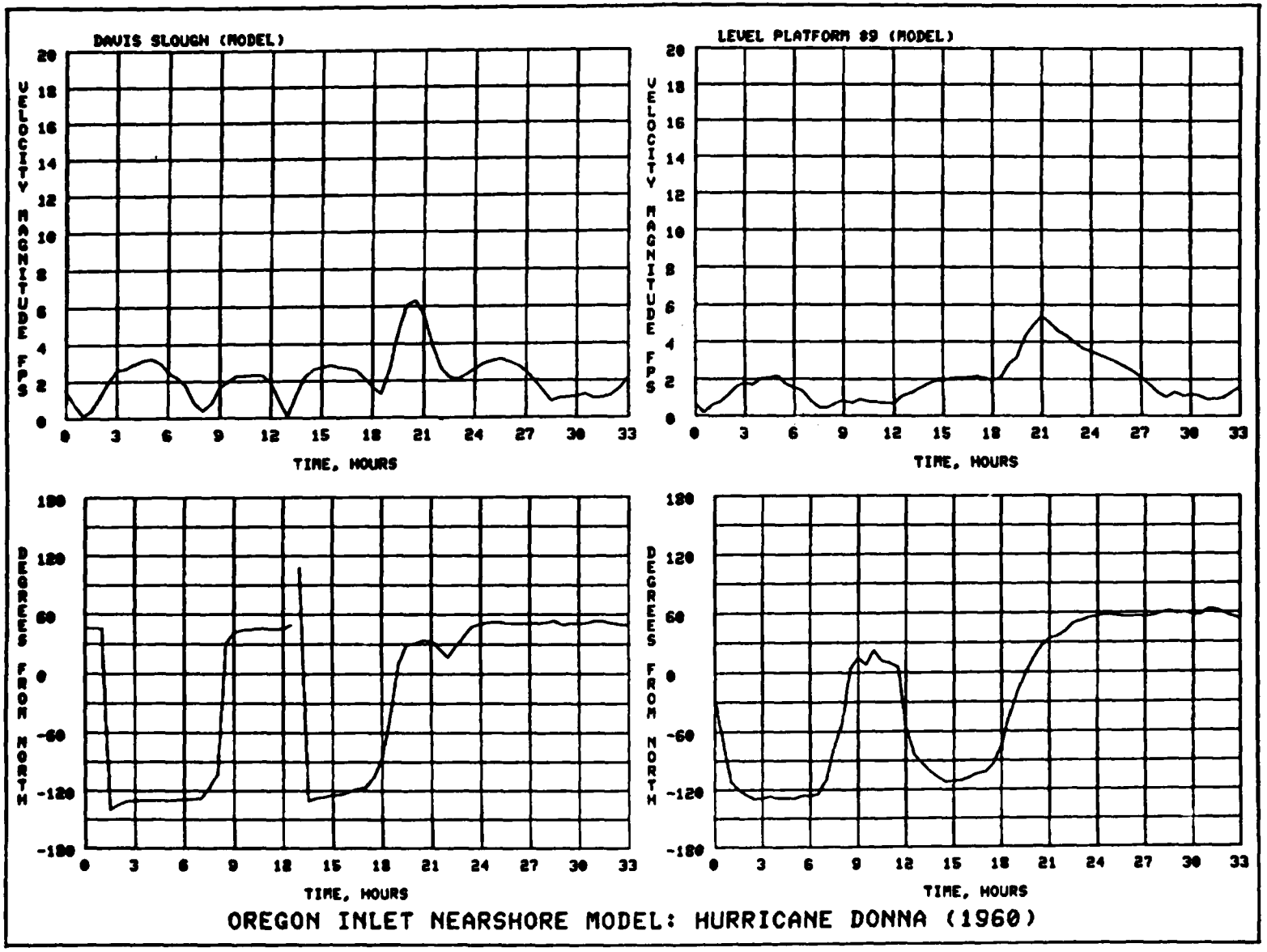

OREGON INLET NEARSHORE MODEL: HURRICANE DONNA (1960)

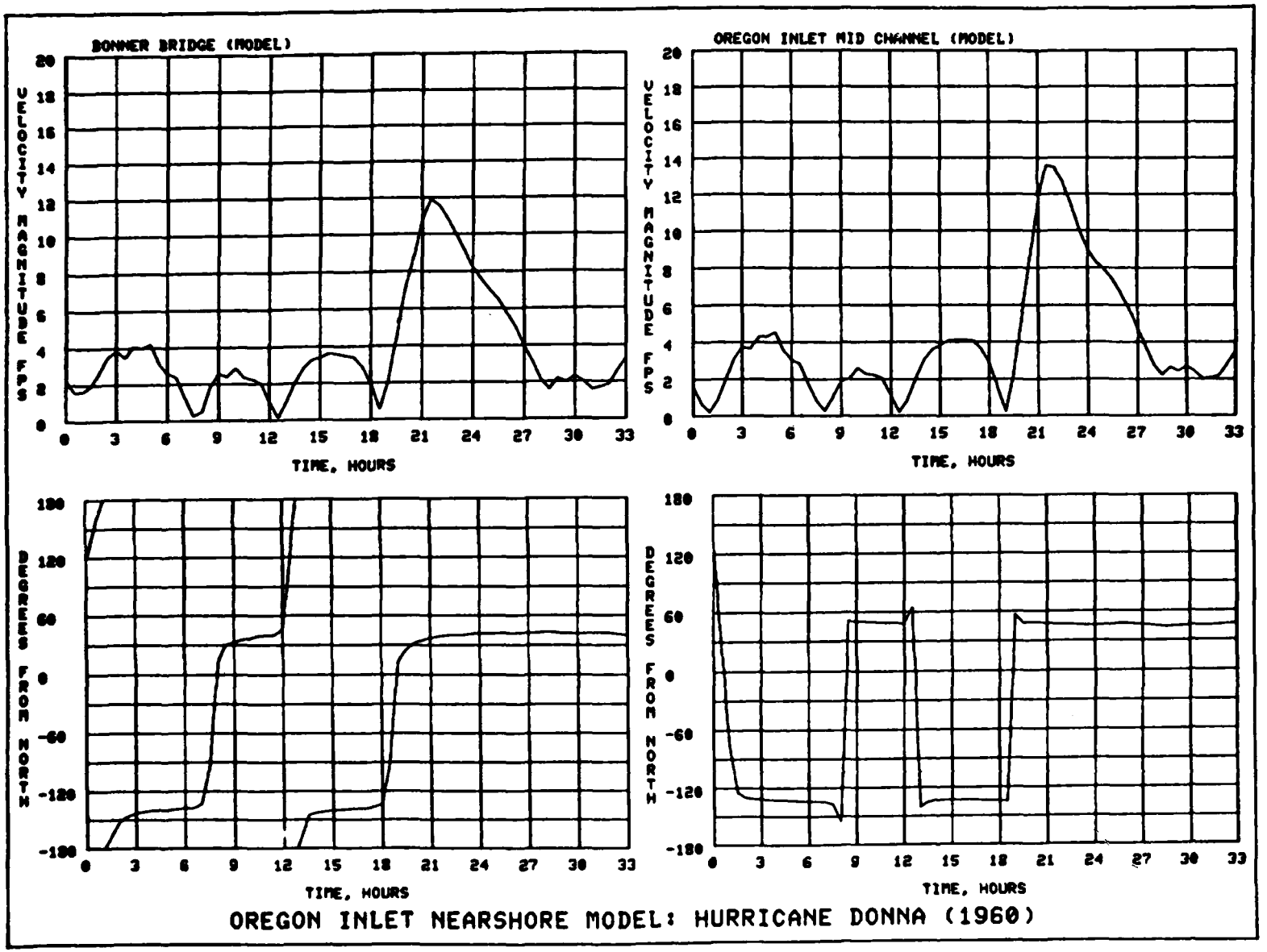

OREGON INLET NEARSHORE MODEL: HURRICANE DONNA (1960)

PLATE 35

PLATE 36

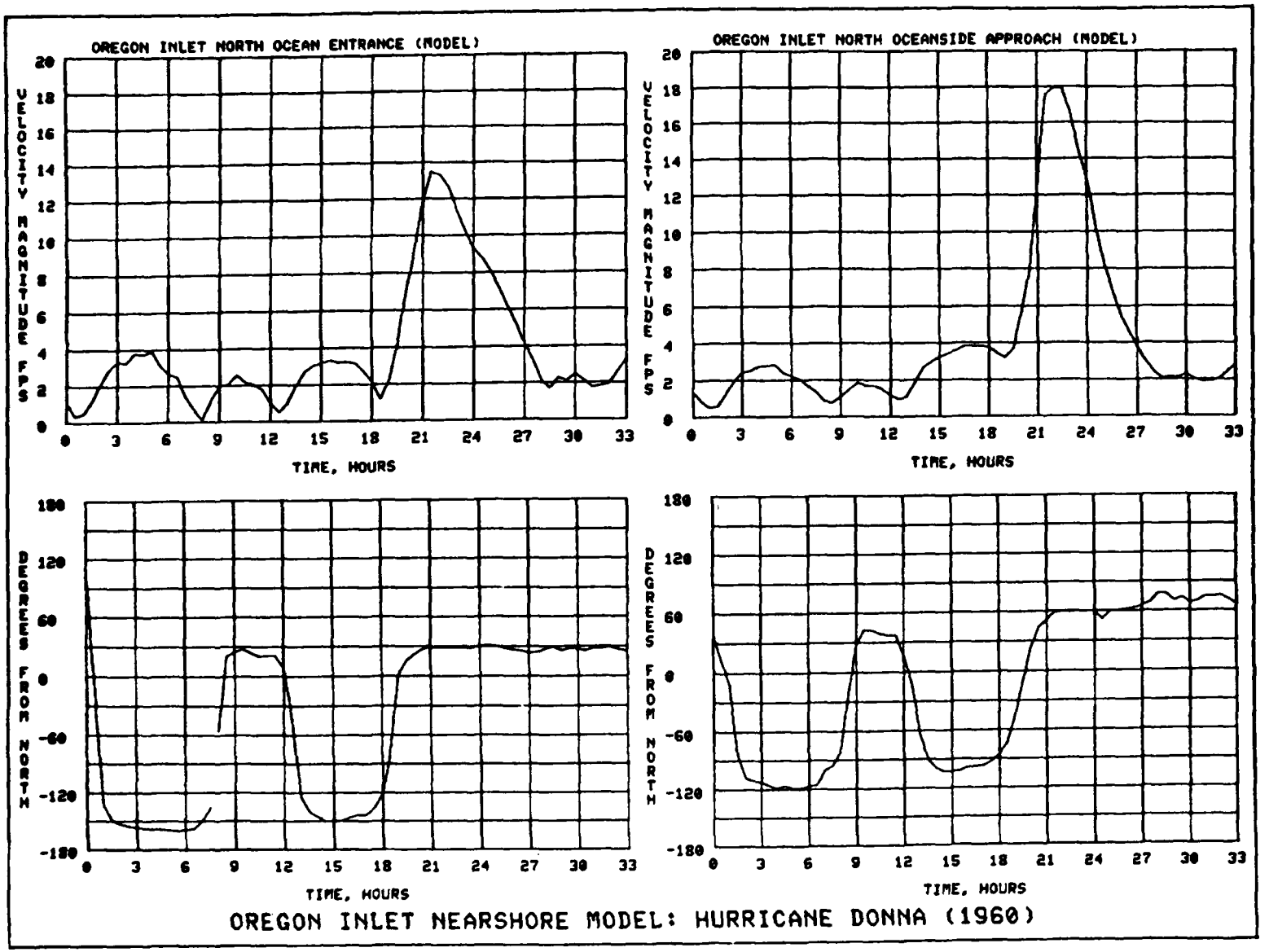

OREGON INLET NEARSHORE MODEL: HURRICANE DONNA (1960)

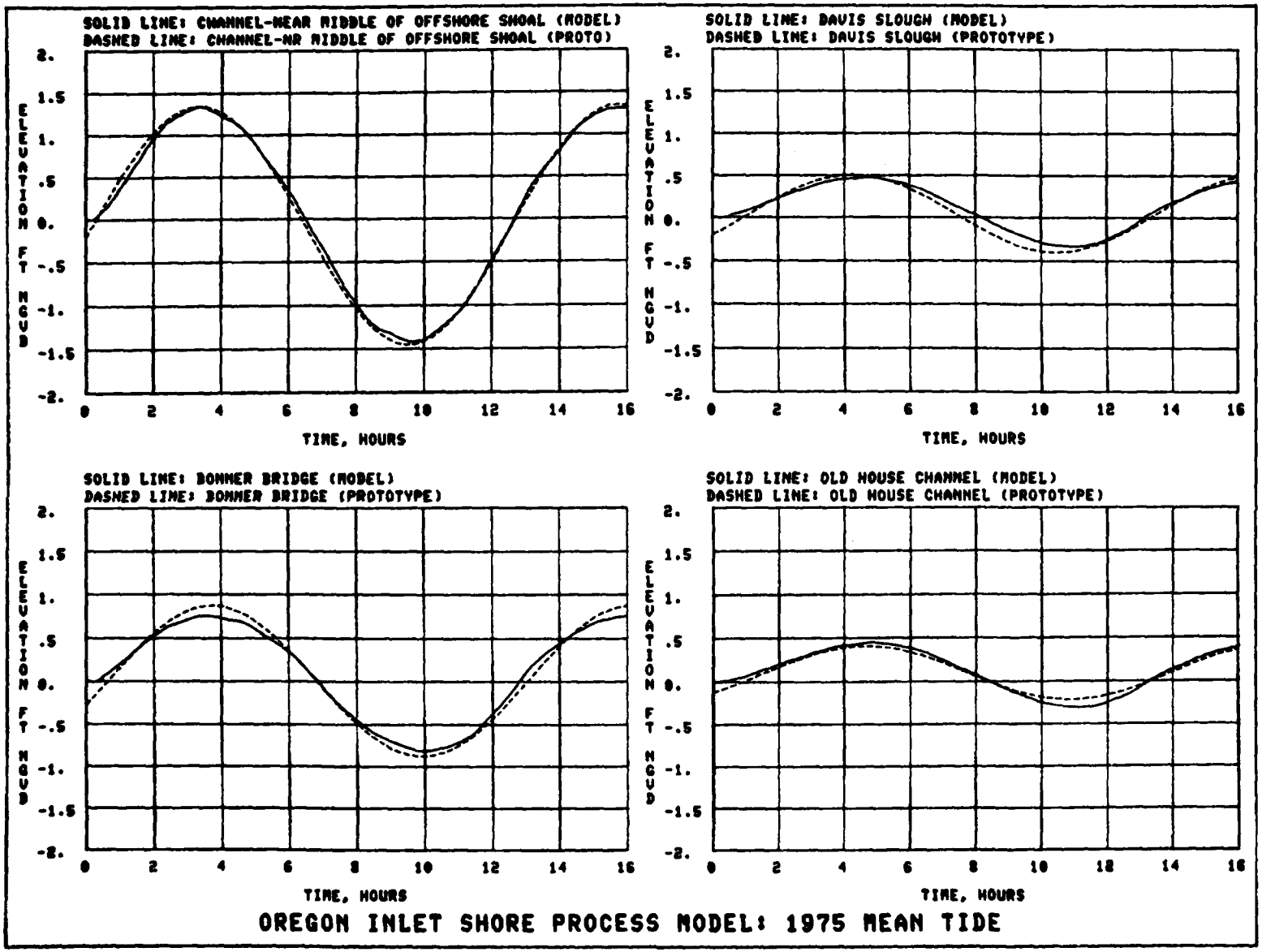

OREGON INLET SHORE PROCESS MODEL: 1975 MEAN TIDE

PLATE 37

PLATE 38

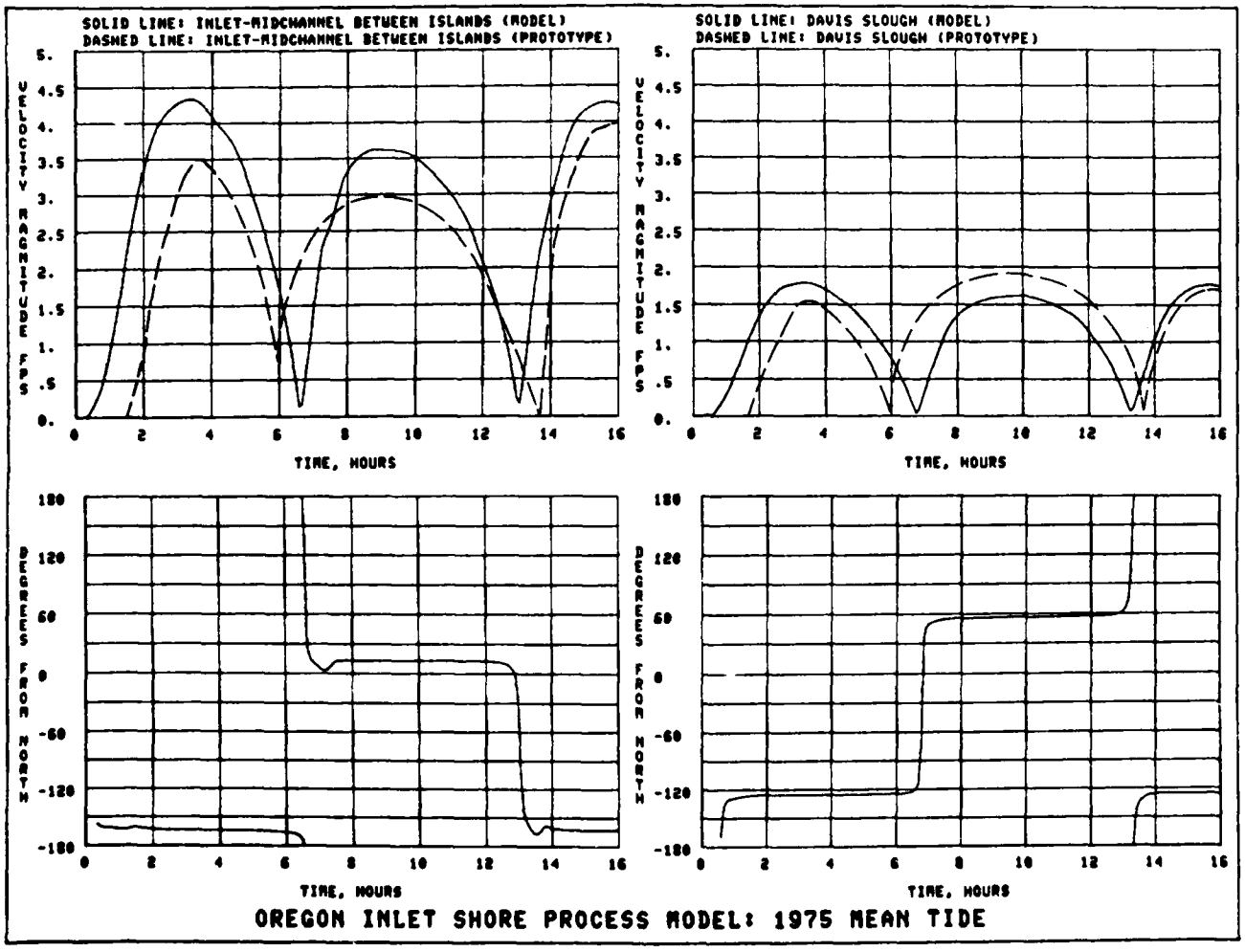

OREGON INLET SHORE PROCESS MODEL: 1975 MEAN TIDE

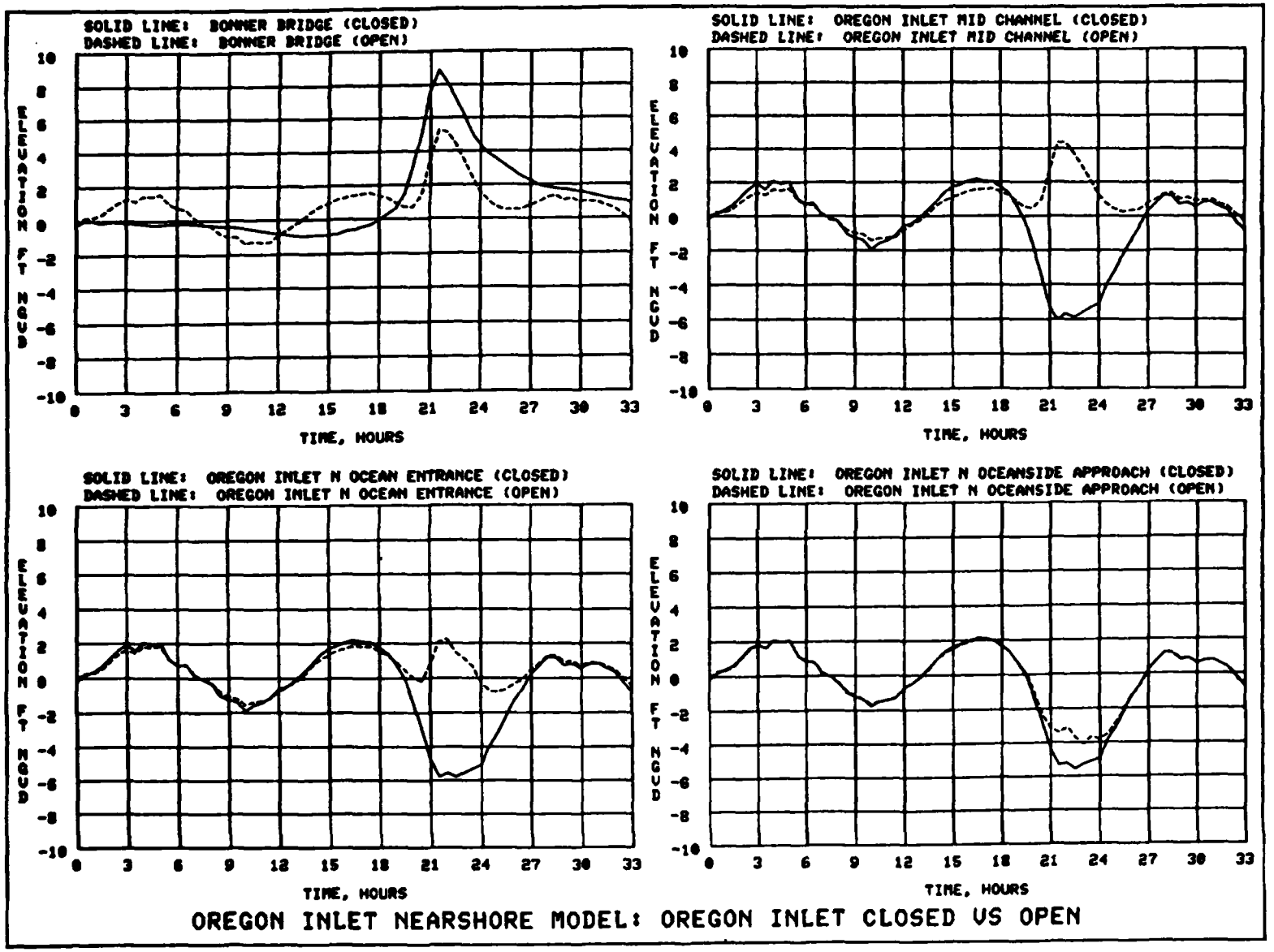

OREGON INLET NEARSHORE MODEL: OREGON INLET CLOSED VS OPEN

PLATE 39

PLATE 40

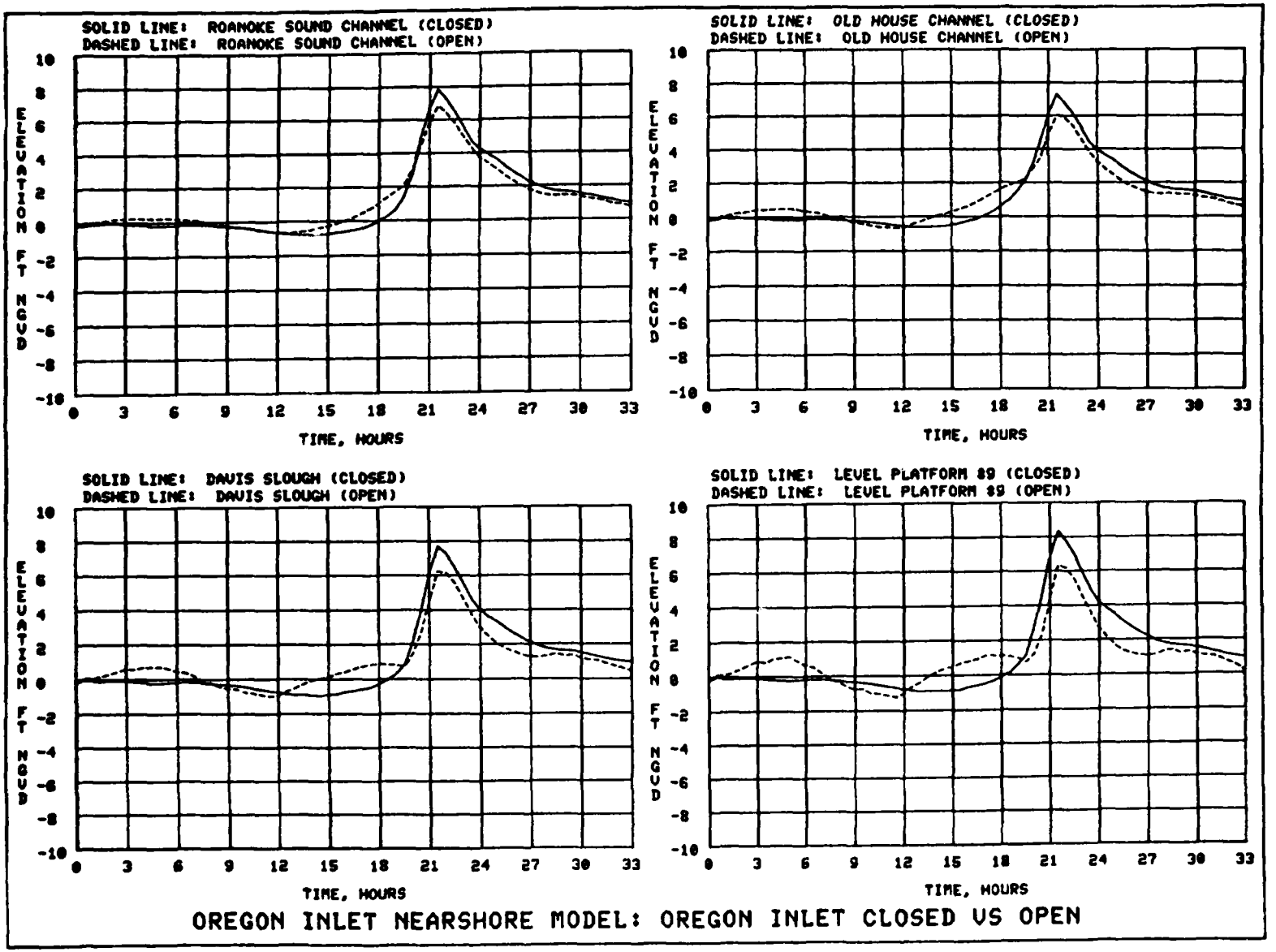

OREGON INLET NEARSHORE MODEL: OREGON INLET CLOSED VS OPEN

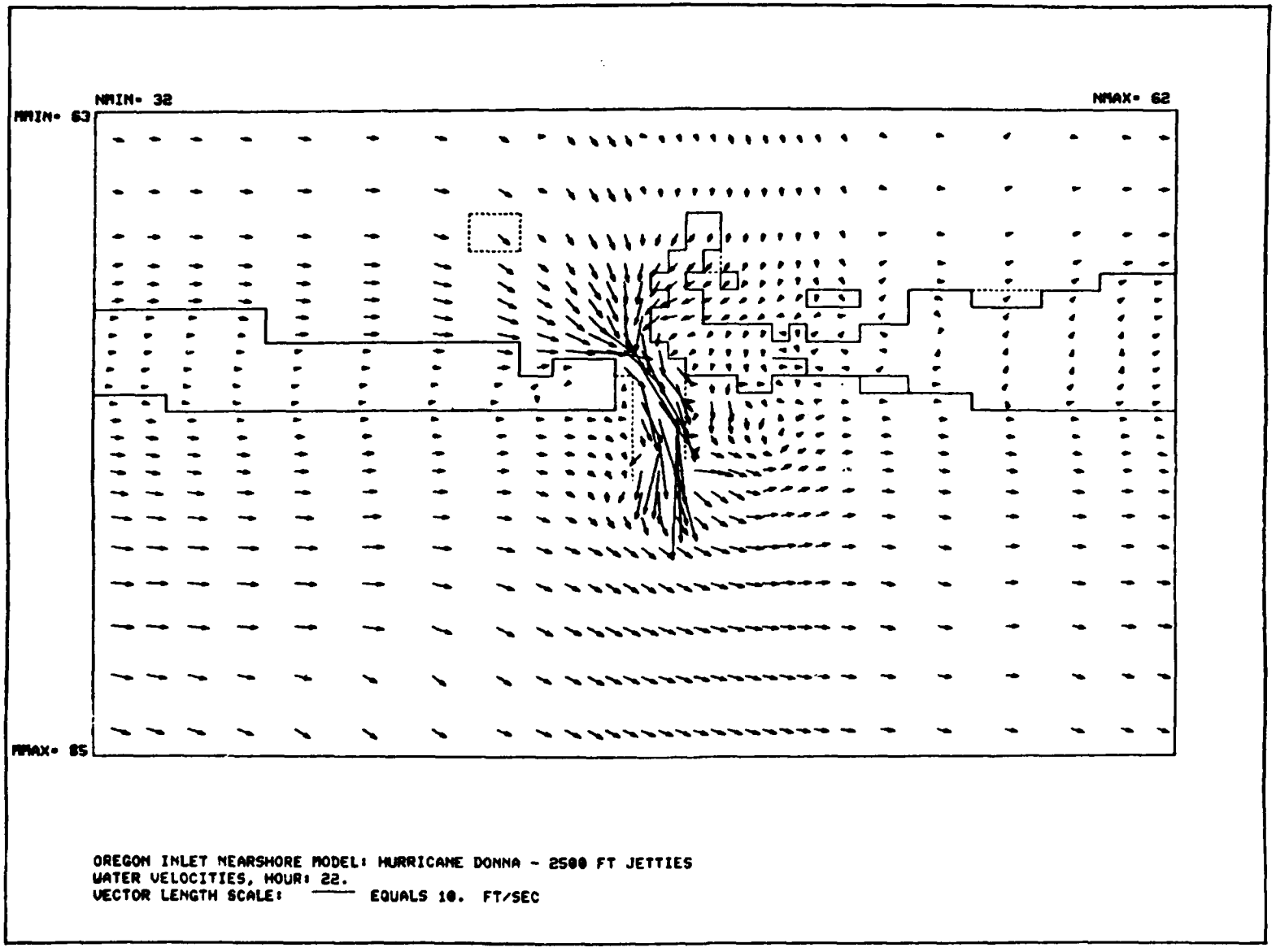

OREGON INLET NEARSHORE MODEL: HURRICANE DONNA - 2500 FT JETTIES
WATER VELOCITIES, HOUR: 22.
VECTOR LENGTH SCALE: ——— EQUALS 10. FT/SEC

PLATE 41

AD-A142 920 NUMERICAL SIMULATION OF OREGON INLET CONTROL STRUCTURES' EFFECTS ON STORM..(U) COASTAL ENGINEERING RESEARCH CENTER VICKSBURG MS D A LEENKNECHT ET AL. 2/2

UNCLASSIFIED APR 84 CERC-TR-84-2 F/G 8/3 NL

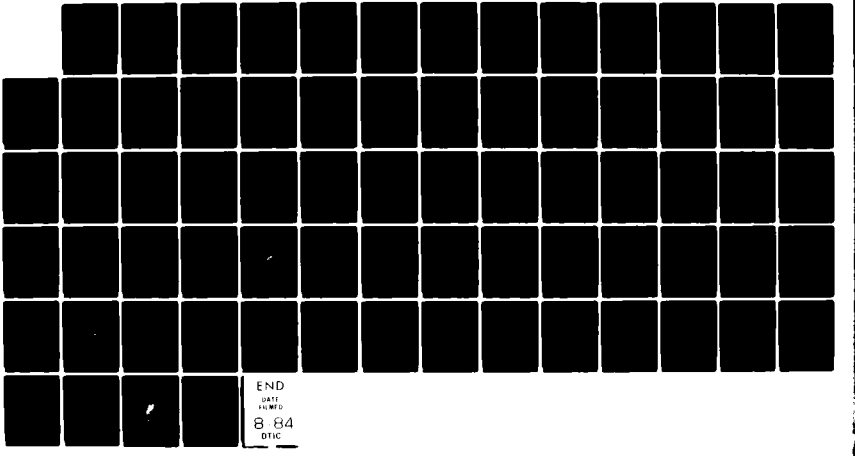

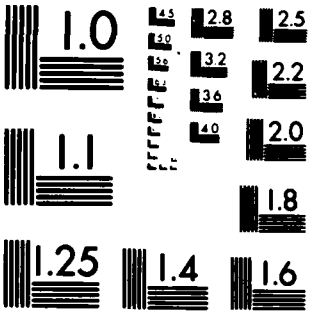

MICROCOPY RESOLUTION TEST CHART
NATIONAL BUREAU OF STANDARDS-1963-A

PLATE 42

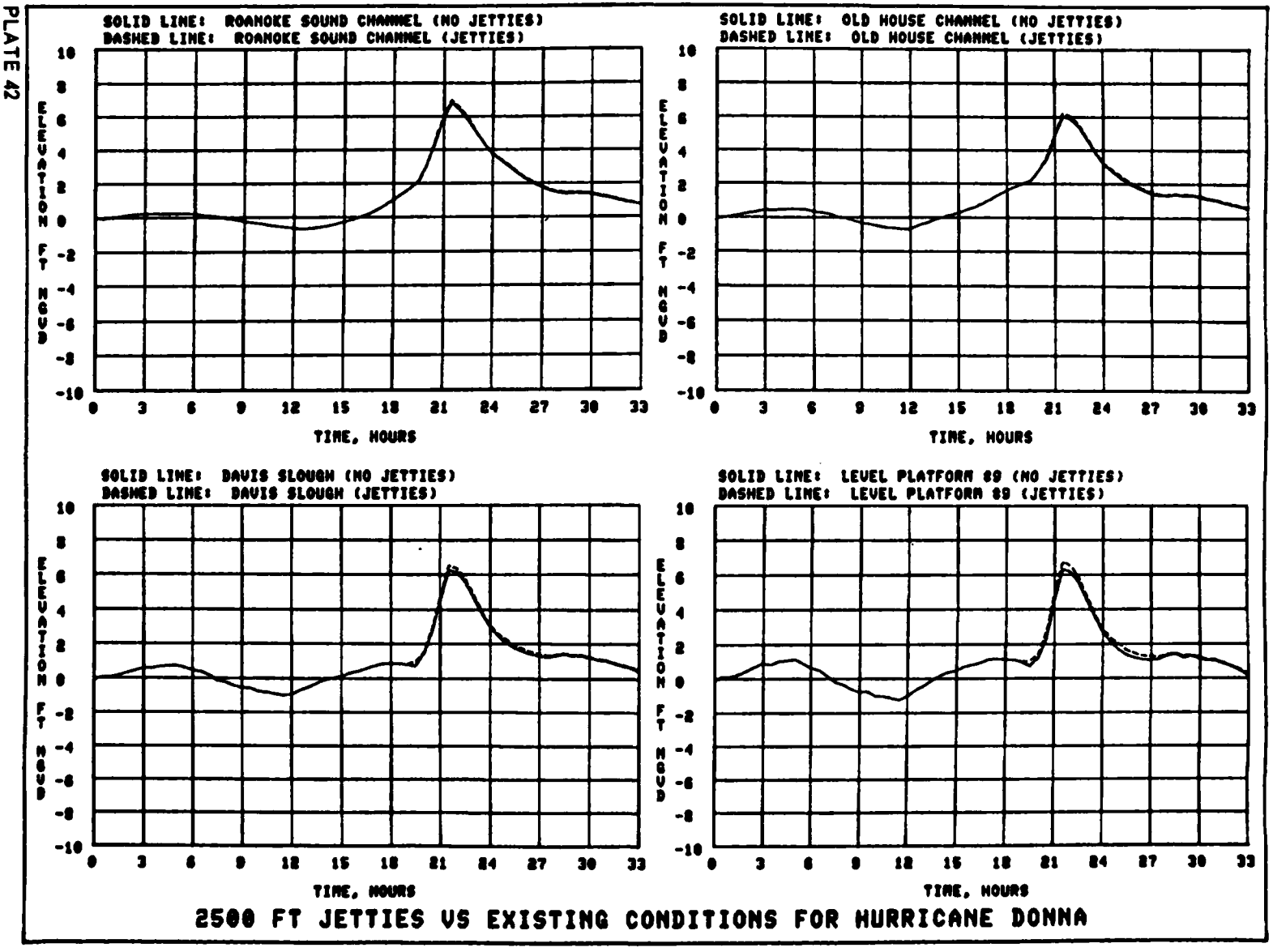
SOLID LINE: ROANOKE SOUND CHANNEL (NO JETTIES)
DASHED LINE: ROANOKE SOUND CHANNEL (JETTIES)
ELEVATION FT NGVD
TIME, HOURS
SOLID LINE: OLD HOUSE CHANNEL (NO JETTIES)
DASHED LINE: OLD HOUSE CHANNEL (JETTIES)
ELEVATION FT NGVD
TIME, HOURS
SOLID LINE: DAVIS SLOUGH (NO JETTIES)
DASHED LINE: DAVIS SLOUGH (JETTIES)
ELEVATION FT NGVD
TIME, HOURS
SOLID LINE: LEVEL PLATFORM 89 (NO JETTIES)
DASHED LINE: LEVEL PLATFORM 89 (JETTIES)
ELEVATION FT NGVD
TIME, HOURS
2500 FT JETTIES VS EXISTING CONDITIONS FOR HURRICANE DONNA

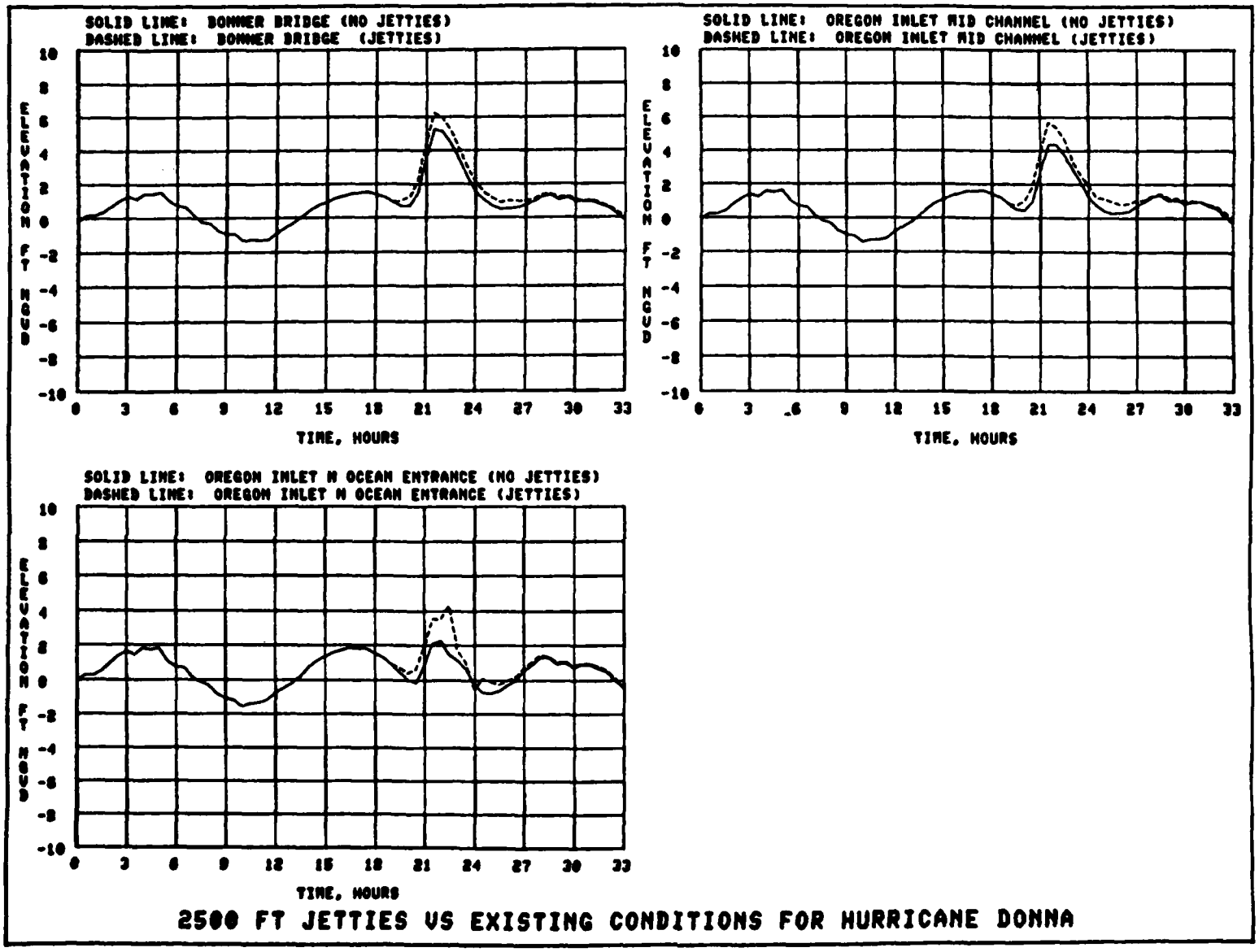

PLATE 43

2500 FT JETTIES VS EXISTING CONDITIONS FOR HURRICANE DONNA

PLATE 44

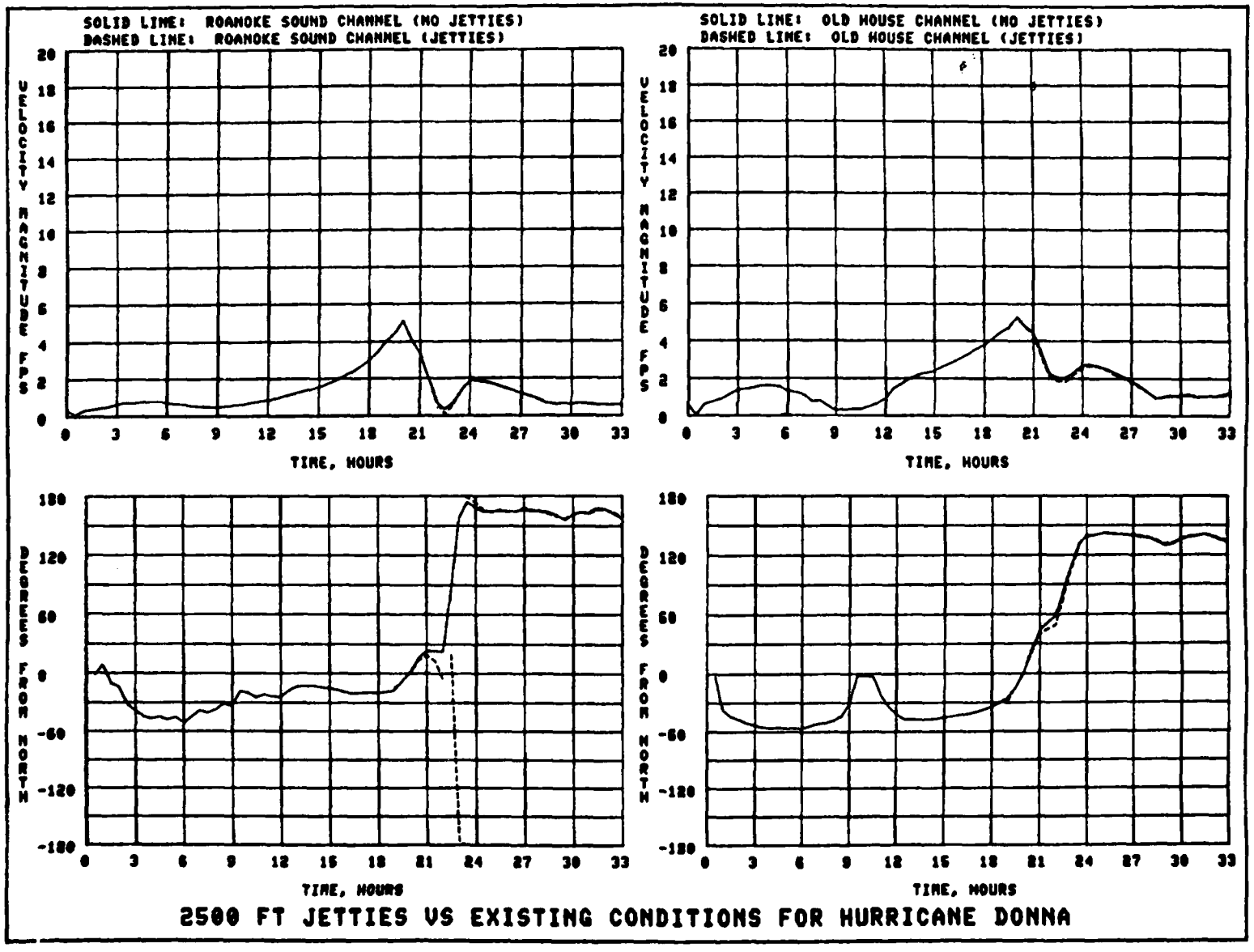

2500 FT JETTIES VS EXISTING CONDITIONS FOR HURRICANE DONNA

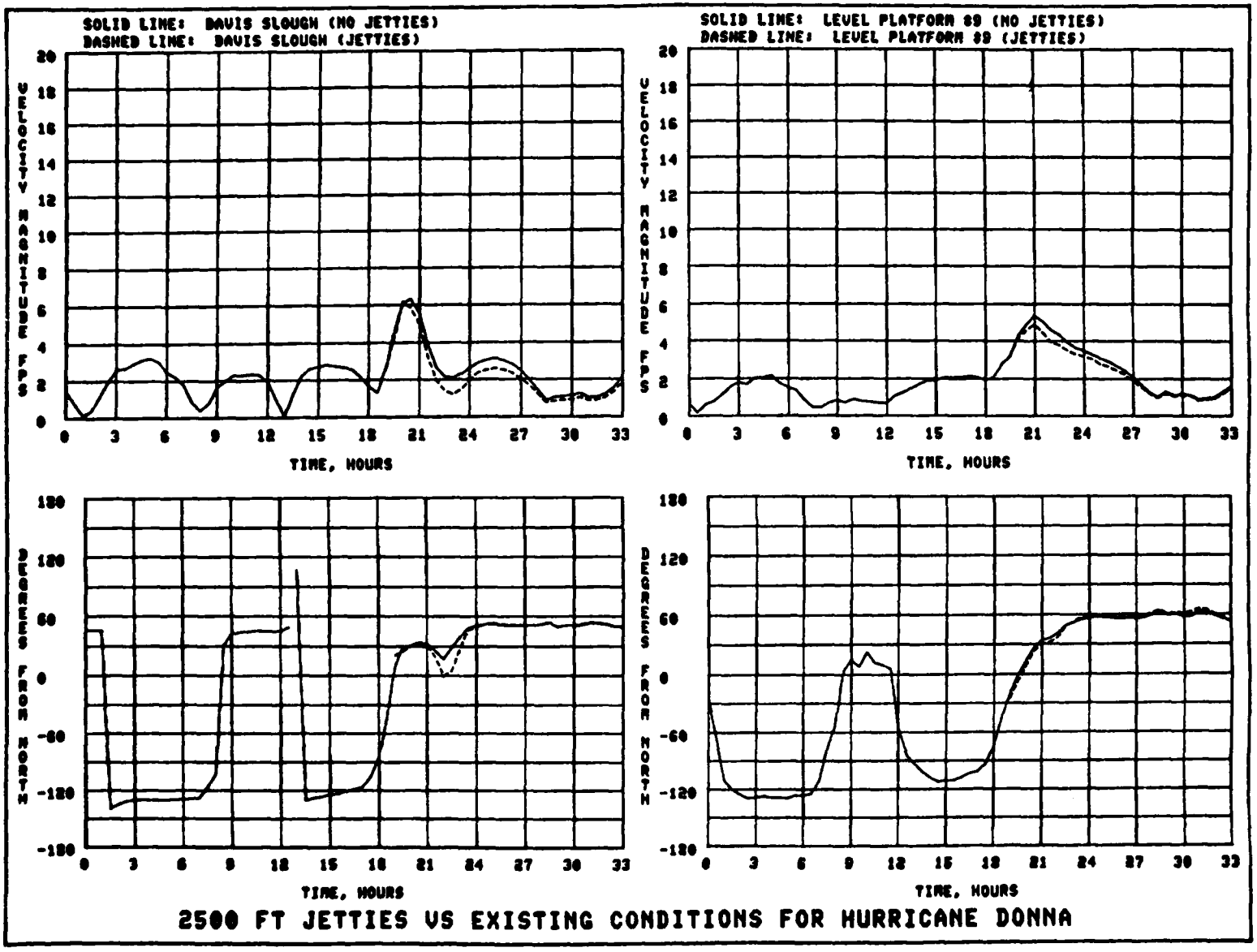

PLATE 45

2500 FT JETTIES VS EXISTING CONDITIONS FOR HURRICANE DONNA

PLATE 46

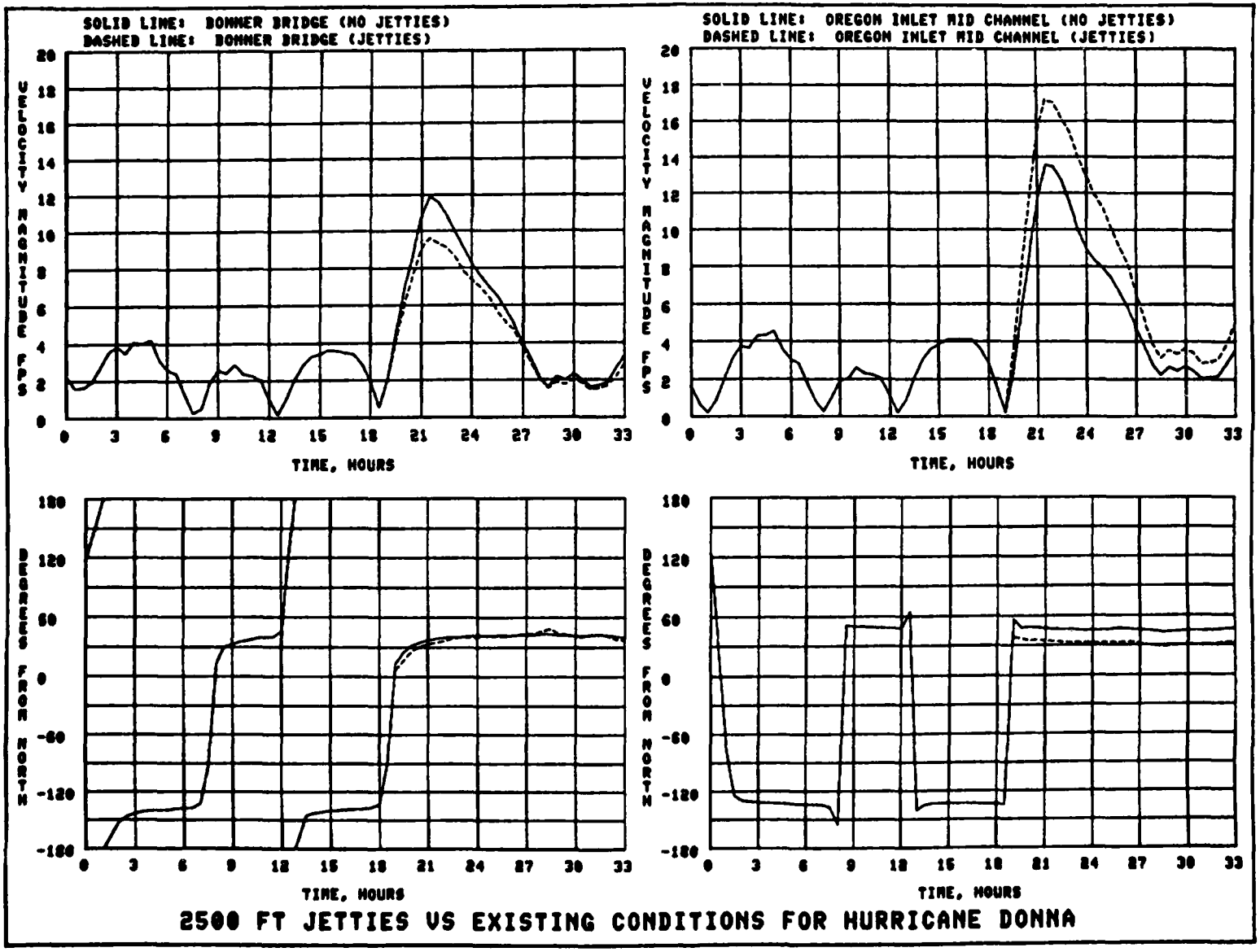

2500 FT JETTIES VS EXISTING CONDITIONS FOR HURRICANE DONNA

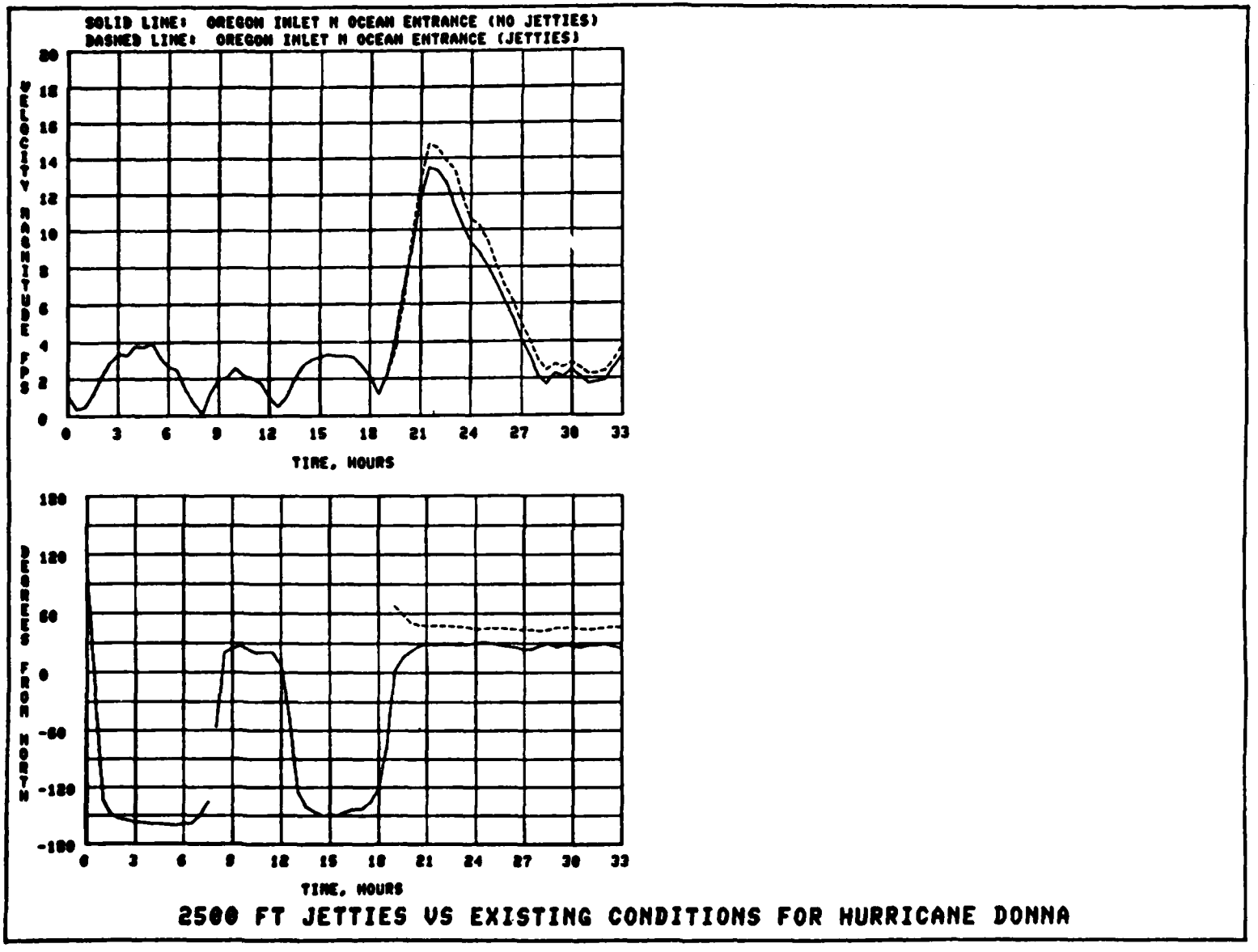

PLATE 47

2500 FT JETTIES VS EXISTING CONDITIONS FOR HURRICANE DONNA

PLATE 48

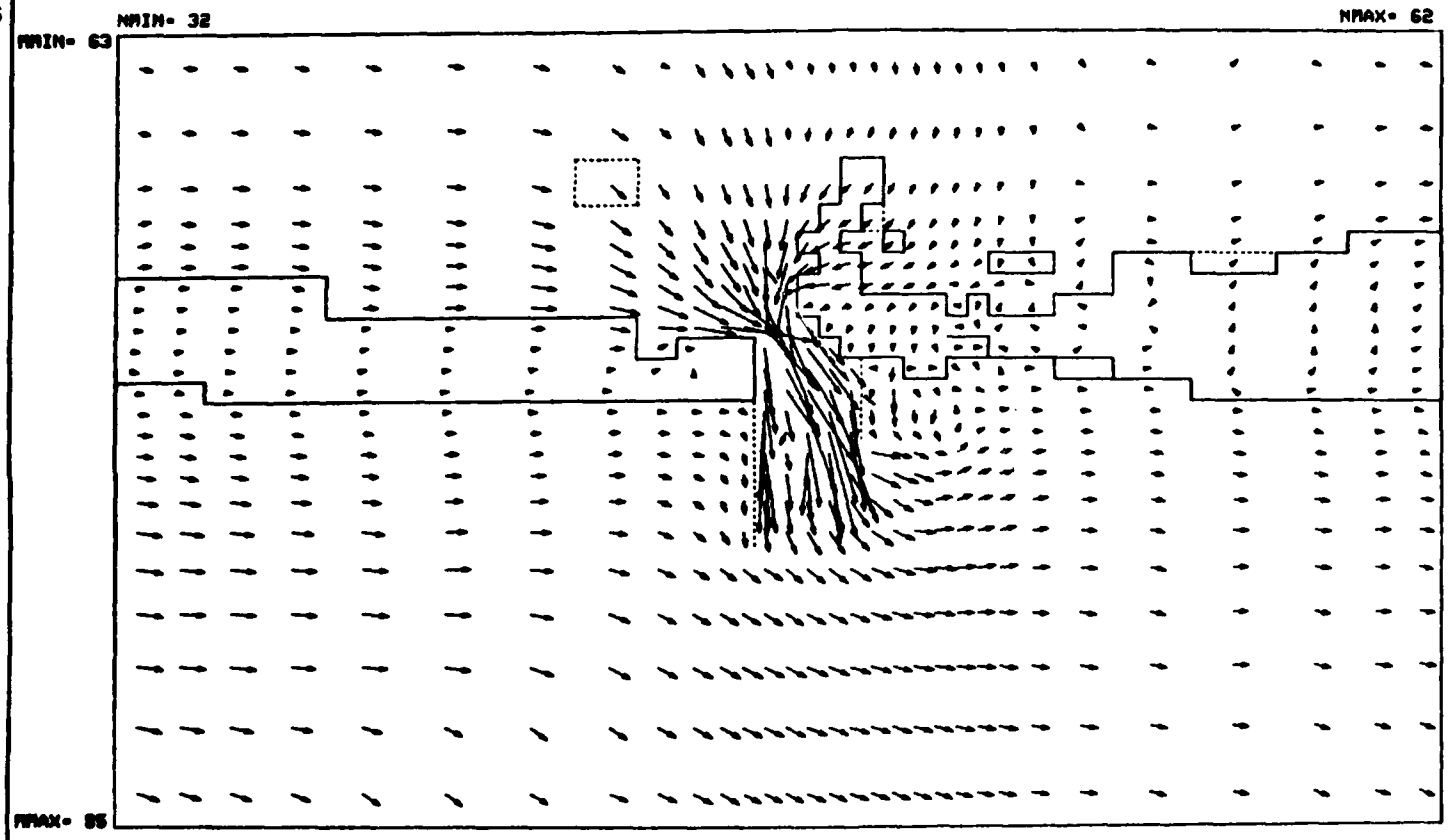

OREGON INLET NEARSHORE MODEL: HURRICANE DONNA - 5000 FT JETTIES
WATER VELOCITIES, HOUR: 22.
VECTOR LENGTH SCALE: ——— EQUALS 10. FT/SEC

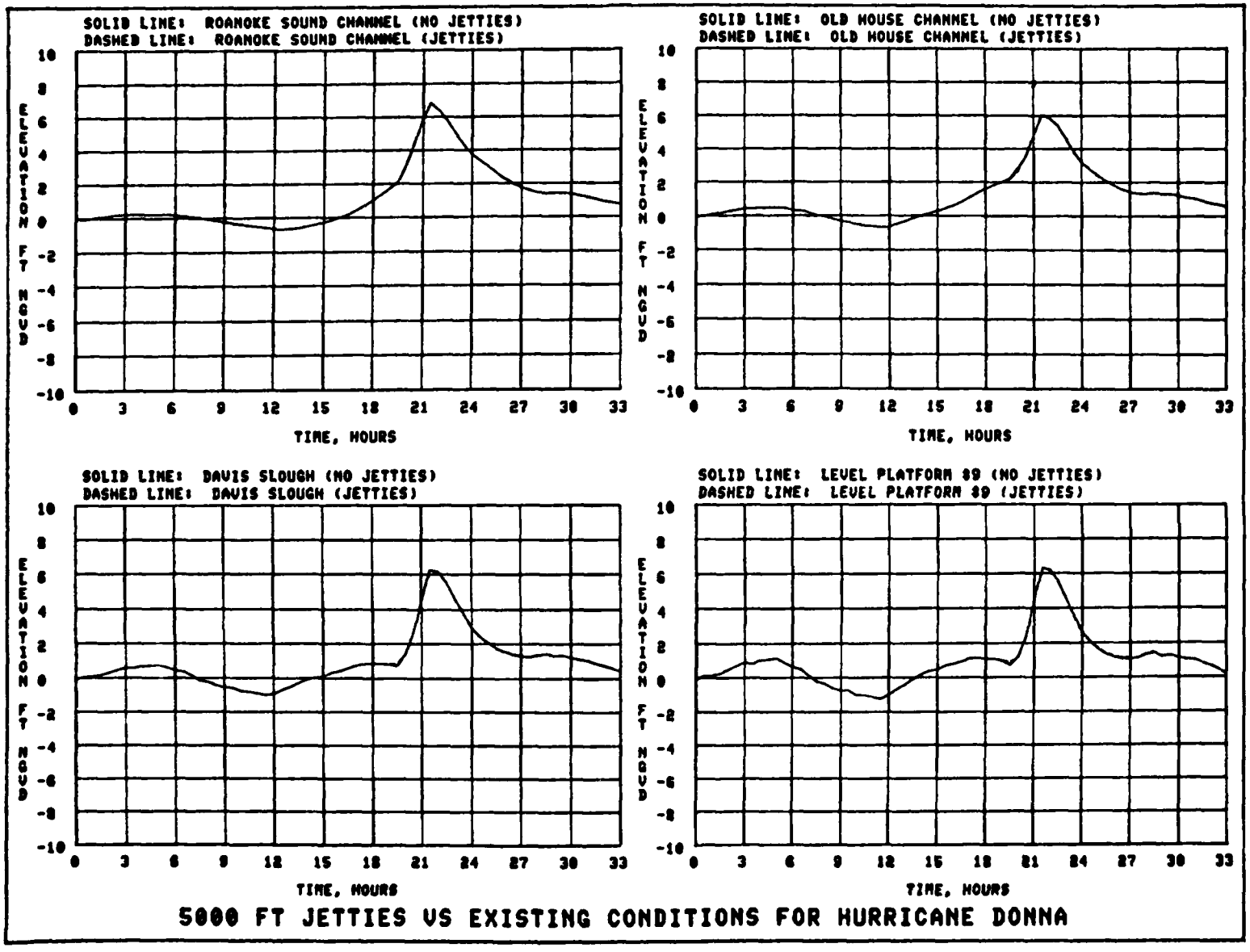

5000 FT JETTIES VS EXISTING CONDITIONS FOR HURRICANE DONNA

PLATE 49

PLATE 50

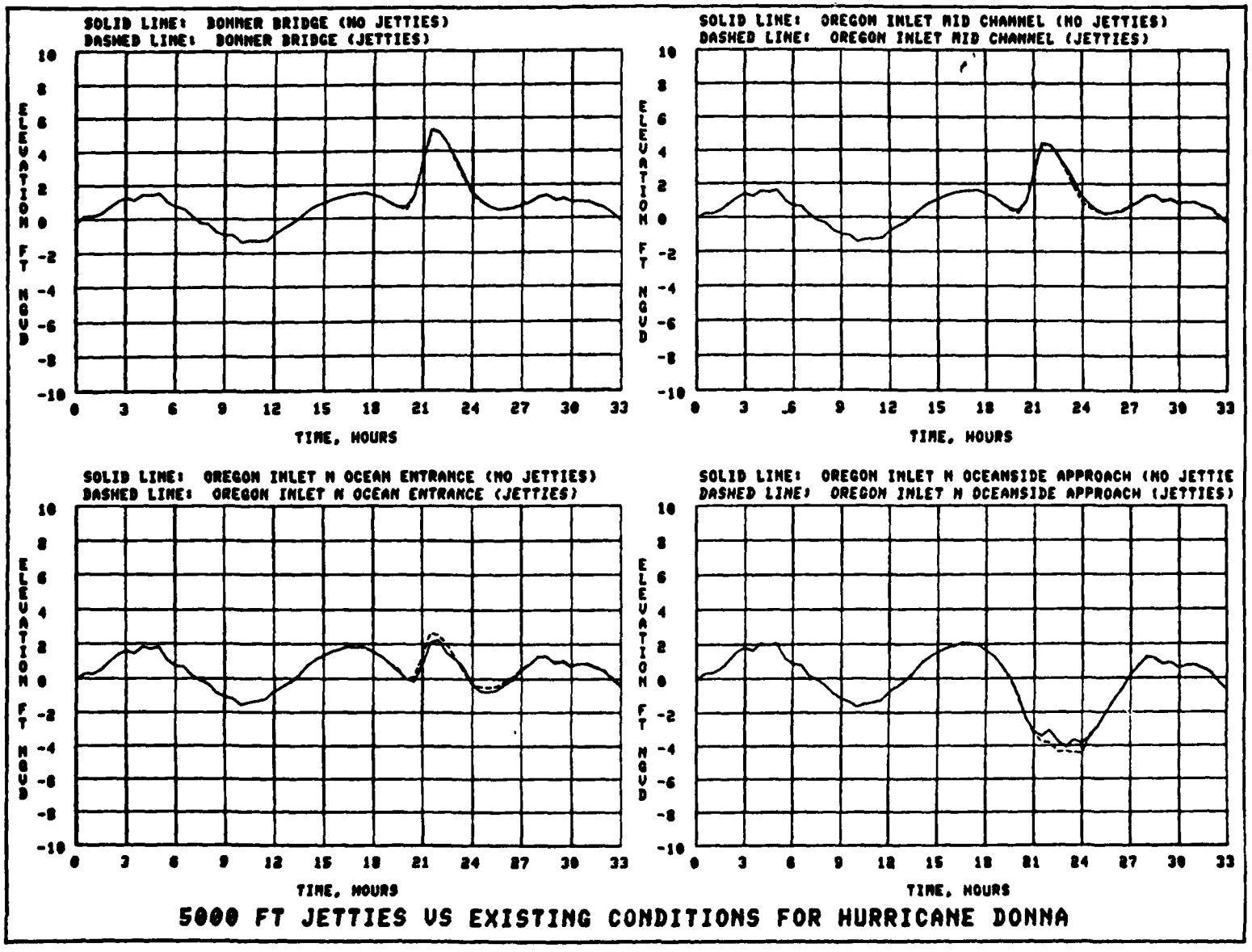

5000 FT JETTIES VS EXISTING CONDITIONS FOR HURRICANE DONNA

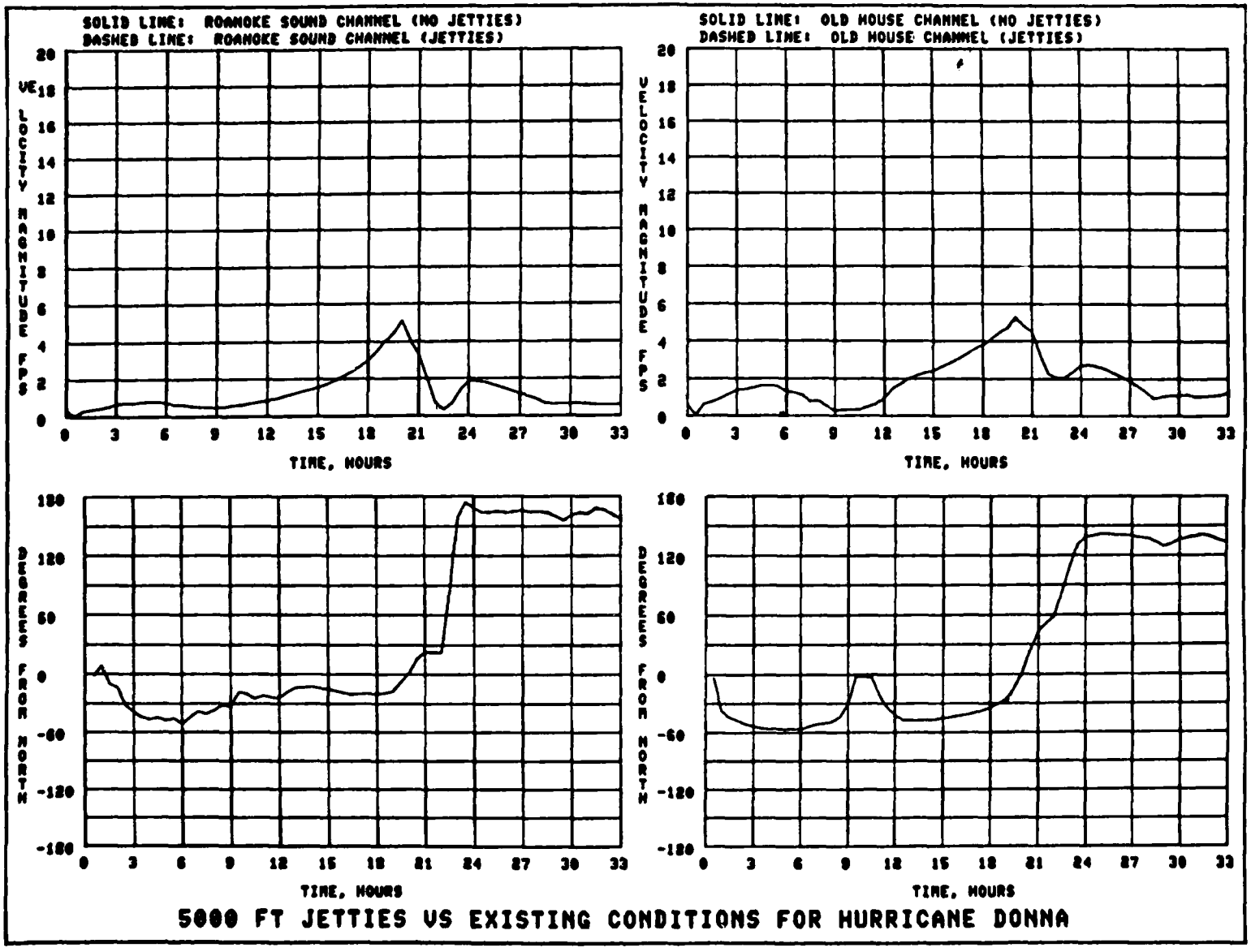

5000 FT JETTIES VS EXISTING CONDITIONS FOR HURRICANE DONNA

PLATE 51

PLATE 52

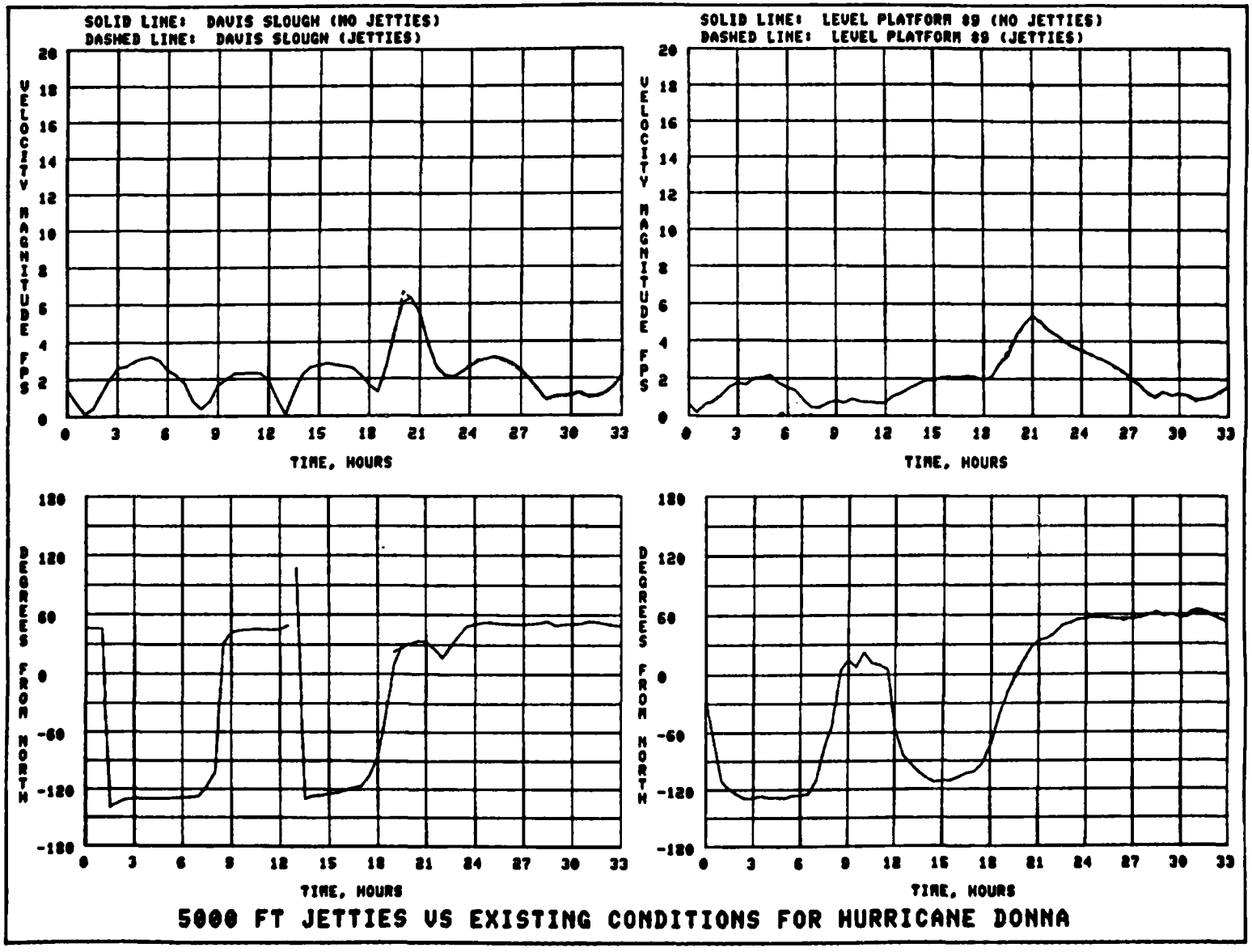

5000 FT JETTIES VS EXISTING CONDITIONS FOR HURRICANE DONNA

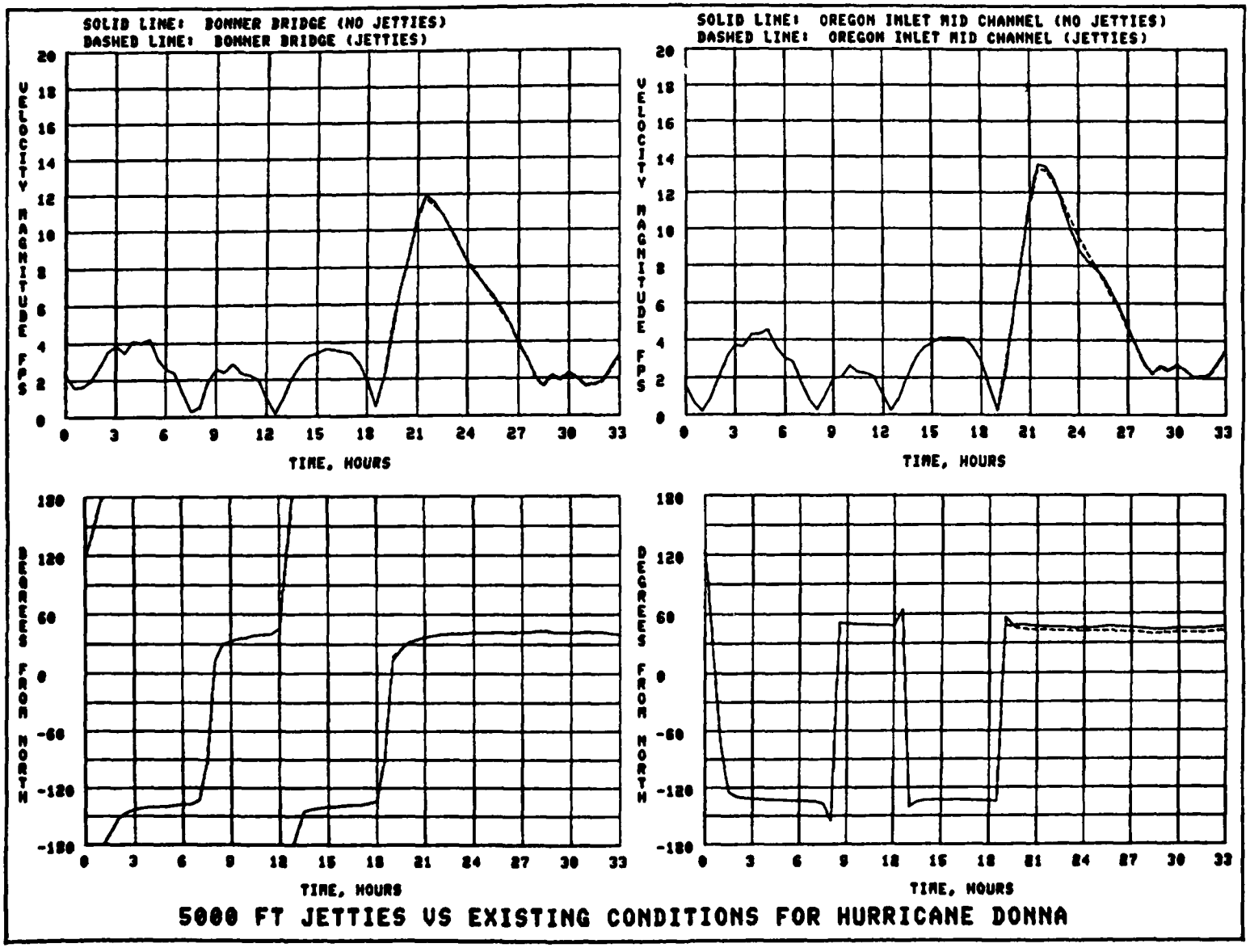

PLATE 53

5000 FT JETTIES VS EXISTING CONDITIONS FOR HURRICANE DONNA

PLATE 54

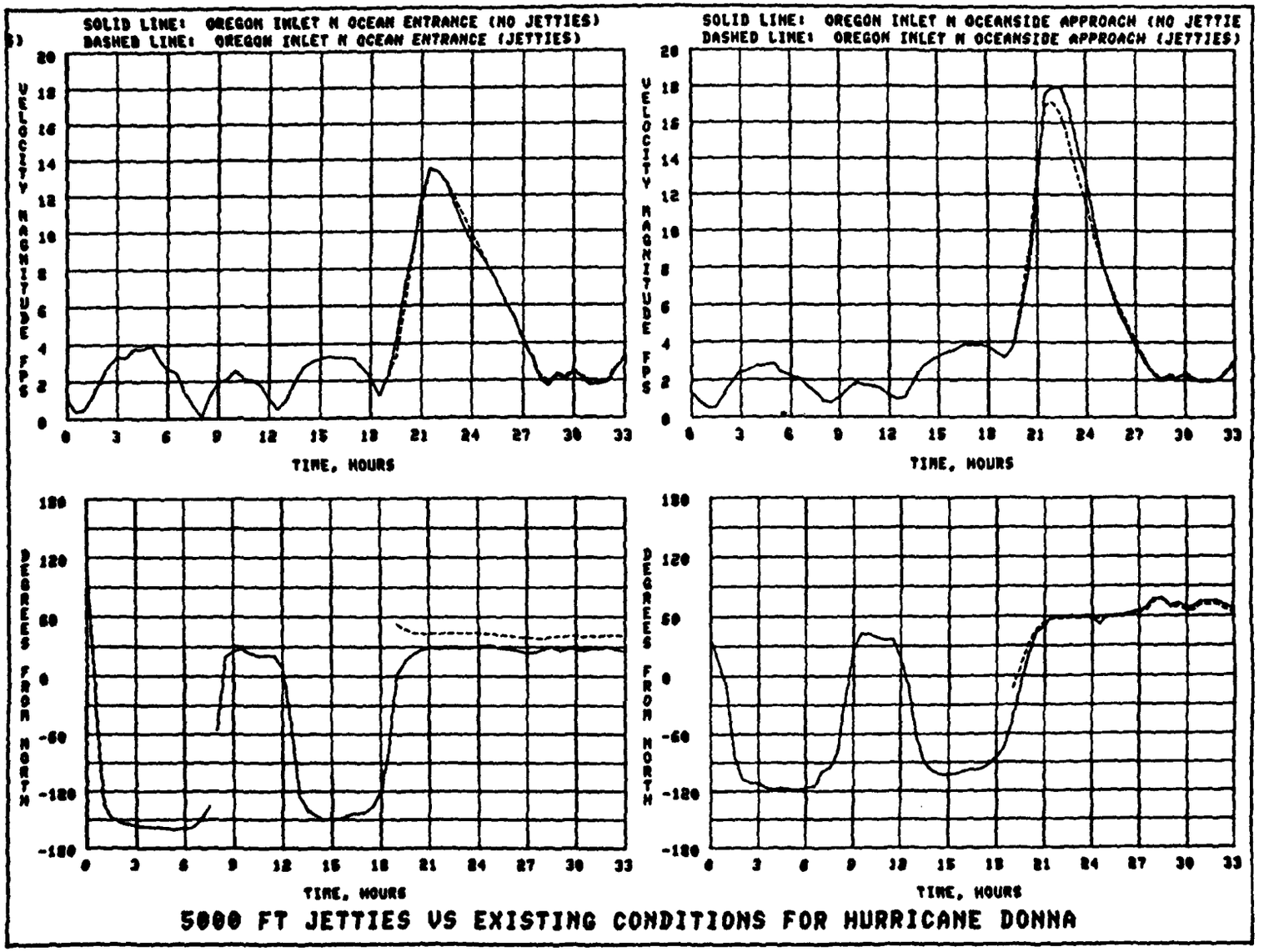

5000 FT JETTIES VS EXISTING CONDITIONS FOR HURRICANE DONNA

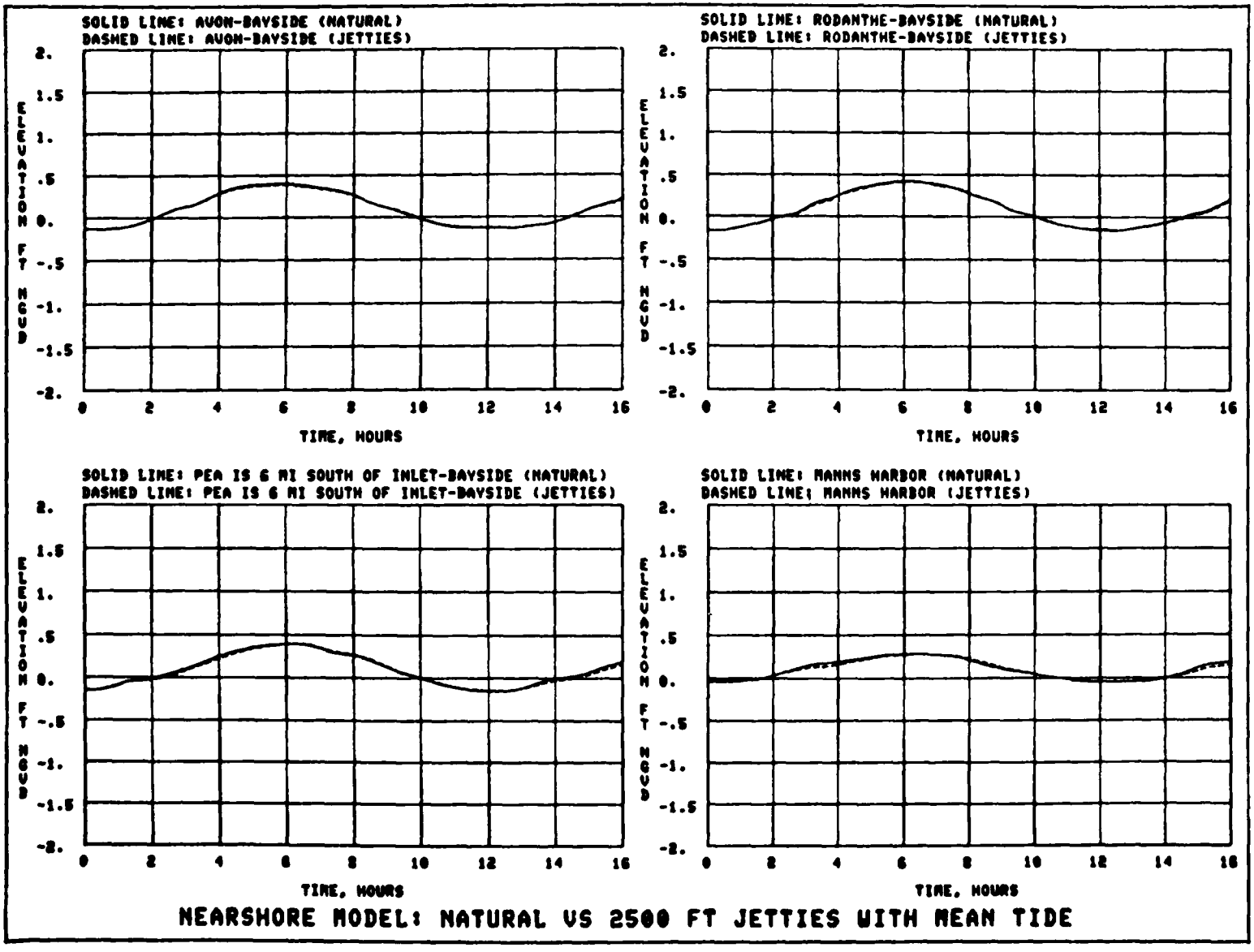

NEARSHORE MODEL: NATURAL VS 2500 FT JETTIES WITH MEAN TIDE

PLATE 55

PLATE 56

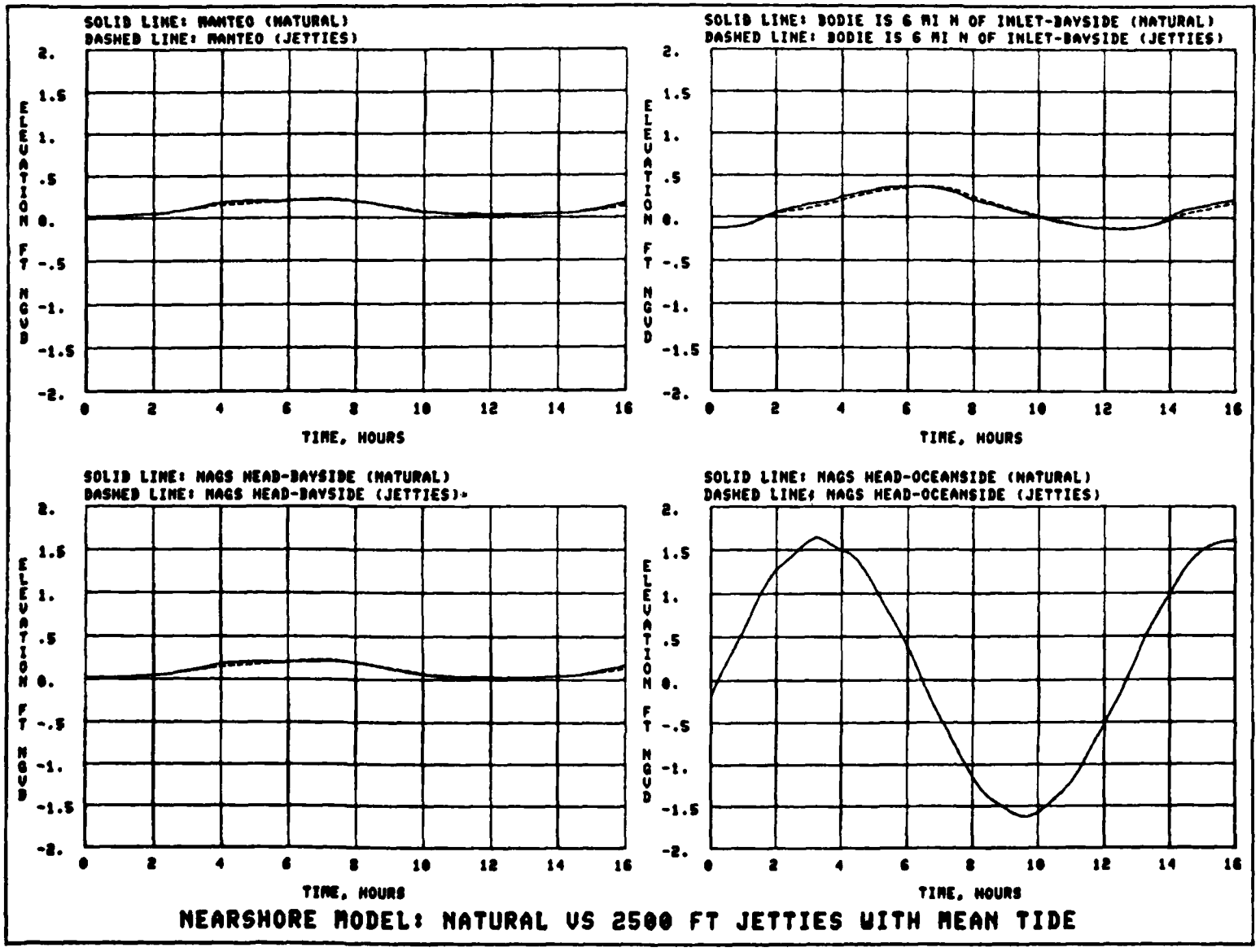

NEARSHORE MODEL: NATURAL VS 2500 FT JETTIES WITH MEAN TIDE

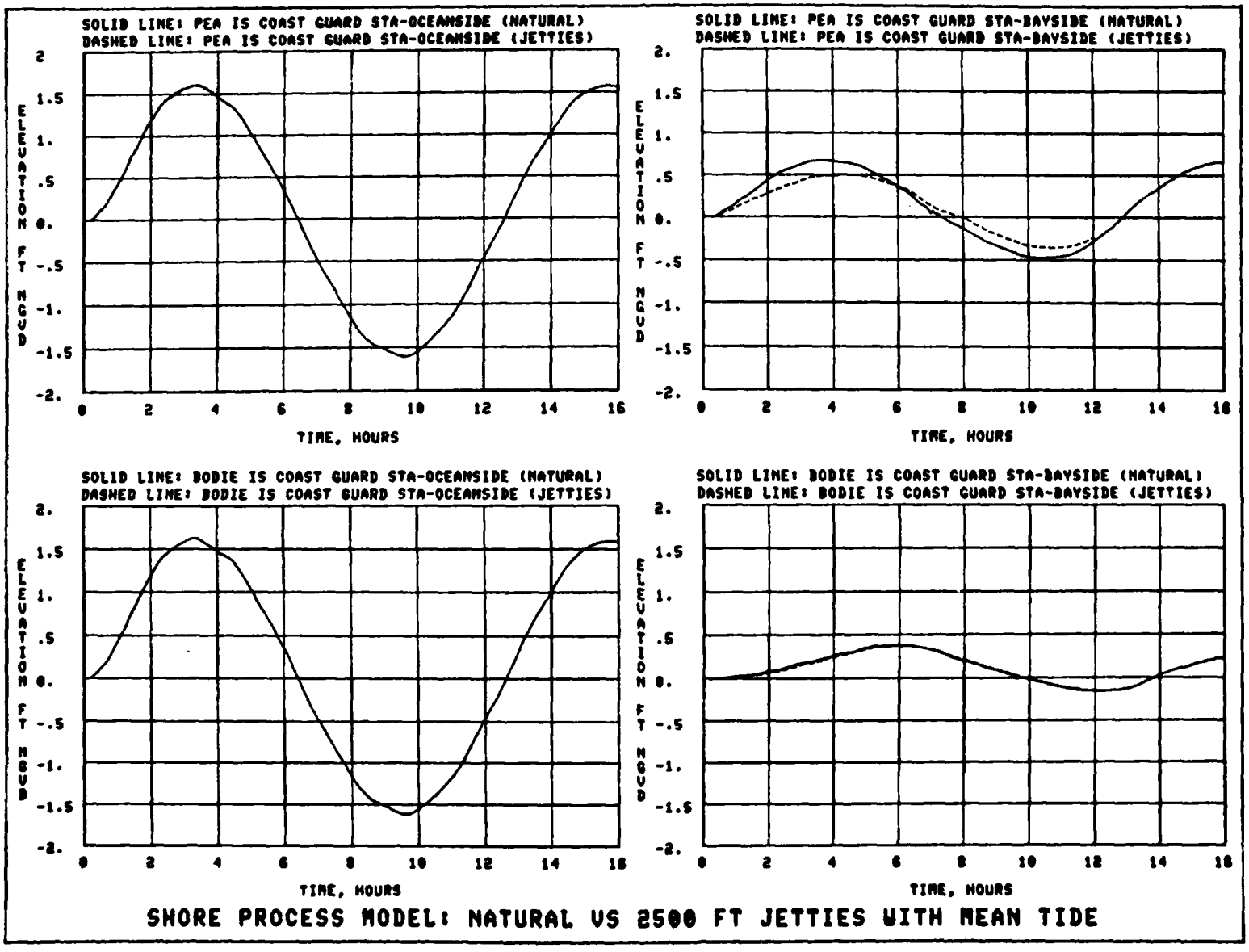

SHORE PROCESS MODEL: NATURAL VS 2500 FT JETTIES WITH MEAN TIDE

PLATE 57

PLATE 58

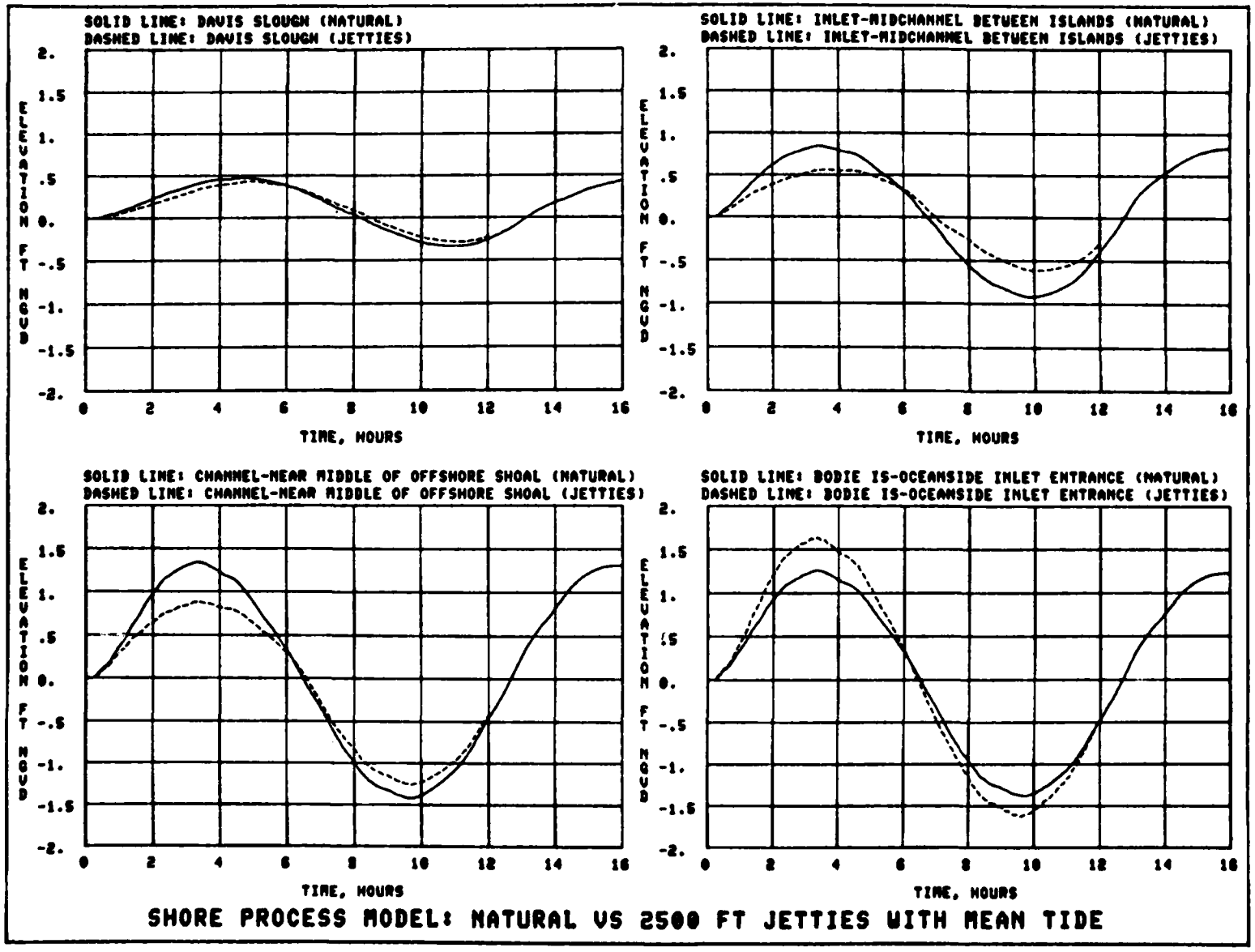

SHORE PROCESS MODEL: NATURAL VS 2500 FT JETTIES WITH MEAN TIDE

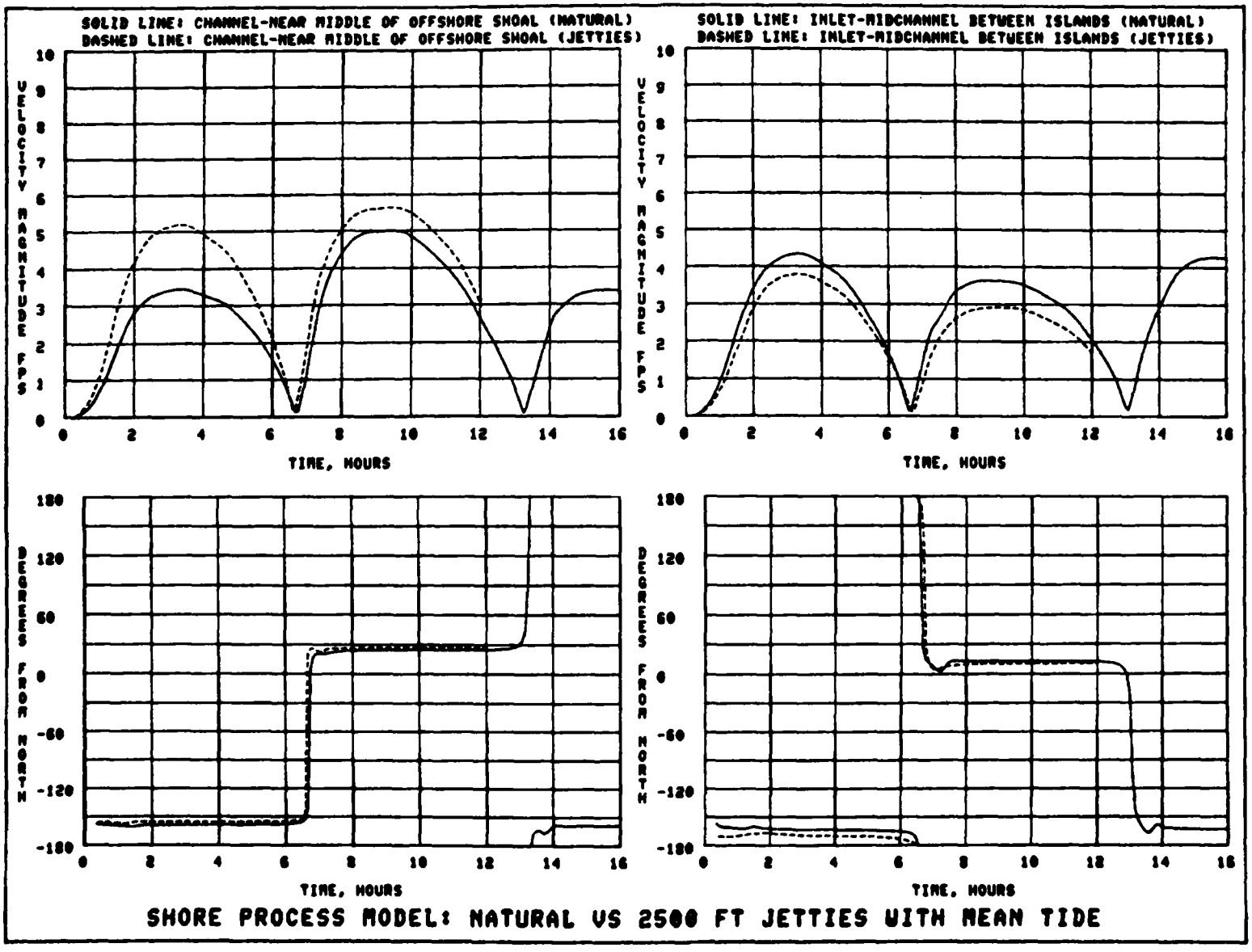

SHORE PROCESS MODEL: NATURAL VS 2500 FT JETTIES WITH MEAN TIDE

PLATE 59

PLATE 60

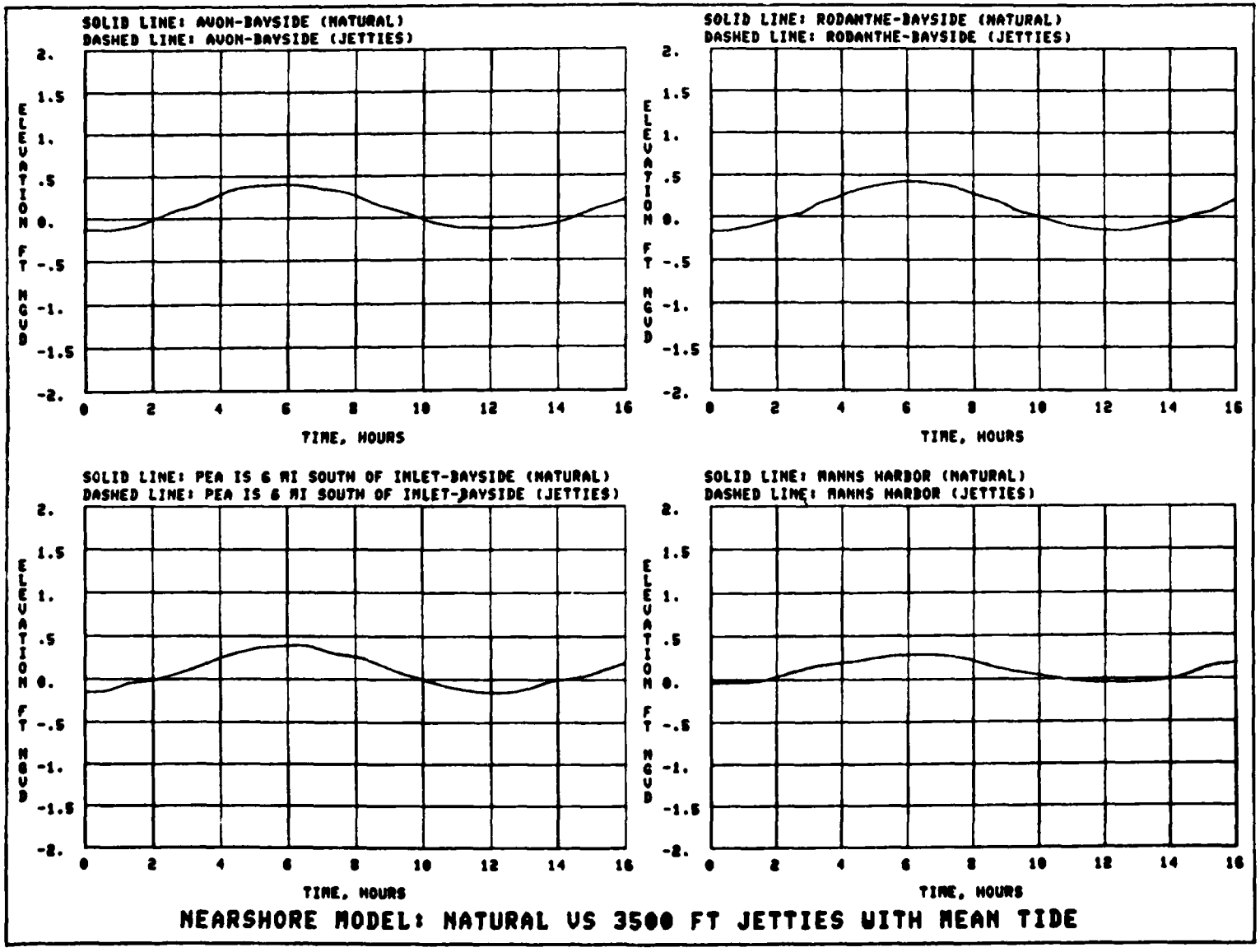
SOLID LINE: AVON-BAYSIDE (NATURAL)
DASHED LINE: AVON-BAYSIDE (JETTIES)
SOLID LINE: RODANTHE-BAYSIDE (NATURAL)
DASHED LINE: RODANTHE-BAYSIDE (JETTIES)
SOLID LINE: PEA IS 6 MI SOUTH OF INLET-BAYSIDE (NATURAL)
DASHED LINE: PEA IS 6 MI SOUTH OF INLET-BAYSIDE (JETTIES)
SOLID LINE: MANNS HARBOR (NATURAL)
DASHED LINE: MANNS HARBOR (JETTIES)
ELEVATION FT NGVD
2.
1.5
1.
.5
0.
-.5
-1.
-1.5
-2.
0
2
4
6
8
10
12
14
16
TIME, HOURS
NEARSHORE MODEL: NATURAL VS 3500 FT JETTIES WITH MEAN TIDE

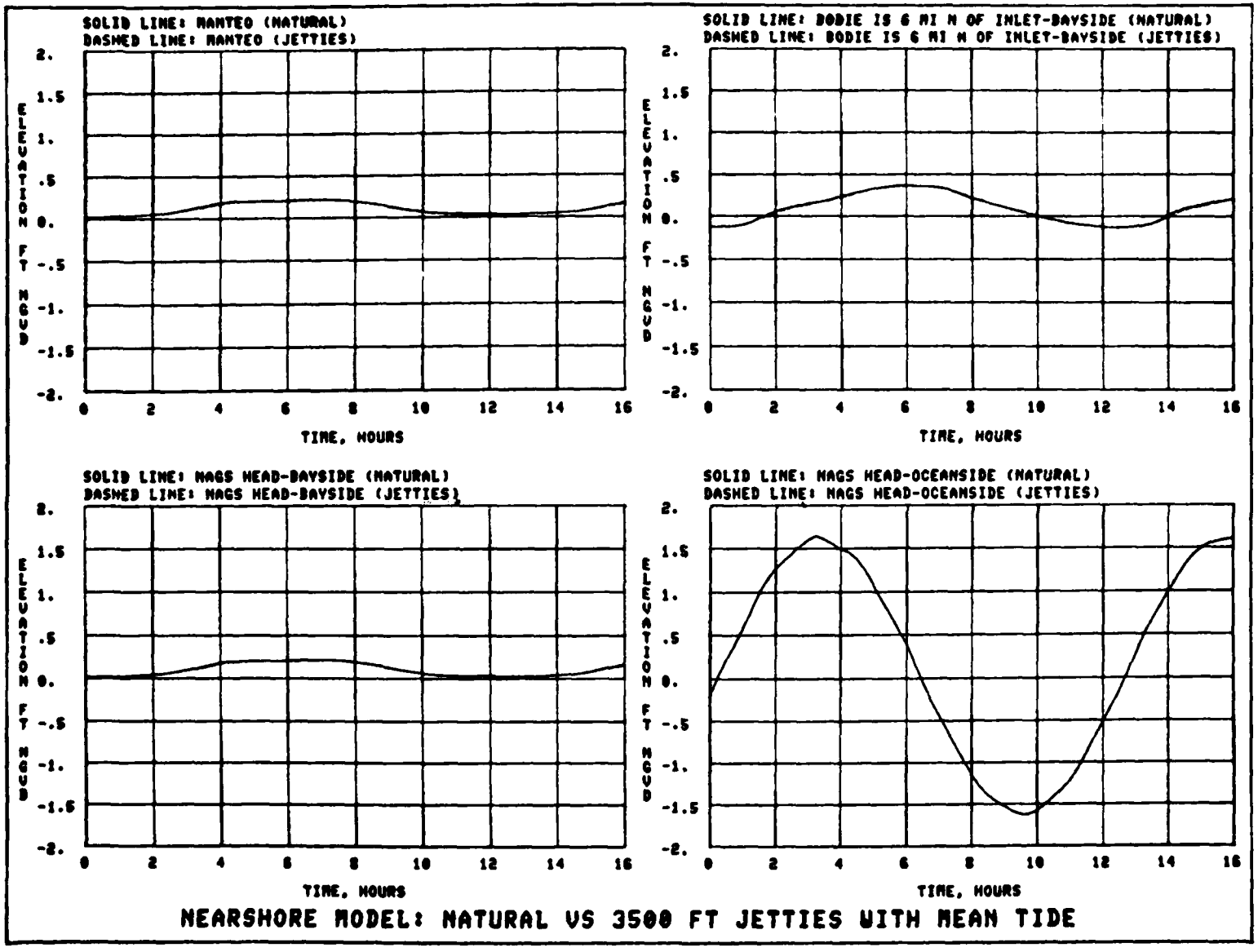

NEARSHORE MODEL: NATURAL VS 3500 FT JETTIES WITH MEAN TIDE

PLATE 61

PLATE 62

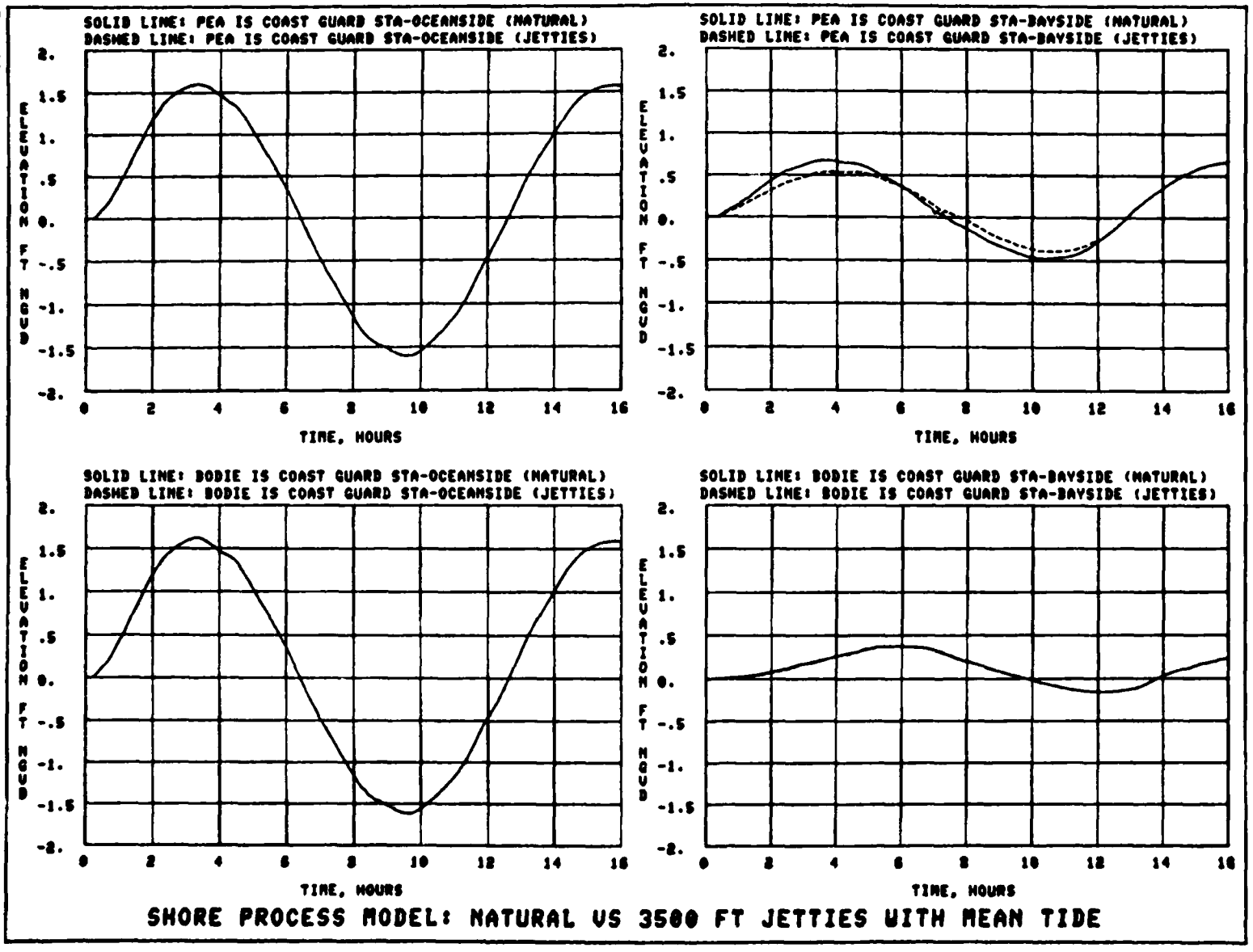
SOLID LINE: PEA IS COAST GUARD STA-OCEANSIDE (NATURAL)
DASHED LINE: PEA IS COAST GUARD STA-OCEANSIDE (JETTIES)
ELEVATION FT NGVD
TIME, HOURS
SOLID LINE: PEA IS COAST GUARD STA-BAYSIDE (NATURAL)
DASHED LINE: PEA IS COAST GUARD STA-BAYSIDE (JETTIES)
ELEVATION FT NGVD
TIME, HOURS
SOLID LINE: BODIE IS COAST GUARD STA-OCEANSIDE (NATURAL)
DASHED LINE: BODIE IS COAST GUARD STA-OCEANSIDE (JETTIES)
ELEVATION FT NGVD
TIME, HOURS
SOLID LINE: BODIE IS COAST GUARD STA-BAYSIDE (NATURAL)
DASHED LINE: BODIE IS COAST GUARD STA-BAYSIDE (JETTIES)
ELEVATION FT NGVD
TIME, HOURS
SHORE PROCESS MODEL: NATURAL VS 3500 FT JETTIES WITH MEAN TIDE

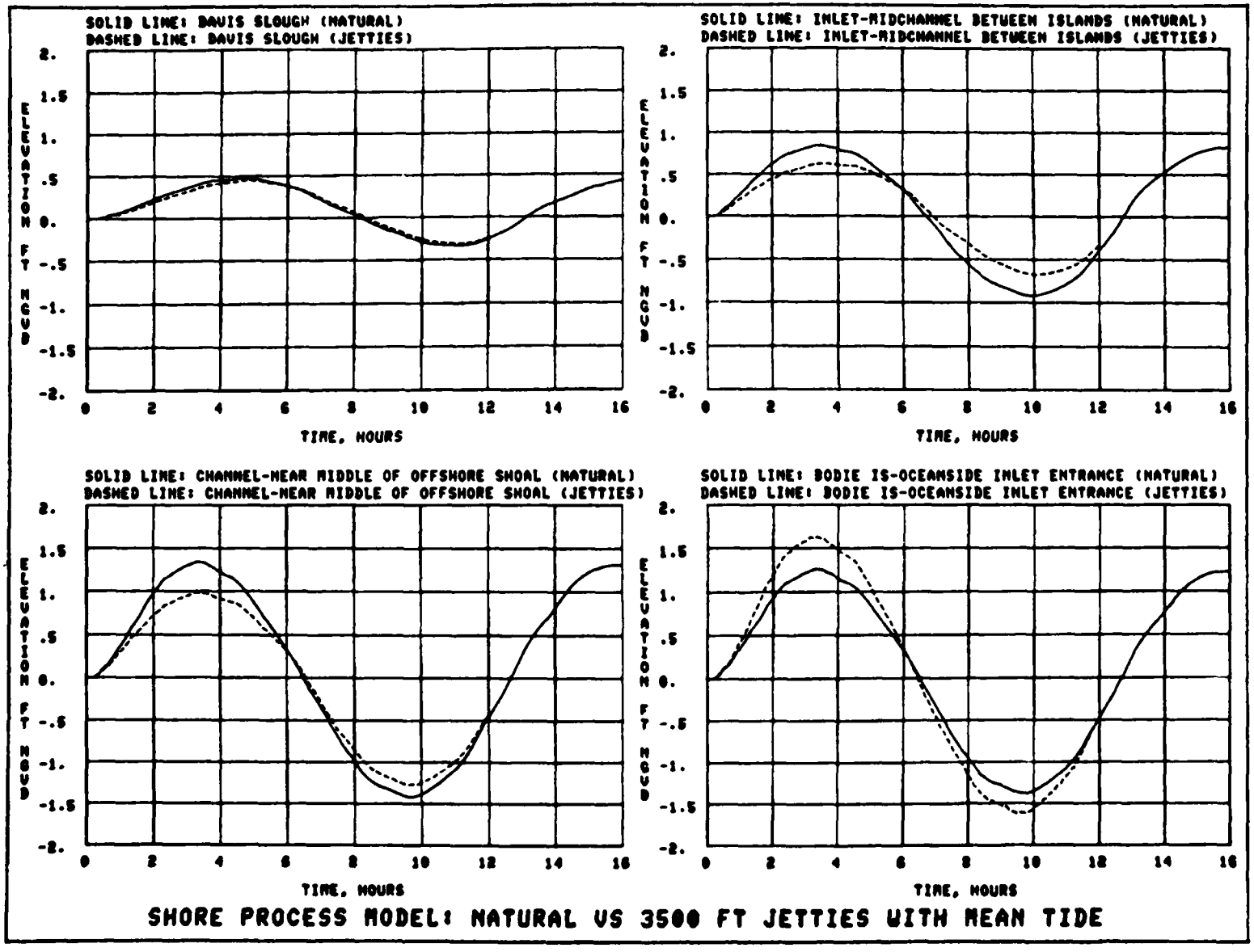

SHORE PROCESS MODEL: NATURAL VS 3500 FT JETTIES WITH MEAN TIDE

PLATE 63

PLATE 64

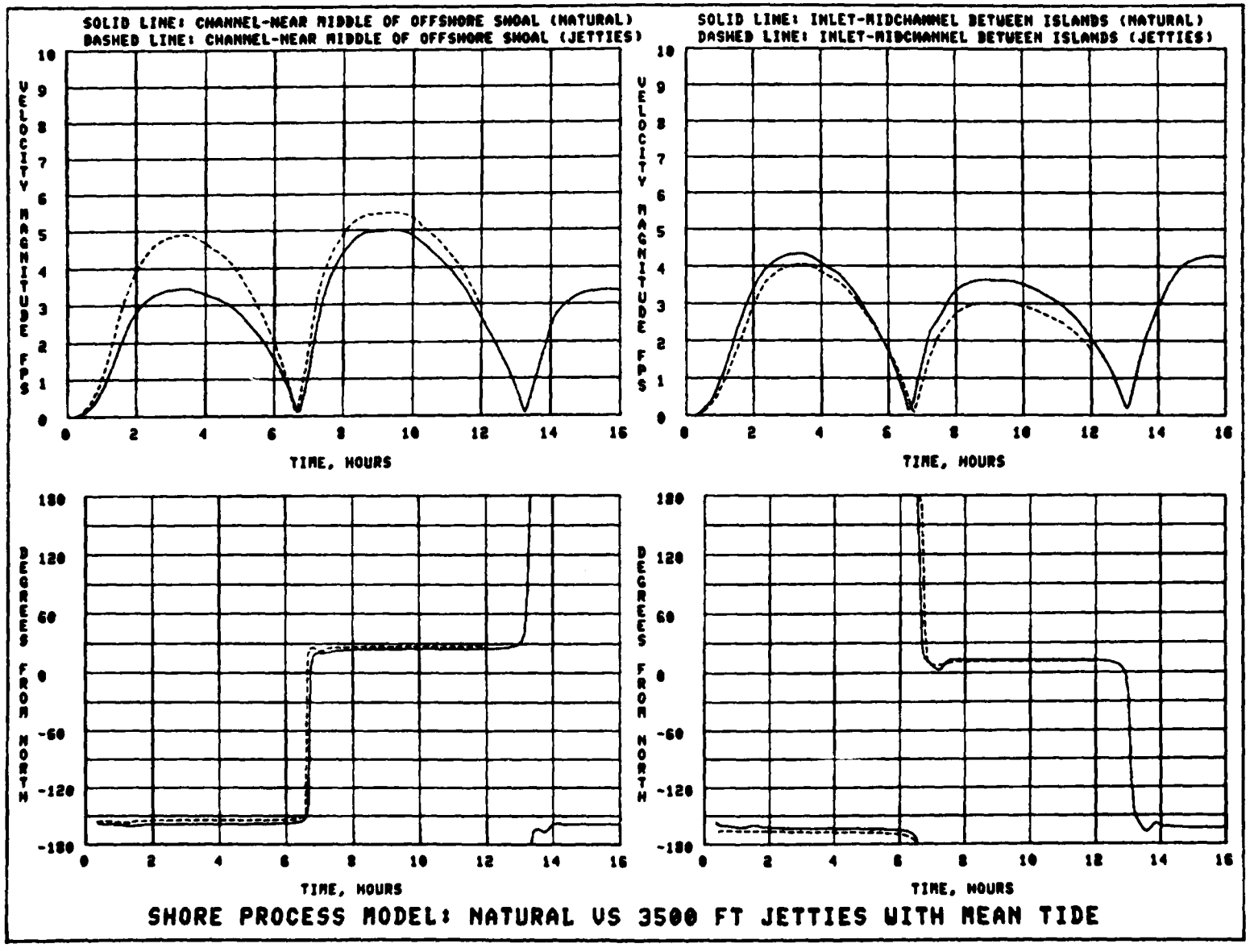
SOLID LINE: CHANNEL-NEAR MIDDLE OF OFFSHORE SHOAL (NATURAL)
DASHED LINE: CHANNEL-NEAR MIDDLE OF OFFSHORE SHOAL (JETTIES)
VELOCITY MAGNITUDE FPS
TIME, HOURS
SOLID LINE: INLET-MIDCHANNEL BETWEEN ISLANDS (NATURAL)
DASHED LINE: INLET-MIDCHANNEL BETWEEN ISLANDS (JETTIES)
VELOCITY MAGNITUDE FPS
TIME, HOURS
DEGREES FROM NORTH
TIME, HOURS
DEGREES FROM NORTH
TIME, HOURS
SHORE PROCESS MODEL: NATURAL VS 3500 FT JETTIES WITH MEAN TIDE

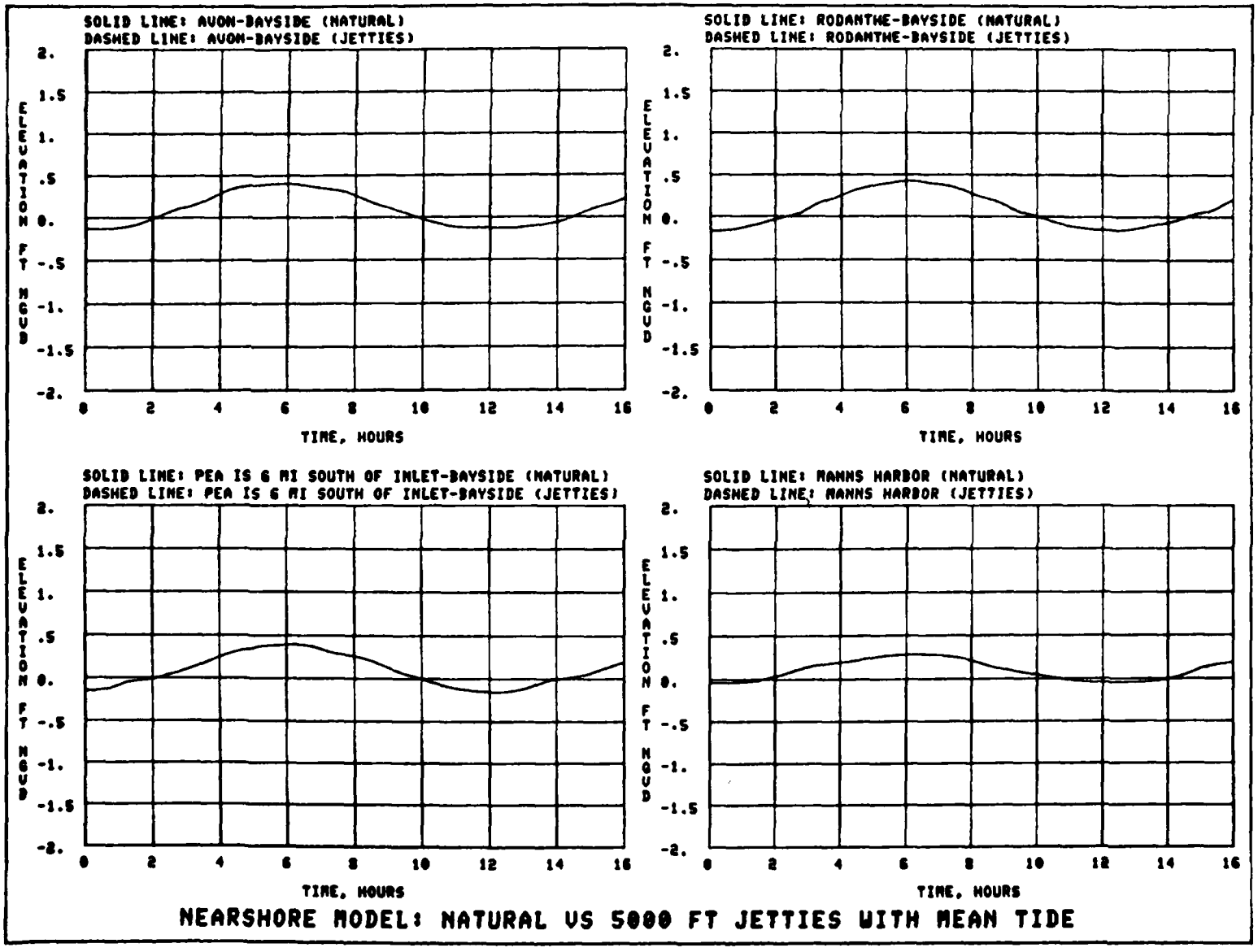

NEARSHORE MODEL: NATURAL VS 5000 FT JETTIES WITH MEAN TIDE

PLATE 65

PLATE 66

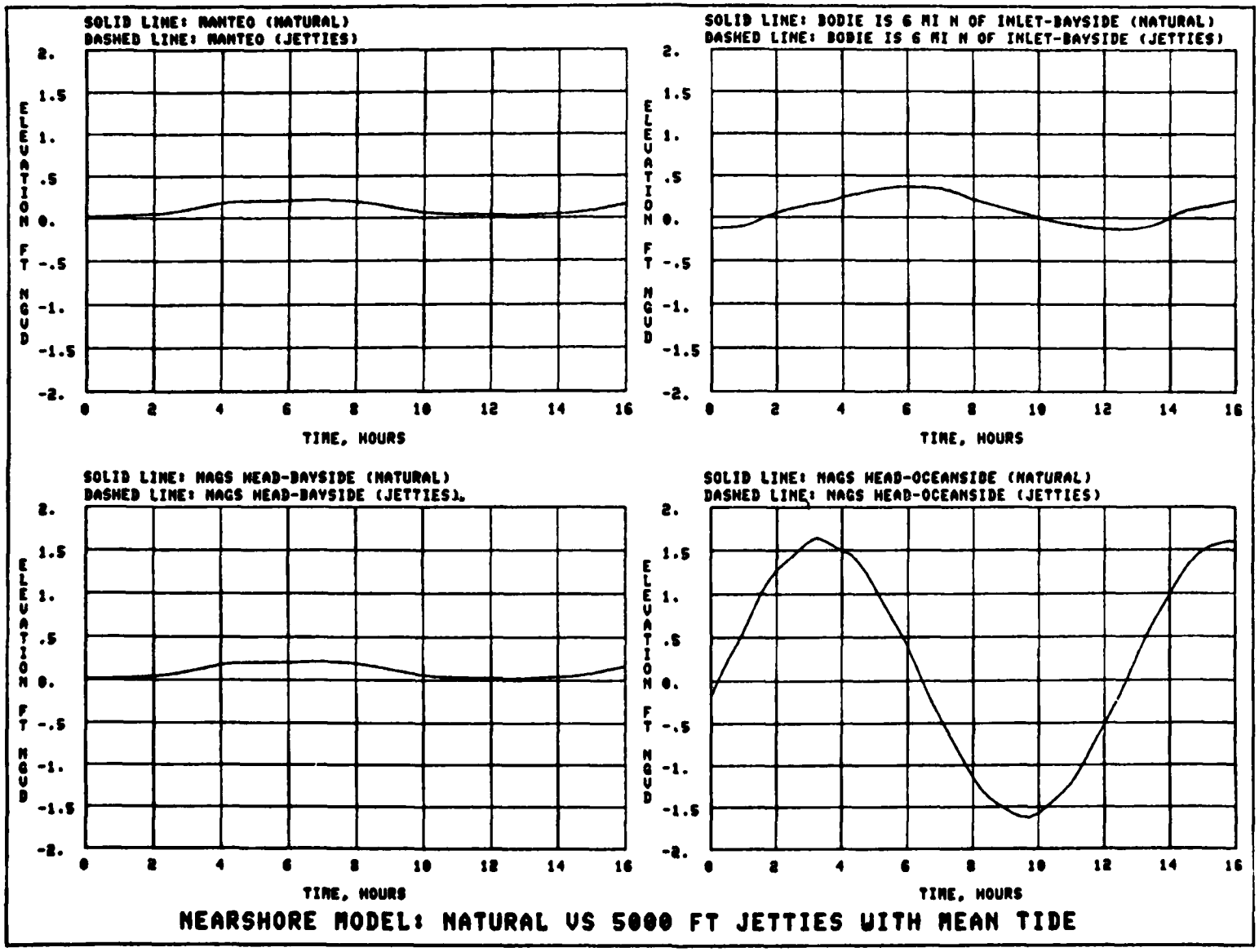
SOLID LINE: MANTEO (NATURAL)
DASHED LINE: MANTEO (JETTIES)
SOLID LINE: BODIE IS 6 MI N OF INLET-BAYSIDE (NATURAL)
DASHED LINE: BODIE IS 6 MI N OF INLET-BAYSIDE (JETTIES)
SOLID LINE: NAGS HEAD-BAYSIDE (NATURAL)
DASHED LINE: NAGS HEAD-BAYSIDE (JETTIES)
SOLID LINE: NAGS HEAD-OCEANSIDE (NATURAL)
DASHED LINE: NAGS HEAD-OCEANSIDE (JETTIES)
ELEVATION FT NGVD
2.
1.5
1.
.5
0.
-.5
-1.
-1.5
-2.
0
2
4
6
8
10
12
14
16
TIME, HOURS
NEARSHORE MODEL: NATURAL VS 5000 FT JETTIES WITH MEAN TIDE

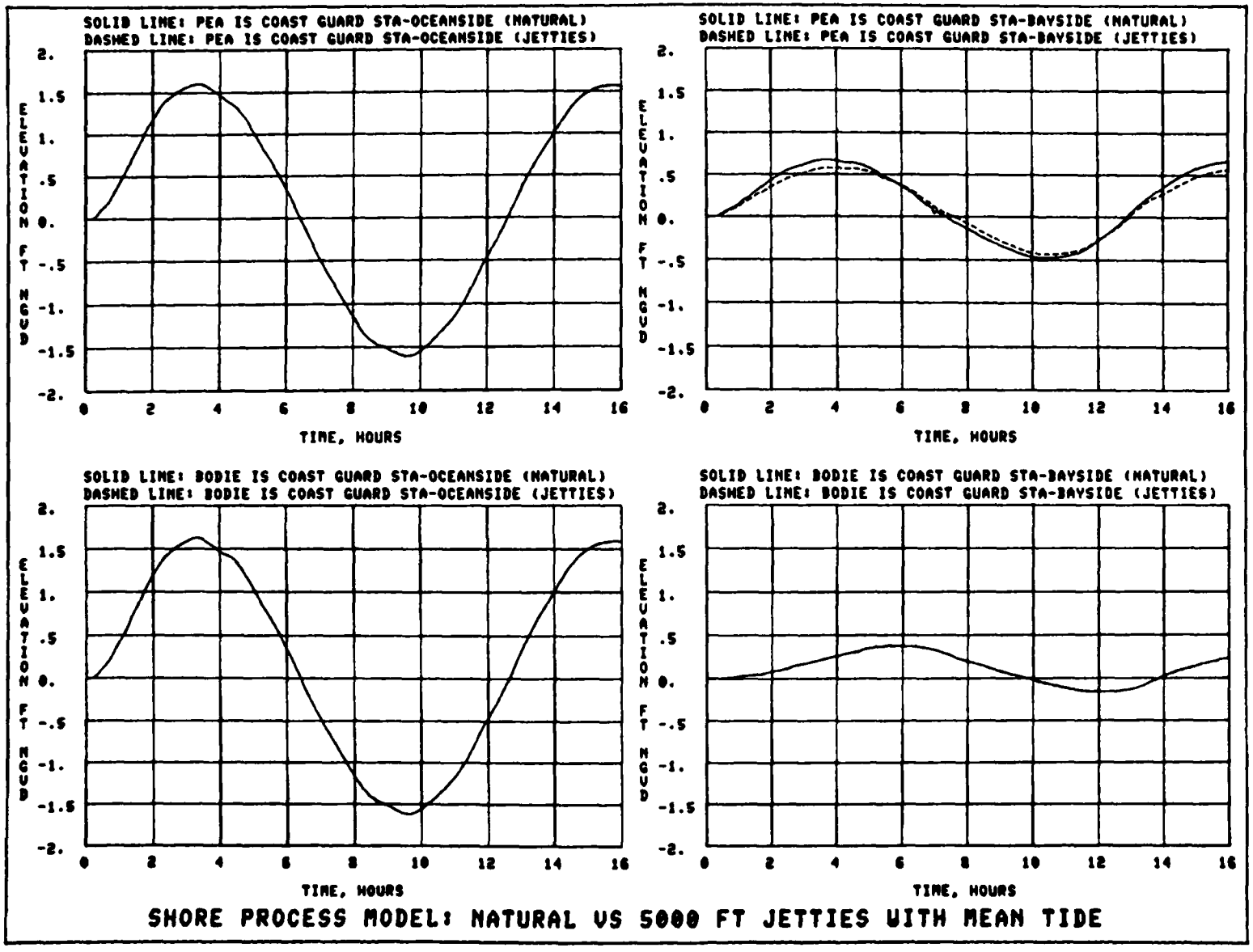
SOLID LINE: PEA IS COAST GUARD STA-OCEANSIDE (NATURAL)
DASHED LINE: PEA IS COAST GUARD STA-OCEANSIDE (JETTIES)
ELEVATION FT NGVD
TIME, HOURS
SOLID LINE: PEA IS COAST GUARD STA-BAYSIDE (NATURAL)
DASHED LINE: PEA IS COAST GUARD STA-BAYSIDE (JETTIES)
ELEVATION FT NGVD
TIME, HOURS
SOLID LINE: BODIE IS COAST GUARD STA-OCEANSIDE (NATURAL)
DASHED LINE: BODIE IS COAST GUARD STA-OCEANSIDE (JETTIES)
ELEVATION FT NGVD
TIME, HOURS
SOLID LINE: BODIE IS COAST GUARD STA-BAYSIDE (NATURAL)
DASHED LINE: BODIE IS COAST GUARD STA-BAYSIDE (JETTIES)
ELEVATION FT NGVD
TIME, HOURS
SHORE PROCESS MODEL: NATURAL VS 5000 FT JETTIES WITH MEAN TIDE

PLATE 67

PLATE 68

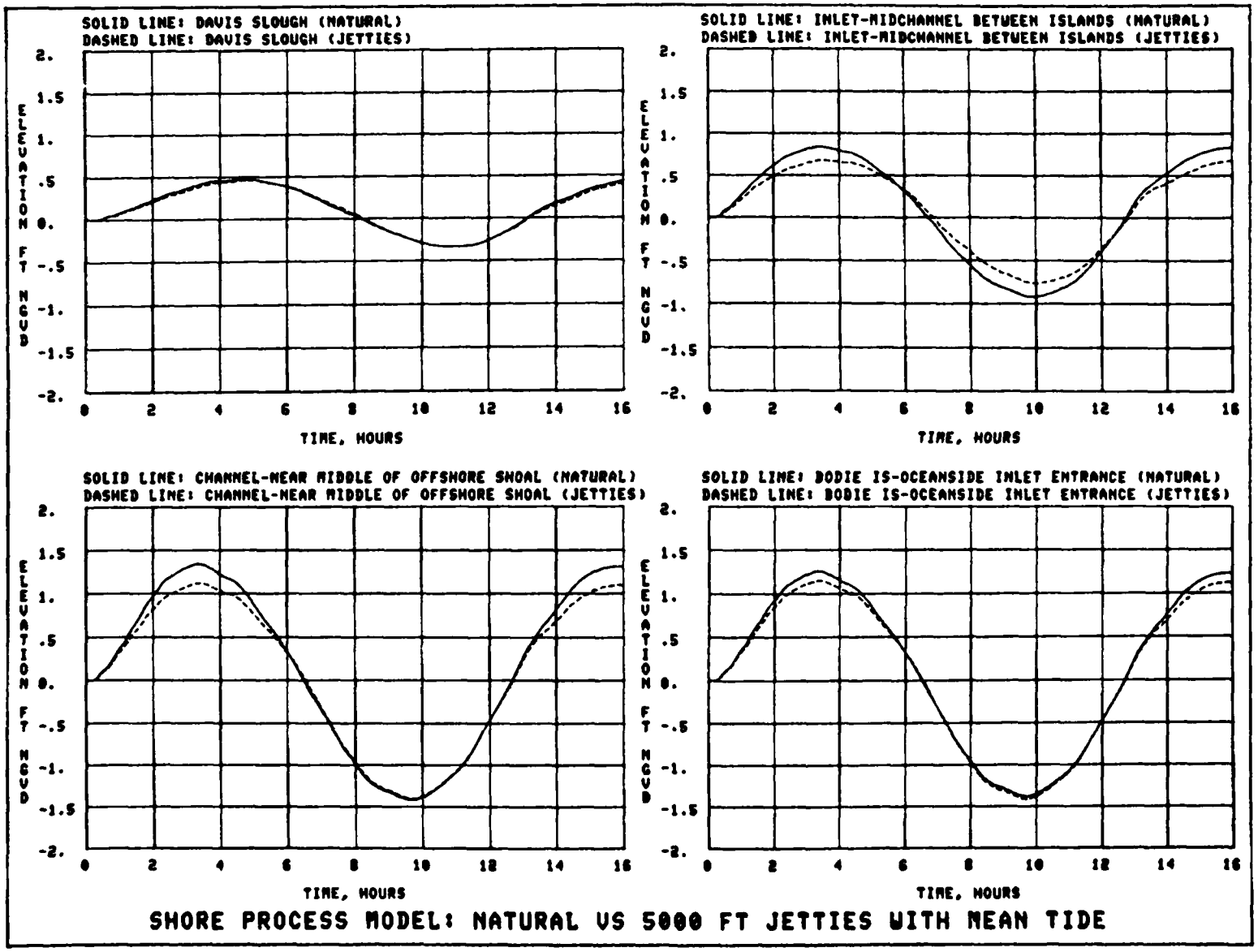

SHORE PROCESS MODEL: NATURAL VS 5000 FT JETTIES WITH MEAN TIDE

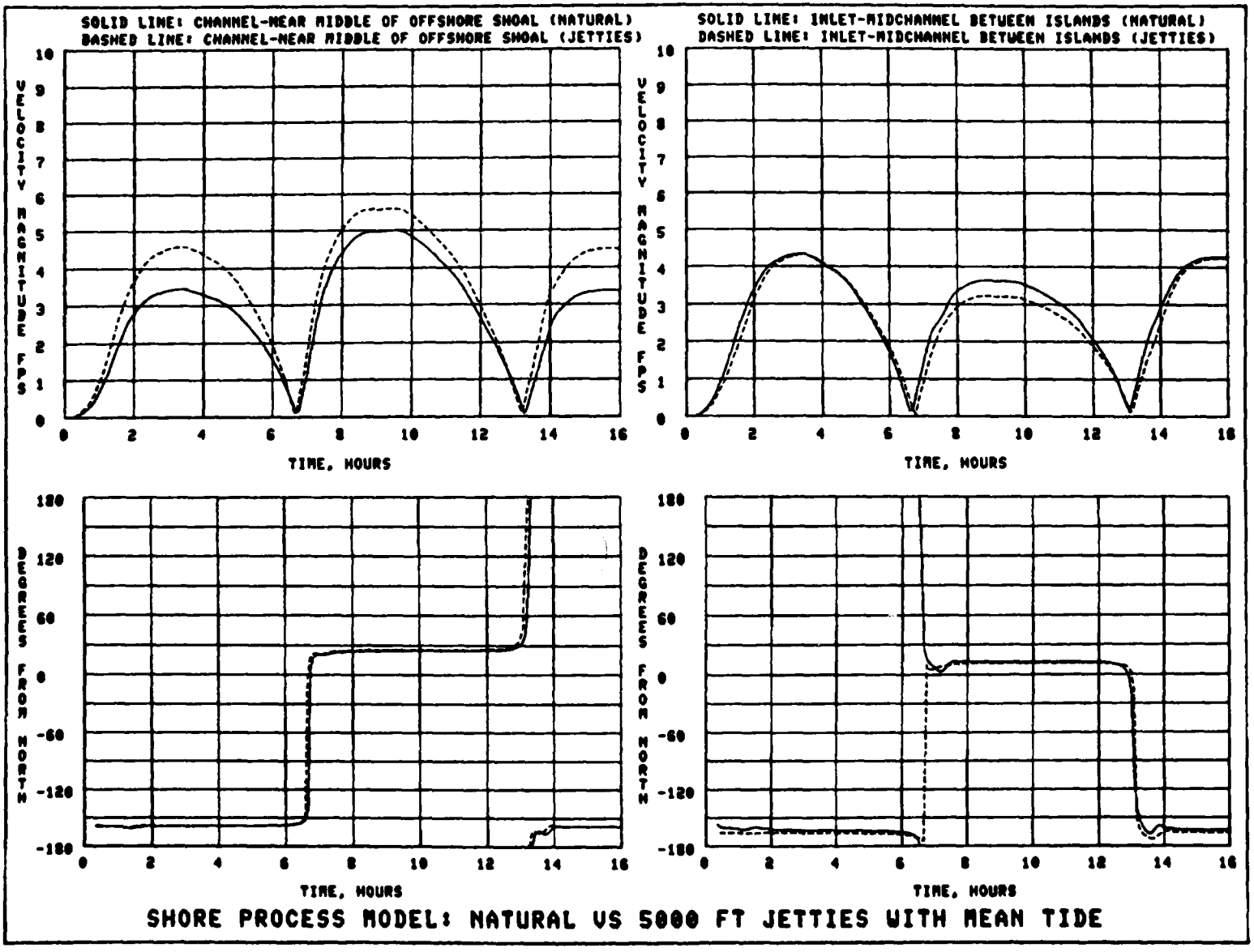

SHORE PROCESS MODEL: NATURAL VS 5000 FT JETTIES WITH MEAN TIDE

PLATE 69

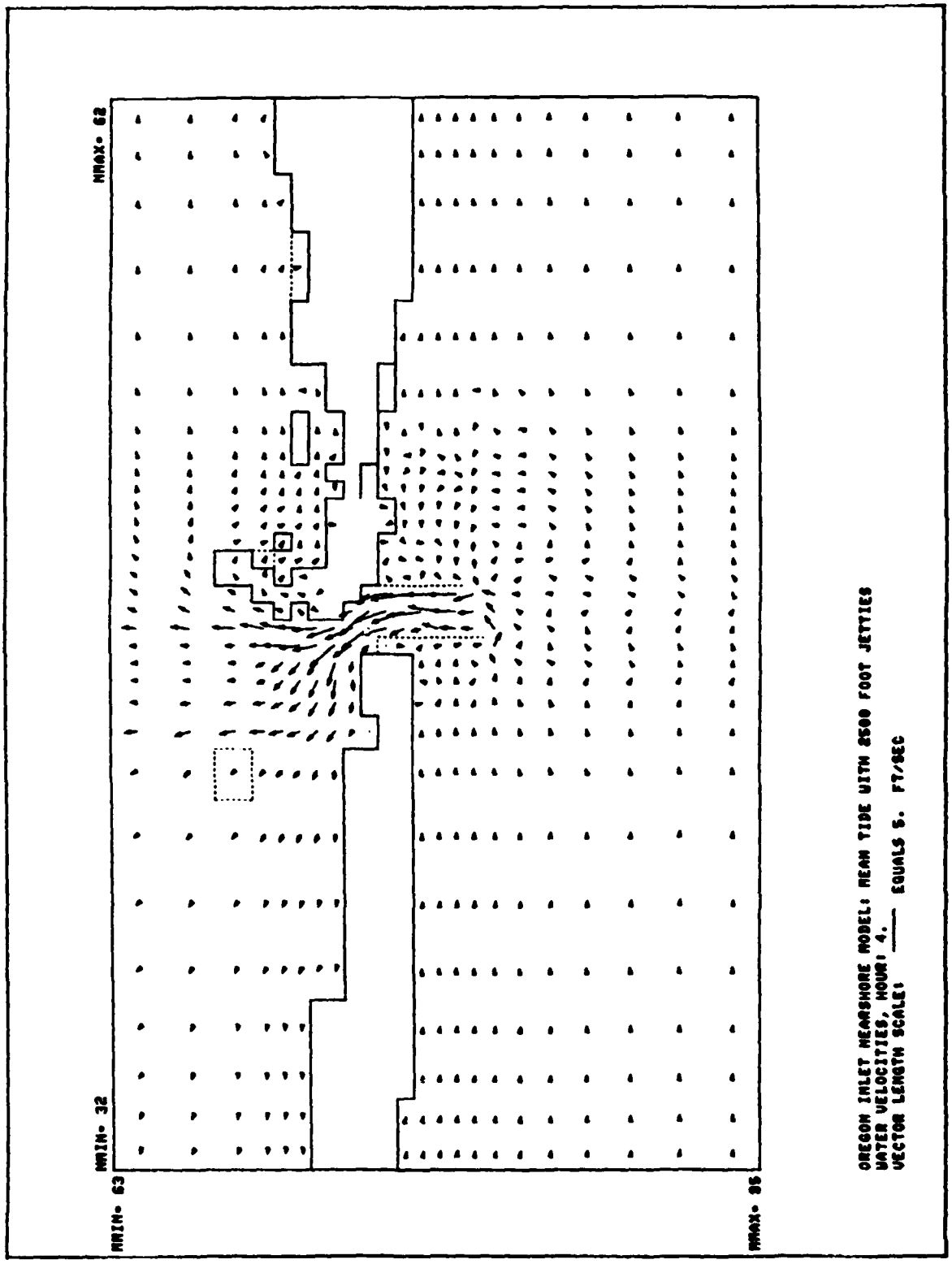
NMAX= 68
NMIN= 32
MMIN= 63
MMAX= 95
OREGON INLET NEARSHORE MODEL: MEAN TIDE WITH 8500 FOOT JETTIES
WATER VELOCITIES, HOUR: 4.
VECTOR LENGTH SCALE: —— EQUALS 5. FT/SEC

PLATE 70

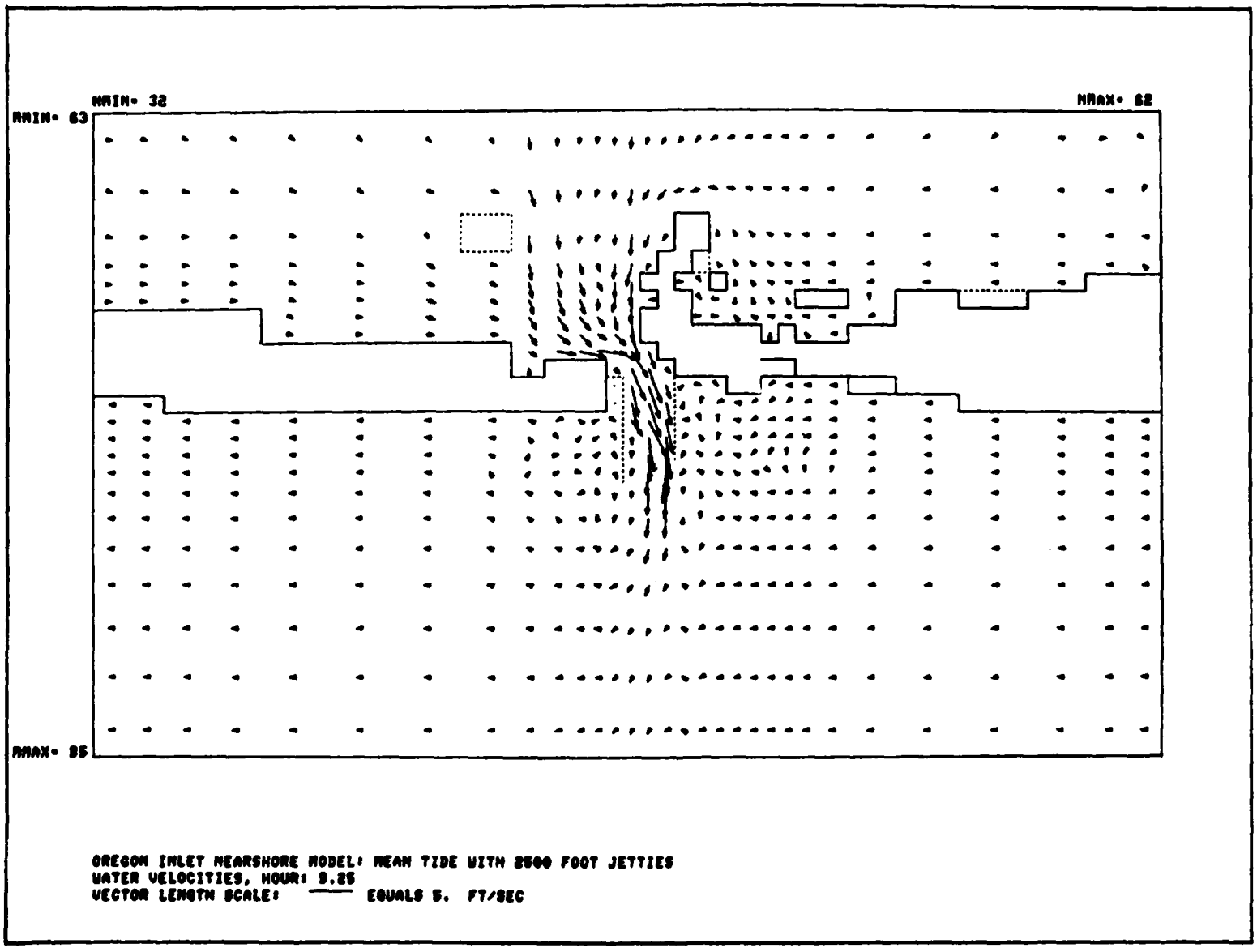

OREGON INLET NEARSHORE MODEL: MEAN TIDE WITH 2500 FOOT JETTIES
WATER VELOCITIES, HOUR: 9.25
VECTOR LENGTH SCALE: ——— EQUALS 5. FT/SEC

PLATE 71

PLATE 72

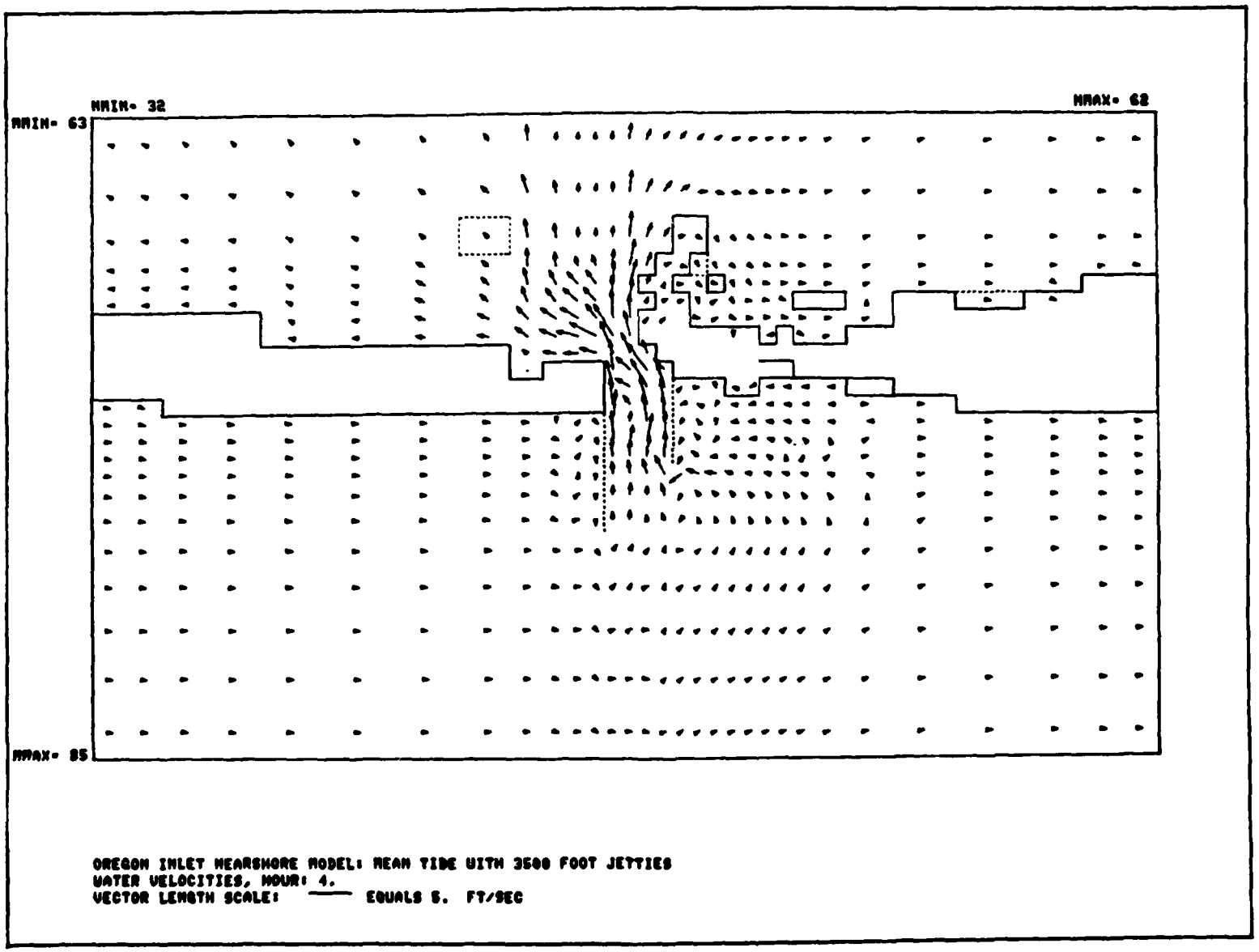

OREGON INLET NEARSHORE MODEL: MEAN TIDE WITH 3500 FOOT JETTIES
WATER VELOCITIES, HOUR: 4.
VECTOR LENGTH SCALE: —— EQUALS 5. FT/SEC

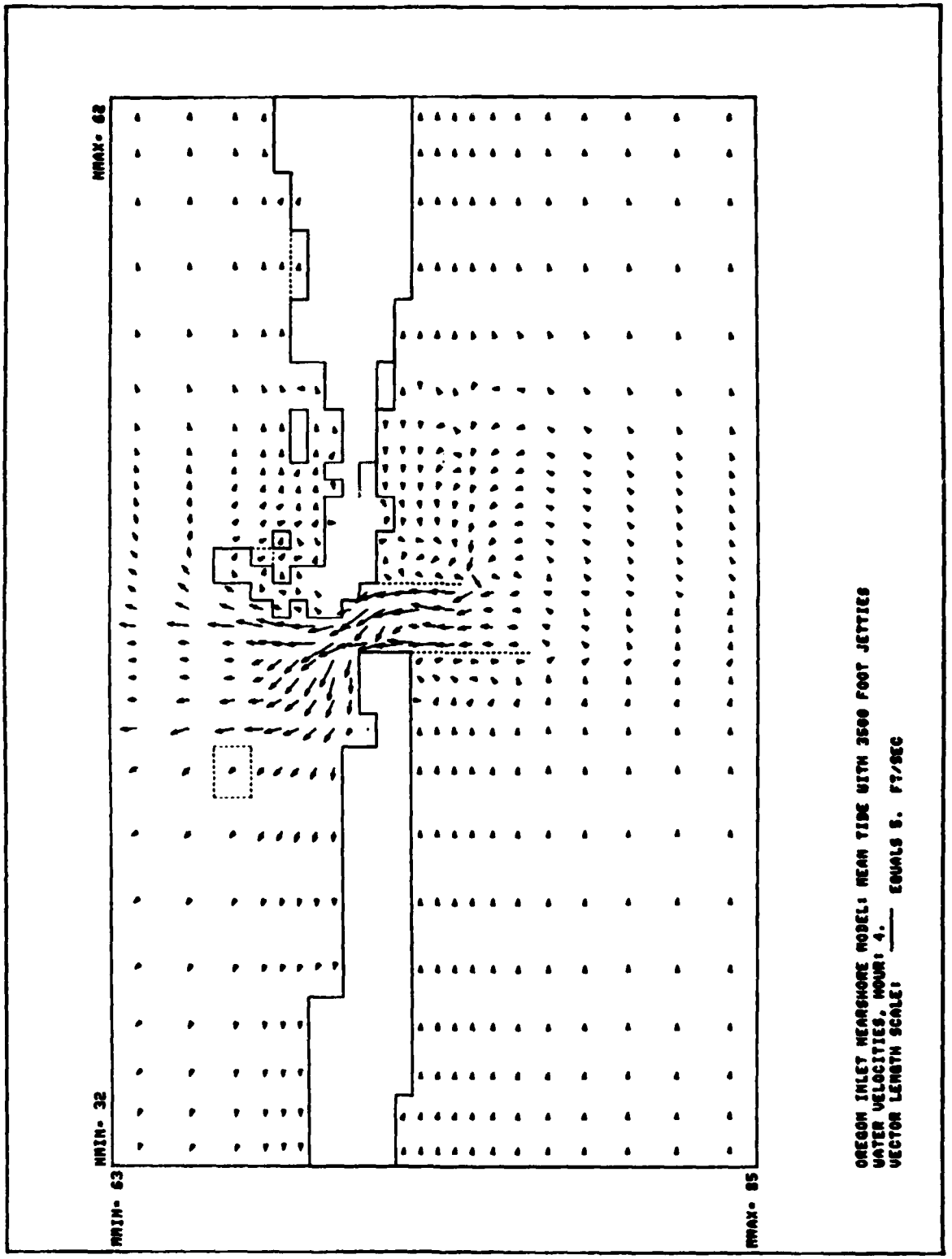
NMAX= 62
NMIN= 32
MMIN= 63
MMAX= 85
OREGON INLET NEARSHORE MODEL: MEAN TIDE WITH 3500 FOOT JETTIES
WATER VELOCITIES, HOUR: 4.
VECTOR LENGTH SCALE: —— EQUALS 5. FT/SEC

PLATE 72

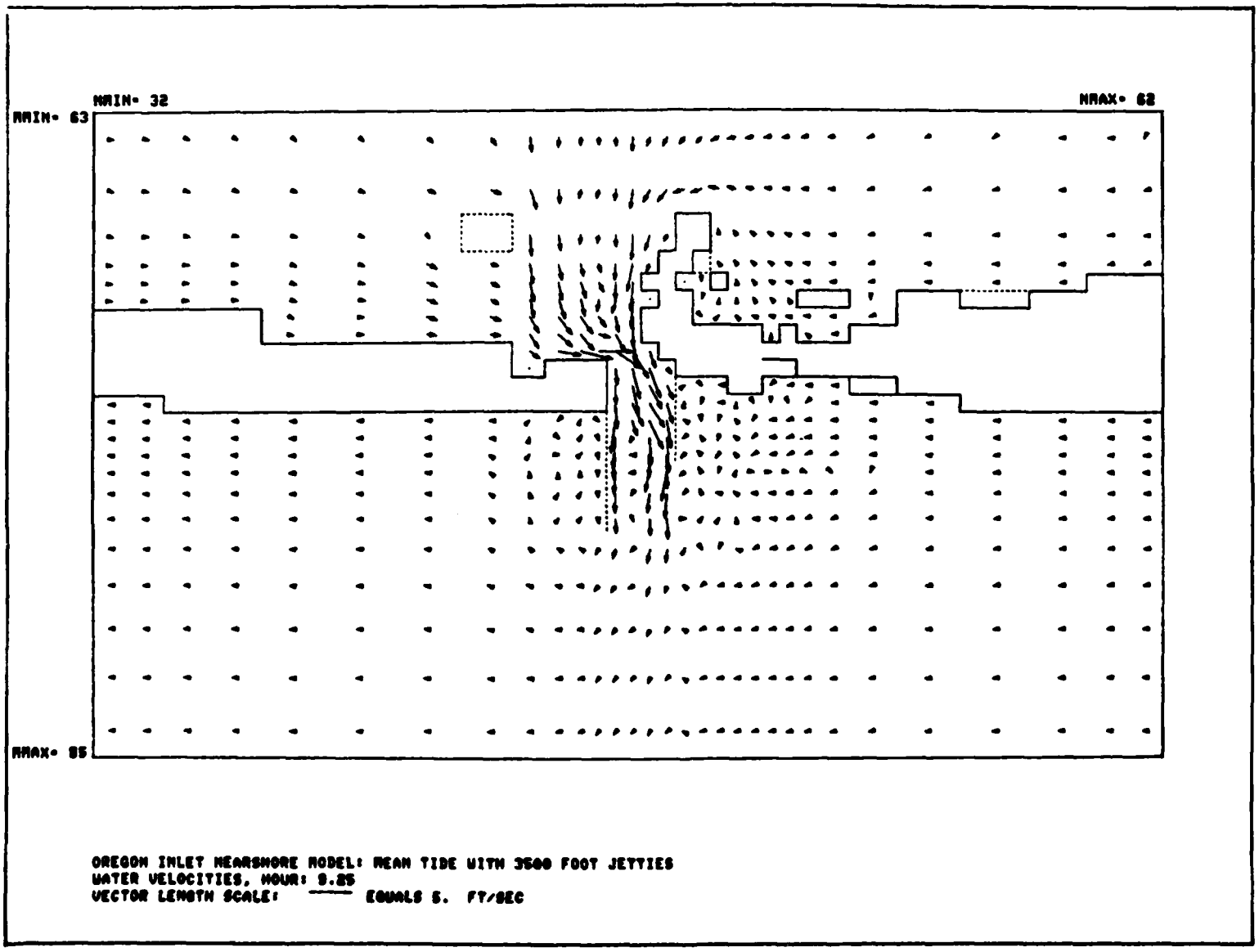

OREGON INLET NEARSHORE MODEL: MEAN TIDE WITH 3500 FOOT JETTIES
WATER VELOCITIES, HOUR: 9.25
VECTOR LENGTH SCALE: ——— EQUALS 5. FT/SEC

PLATE 73

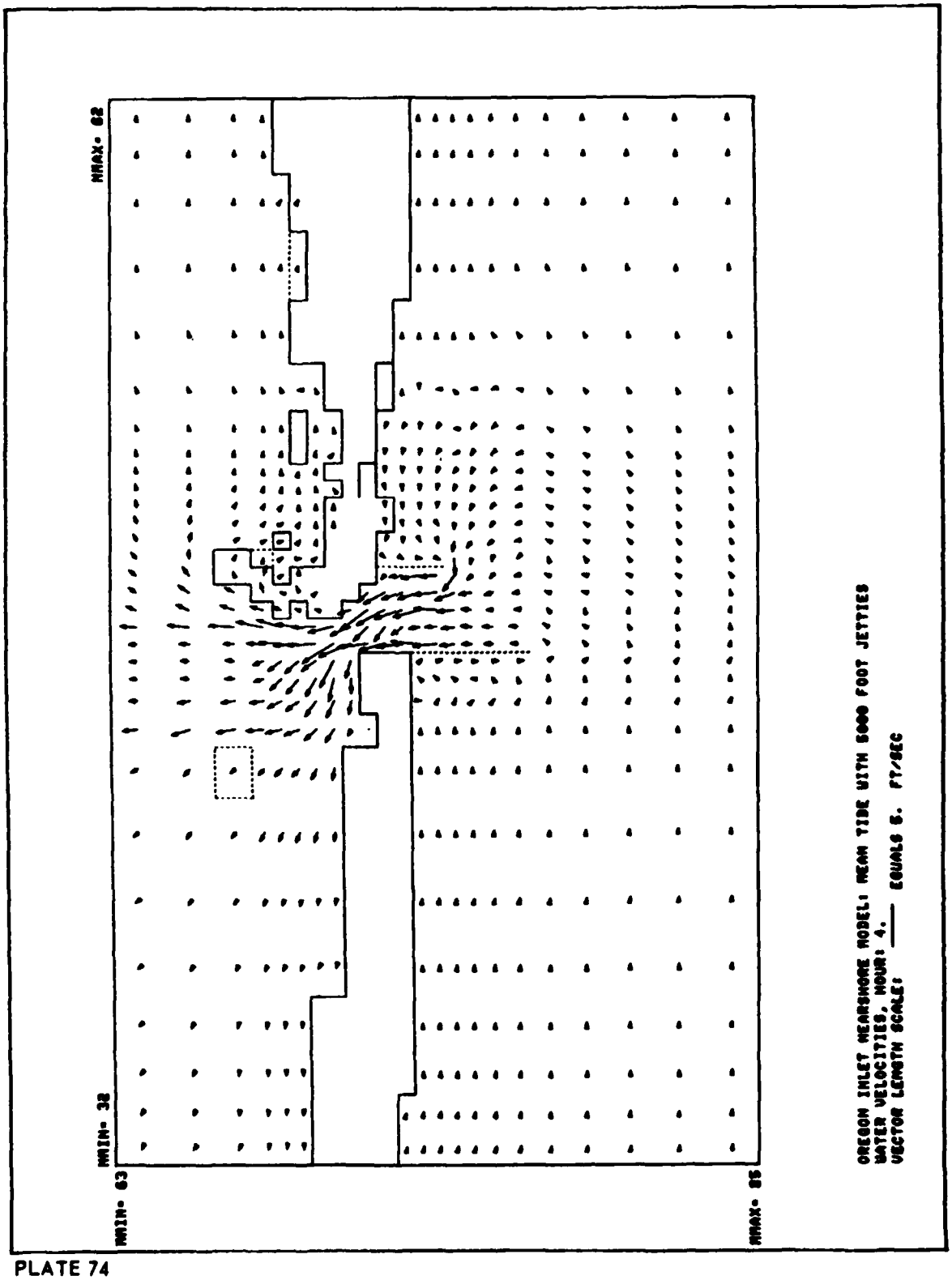
NMAX= 62
NMIN= 32
NMIN= 63
NMAX= 95
OREGON INLET NEARSHORE MODEL: MEAN TIDE WITH 5000 FOOT JETTIES
WATER VELOCITIES, HOUR: 4.
VECTOR LENGTH SCALE: —— EQUALS 6. FT/SEC

PLATE 74

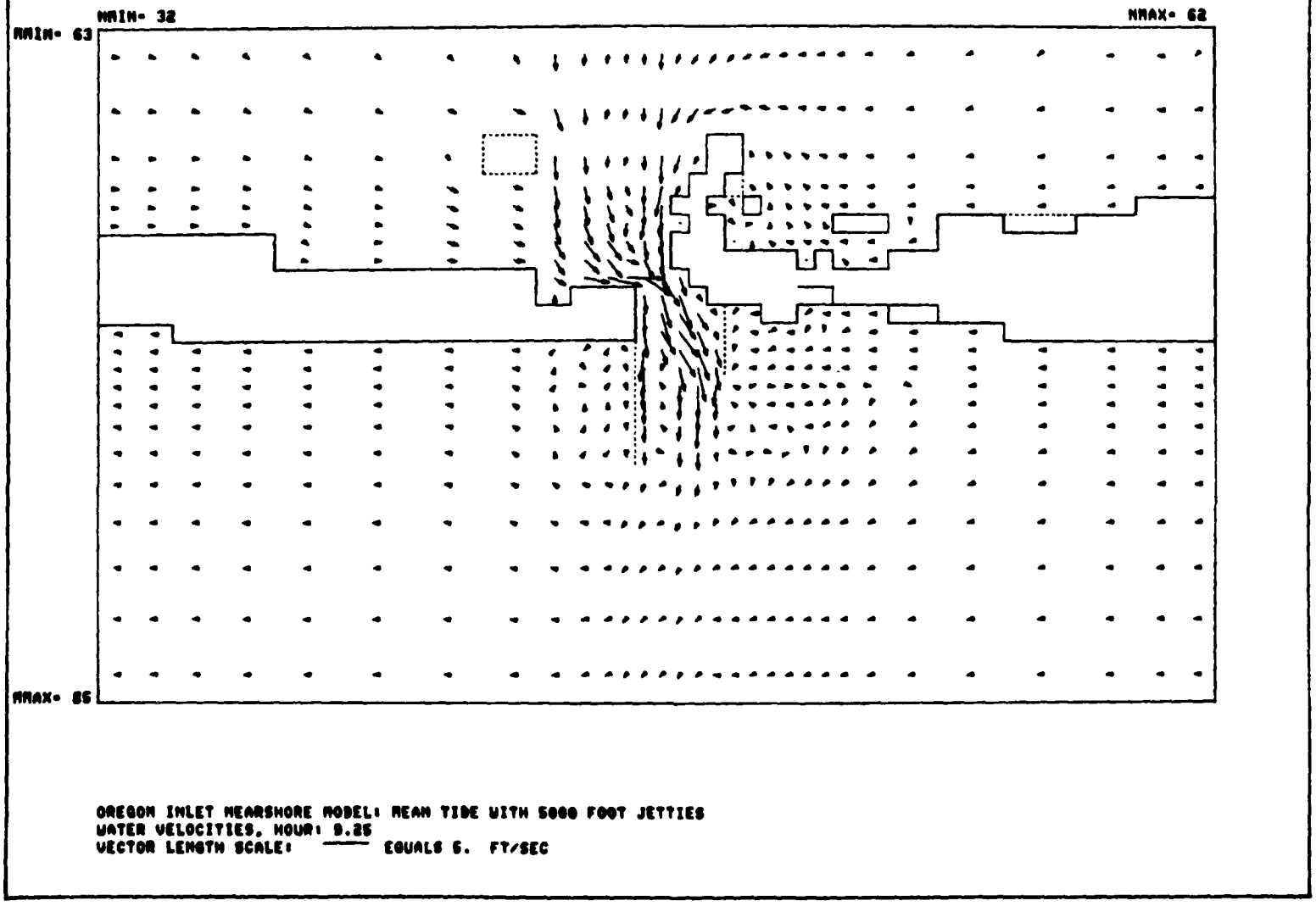

OREGON INLET NEARSHORE MODEL: MEAN TIDE WITH 5000 FOOT JETTIES
WATER VELOCITIES, HOUR: 9.25
VECTOR LENGTH SCALE: ——— EQUALS 6. FT/SEC

PLATE 75

PLATE 76

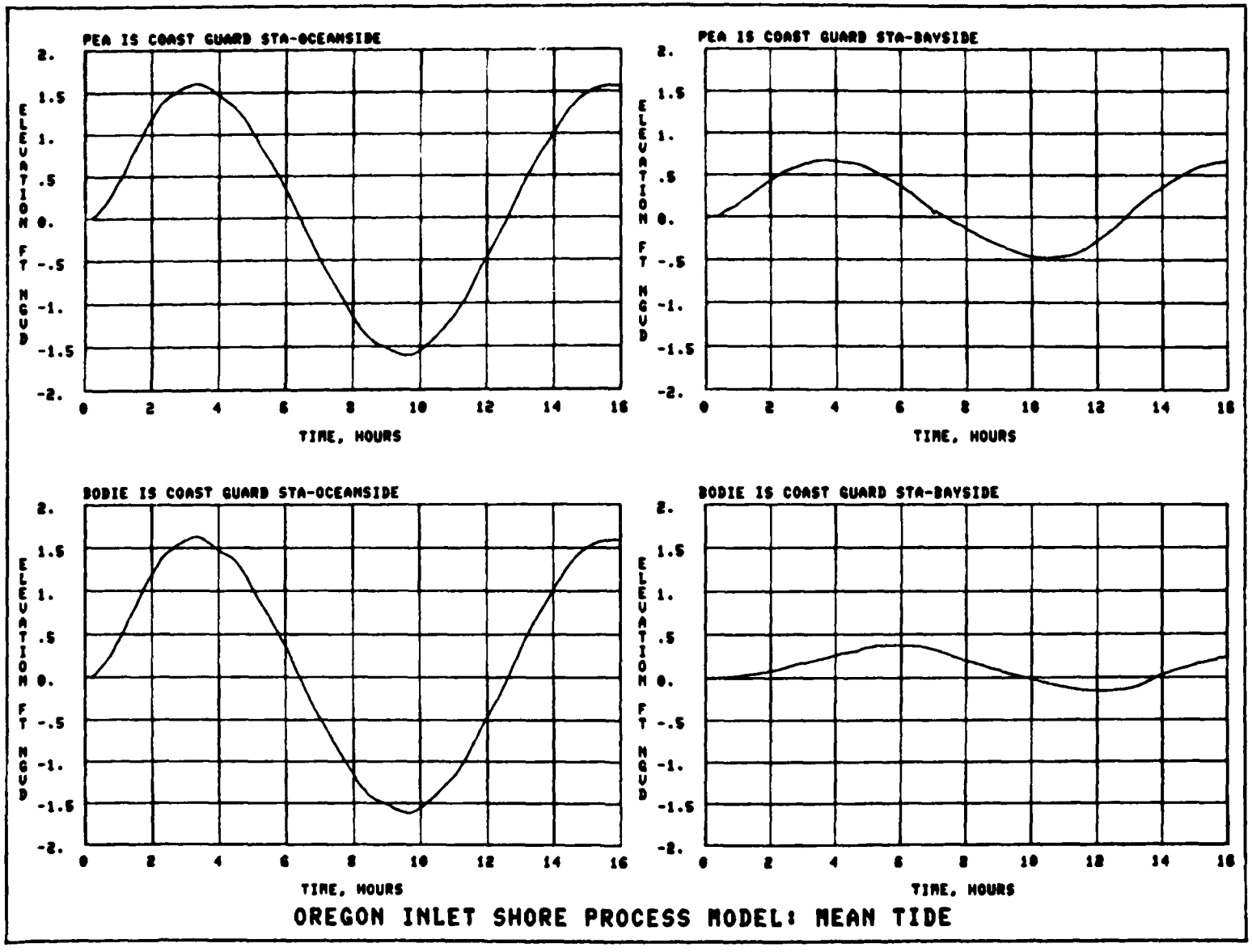

OREGON INLET SHORE PROCESS MODEL: MEAN TIDE

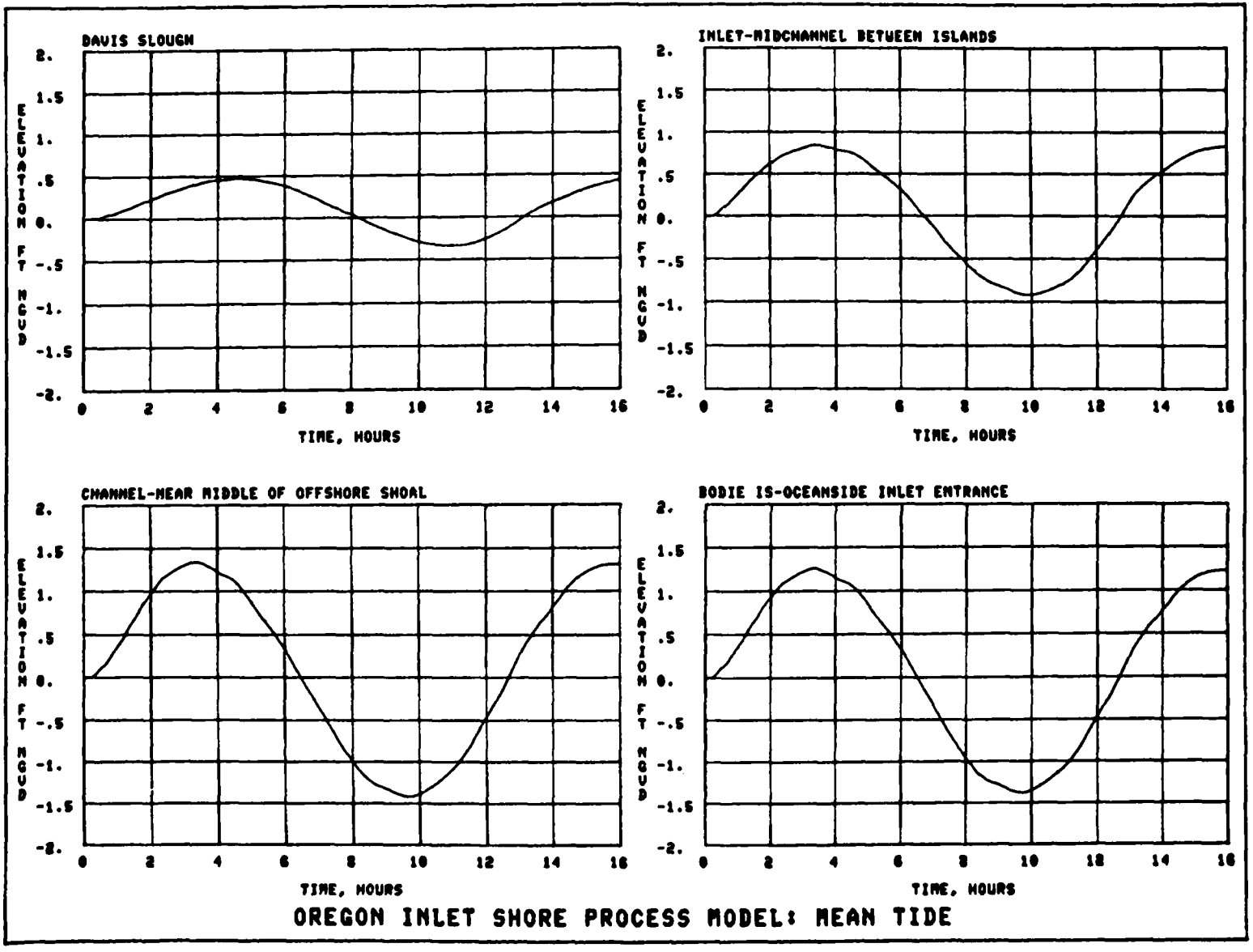

OREGON INLET SHORE PROCESS MODEL: MEAN TIDE

PLATE 77

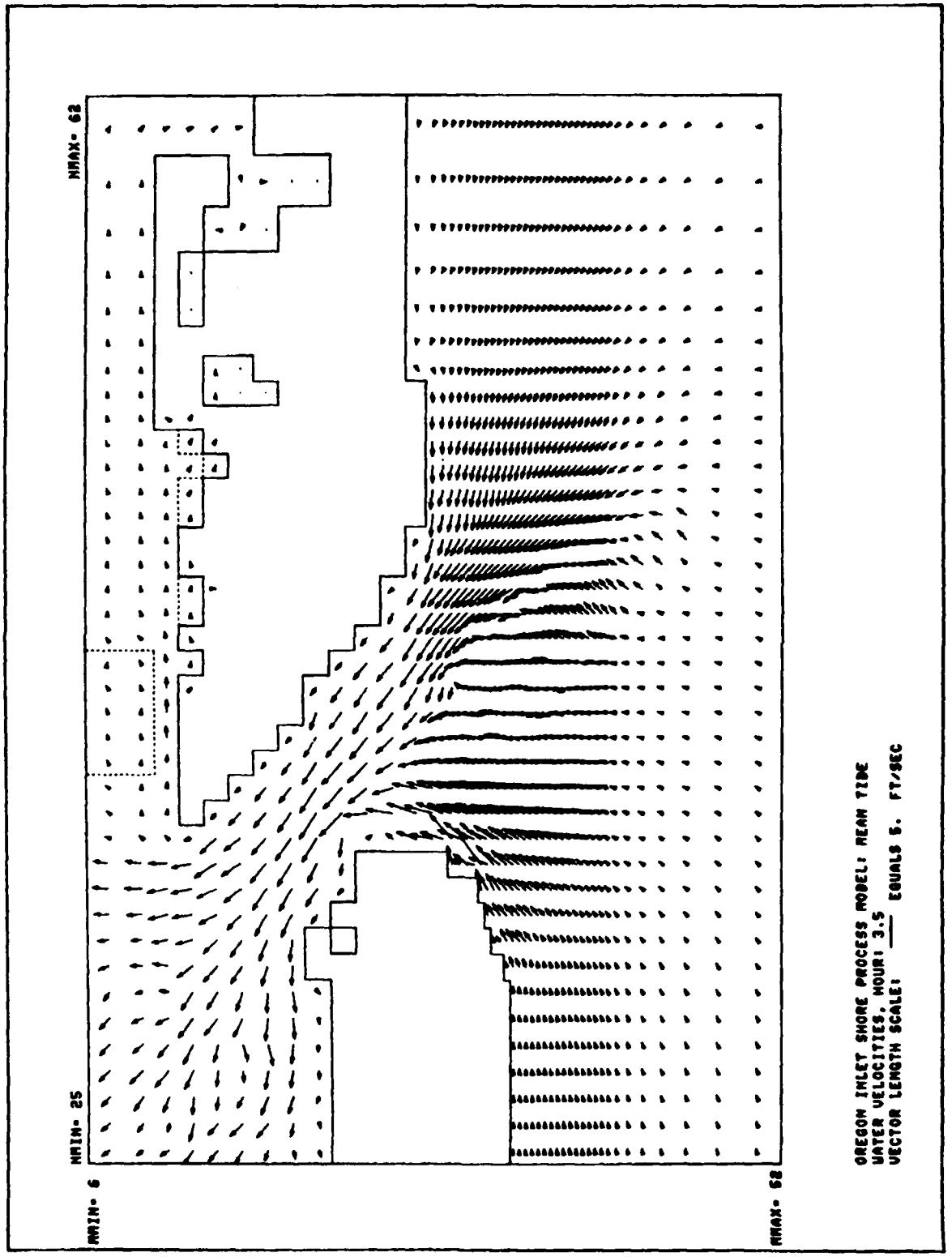
NMAX= 68
NMIN= 25
MMIN= 6
MMAX= 68
OREGON INLET SHORE PROCESS MODEL: MEAN TIDE
WATER VELOCITIES, HOUR: 3.5
VECTOR LENGTH SCALE: —— EQUALS 5. FT/SEC

PLATE 78

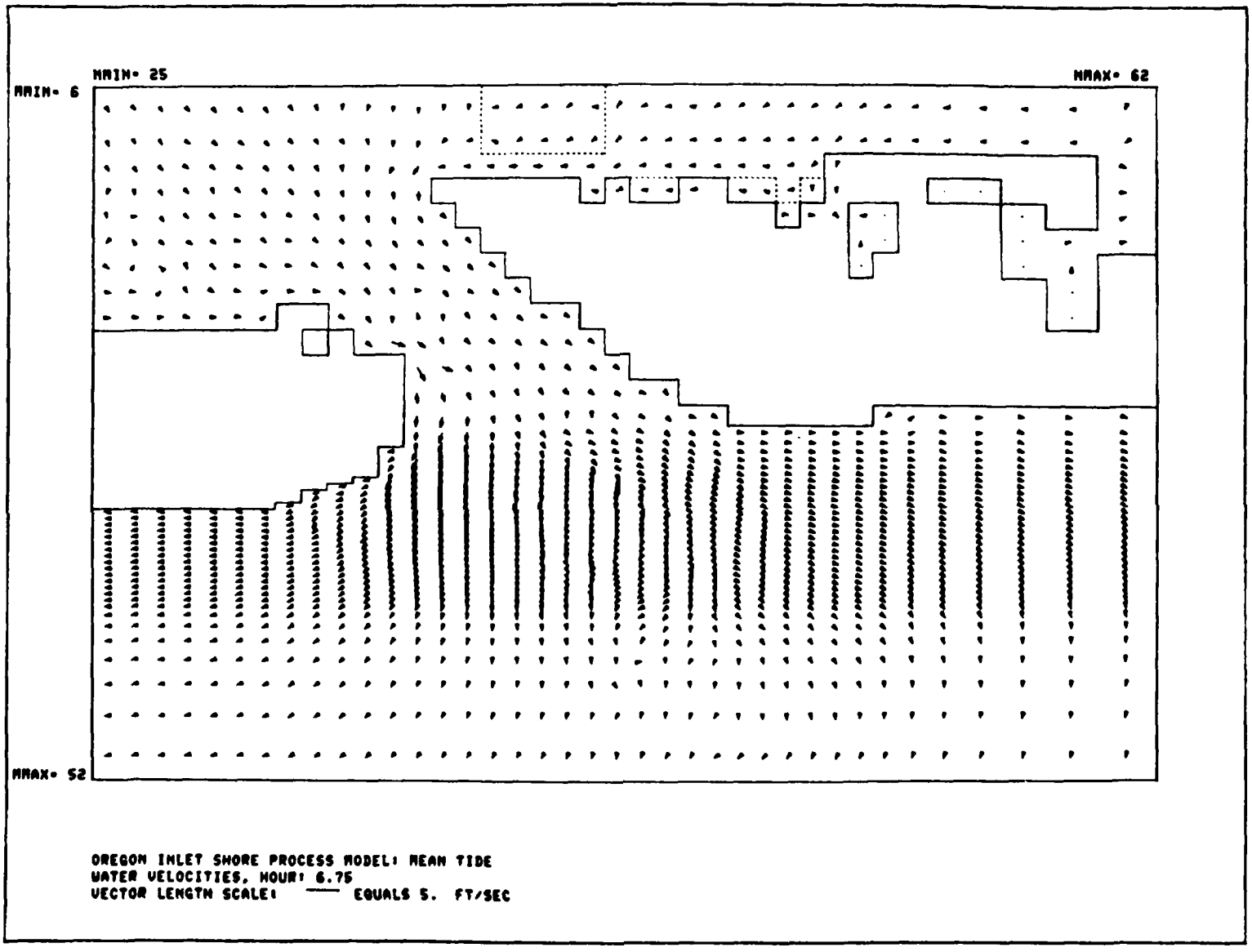

OREGON INLET SHORE PROCESS MODEL: MEAN TIDE
WATER VELOCITIES, HOUR: 6.75
VECTOR LENGTH SCALE: —— EQUALS 5. FT/SEC

PLATE 79

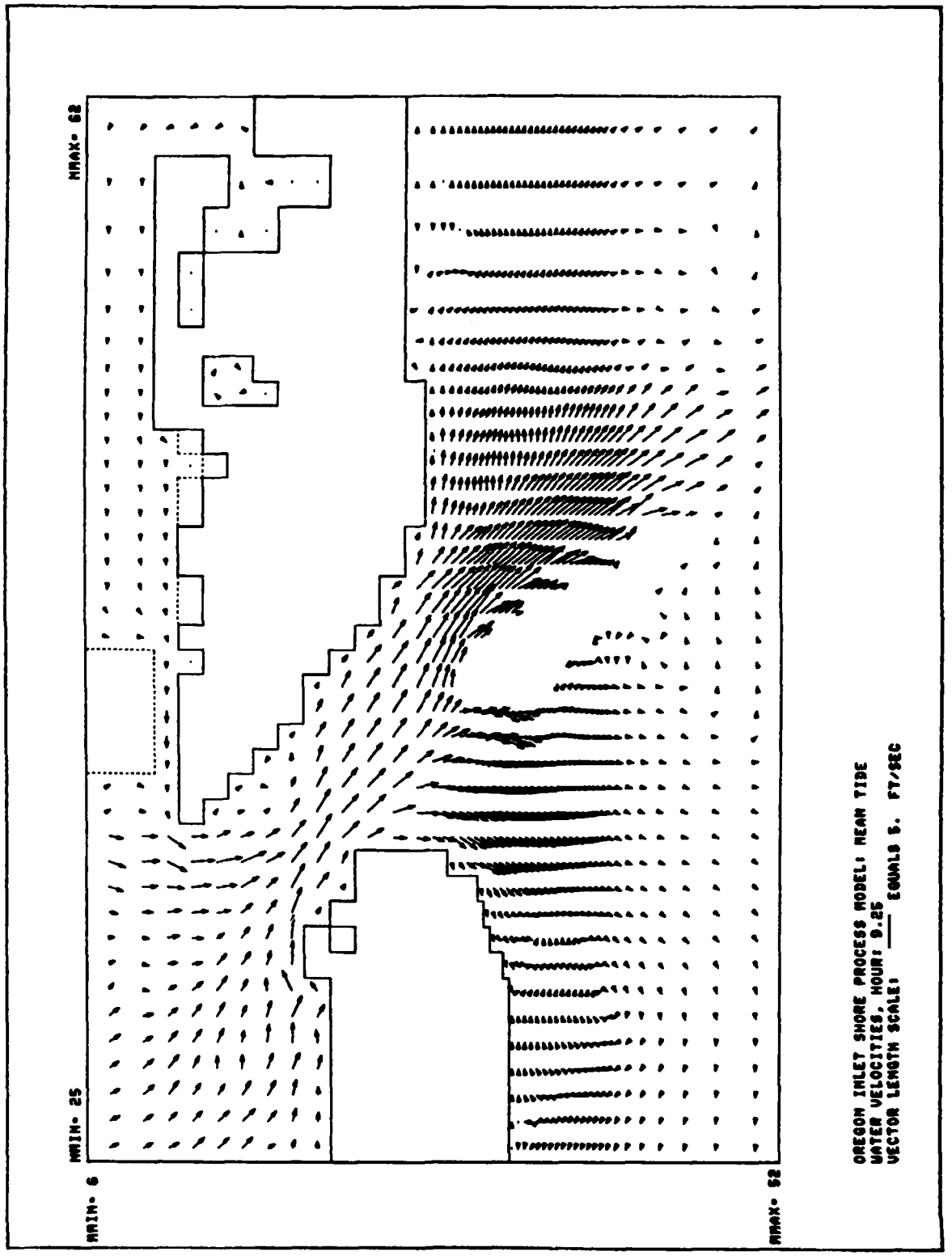
NMAX= 68
MMIN= 25
MMIN= 6
MMAX= 52
OREGON INLET SHORE PROCESS MODEL: MEAN TIDE
WATER VELOCITIES, HOUR: 9.25
VECTOR LENGTH SCALE: ___ EQUALS 5. FT/SEC

PLATE 80

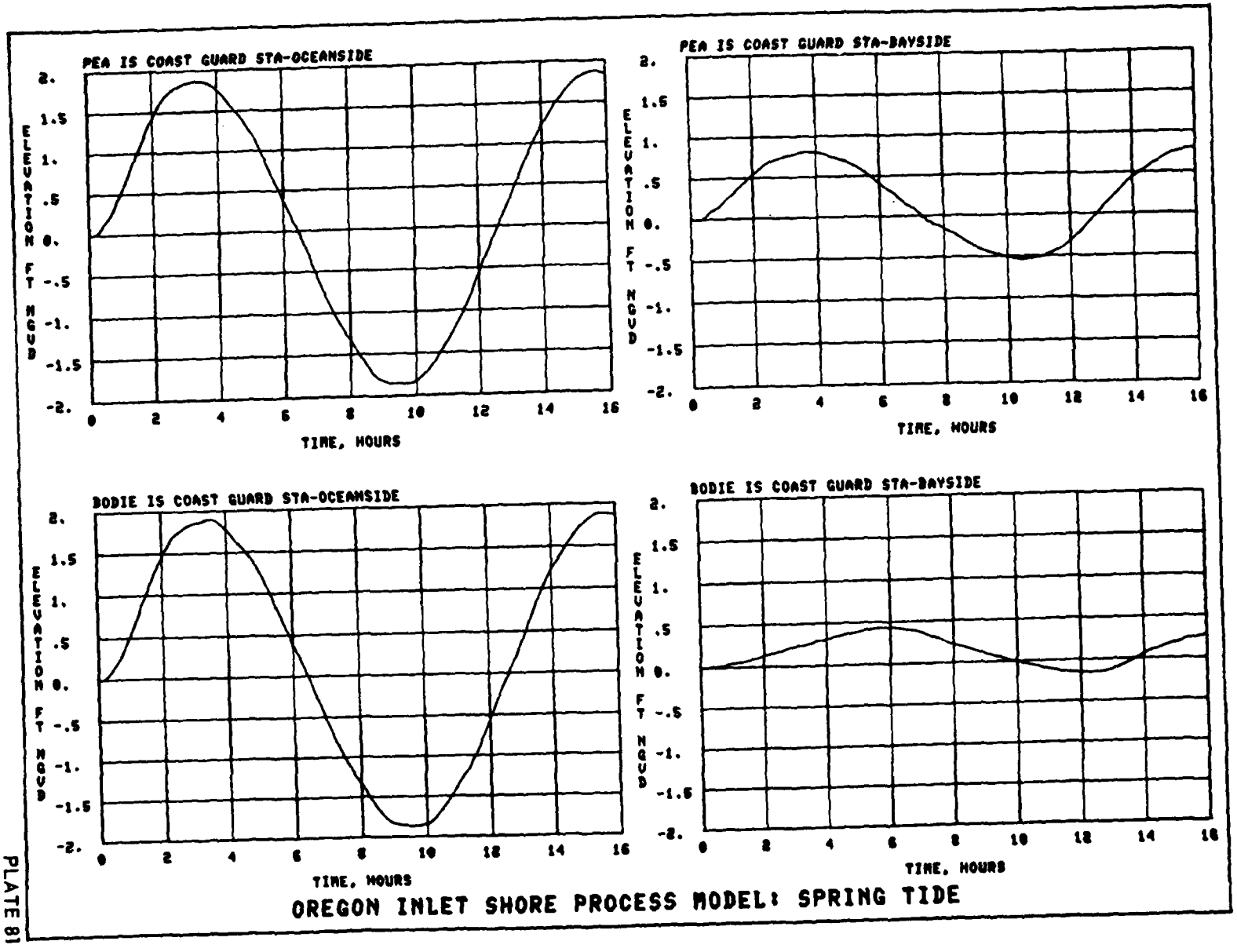

OREGON INLET SHORE PROCESS MODEL: SPRING TIDE

PLATE 81

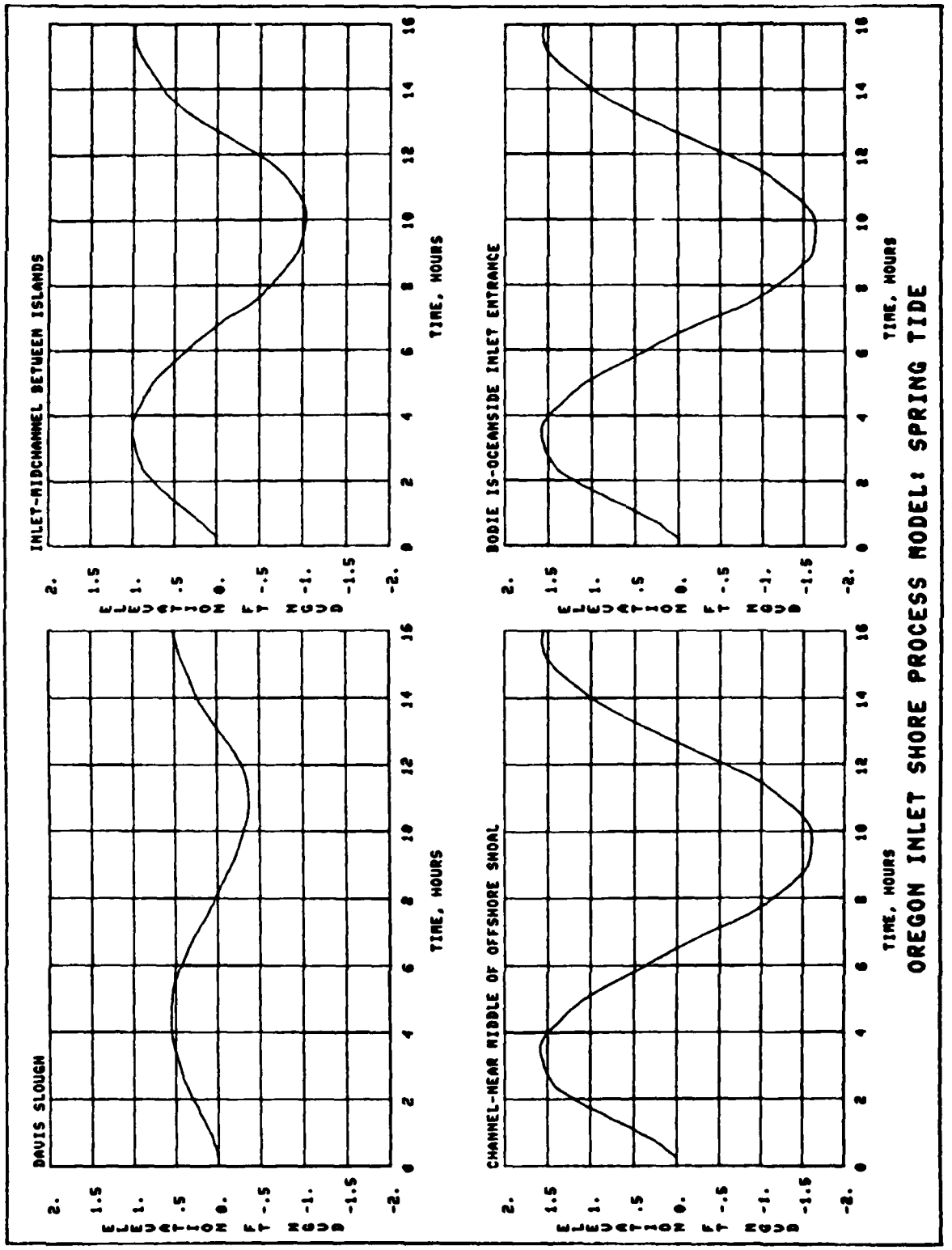

OREGON INLET SHORE PROCESS MODEL: SPRING TIDE

PLATE 82

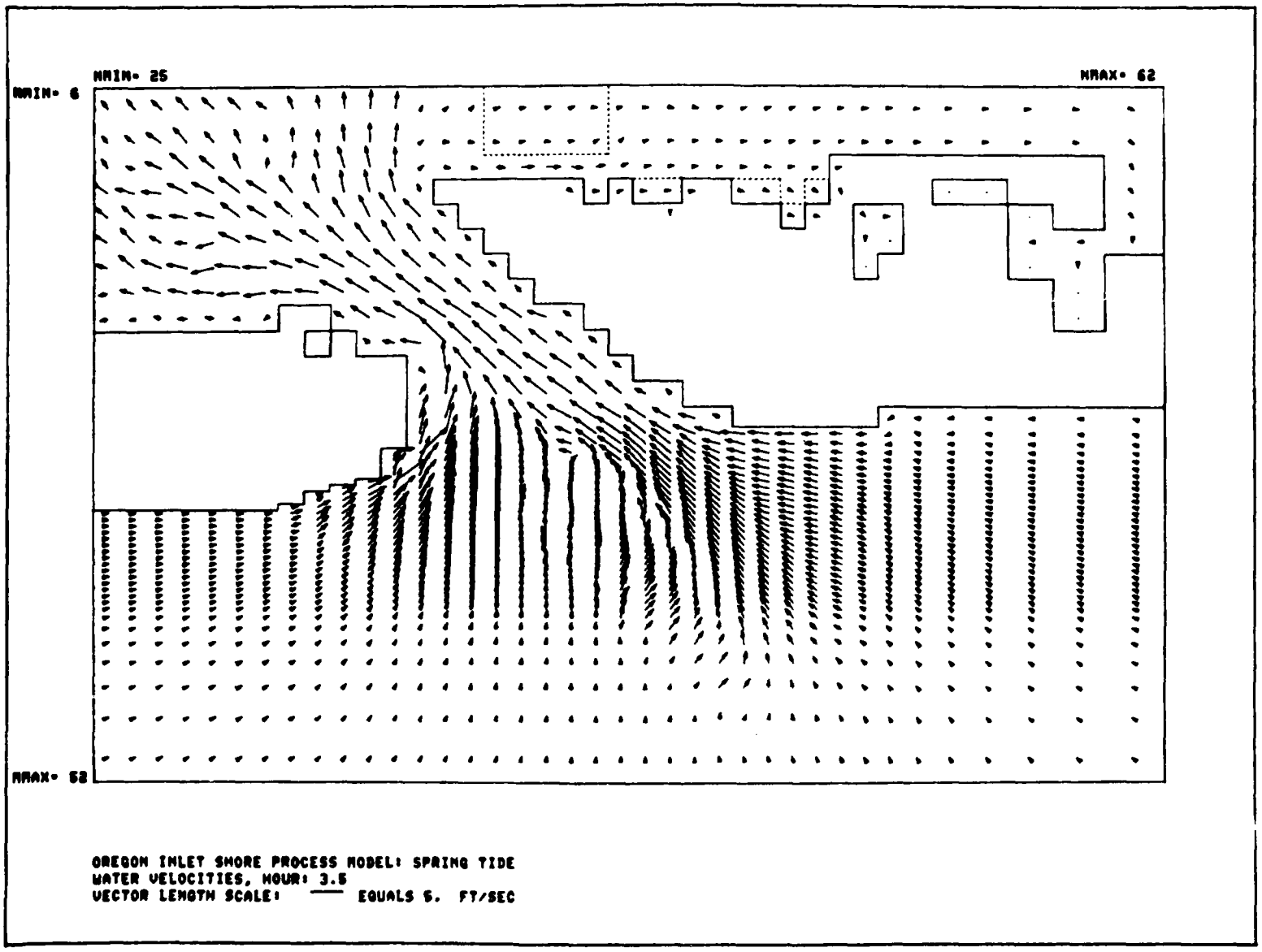

OREGON INLET SHORE PROCESS MODEL: SPRING TIDE
WATER VELOCITIES, HOUR: 3.5
VECTOR LENGTH SCALE: —— EQUALS 5. FT/SEC

PLATE 83

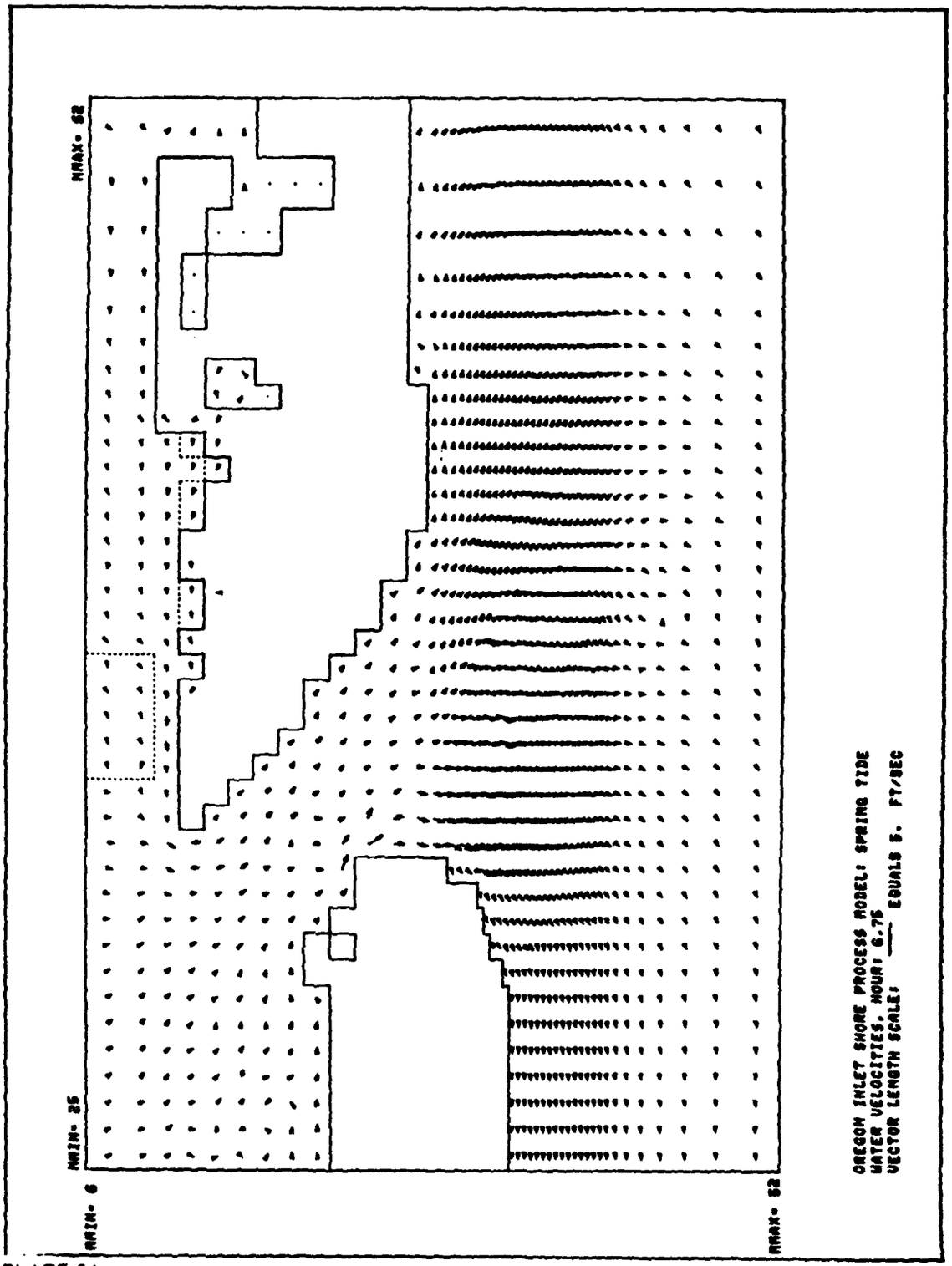
NMAX= 62
NMIN= 25
MMIN= 6
MMAX= 53
OREGON INLET SHORE PROCESS MODEL: SPRING TIDE
WATER VELOCITIES, HOUR: 6.75
VECTOR LENGTH SCALE: ——— EQUALS 5. FT/SEC

PLATE 84

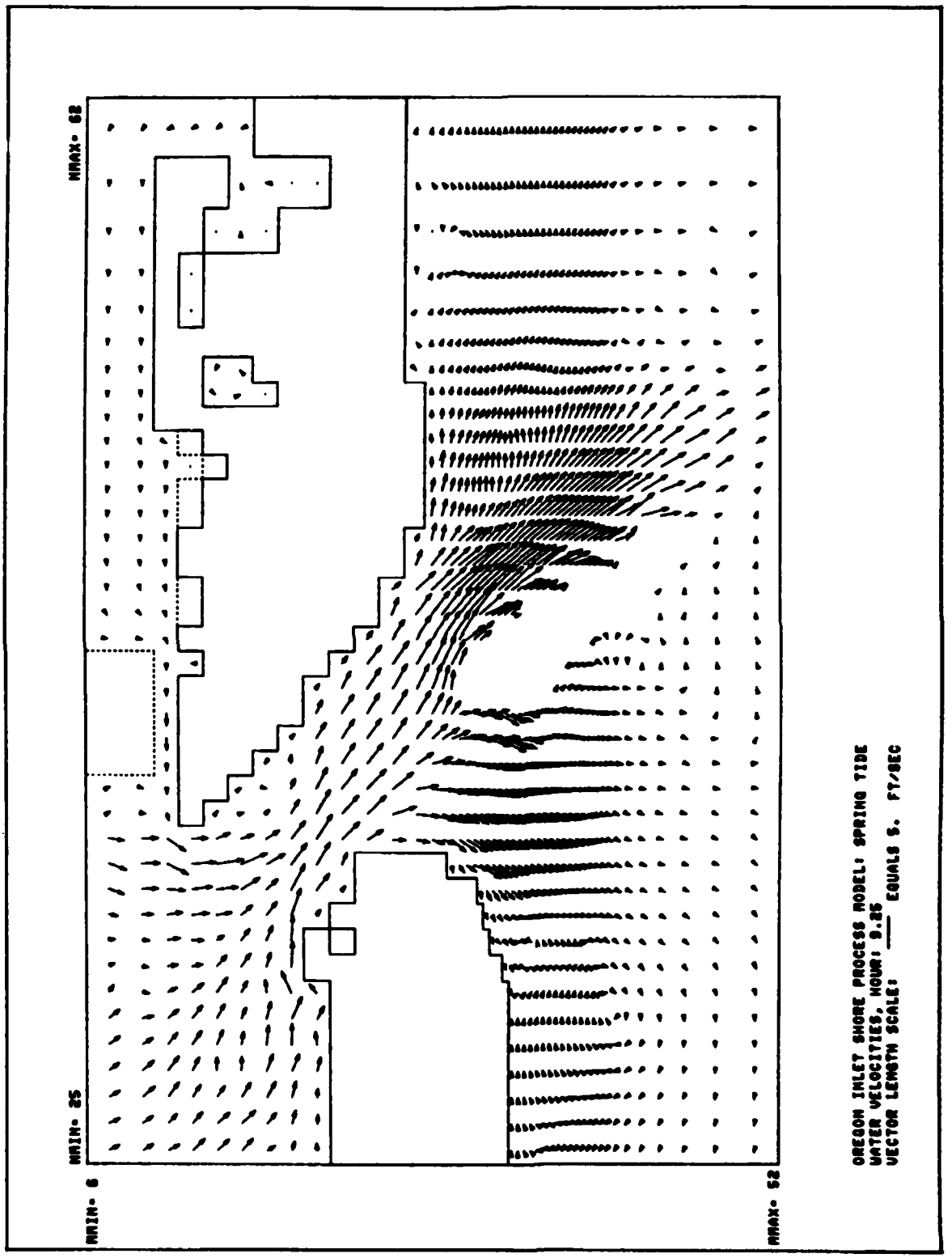
NMAX= 68
NMIN= 25
NMIN= 6
NMAX= 52
OREGON INLET SHORE PROCESS MODEL: SPRING TIDE
WATER VELOCITIES, HOUR: 9.25
VECTOR LENGTH SCALE: —— EQUALS 5. FT/SEC

PLATE 85

PLATE 86

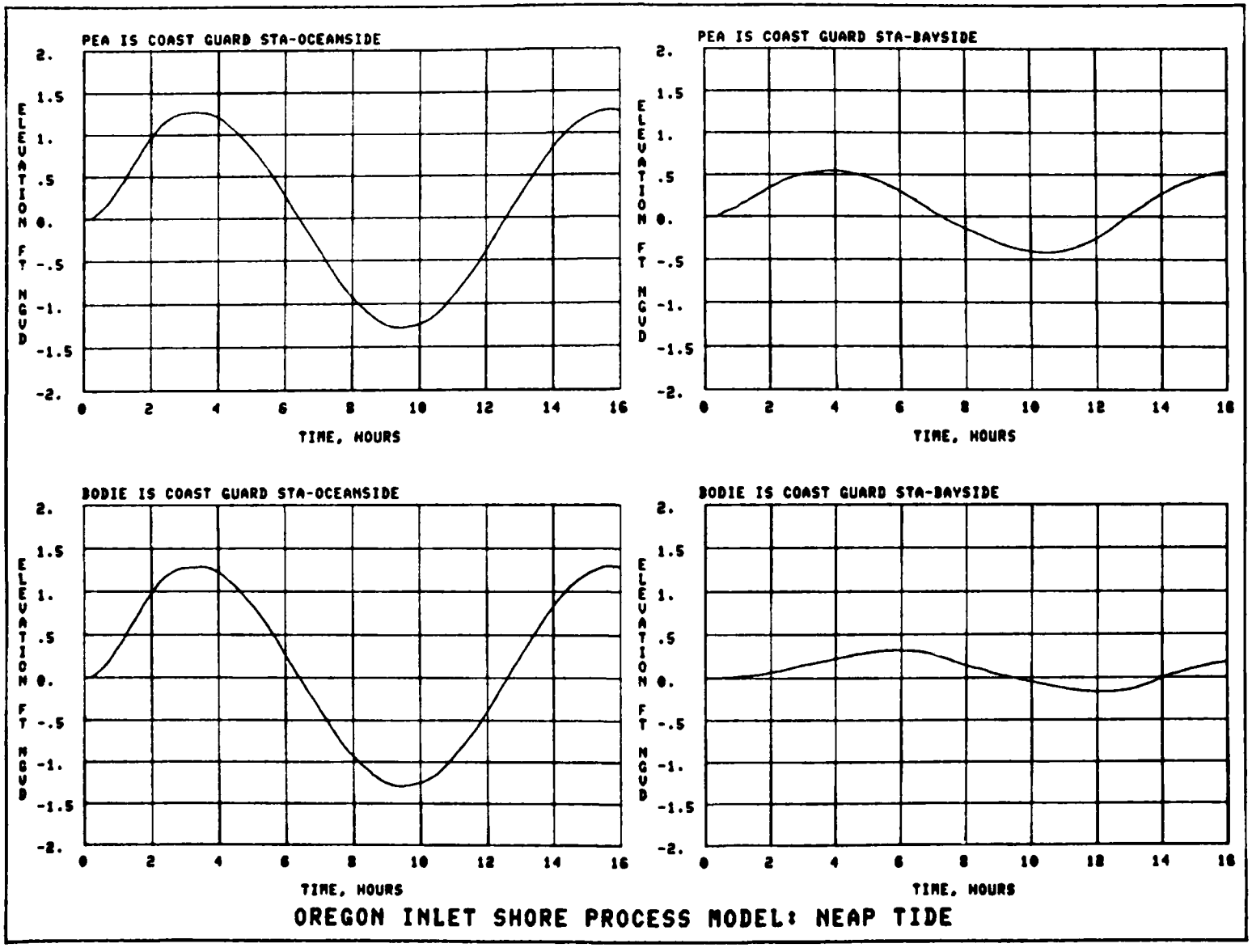

OREGON INLET SHORE PROCESS MODEL: NEAP TIDE

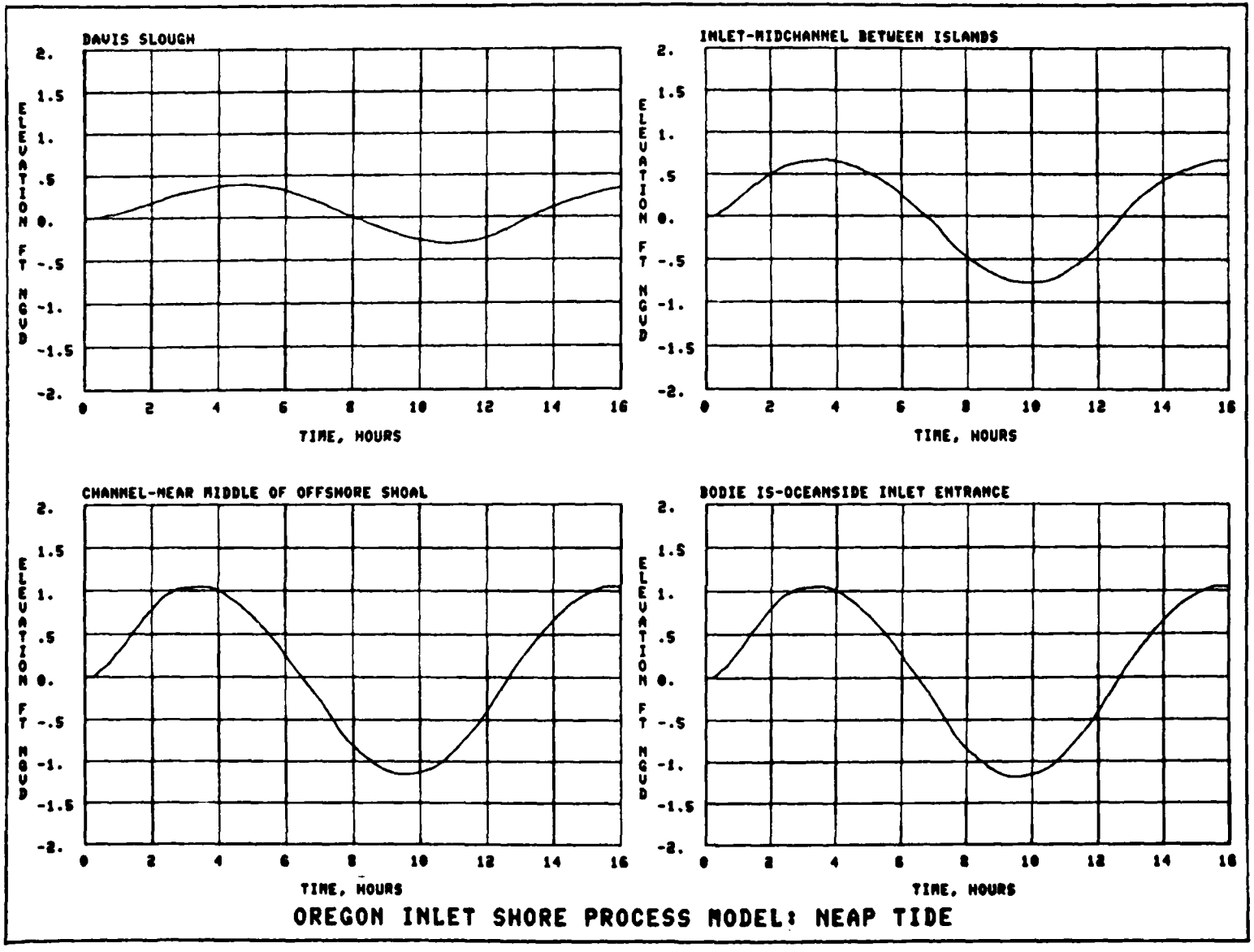

OREGON INLET SHORE PROCESS MODEL: NEAP TIDE

PLATE 87

PLATE 88

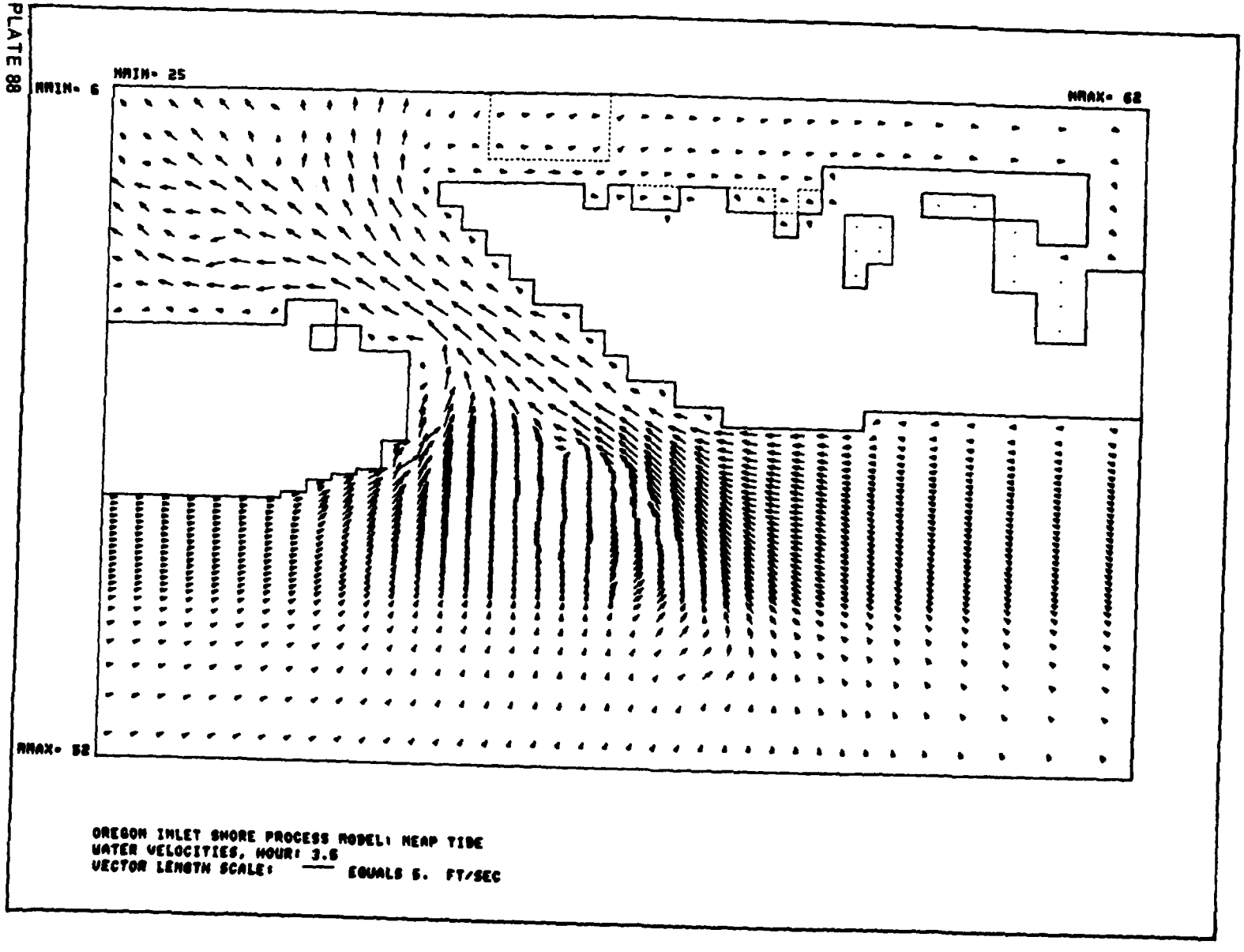

OREGON INLET SHORE PROCESS MODEL: NEAP TIDE
WATER VELOCITIES, HOUR: 3.6
VECTOR LENGTH SCALE: —— EQUALS 5. FT/SEC

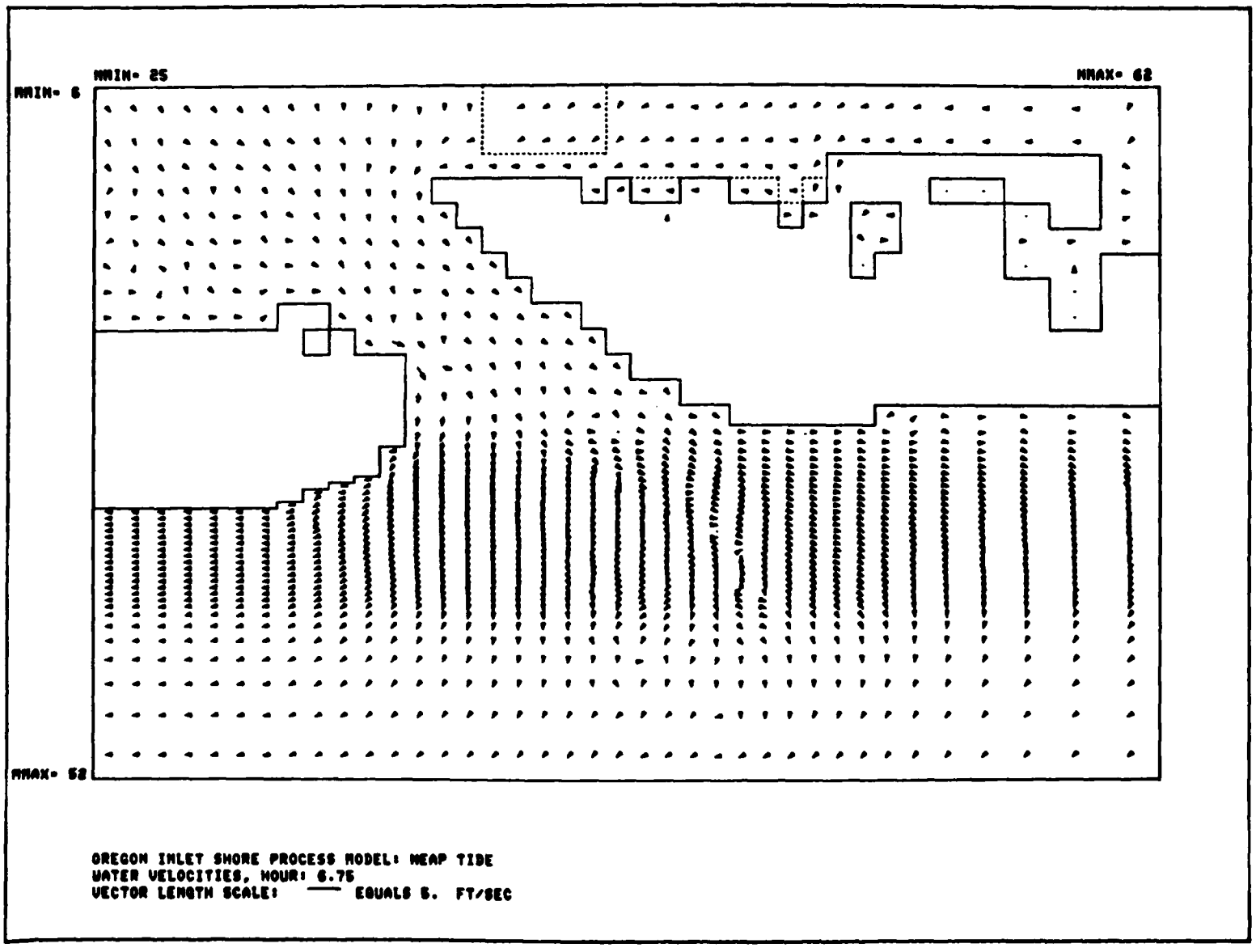

OREGON INLET SHORE PROCESS MODEL: MEAP TIDE
WATER VELOCITIES, HOUR: 6.75
VECTOR LENGTH SCALE: —— EQUALS 5. FT/SEC

PLATE 89

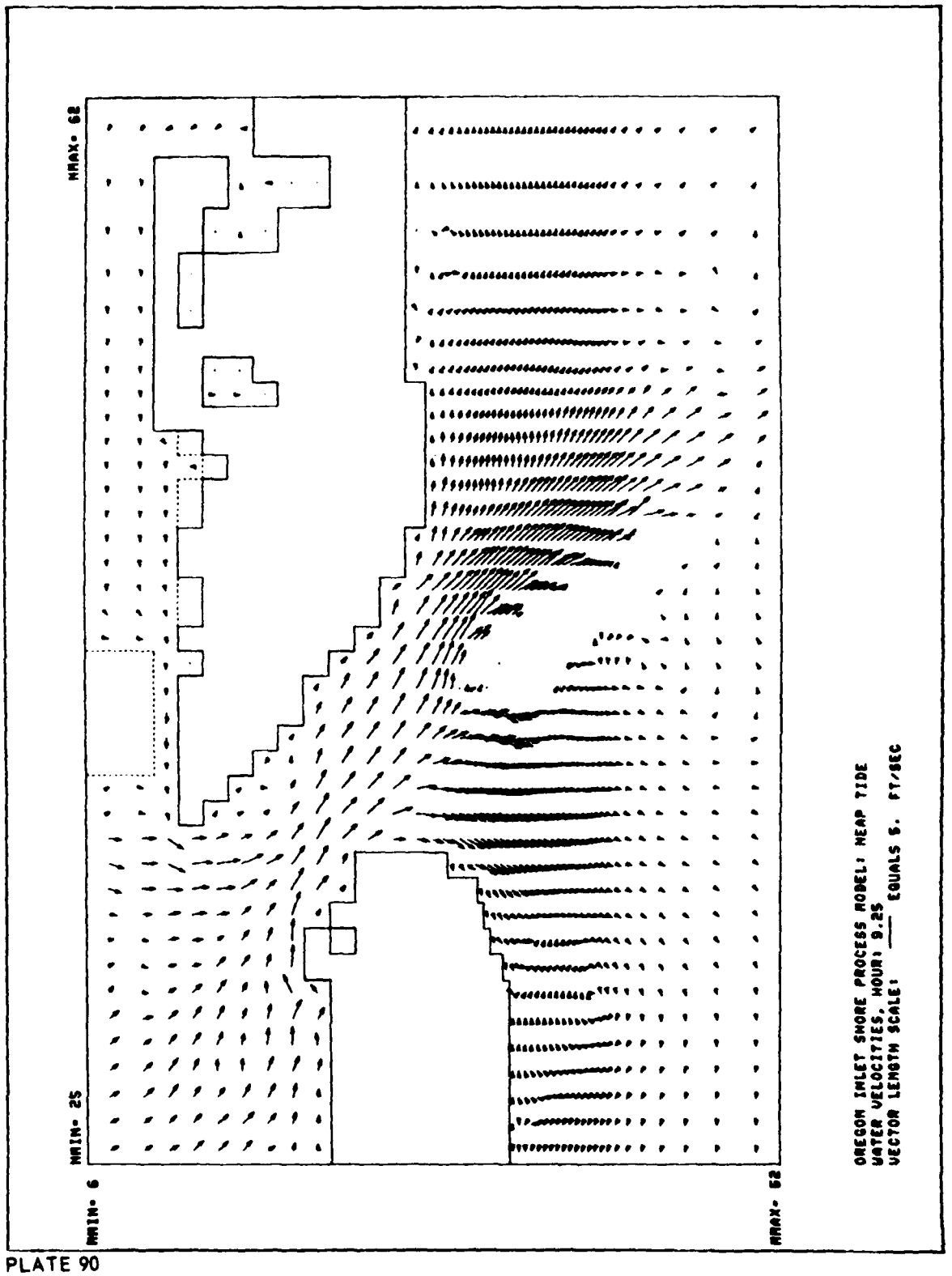
MAX= 68
MIN= 25
MIN= 6
MAX= 62
OREGON INLET SHORE PROCESS MODEL: NEAP TIDE
WATER VELOCITIES, HOUR: 9.25
VECTOR LENGTH SCALE: —— EQUALS 5. FT/SEC

PLATE 90

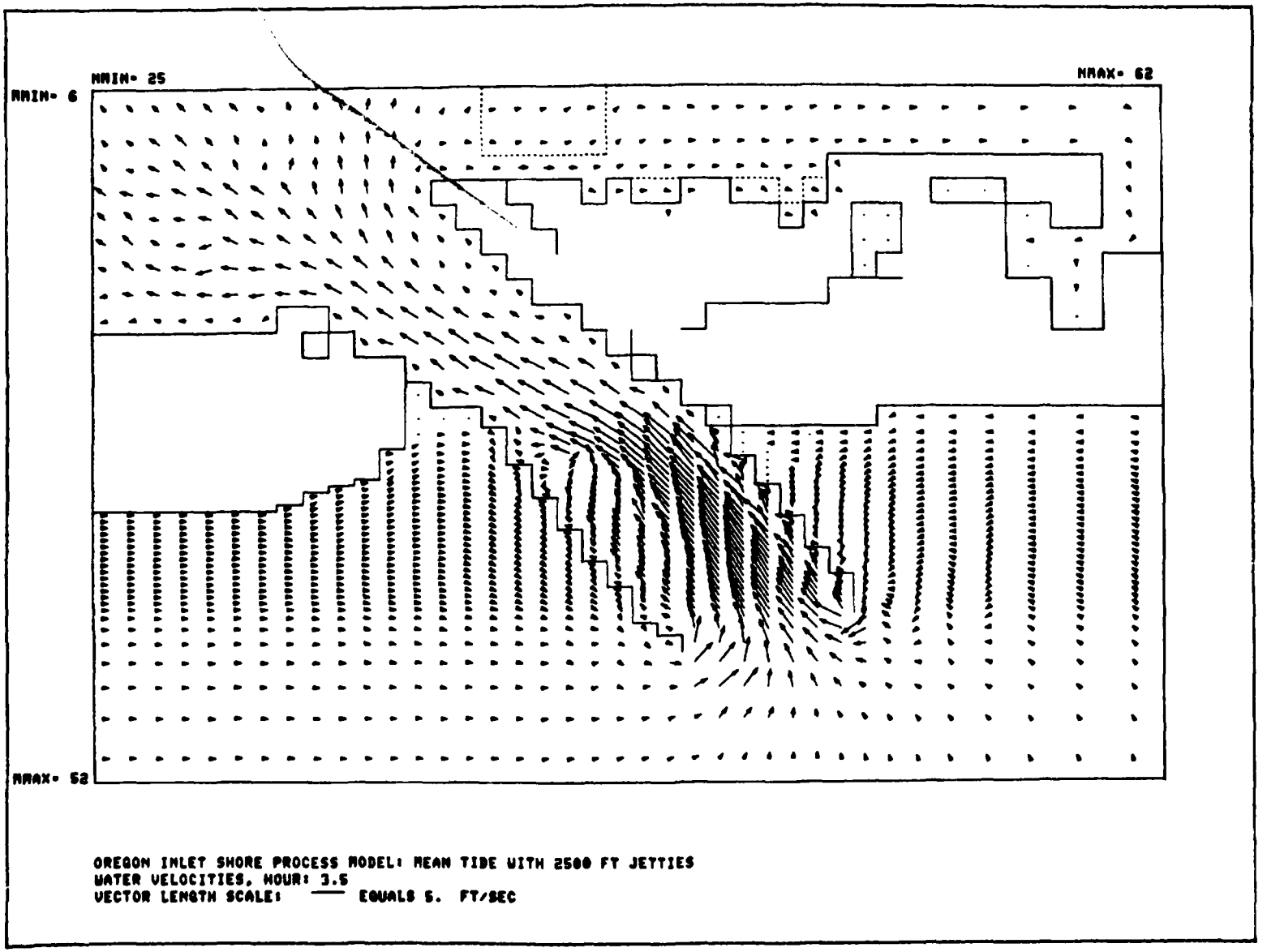

OREGON INLET SHORE PROCESS MODEL: MEAN TIDE WITH 2500 FT JETTIES
WATER VELOCITIES, HOUR: 3.5
VECTOR LENGTH SCALE: —— EQUALS 5. FT/SEC

PLATE 91

PLATE 92

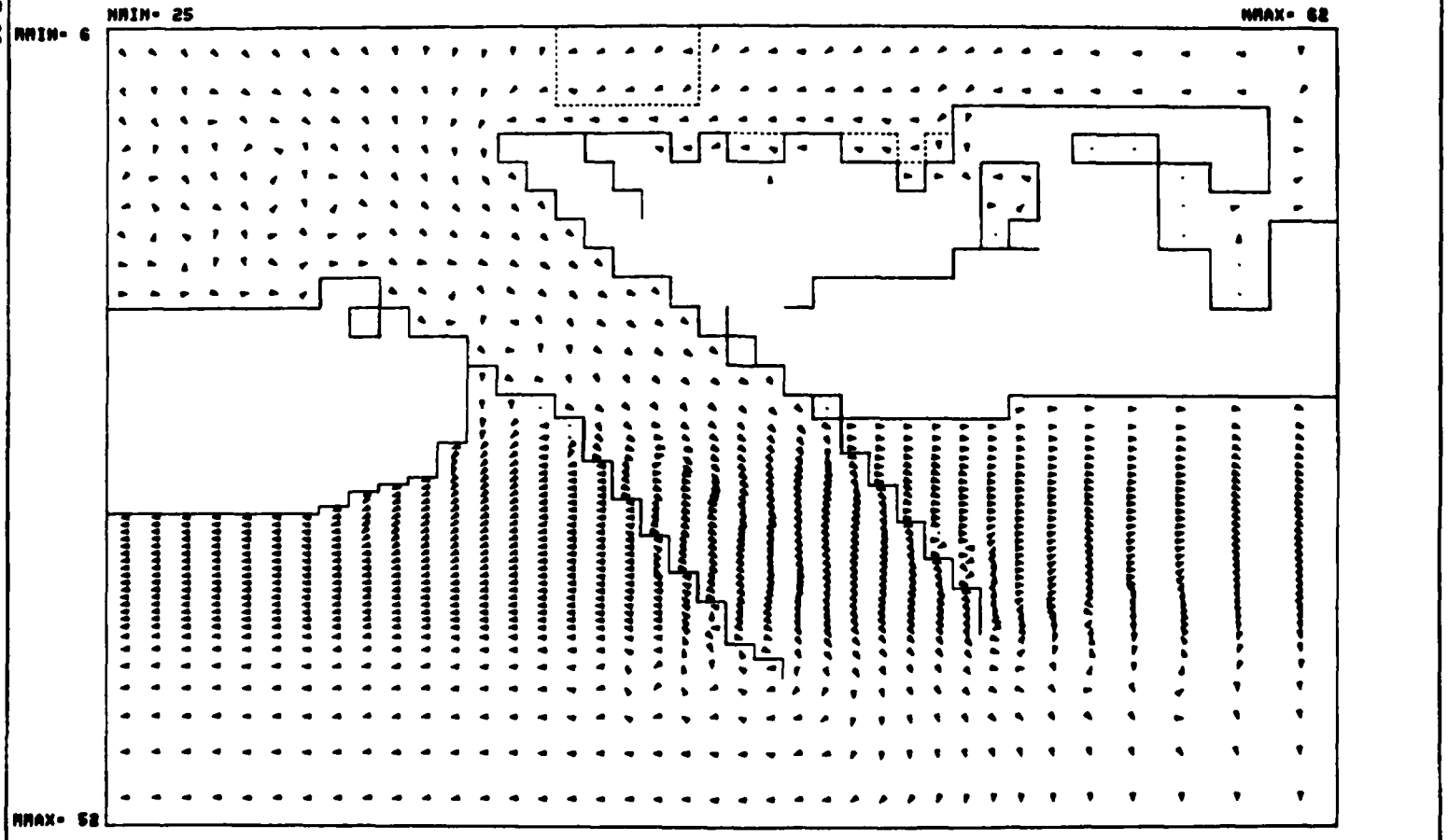

OREGON INLET SHORE PROCESS MODEL: MEAN TIDE WITH 2500 FT JETTIES
WATER VELOCITIES, HOUR: 6.75
VECTOR LENGTH SCALE: —— EQUALS 5. FT/SEC

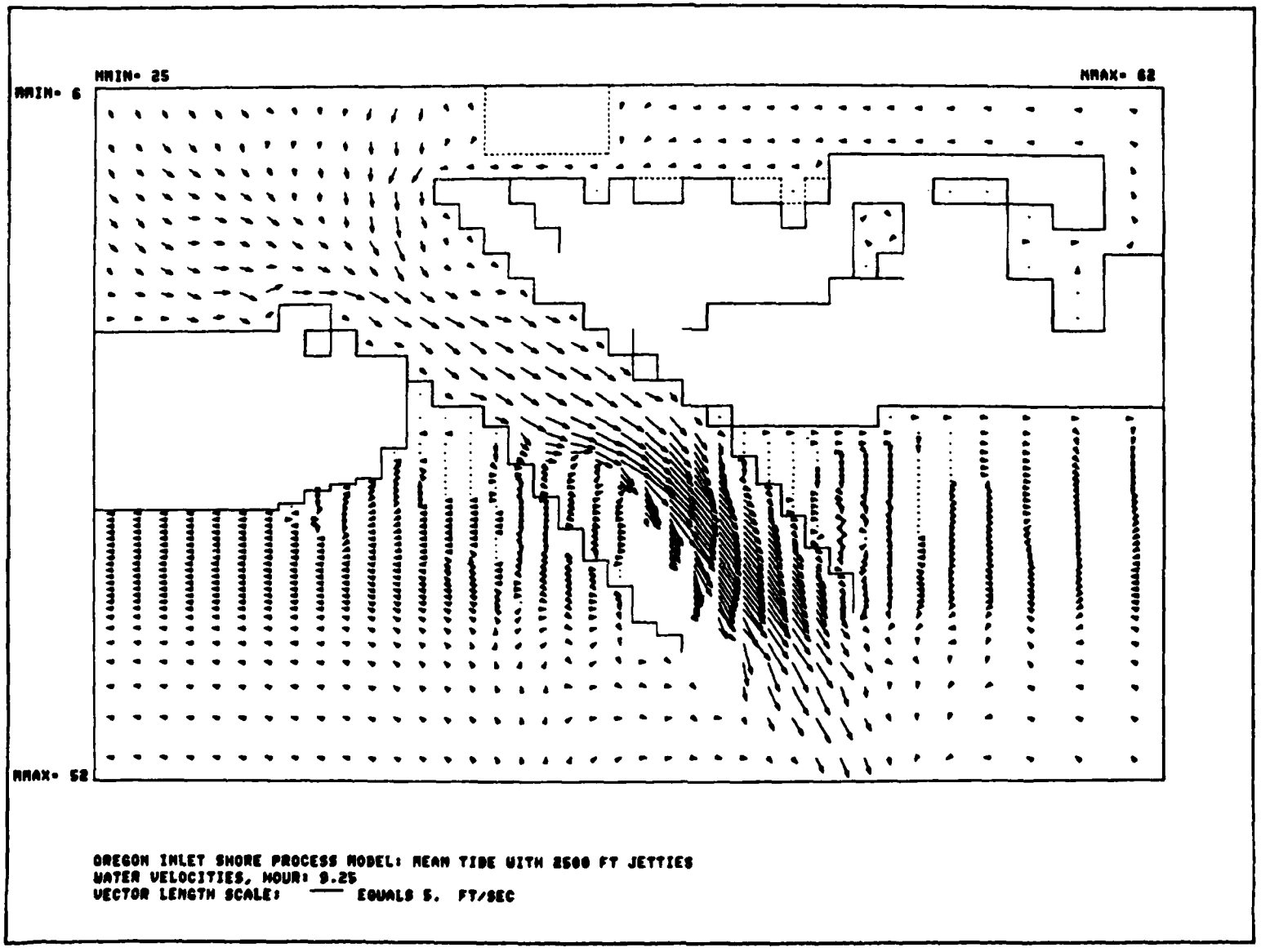

OREGON INLET SHORE PROCESS MODEL: MEAN TIDE WITH 2500 FT JETTIES
WATER VELOCITIES, HOUR: 9.25
VECTOR LENGTH SCALE: —— EQUALS 5. FT/SEC

PLATE 93

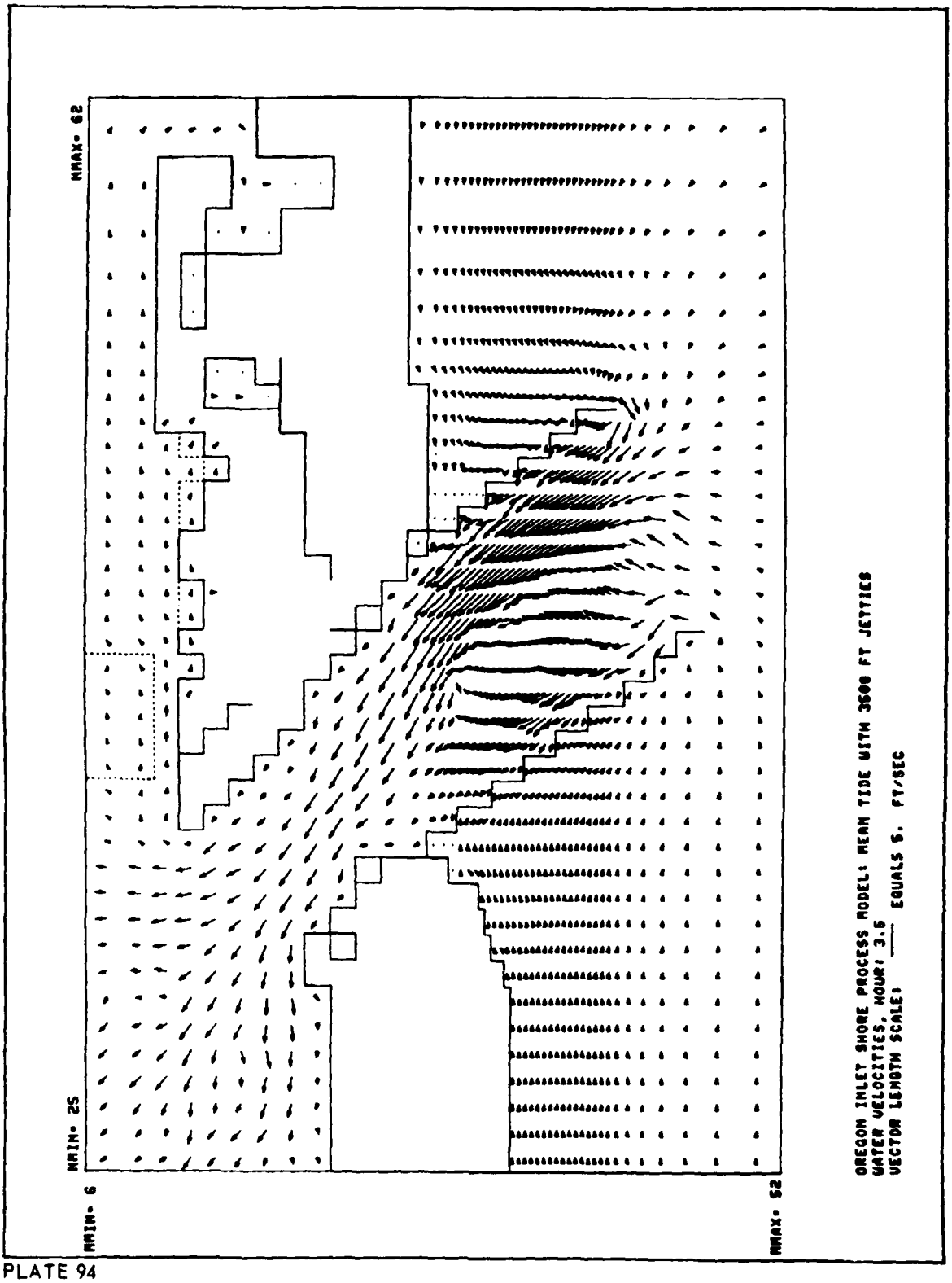
NMAX= 62
NMIN= 25
MMIN= 6
MMAX= 52
OREGON INLET SHORE PROCESS MODEL: MEAN TIDE WITH 3500 FT JETTIES
WATER VELOCITIES, HOUR: 3.5
VECTOR LENGTH SCALE: ____ EQUALS 5. FT/SEC

PLATE 94

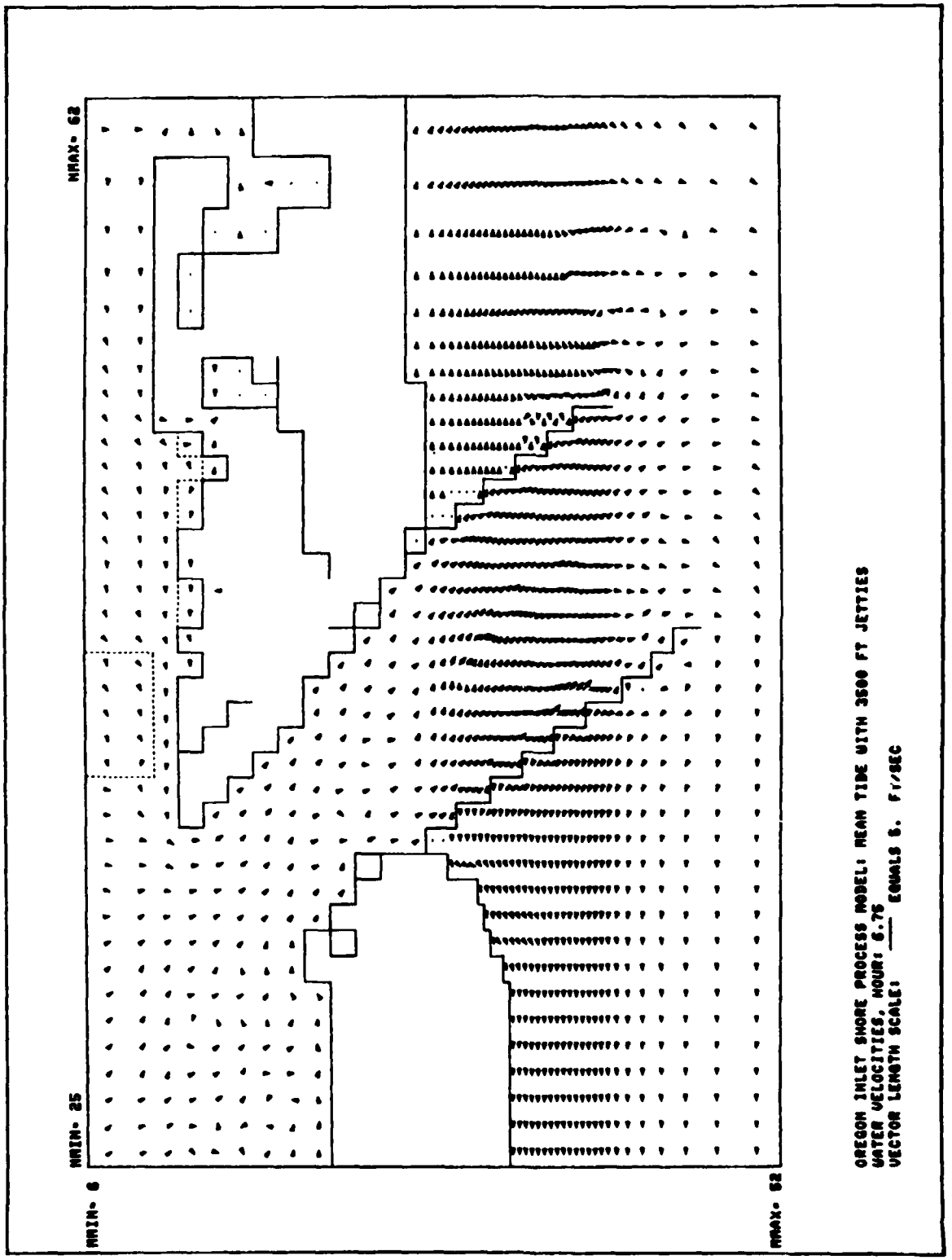
NMAX= 68
NMIN= 25
NMIN= 6
NMAX= 62
OREGON INLET SHORE PROCESS MODEL: MEAN TIDE WITH 3500 FT JETTIES
WATER VELOCITIES, HOUR: 6.75
VECTOR LENGTH SCALE: ___ EQUALS 6. FT/SEC

PLATE 95

PLATE 96

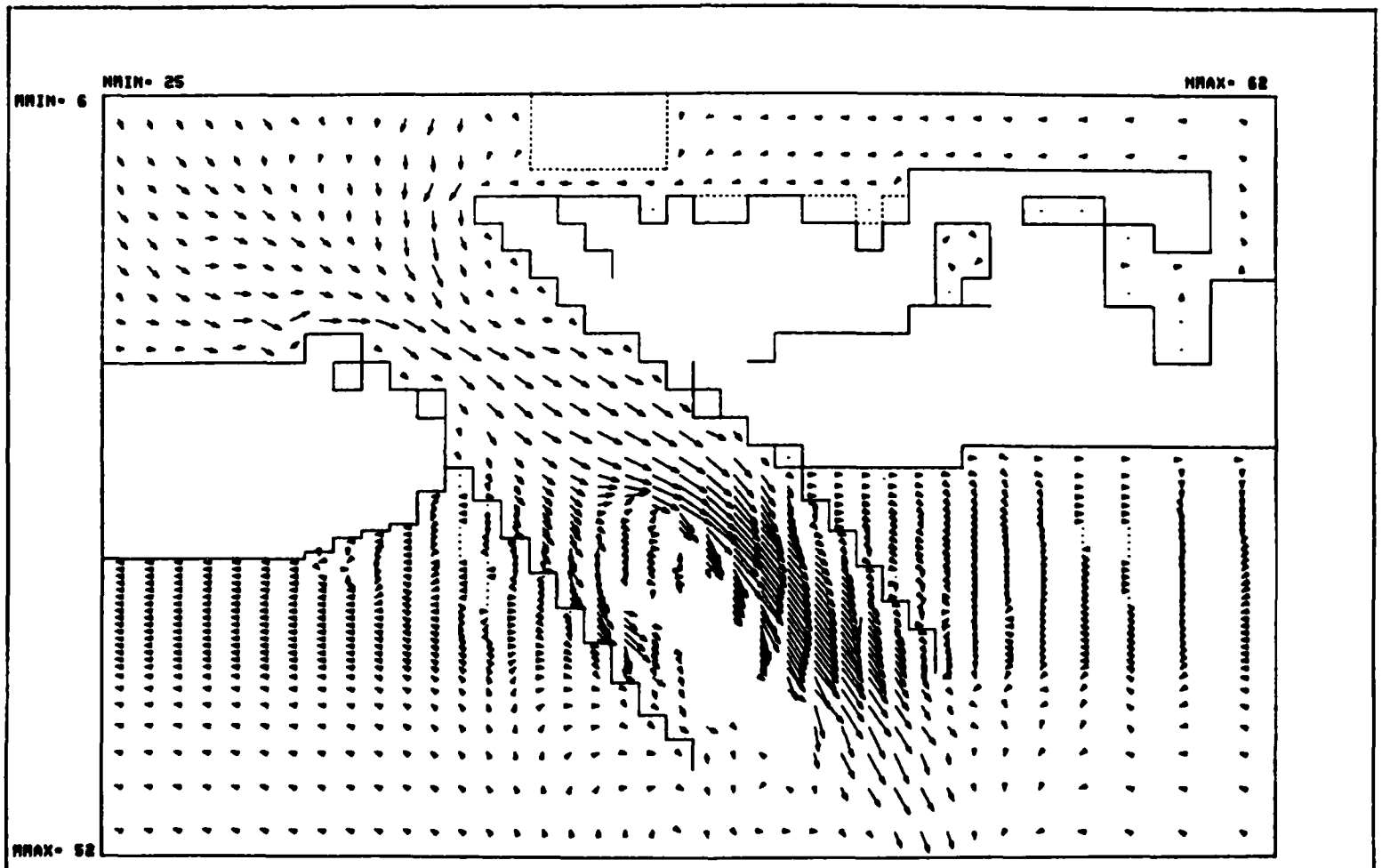

OREGON INLET SHORE PROCESS MODEL: MEAN TIDE WITH 3600 FT JETTIES
WATER VELOCITIES, HOUR: 9.25
VECTOR LENGTH SCALE: —— EQUALS 5. FT/SEC

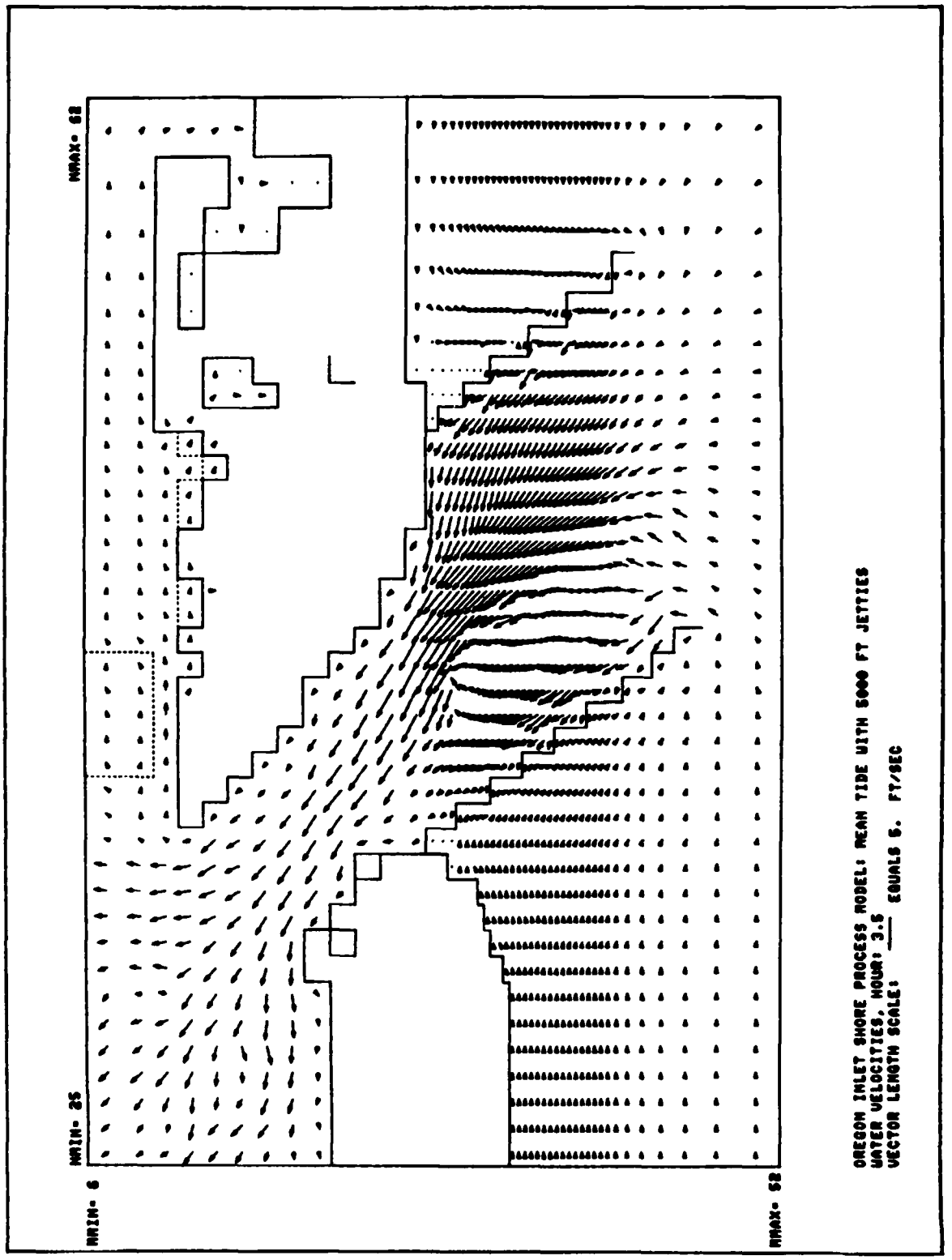
NMAX= 62
NMIN= 25
NMIN= 6
NMAX= 52
OREGON INLET SHORE PROCESS MODEL: MEAN TIDE WITH 5000 FT JETTIES
WATER VELOCITIES, HOUR: 3.5
VECTOR LENGTH SCALE: —— EQUALS 5. FT/SEC

PLATE 97

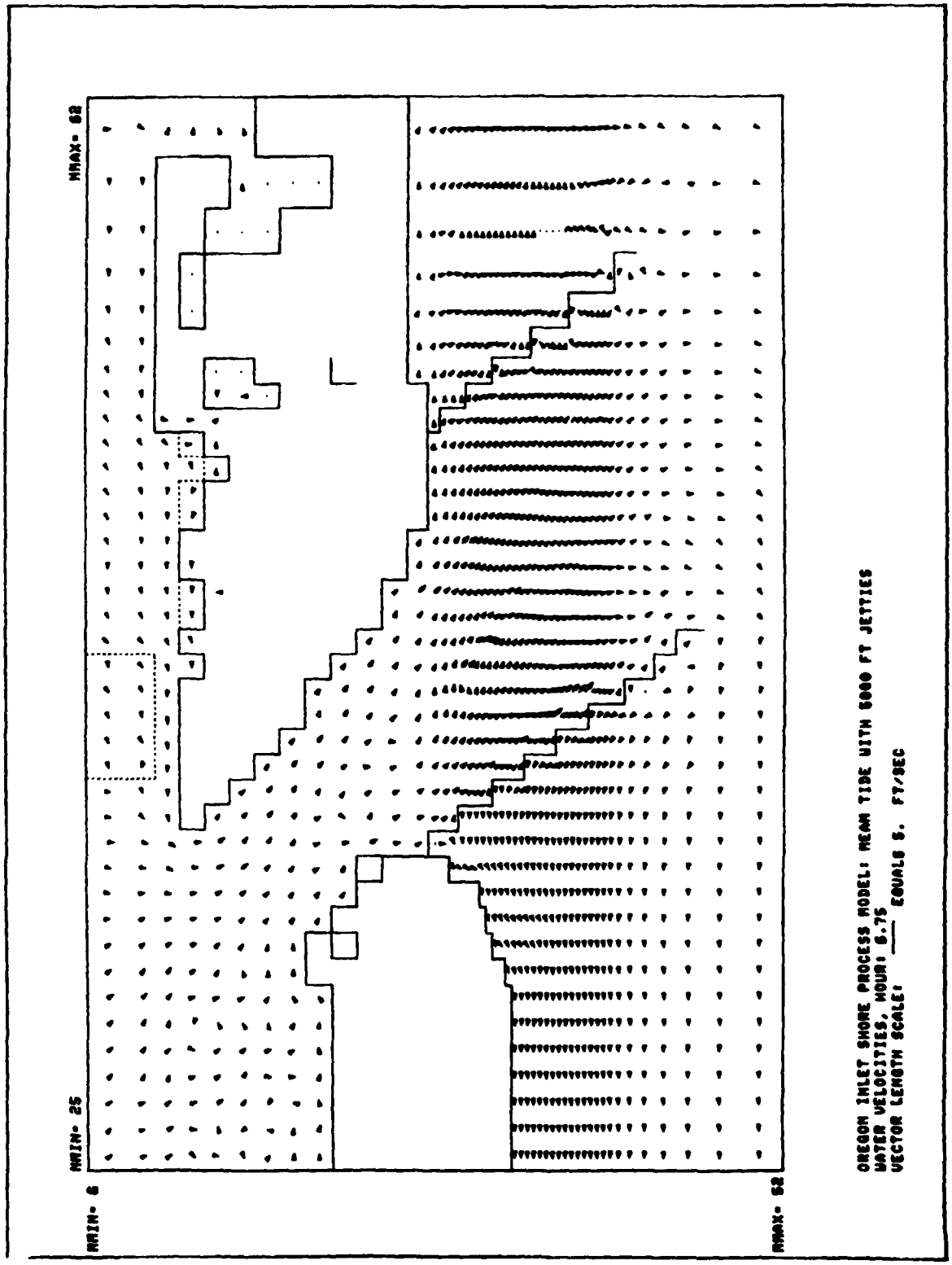
NMAX= 62
NMIN= 25
MMIN= 6
MMAX= 52
OREGON INLET SHORE PROCESS MODEL: MEAN TIDE WITH 6000 FT JETTIES
WATER VELOCITIES, HOUR: 6.75
VECTOR LENGTH SCALE: ___ EQUALS 5. FT/SEC

PLATE 98

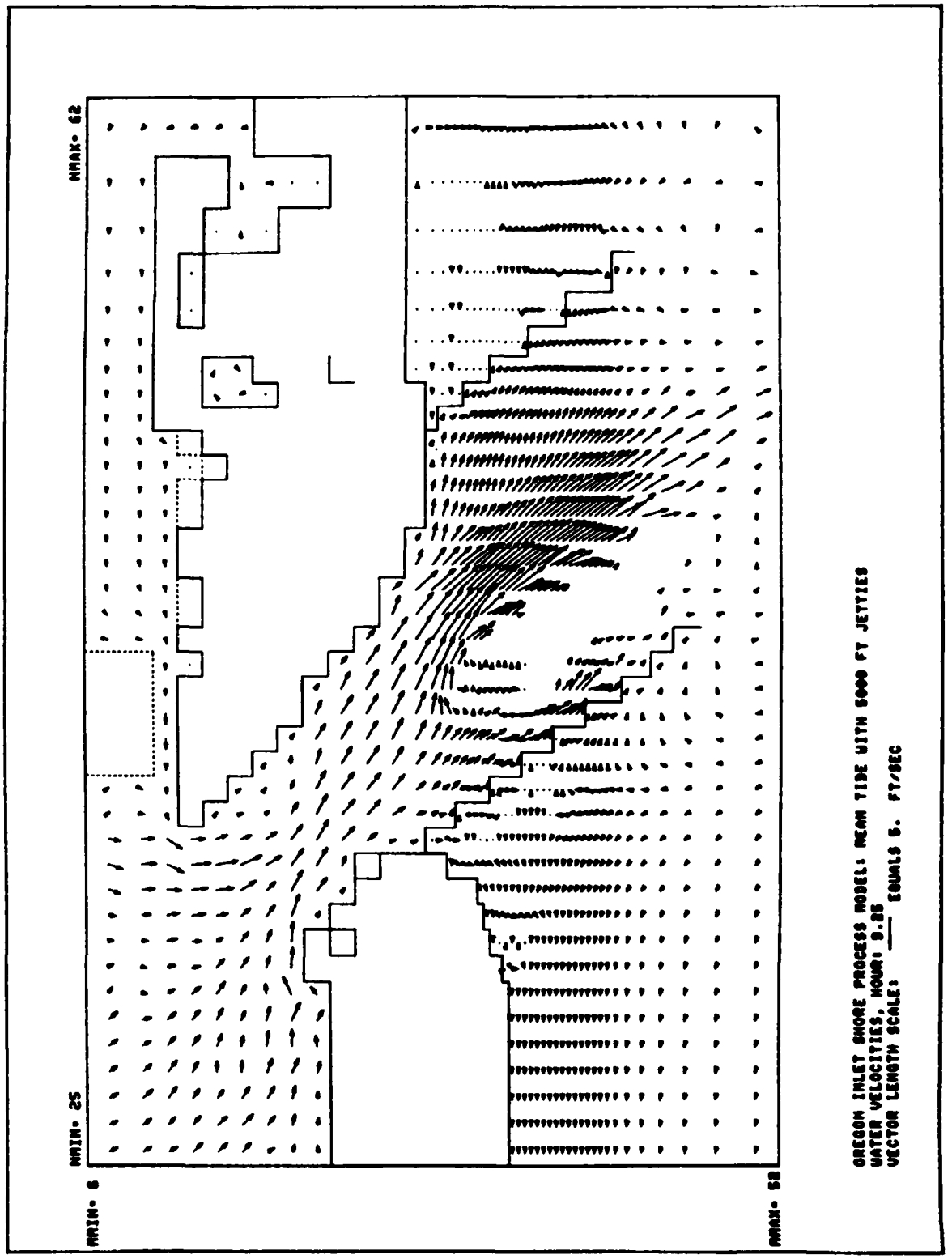
NMAX= 62
NMIN= 25
MMIN= 6
MMAX= 58
OREGON INLET SHORE PROCESS MODEL: MEAN TIDE WITH 6000 FT JETTIES
WATER VELOCITIES, HOUR: 9.25
VECTOR LENGTH SCALE: ___ EQUALS 5. FT/SEC

PLATE 99

PLATE 100

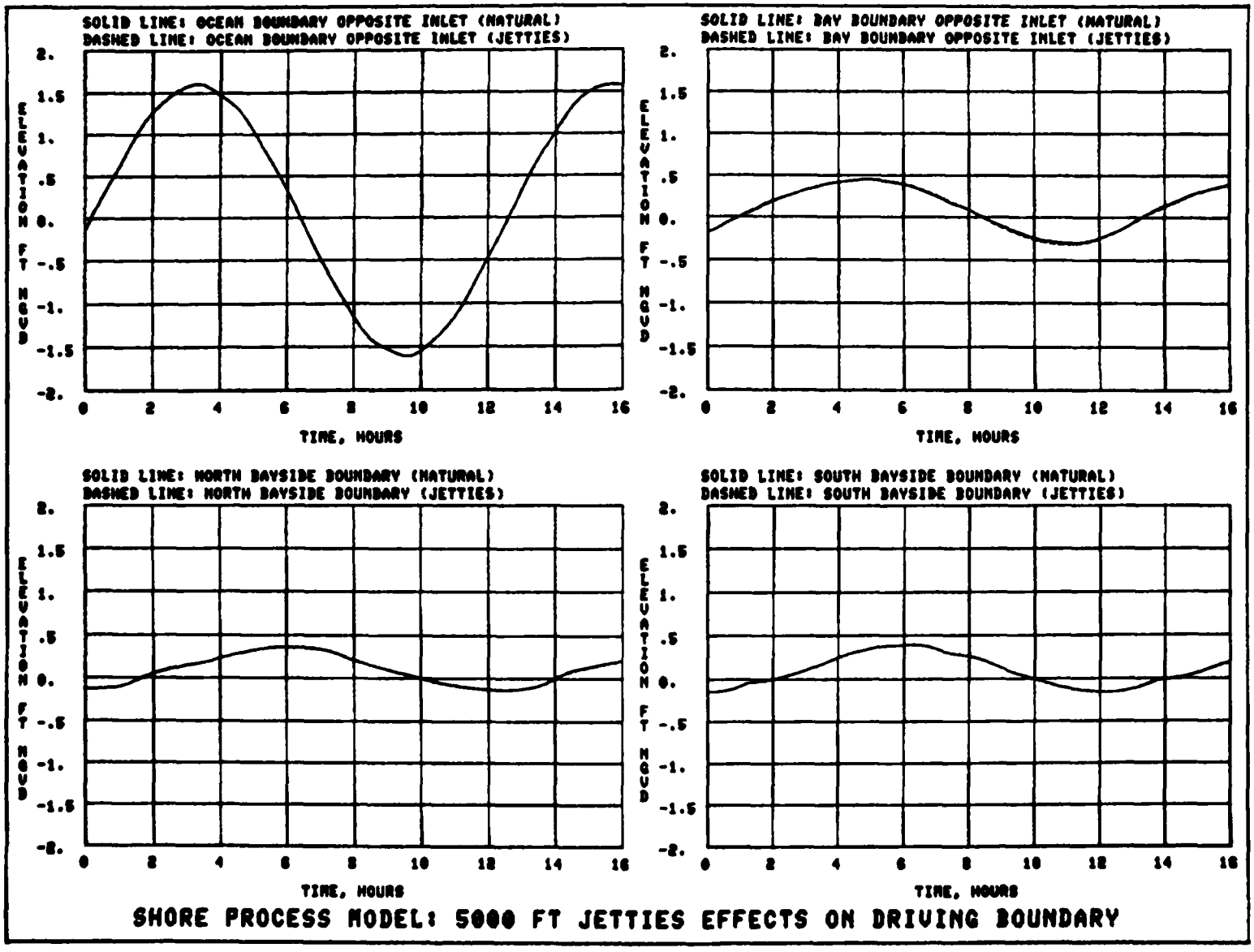

SHORE PROCESS MODEL: 5000 FT JETTIES EFFECTS ON DRIVING BOUNDARY

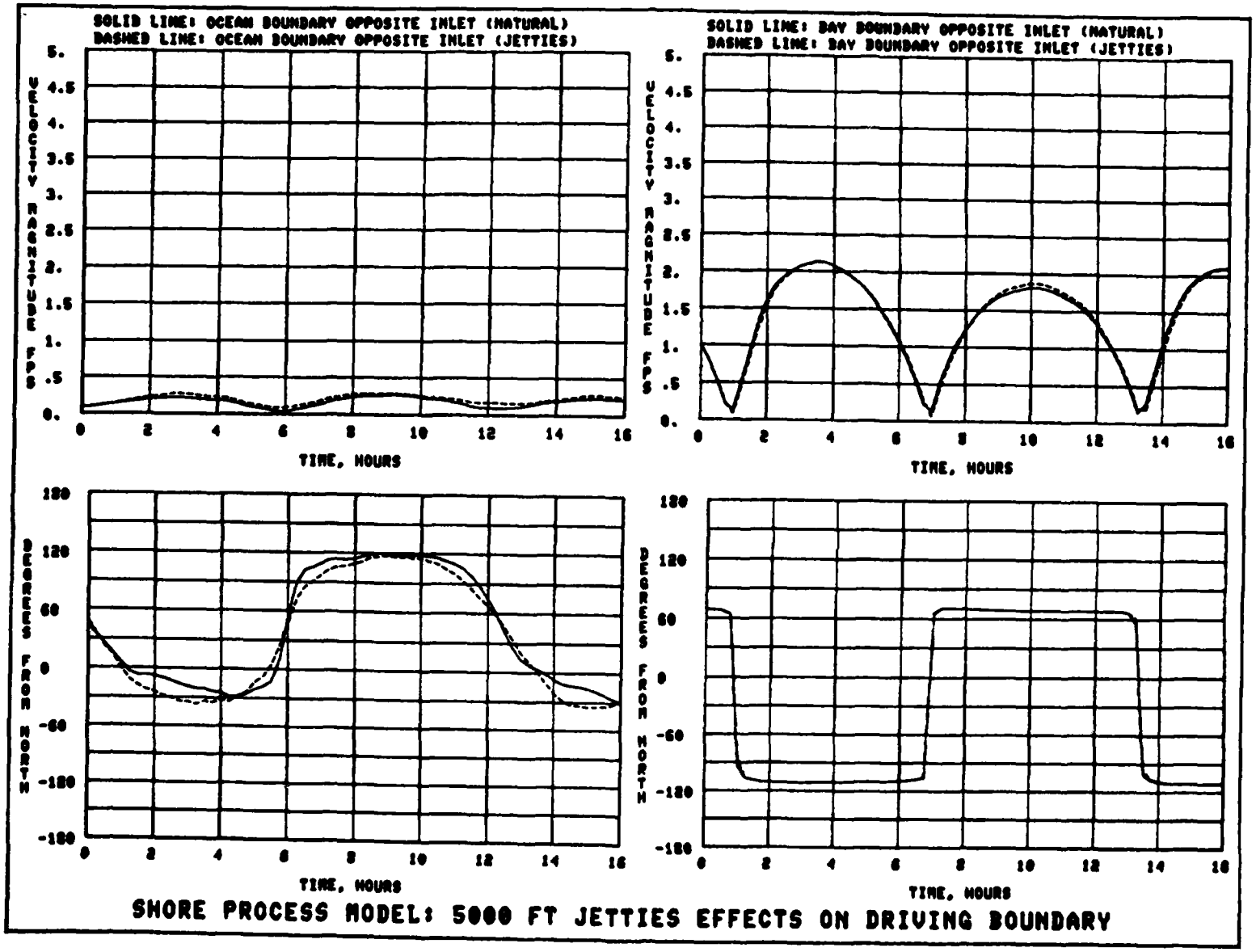

SHORE PROCESS MODEL: 5000 FT JETTIES EFFECTS ON DRIVING BOUNDARY

PLATE 101

PLATE 102

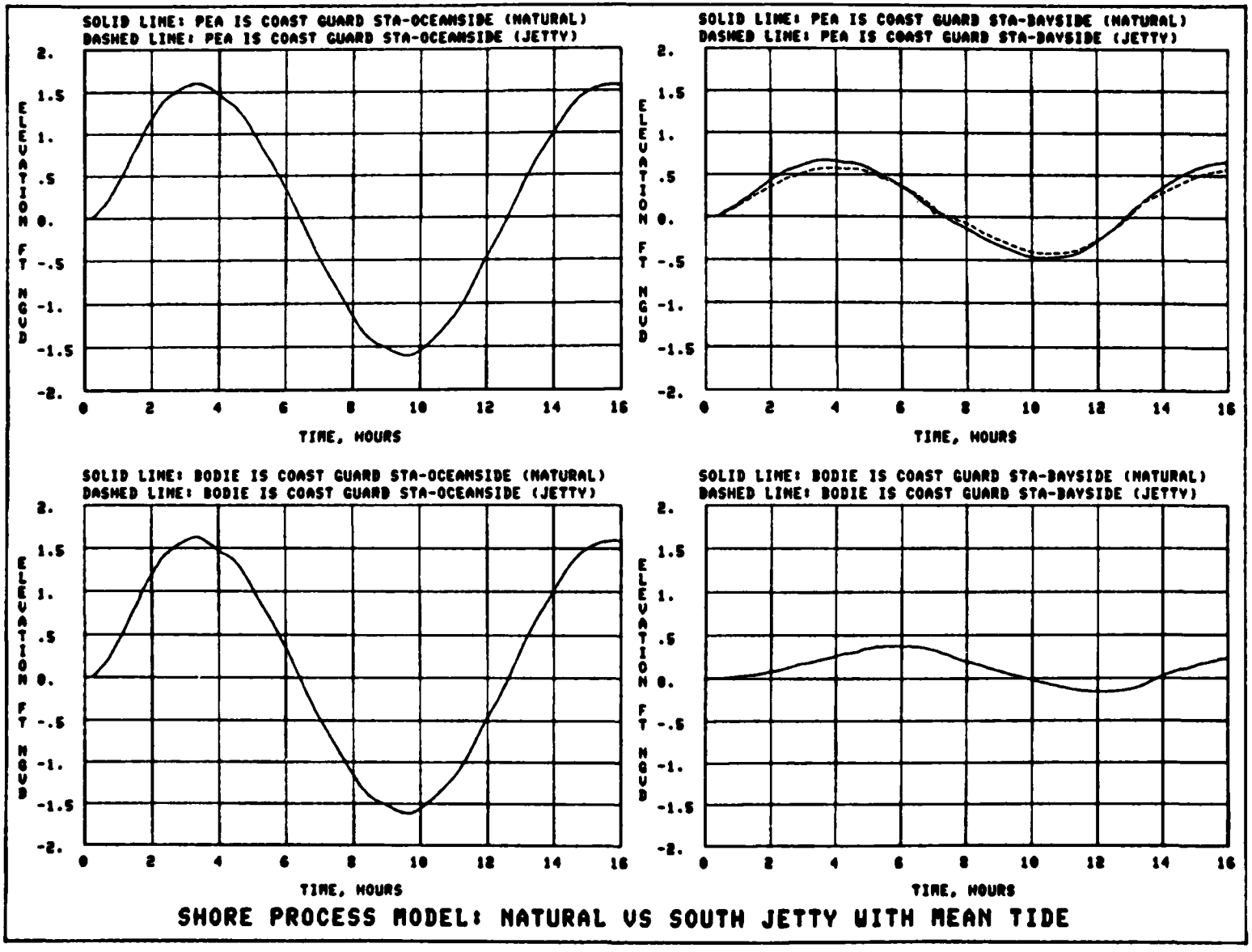
SOLID LINE: PEA IS COAST GUARD STA-OCEANSIDE (NATURAL)
DASHED LINE: PEA IS COAST GUARD STA-OCEANSIDE (JETTY)
SOLID LINE: PEA IS COAST GUARD STA-BAYSIDE (NATURAL)
DASHED LINE: PEA IS COAST GUARD STA-BAYSIDE (JETTY)
SOLID LINE: BODIE IS COAST GUARD STA-OCEANSIDE (NATURAL)
DASHED LINE: BODIE IS COAST GUARD STA-OCEANSIDE (JETTY)
SOLID LINE: BODIE IS COAST GUARD STA-BAYSIDE (NATURAL)
DASHED LINE: BODIE IS COAST GUARD STA-BAYSIDE (JETTY)
ELEVATION FT NGVD
2.
1.5
1.
.5
0.
-.5
-1.
-1.5
-2.
0
2
4
6
8
10
12
14
16
TIME, HOURS
SHORE PROCESS MODEL: NATURAL VS SOUTH JETTY WITH MEAN TIDE

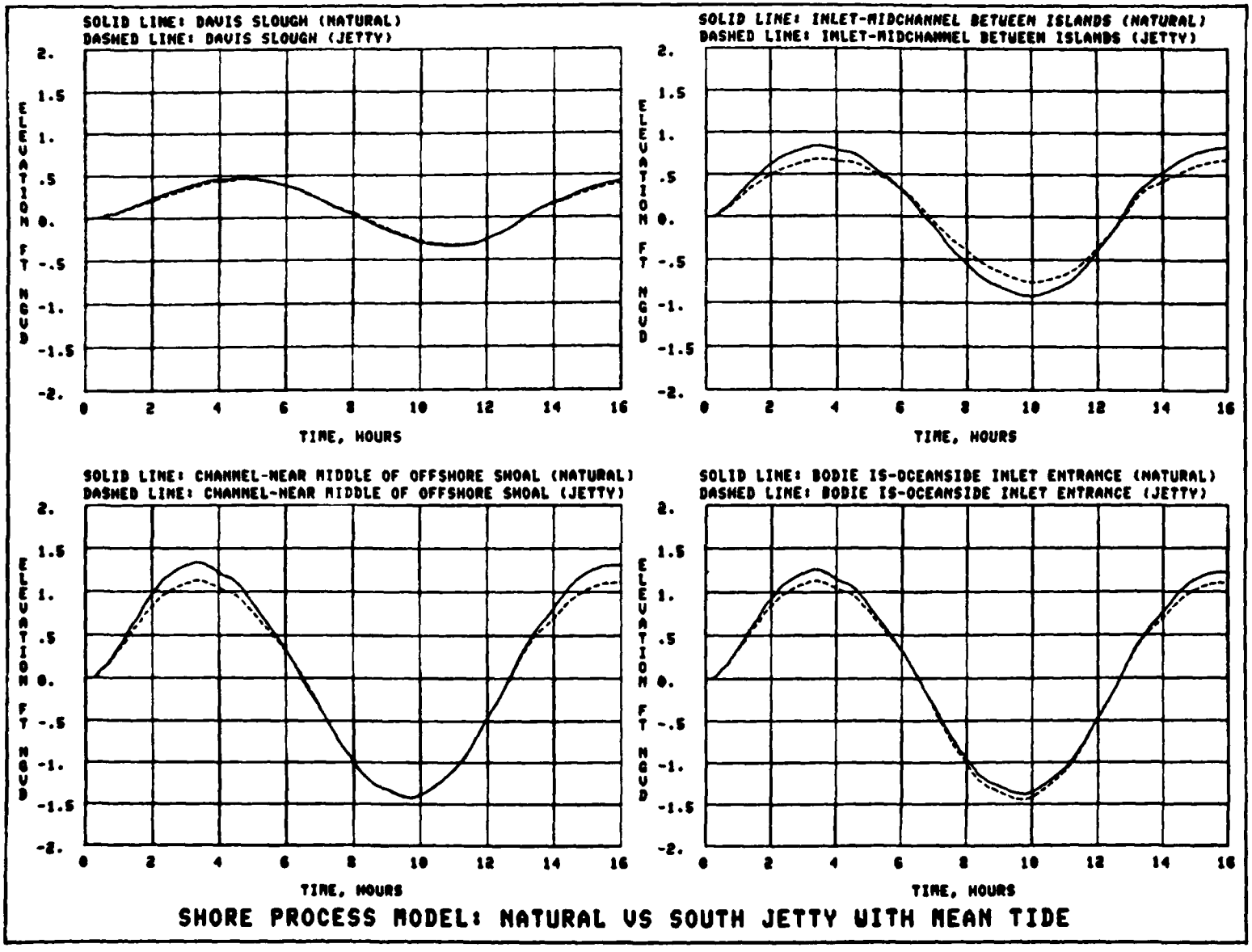

SHORE PROCESS MODEL: NATURAL VS SOUTH JETTY WITH MEAN TIDE

PLATE 103

PLATE 104

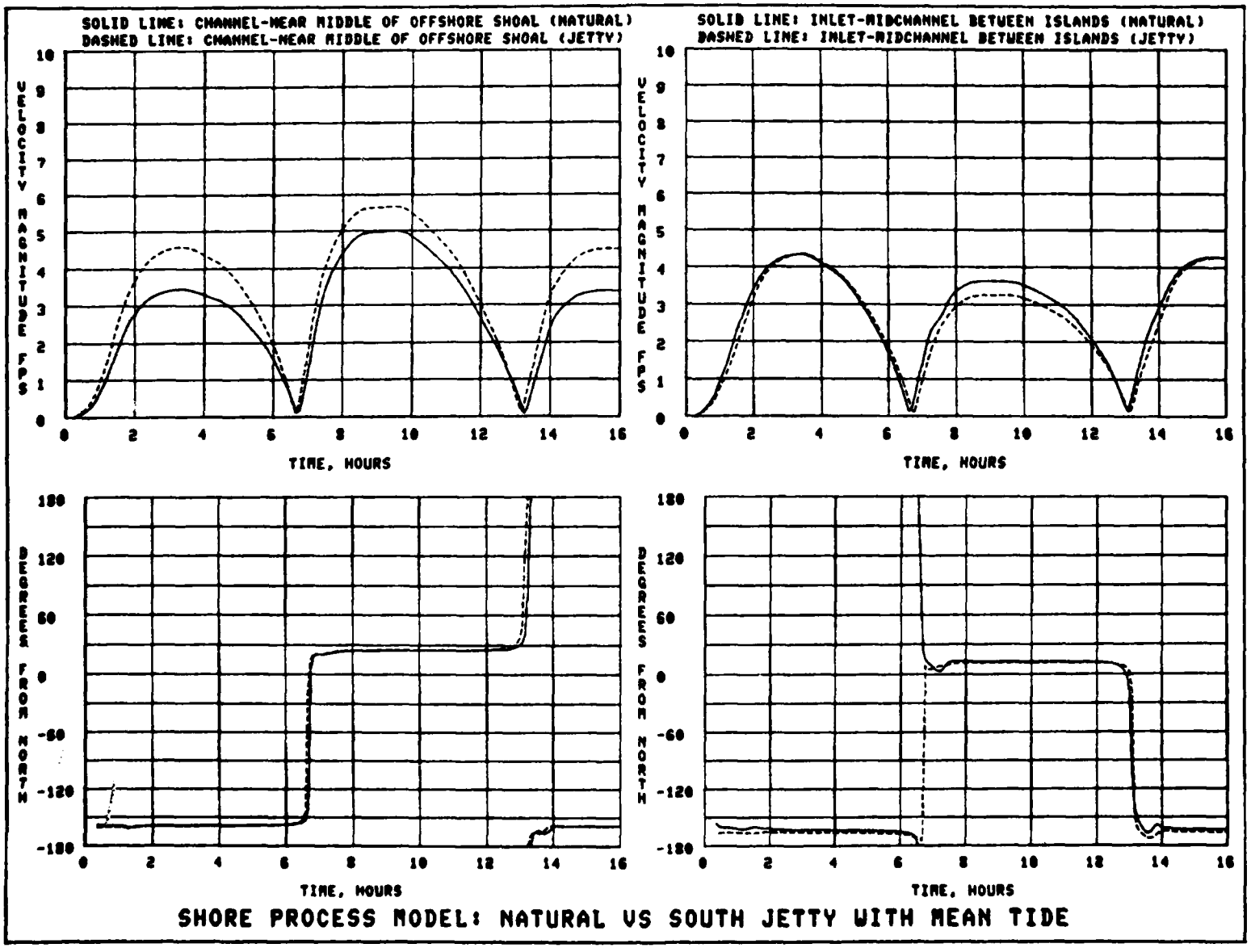

SHORE PROCESS MODEL: NATURAL VS SOUTH JETTY WITH MEAN TIDE

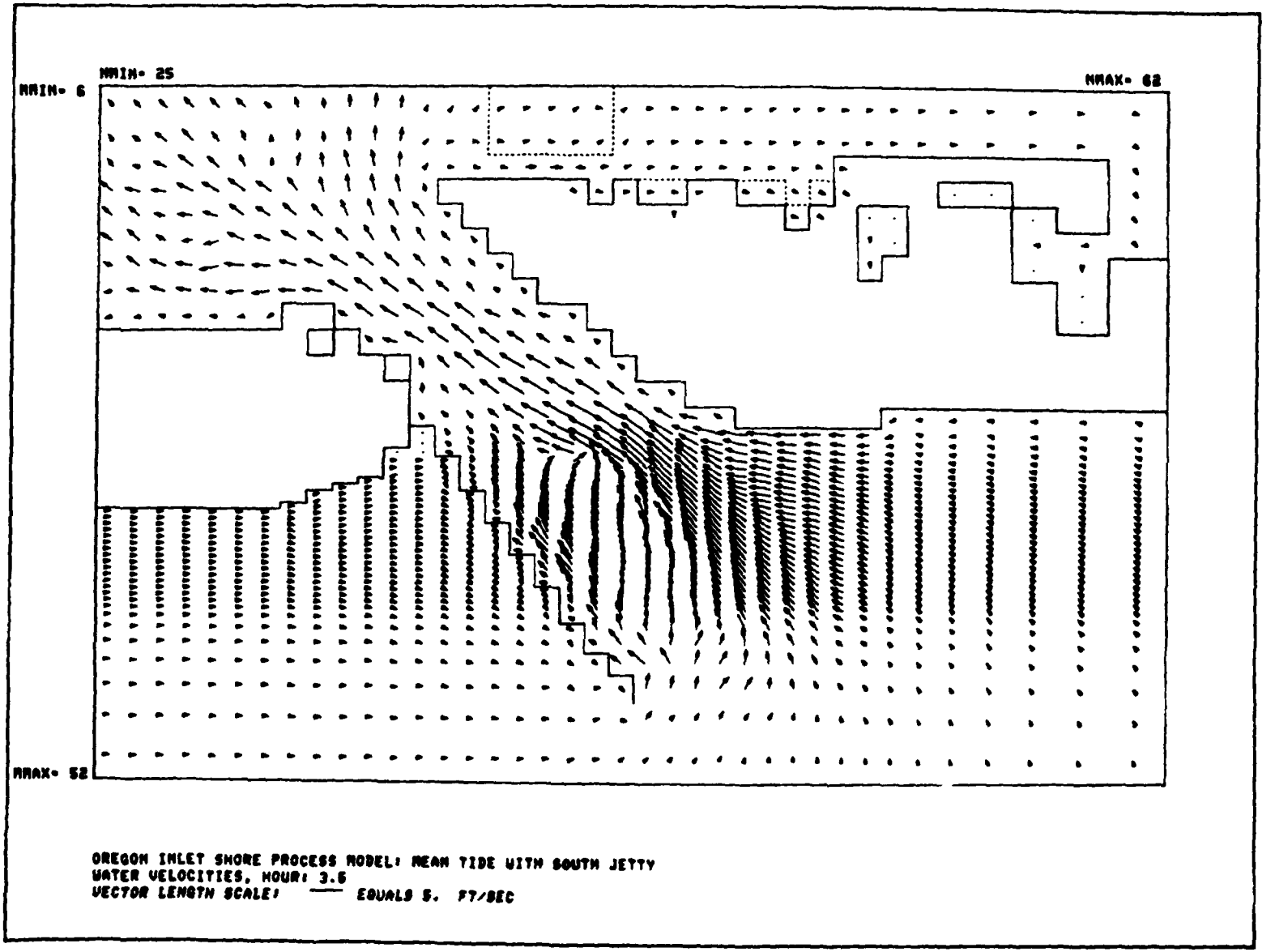

OREGON INLET SHORE PROCESS MODEL: MEAN TIDE WITH SOUTH JETTY
WATER VELOCITIES, HOUR: 3.6
VECTOR LENGTH SCALE: —— EQUALS 5. FT/SEC

PLATE 105

PLATE 106

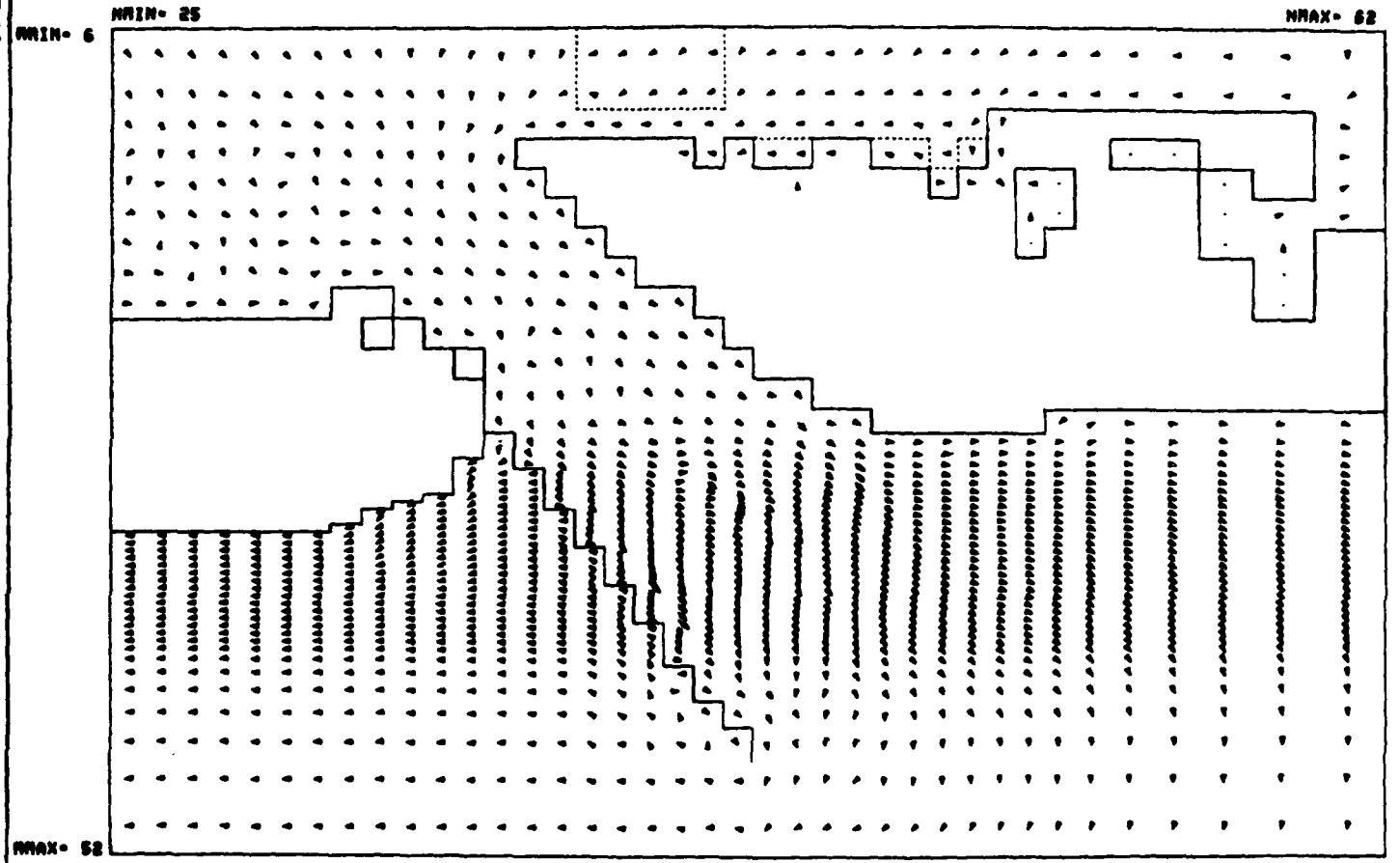

OREGON INLET SHORE PROCESS MODEL: MEAN TIDE WITH SOUTH JETTY
WATER VELOCITIES, HOUR: 6.75
VECTOR LENGTH SCALE: —— EQUALS 5. FT/SEC

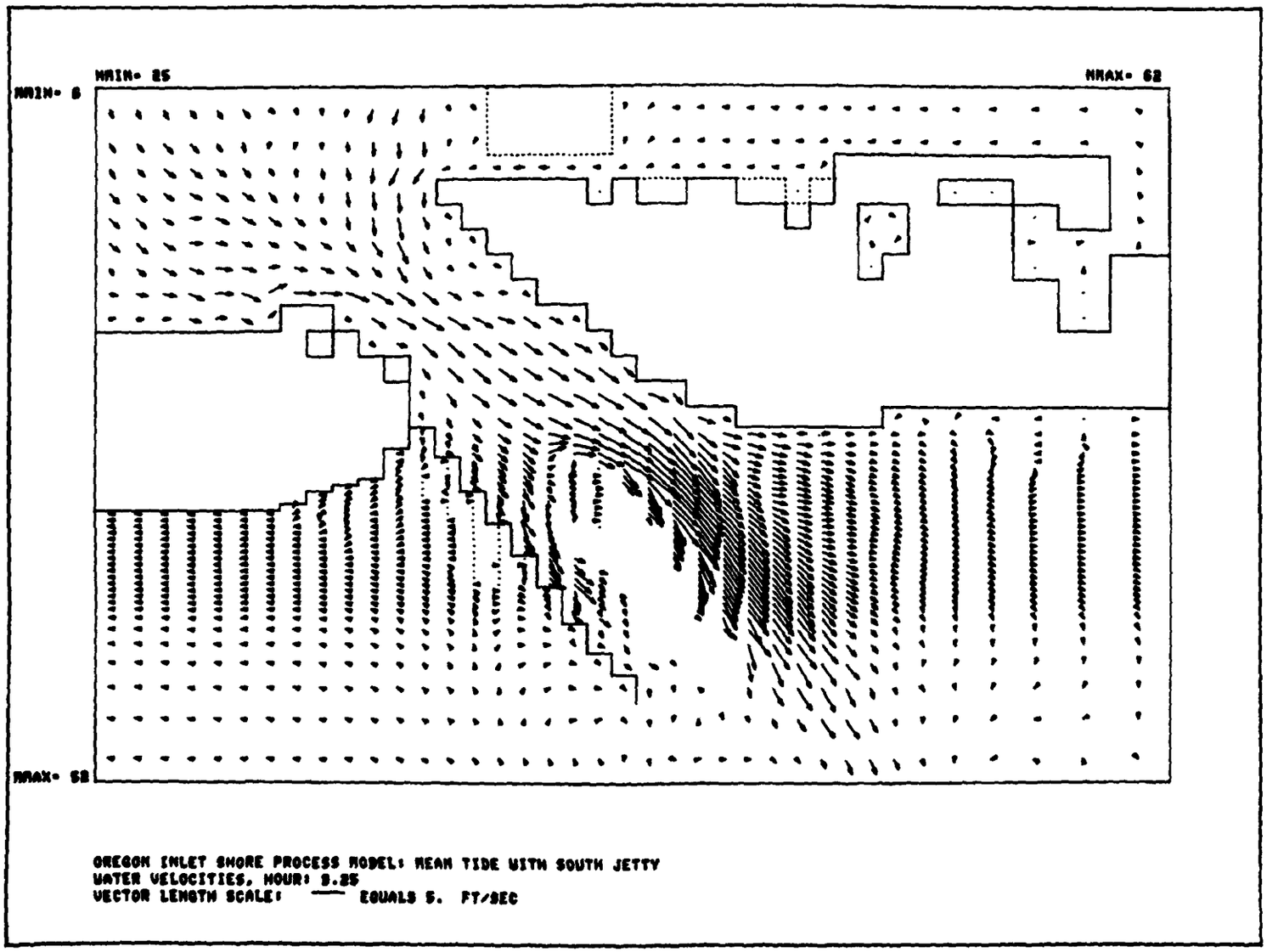

OREGON INLET SHORE PROCESS MODEL: MEAN TIDE WITH SOUTH JETTY
WATER VELOCITIES, HOUR: 9.25
VECTOR LENGTH SCALE: —— EQUALS 5. FT/SEC

PLATE 107

PLATE 108

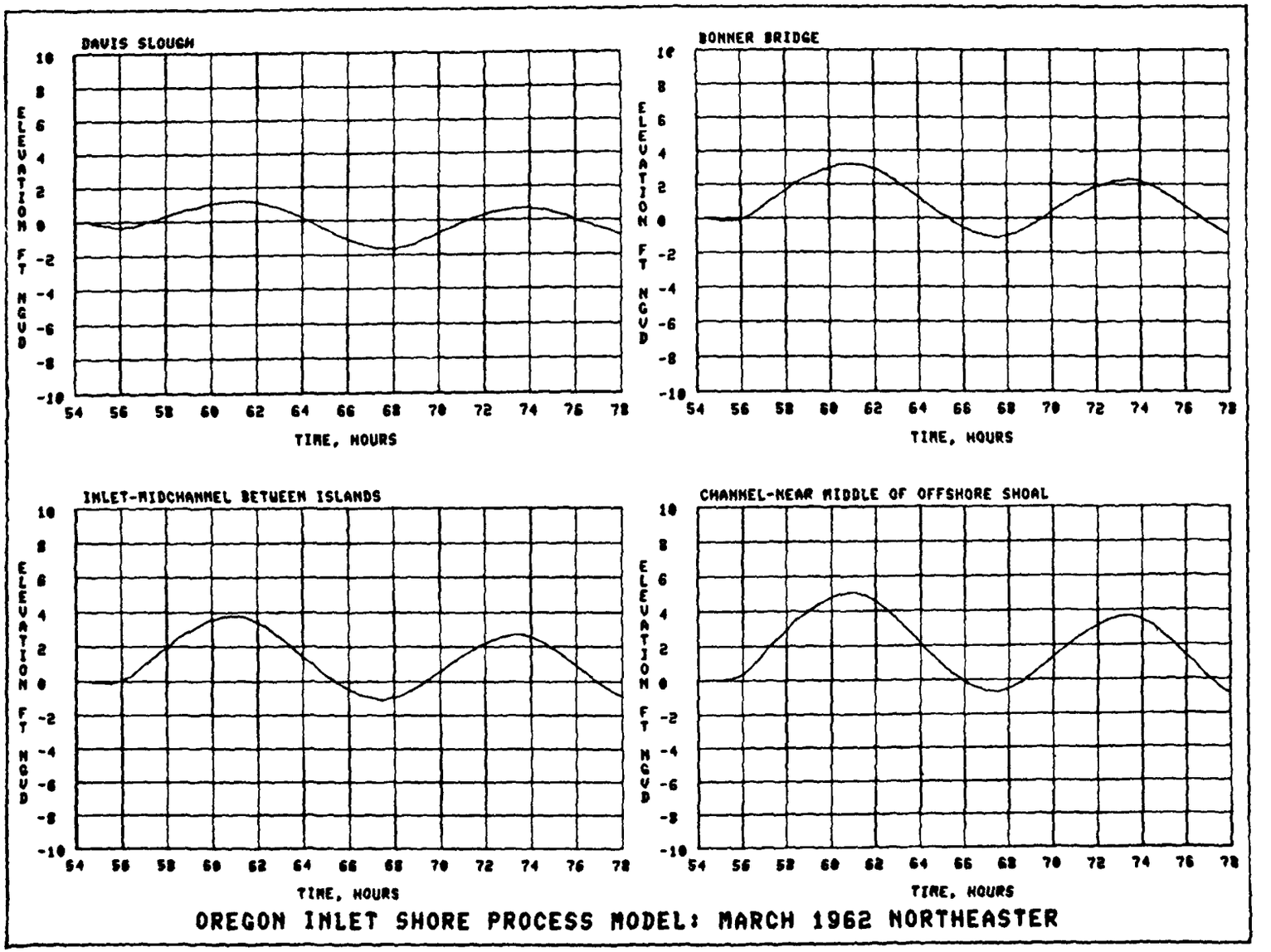

OREGON INLET SHORE PROCESS MODEL: MARCH 1962 NORTHEASTER

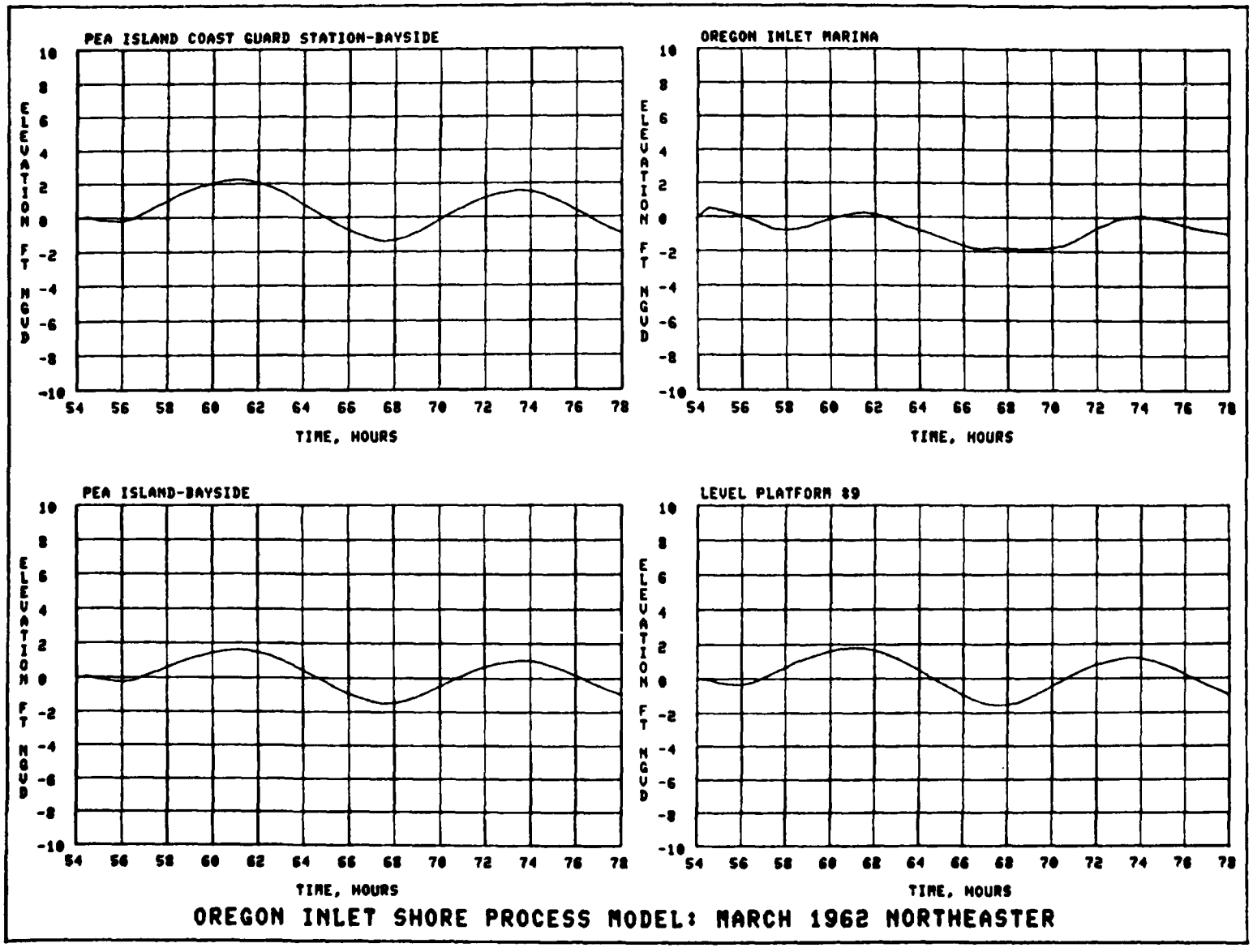

OREGON INLET SHORE PROCESS MODEL: MARCH 1962 NORTHEASTER

PLATE 109

PLATE 110

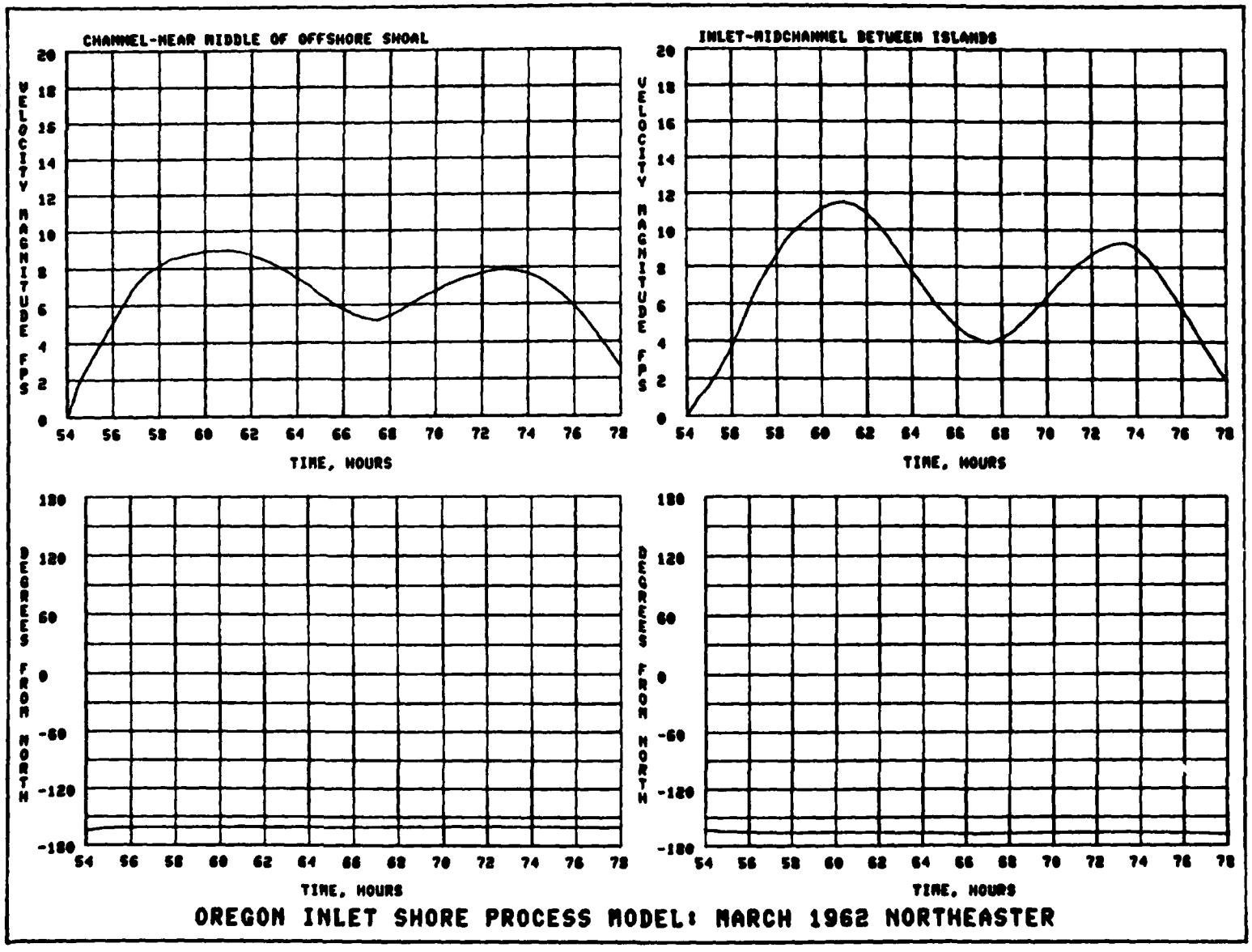

OREGON INLET SHORE PROCESS MODEL: MARCH 1962 NORTHEASTER

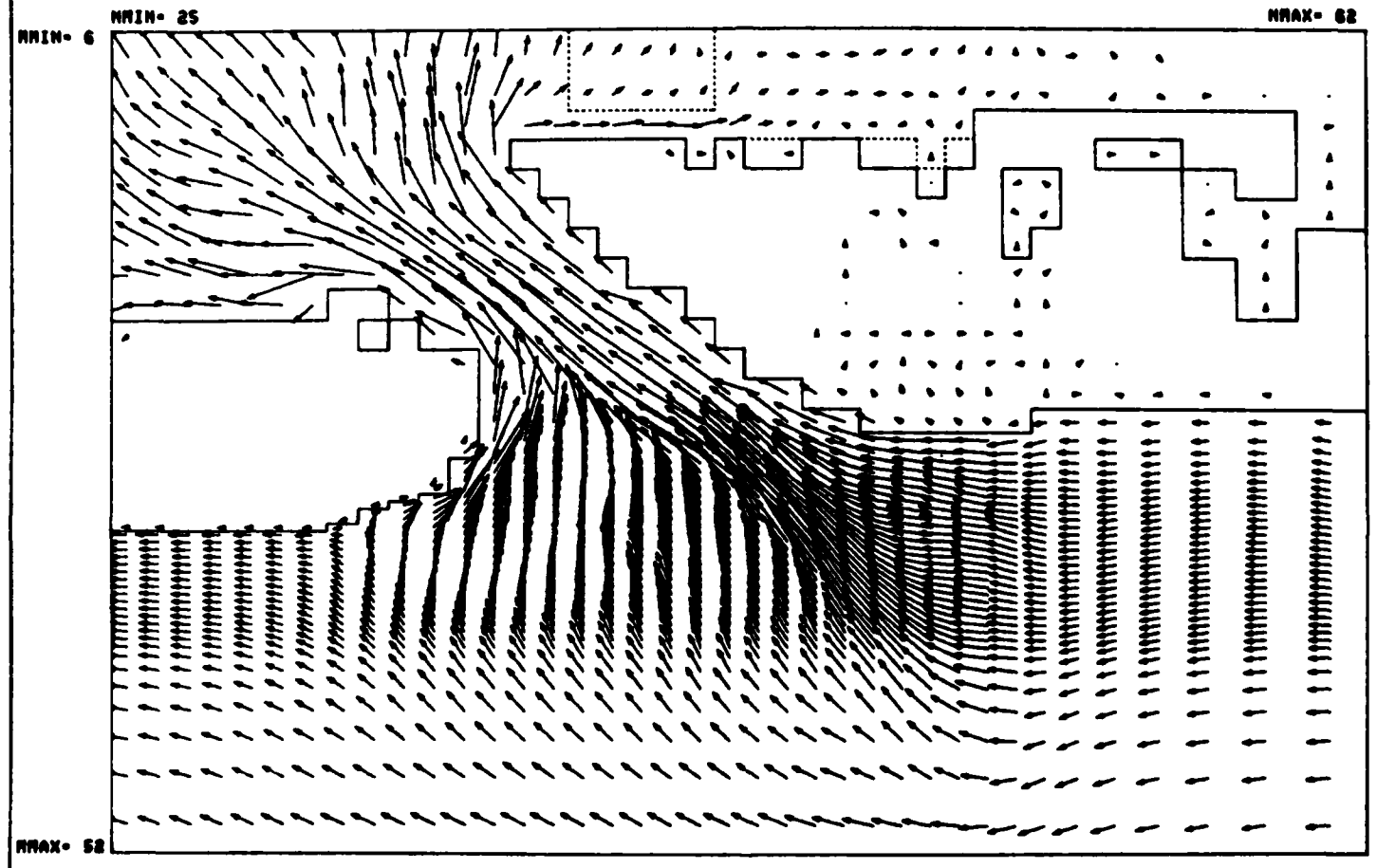

OREGON INLET SHORE PROCESS MODEL: MARCH 1962 NORTHEASTER
WATER VELOCITIES, HOUR: 60.
VECTOR LENGTH SCALE: —— EQUALS 5. FT/SEC

PLATE 111

APPENDIX A: NOTATION

a,b,c	Regional constants derived from stretching transformation of coordinate system
A,B	Coefficient matrices
C	Chezy friction coefficient
C_D	Wind drag coefficient
d	Total depth of water column $d = \eta - h$
f	Coriolis parameter
F_x,F_y	Terms representing external forces such as wind stress
g	Acceleration due to gravity
h	Local ground (cell) elevation above datum
k	Integer time-step counter
n	Dimensionaless parameter used to characterize stability criterion
R	Rate of water volume change in the system (for example through rainfall or evaporation)
t	Time
u	Vertically averaged water velocity in x-direction
U	Matrix consisting of η, u, and v as functions of x, y and t
v	Vertically averaged water velocity in y-direction
V	Largest velocity encountered at a computational cell
W	10-metre wind speed
x,y	Cartesian coordinate system axes names
ΔX	Smaller value of Δx and Δy
Δt	Time-step
$\Delta x,\Delta y$	Length of computational cell in x- and y-directions
ϵ	Eddy viscosity coefficient
η	Water-surface elevation above datum
η_a	Hydrostatic water elevation due to atmospheric pressure differences
$\lambda_x,\lambda_y,S_x,S_y$	Two-dimensional differences operators
ρ	Air density
τ	Surface stress of wind
$*$	Intermediate time-step level
∂	Positive integer representing computational grid line

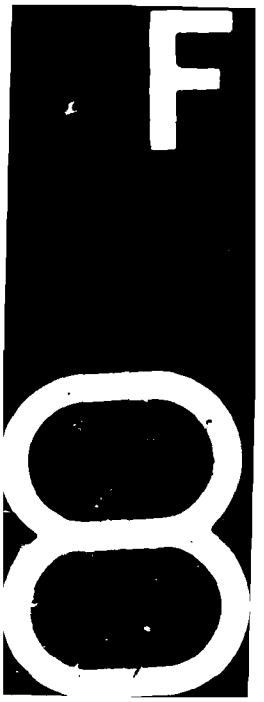
F
8